THÈSE PRÉSENTÉE À

L'UNIVERSITÉ DU QUÉBEC À CHICOUTIMI

COMME EXIGENCE PARTIELLE

DU DOCTORAT EN SCIENCES DE LA TERRE ET DE L'ATMOSPHÈRE

PAR

JULIEN WALTER

MODÈLE D'ÉVOLUTION NATURELLE DE L'EAU SOUTERRAINE DANS UNE RÉGION DU BOUCLIER CANADIEN À PARTIR DE LA DÉTERMINATION DE PÔLES HYDROGÉOCHIMIQUES RÉGIONAUX

MAI 2018

RÉSUMÉ

Les modèles d'évolution des faciès chimiques de l'eau souterraine en fonction de la profondeur et de la distance parcourue entre les zones de recharge et de décharge (cellules d'écoulement locales ou régionales), permettent d'expliquer qualitativement la variabilité spatiale hydrogéochimique. Au Saguenay-Lac-Saint-Jean (SLSJ), cette variabilité est observée pour des résultats d'analyses chimiques de 321 échantillons d'eaux souterraines collectés dans le cadre du Programme d'acquisition de connaissances sur les eaux souterraines de la région Saguenay-Lac-St-Jean (PACES-SLSJ) et pour lesquels environ 40 paramètres physico-chimiques ont été mesurés. Les résultats de travaux antérieurs suggèrent 3 principales sources d'eau d'infiltration (météoritique, marine et sous-glaciaire). Au moment de la recharge, l'eau d'infiltration entre en interaction avec les unités lithologiques régionales. Ces dernières sont groupées en 2 principaux réservoirs sur la base de leur comportement hydraulique général (réservoirs rocheux fracturés et réservoirs granulaires poreux). Ainsi, ce projet vise la détermination de pôles compositionnels hydrogéochimiques de l'évolution naturelle de l'eau d'infiltration en fonction des réservoirs géologiques régionaux, et l'identification de traceurs géochimiques caractéristiques des mécanismes d'interaction eau-roche proposés.

Les pôles hydrogéochimiques sont obtenus selon un traitement qui combine les techniques statistiques standards, l'analyse statistique multivariée et la mise en graphique des résultats. L'analyse statistique multivariée est appliquée en deux temps. Dans un

premier temps, la base de données est considérée dans son ensemble, et dans un second temps, l'analyse est appliquée à un sous-ensemble de données, lesquelles sont sélectionnées à partir de leurs caractéristiques géochimiques. Cette méthode nous conduit à définir 2 pôles hydrogéochimiques régionaux distincts du point de vue de leur composition chimique : 1) un pôle compositionnel régional de l'évolution de l'eau souterraine en milieu rocheux fracturé, et 2) un pôle compositionnel régional de l'évolution de l'eau souterraine en milieu granulaire poreux confiné par l'argile marine. La composition chimique de ces pôles est comparée avec les compositions chimiques de saumures de roches cristallines précambriennes tirées de la littérature. Une signature chimique régionale de l'eau de pluie est proposée suite à la compilation de données existantes et aux résultats d'analyse de 4 échantillons. Les différents stades d'évolution de l'eau souterraine sont comparés à l'aide d'une méthode normative multiéléments et les différences observées sont exprimées en indices de maturité. Ces indices de maturité, combinés aux résultats du traitement d'analyse multivariée et à la comparaison de la composition chimique des pôles avec celle d'eaux de référence, nous permettent de proposer des paramètres chimiques caractéristiques de l'évolution naturelle de l'eau souterraine vers l'un ou l'autre de ces pôles. Le tout fait l'objet d'un modèle conceptuel schématique qui inclut les caractéristiques stratigraphiques simplifiées de la région et leurs impacts sur la composition chimique de l'eau souterraine.

REMERCIEMENTS

Je remercie **Dr. Alain Rouleau**, professeur d'hydrogéologie à l'UQAC pendant plus de trente ans. Il m'a ouvert la voie de la recherche en 2003, m'a offert la charge du projet PACES-SLSJ, façonnant ainsi à bien des égards l'hydrogéologue que je suis aujourd'hui. Il m'a ensuite encouragé à entreprendre mes études de doctorat. Du fond du cœur, merci pour tout.

Je remercie mon directeur de recherche, et maintenant ami, **Dr. Romain Chesnaux**. Une des personnes les plus humaines qu'il m'ait été permis de côtoyer, dotée d'une simplicité et d'une gentillesse sans égale, et surtout, d'un immense savoir qu'il diffuse sans retenu. Romain, tu m'impressionnes d'allier avec autant de brio ta fleurissante vie professionnelle et ton amour inconditionnel pour les bonnes choses. Merci de m'avoir fait confiance tout au long de l'aventure, et de m'avoir montré que la rigueur et le plaisir vont de pair dans la réalisation de grands projets.

Je remercie mes co-directeurs : **Dr. Vincent Cloutier**, pour sa très grande disponibilité, sa promptitude à commenter mes travaux et à répondre de façon détaillée à toutes mes interrogations; et **Dr. Damien Gaboury**, pour l'énergie déployée à la mise en fonction de son formidable *Système d'hydrothermalisme expérimentale*, pour cette capacité incomparable qu'il possède de ne pas couper les cheveux en quatre et d'aller de l'avant sans se soucier des « qu'en dira-t-on », c'est aussi comme ça qu'on finit par finir.

Je remercie mon fidèle partenaire de terrain, et ami, **David Noël**, expert incontestable de tous les aspects techniques de l'hydrogéologie, et même plus! Car la passion qui l'anime le fait innover sans cesse. David, ta grande débrouillardise, tes compétences variées, et ta grande pédagogie font de toi un atout inestimable au sein d'une équipe. L'UQAC est chanceuse de t'avoir.

Je remercie mes collègues et amis : **Denis Germaneau, Mélanie Lambert et Marie-Line Tremblay** pour toutes ces années passées ensemble à chercher comment ne jamais refaire de la même manière ce qu'on avait déjà fait.

Je remercie aussi **Dr. Philippe Pagé**, pour nos multiples rencontres lors desquelles nous parlions géologie, entre autre. Merci pour l'intérêt que tu portes à mes travaux, et merci de m'avoir partagé sans retenue ta vaste connaissance de la géochimie.

Je remercie avec tout l'amour et la passion dont je suis capable, **Annick Fortin**, non seulement ma partenaire de vie, mais aussi ma meilleure amie. Annick, pendant ce doctorat, tu as donné naissance à nos deux magnifiques garçons, et depuis, tu n'as jamais cessé d'être là pour eux, comme pour moi, pour le meilleur et pour le pire. Tu m'as donné toute la force nécessaire pour aller au bout de ce grand défi, le temps aussi, ce temps si précieux qui nous manque toujours trop. Merci pour tout ce que tu as fait.

Je dédie cette thèse à mes parents, **Philippe Walter et Marièle Walter née Ziegler**, sans qui, rien de tout cela ne serait arrivé. Je vous porte dans mon cœur pour l'éternité.

Je dédie aussi cette thèse à mes enfants, **Eugénie, Milan et Théo Walter**, en espérant qu'ils apprennent comme moi que lorsque la passion, la conviction et la persévérance guident nos pas, il ne reste plus beaucoup de limite infranchissable.

TABLE DES MATIÈRES

LISTE DES FIGURES

CHAPITRE 1

CHAPITRE 2

LISTE DES TABLEAUX

CHAPITRE 4

CHAPITRE 5

LISTE DES ANNEXES

CHAPITRE 1

INTRODUCTION

Tales sunt aquae, qualis terra per quam fluunt

(L'eau acquiert sa nature des strates à travers lesquelles elle circule)

De *Gaius Plinius Secundus, écrivain naturaliste du 1er siècle.*

1.1 PROBLÉMATIQUE GÉNÉRALE

Il est maintenant bien connu en géochimie des eaux qu'une partie de la minéralisation des eaux souterraines est gouvernée par la capacité des milieux aquifères à imprimer leur signature chimique à la nappe (Chebotarev, 1955; Derron, 2004, Adiaffi et al., 2012). La couleur et certains goûts inhabituels en sont souvent les premiers indicateurs mais c'est surtout l'observation d'une importante variabilité spatiale qui en atteste, et qui a conduit certains auteurs à définir des modèles d'évolution de la chimie de l'eau souterraine. Dans cette thèse doctorale, la région du Saguenay-Lac-Saint-Jean, à la physiographie particulière et située dans le Bouclier Canadien au Québec, constituera notre laboratoire d'étude compte tenu notamment de l'importance de valoriser la grande quantité de connaissances hydrogéochimiques et hydrogéologiques acquises au cours des dix dernières années.

1.1.1 VARIABILITÉ CHIMIQUE DE L'EAU SOUTERRAINE

Selon une approche essentiellement qualitative, Chebotarev (1955), suggère que quasiment tous les minéraux (primaires et secondaires) retrouvés dans la croûte terrestre sont solubles dans l'eau naturelle. Les résultats d'analyses chimiques d'eaux souterraines de qualité variable le conduisent à proposer un premier groupement des eaux naturelles en fonction de leur contenu minéral exprimé en mg/L (Tableau 1.1).

Tableau 1.1 : Regroupement qualitatif des eaux naturelles (Chebotarev, 1955)

Groupes d'eaux naturelles		Salinité approximative (mg/L)
Groupes majeurs	Subdivisions	
Eaux fraîches	Potable	Moins de 500
	Fraîche	Moins de 700
	Assez fraîche	700 – 1500
	Passablement fraîche	1 500 – 2 500
Eaux saumâtres	Légèrement saumâtre	2 500 – 3 200
	Saumâtre	3 200 – 4 000
	Assurément saumâtre	4 000 – 5 000
Eaux salées	Légèrement salée	5 000 – 6 500
	Salée	6 500 – 7 000
	Très salée	7 000 – 10 000
	Extrêmement salée	Plus de 10 000

Remarque : la salinité de l'eau de mer est de l'ordre de 35 000 mg/L

Toujours selon Chebotarev (1955), la proportion et le type de matières solubles sont fonction de plusieurs facteurs comme la nature des formations géologiques, les éléments structuraux du milieu réservoir, la température de l'eau, la concentration en sels dissous et l'abondance de certains ions dans l'eau, la quantité d'eau circulant dans l'aquifère et sa vitesse d'écoulement. Il ajoute que si certaines substances sont intensément affectées par l'eau et se retrouvent rapidement en solution, d'autres composés chimiques sont plus résistants aux processus d'altération. Ainsi, la composition chimique des eaux naturelles peut grandement différer d'un endroit à l'autre. Pour Chebotarev (1955), l'eau souterraine présentant de grandes concentrations en éléments dissous est généralement retrouvée dans les parties profondes des structures géologiques où des conditions de stagnation dominent, sans égards à la nature de la formation aquifère. À l'inverse, lorsque l'eau souterraine présente un échange actif avec la surface

terrestre (eaux à renouvellement « rapide » et abondante), sa salinité est généralement faible.

L'étude de Casanova et al. (2004) a permis l'élaboration d'une base de données contenant plus de 1 800 échantillons avec une analyse de la chimie de l'eau (éléments majeurs et traces) provenant de l'Europe (France, Allemagne, Angleterre, Espagne, Suisse, Finlande, Suède, Lituanie, Ukraine), du Canada et de l'Antarctique. En général, les anions principaux sont Cl^- et HCO_3^- et dans de rares cas SO_4^{2-}. Les eaux souterraines de sites granitiques au Canada, en Fenno-Scandinavie et en France ont des signatures témoignant plus ou moins de la composition résultant de l'histoire magmatique et hydrothermale associée à la mise en place des granites, ou de modifications ultérieures liées à différents processus géodynamiques, ou encore témoignent d'interactions granite-eaux interstitielles très anciennes (Casanova et al., 2004). Le Tableau 1.2 de Casanova et al. (2004) présente la variabilité géographique des types d'eau considérés dans leur étude et la figure 1.1 illustre la variabilité de leur contenu minéral (i.e. total des solides dissous; TSD) sur un diagramme de Piper (1944).

La région à l'étude se situe dans le Bouclier précambrien canadien où des fluides minéralisés sont documentés avec des teneurs supérieures à 150 g/L (Frape et al., 1984). Ceci est similaire à ce qui est trouvé dans des contexte géologique similaire comme dans le Bouclier fenno-scandinave et sur le continent européen (où des socles anciens sont présents) avec des teneurs dépassant 45 g/L (Lodemann et Fritz, 1997; Laaksoharju et

al.,1995). Parmi les ions majeurs, le sodium, le calcium et les chlorures sont en plus fortes concentrations dans les eaux souterraines profondes (> 500 m) du socle cristallin de la croûte continentale (Edmunds et al. 1984; Fritz et Frape, 1987; Fritz, 1997).

Tableau 1.2: Types d'eau et leurs localisations géographiques selon Casanova et al. (2004)

Type d'eau	Localisation géographique
Na-Cl	Canada, Aspö, Palmottu, Lituanie, Finlande (Parainen, Kerimaki, Stripa), Massif Armoricain, Massif Central, Forêt Noire, Vosges
Ca-Cl	KTB (Allemagne), Canada, Aspö, Finlande (Outokumpo, Okiluoto, Hästholmen), Antarctique, Carnemellis (Angleterre)
Ca-Cl-SO_4	Forêt Noire, Alpes, Corse, Canada (Luppin), Palmottu, Massif Armoricain
Na-Cl-HCO_3	Forêt Noire, Canada, Aspö, Palmottu, Massif Armoricain, Massif Central, Stripa
Na-Cl-NO_3	Massif Armoricain
Ca-HCO_3	El Berrocal (Espagne), Forêt Noire, Vosges, Canada, Aspö, Palmottu, Massif Armoricain, Massif Central, Vosges, Corse, Finlande (Outokumpo, Stripa)
Na-HCO_3	Corse, Forêt Noire, Canada, Aspö, Palmottu, Massif Armoricain, Massif Central, El Berrocal
Ca-SO_4	Alpes, Vosges, Canada, Massif Central
Na-SO_4	Forêt Noire, Palmottu, Massif Central, Alpes, Corse, Suisse, Vosges, Massif Armoricain, Aspö, UK, Palmottu, Canada
NO_3	Massif Armoricain

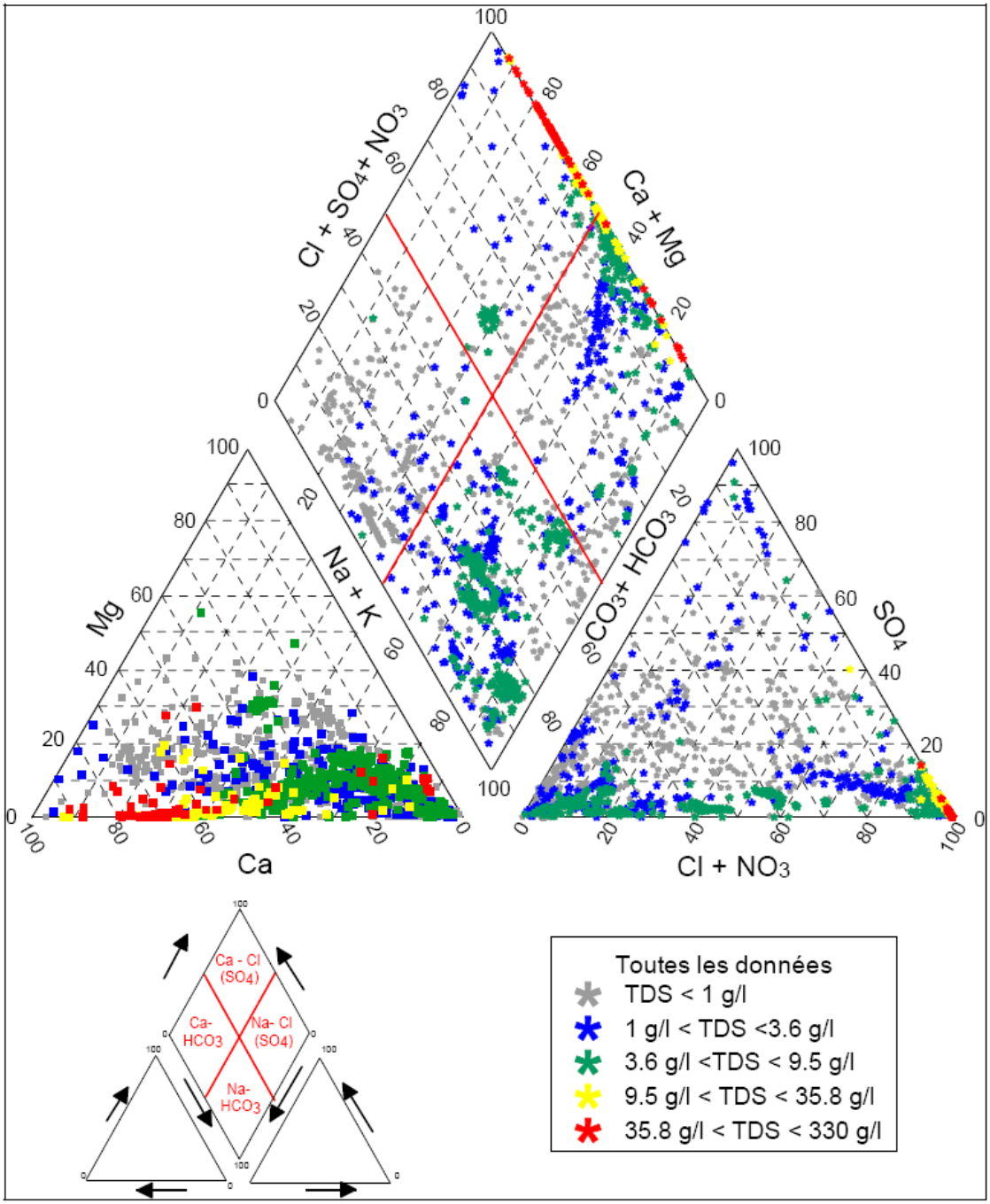

Figure 1.1 : Classification de 1800 échantillons d'eau souterraine au sein d'un diagramme de Piper en fonction de leur TSD. Ces eaux proviennent de différents endroits à travers le monde (Europe, Canada, Fenno-scandinavie, Antarctique) (Tirée de Casanova et al., 2004).

1.1.2 MODÈLES D'ÉVOLUTION DE LA CHIMIE DE L'EAU SOUTERRAINE

Pour Gascoyne et Kamineni (1994), la composition des eaux souterraines des milieux fracturés cristallins est contrôlée principalement par l'interaction entre l'eau et la roche dans les environnements superficiels où les phénomènes d'advection dominent sur les phénomènes de diffusion. Les auteurs proposent une série de réactions pour expliquer la composition chimique de leurs échantillons d'eau souterraine. Pour eux, sans distinction pour le type considéré de roches granitiques, l'hydrolyse des feldspaths est le processus chimique prédominant. Avec la dissolution et la dissociation du CO_2 dans l'eau souterraine (équation 1), l'altération des feldspaths (équations 2 et 3) permet d'expliquer l'augmentation du pH obtenue. La diminution du calcium dissous est expliquée par la précipitation de la calcite (équation 4) et par des phénomènes d'échanges ioniques avec les minéraux argileux néoformés (équation 5). La dominance des minéraux argileux, kaolinite et illite, dans les roches granitiques est expliquée par l'altération des deux principaux composants minéralogiques de ce type de roche, la biotite et le feldspath potassique (équation 6 et 7). Bien que ces réactions d'altération produisent du potassium et du magnésium dissous, Gascoyne et Kamineni (1994) expliquent les faibles teneurs de l'eau souterraine en ces éléments (<10 mg/L) en évoquant des phénomènes d'échanges ioniques avec les minéraux argileux et la faible solubilité des hydroxydes et des carbonates à des pH élevés. À de plus grandes profondeurs, les effets de l'advection diminuent et les temps de résidence augmentent (> 10^6 années), ce qui permet la dissolution de sels

contenus dans la matrice poreuse des roches. Partant de ces hypothèses, Gascoyne et Kamineny (1994) propose un modèle d'évolution naturelle de l'eau souterraine.

$H_2O + CO_2 \Leftrightarrow H_2CO_3 \Leftrightarrow H^+ + HCO_3^-$ (Équation 1)

$2NaAlSi_3O_8 + 2H^+ + H_2O \rightarrow 2Na^+ + Al_2Si_2O_5(OH)_4 + 4SiO_2$ (Équation 2)

(albite) (kaolinite)

$CaAl_2Si_2O_8 + 2H^+ + H_2O \rightarrow Ca^{2+} + Al_2Si_2O_5(OH)_4$ (Équation 3)

(anorthite) (kaolinite)

$Ca^{2+} + 2HCO_3^- \leftrightarrow CaCO_3 + H_2O + CO_2$ (Équation 4)

(calcite)

$2Ca^{2+} + 2Na\text{-}X(s) \Leftrightarrow 2Na^+ + 2Ca\text{-}X(s)$ (Équation 5)

$2KMg_3AlSi_3O_{10}(OH)_2 + 14H^+ \rightarrow 2K^+ + 6Mg^{2+} + 7H2O + 4SiO_2 + Al_2Si_2O_5(OH)_4$ (Équation 6)

(Biotite) (Kaolinite)

$3KAlSi_3O_8 + 2H^+ \rightarrow 2K^+ + 6SiO_2 + KAl_3Si_3O_{10}(OH)_2$ (Équation 7)

(microcline) (illite)

Ainsi, selon le modèle schématisé à la figure 1.2 appliqué aux différents types de roches plutoniques du Bouclier canadien, les eaux souterraines récentes devraient être faiblement concentrées et légèrement acides et du type Ca-HCO_3. Leur évolution amène ces eaux au type Na-HCO_3. Elles se rencontrent principalement dans les premiers 100 à 200 m de profondeur et sont généralement de très bonne qualité. Par la suite, elles peuvent devenir sulfatées, notamment en présence de minéraux sulfurés. À de plus grandes profondeurs, les eaux deviennent du type chloruré et leur salinité augmente. Cette évolution est observée en fonction de la profondeur ou en fonction de la distance de parcours le long d'une trajectoire d'écoulement et ce, quel que soit le type de roche (plutons de granite, de gabbro et de gneiss). Gasoyne et Kamineny (1994) précisent que passé 1 000 m de profondeur dans le roc cristallin, l'eau souterraine est généralement salée à très salée. À noter que la figure de Gascoyne et Kamineni (1994) illustre uniquement une zone de recharge (Figure 1.2), ce qui a pour effet l'augmentation du temps et de la distance de parcours en fonction de la profondeur uniquement.

Tòth (1985) suggère que la qualité des eaux souterraines est en relation directe avec leur régime hydraulique, de même que la taille de la cellule d'écoulement, laquelle peut être locale, intermédiaire ou régionale. Contrairement à Gascoyne et Kamineni (1994), il met davantage l'accent sur l'écoulement, incluant des zones de recharge et des zones de décharge pour expliquer l'évolution de l'eau souterraine. Pour Tòth (1999), l'interaction et l'écoulement se produisent en même temps à toutes les échelles de temps et d'espace, mais à des taux et à des intensités variables selon les échelles (Figure 1.3). Il

identifie trois types d'interaction entre les eaux souterraines et l'environnement : les interactions chimiques, physiques et cinétiques.

Tòth (1999) considère aussi la présence de vestiges d'eau de salinité différente et généralement plus élevée, comme l'eau de mer, dans des unités géologiques de plus faible perméabilité. Ces eaux « fossiles » constituent une source à long terme pour certaines substances en solution. Dans les modèles de Tòth (1999) et de Gascoyne et Kamineni (1994), la possibilité que certaines composantes puissent venir de la base de la croûte ou même du manteau n'est pas considérée. Cette hypothèse est notamment évoquée pour des sources minérales de l'Europe centrale (Babuska et Plomerova, 2003).

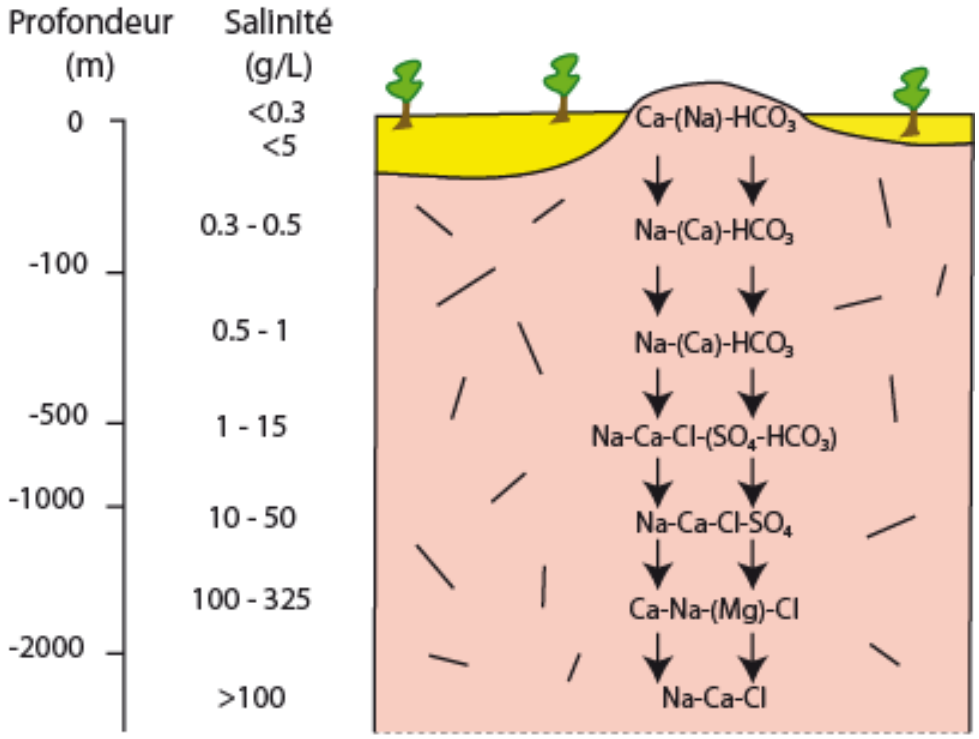

Figure 1.2: Évolution géochimique des fluides dans les roches cristallines en fonction de la profondeur (modifié de Gascoyne et Kamineni, 1994).

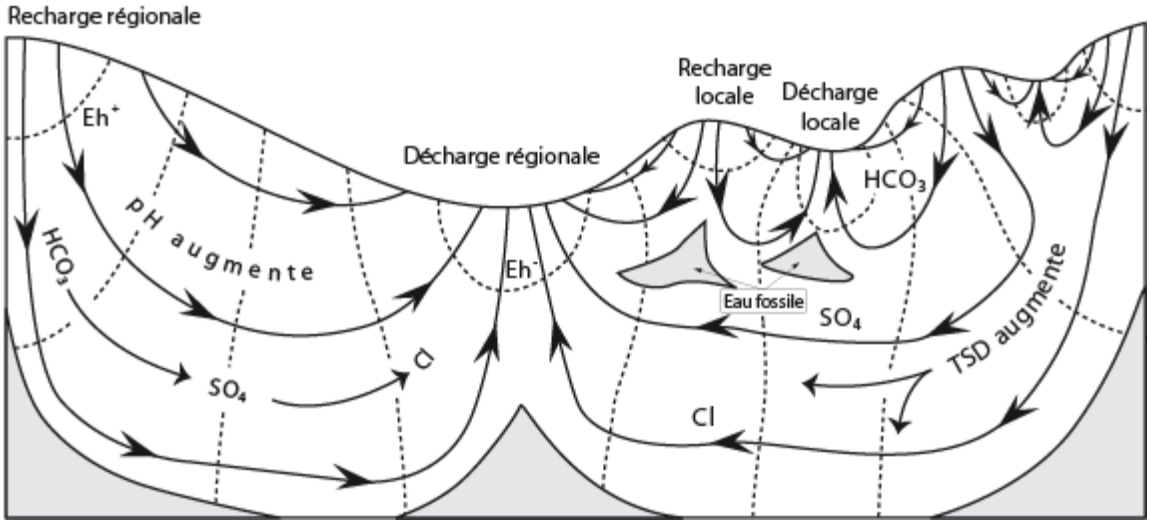

Figure 1.3: Cellules d'écoulement et influence d'une topographie irrégulière sur la taille de ces cellules (locales, intermédiaires et régionales) (modifiée de Tóth, 1999).

1.2 PROBLÉMATIQUE SPÉCIFIQUE

1.2.1 CONTEXTE HYDROGÉOLOGIQUE RÉGIONAL ET VARIABILITÉ CHIMIQUE DE L'EAU SOUTERRAINE AU SAGUENAY-LAC-SAINT-JEAN

Le roc qui occupe le territoire du SLSJ est très majoritairement précambrien et les principales lithologies correspondent à plusieurs phases d'injections magmatiques mésoprotérozoïques (entre 1 500 et 1 000 Ma) de masses anorthositiques, de plutons de composition felsique à intermédiaire et d'un complexe gneissique formé d'orthogneiss et de paragneiss (Hébert et Lacoste, 1998). Ces roches appartiennent à la Province de Grenville (Rivers et al., 1989). Au Cambrien (600 Ma), le socle grenvillien a été découpé le long du fleuve Saint-Laurent lors de la formation d'un rift produit par l'ouverture de

l'océan Iapétus (Kumarapeli, 1985). Dans la région du SLSJ, le complexe alcalin de Saint-Honoré composé de carbonatites et de syénites correspond à un centre volcanique en activité à cette époque. Ce dernier est actuellement exploité pour ses ressources en niobium par la seule mine de la région. Un autre complexe alcalin dans le canton de Crevier, au nord-ouest du lac Saint-Jean, pourrait dater de la même période. Superposés au socle grenvillien, on trouve quelques lambeaux de roche sédimentaire d'âge paléozoïque composés de calcaires et de shale argileux datés à l'Ordovicien moyen (~450 Ma), vestiges d'une mer chaude tropicale, l'océan ordovicien (Desbiens et Lespérance, 1989). La topographie de la région est contrôlée par une succession de divers événements géologiques dont le principal élément est le Graben du Saguenay orienté ONO-ESE (Roy et al., 1993). Les failles majeures bordant le graben divisent les hautes-terres des basses-terres se sont formées lors du démembrement du supercontinent Rodinia au début du Cambrien (~ 450 Ma). Certaines ont été réactivées lors de l'ouverture de l'océan Atlantique actuel et la formation de la vallée du Saint-Laurent (~180 Ma). Plusieurs familles de structures cassantes sont ainsi présente, ce qui confère par endroit un assez bon potentiel aquifère au roc (CERM-PACES, 2013). Pour Walter (2010), la topographie en graben de la région est susceptible de concentrer des zones de décharge d'eaux souterraines profondes (i.e. cellule d'écoulement régional). La géologie se caractérise aussi par la présence d'importants dépôts granulaires d'origine fluvioglaciaire et fluviatile d'âge Quaternaire, constituant les principaux aquifères en exploitation de la région (CERM-PACES, 2013). On y trouve aussi d'importants sédiments d'eau profonde de la mer

de Laflamme (-10 000 ans) ayant submergé les terres suite au retrait de l'inlandsis. Ces sédiments fins sont constitués de silt argileux ou d'argile silteuse grise identifiés à de la farine de roche (Bouchard et al., 1983) et jouent le rôle d'aquitards.

Au cours des dernières années, de nombreux cas de qualité incertaine de l'eau souterraine ont été identifiés au SLSJ (Dessureault, 1975; Simard et Desrosiers, 1979, Walter, 2010; Walter et al. 2011), mais c'est dans le cadre du Programme d'acquisition de connaissances sur les eaux souterraines du Québec (PACES), administré par le Ministère du développement durable, de l'environnement, de la faune et des parcs (MDDEFP), que le portrait hydrogéochimique régional le plus complet a été réalisé entre 2009 et 2013. Ce projet majeur couvrait le territoire municipalisé du SLSJ, soit une superficie de 13 210 km^2 et a permis de réaliser une synthèse des connaissances concernant les aspects quantitatif et qualitatif des eaux souterraines de la région, et de mieux comprendre les particularités hydrogéologiques de cette région (Rouleau et al., 2011; CERM-PACES, 2013). Le PACES constitue ainsi un tremplin évident pour la réalisation d'études plus approfondies pour la compréhension du fonctionnement du « système eaux souterraines » à partir des données existantes et nouvellement acquises dans la région du SLSJ (Chapitre 2.).

Les travaux de terrain effectués en 2010 et 2011 ont permis de collecter 354 échantillons d'eau souterraine à partir de puits distribués sur le territoire municipalisé du SLSJ (figure 1.4). L'étude du CERM-PACES (2013) a montré que l'eau souterraine de la région du SLSJ est majoritairement du type bicarbonaté (HCO_3^-), soit sodique (Na^+) ou

calcique (Ca^{2+}) et correspond généralement à une eau douce de très bonne qualité, malgré un pH légèrement acide dans les milieux aquifères granulaires et légèrement basique dans les milieux aquifères rocheux fracturés. Les travaux hydrogéochimiques réalisés montrent aussi que l'eau souterraine de la région contient des quantités appréciables de fer et de manganèse, et que ces paramètres sont souvent associés entre eux. Cette étude a aussi mis en évidence l'étroite corrélation entre les milieux aquifères de roc fracturé et les concentrations importantes de fluorures dans l'eau souterraine de la région. De plus, plusieurs dépassements des normes du *Règlement sur la qualité de l'eau potable* (MDDEP, 2014; tableau 1.3 et des *recommandations pour la qualité de l'eau potable* de Santé Canada (CFPTEP, 2014; tableau 1.4) ont été identifiés. Les eaux souterraines à salinité élevée présentent un nombre important de dépassements significatifs, notamment en sodium, et en dureté (calcium et magnésium). Ces occurrences demeurent *a priori* marginales et semblent concentrées autour du lac Saint-Jean, sans que ne ressorte clairement le type de milieu aquifère qui les contient, ni les mécanismes à leur origine (CERM-PACES, 2013).

Un examen préliminaire des données a permis des observations sommaires dont certaines ont été formulées par Walter et al. (2011). La comparaison des moyennes arithmétiques et des maxima obtenus pour les paramètres chimiques de groupes d'eau souterraine montre des différences significatives dans leur contenu en ions dissous. Par exemple, pour les aquifères de roc fracturé, une tendance à l'enrichissement est observée pour le lithium, l'argent, le baryum, les bromures, le strontium et l'uranium. Dans cette

étude préliminaire, Walter et al. (2011) ne parviennent pas à expliquer les différences entre les groupes d'eaux souterraines. Pour aller plus loin, ils recommandent de mener une analyse hydrogéochimique plus poussée incluant une analyse statistique multi-variable de l'ensemble des analyses toutes teneurs confondues (Chapitre 3.).

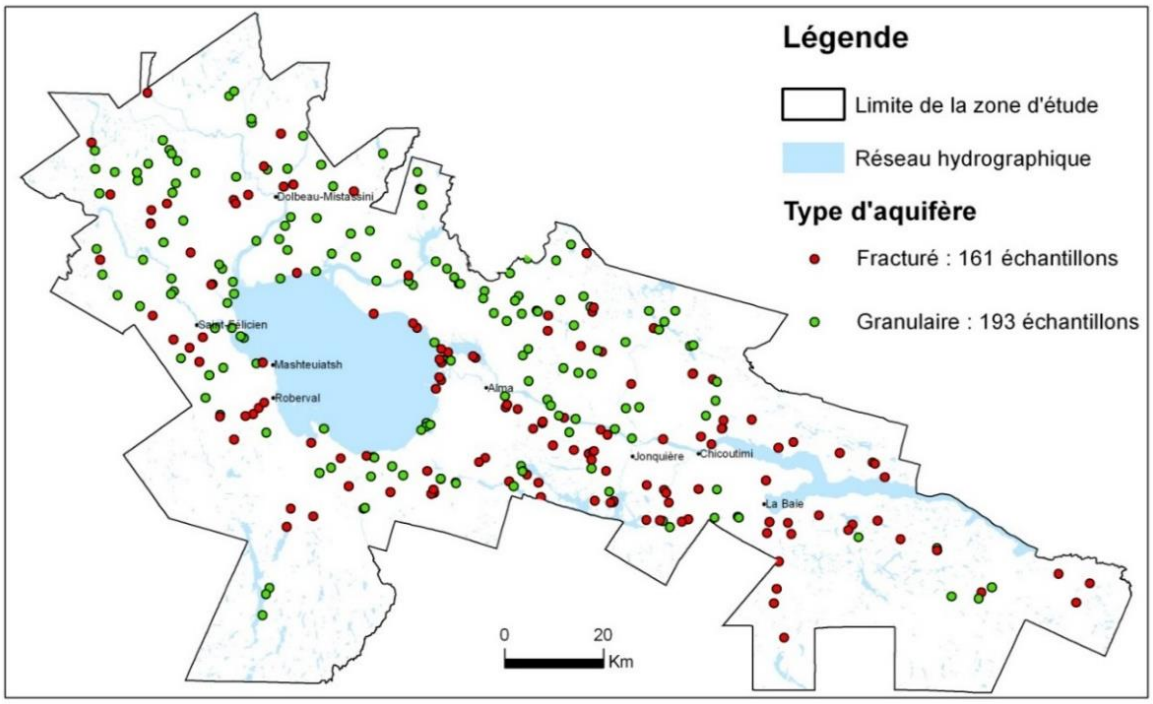

Figure 1.4: Répartition des échantillons d'eau souterraine en fonction du type de milieu aquifère échantillonné (CERM-PACES, 2013).

Dans le cadre d'une étude axée sur les eaux souterraines à salinité élevée autour du lac Saint-Jean, Walter (2010) propose trois mécanismes distincts pour expliquer la signature géochimique particulière de ces eaux souterraines: 1) le lessivage des sédiments marins de la mer de Laflamme, 2) l'évolution naturelle dans le temps et dans l'espace de l'eau souterraine en contact avec les roches cristallines de la région, et 3) l'évolution

naturelle dans le temps et dans l'espace de l'eau souterraine en contact avec les sédiments paléozoïques de la région (calcaires et shales ordoviciens).

Tableau 1.3: Dépassements des objectifs esthétiques (OE) des échantillons collectés dans le cadre du PACES-SLSJ (Recommandations sur la qualité de l'eau potable au Canada; tiré de CERM-PACES, 2013).

Paramètre	Nb	N détection	LD*	Min.	25%	Médiane	75%	Max.	OE	N dépassements
Cl (mg/L)	316	312	0,05	0,14	1,9	8,7	36,25	4200	250	23
Dureté (mg/L)	316	279	-	0,39	36,6	88,4	162,7	3757	200	51
MDT (mg/L)	316	316	-	15	136	248	396	7240	500	40
Na (mg/L)	316	315	0,1	0,89	3,3	11	45,5	1800	200	20
pH	316	316	-	4,38	6,48	7,57	8,1	10,1	6,5 - 8,5	110
Sulfures (mg/L)	15	15	0,02	0,02	0,05	0,16	0,55	16	0,05	11
Temp (°C)	316	316	-	1,68	6,9	7,49	8,64	17,5	15	5
Al (mg/L)	316	285	0,001	0,001	0,004	0,007	0,016	0,23	0,1	6
Fe (mg/L)	316	142	0,1	0,03	0,062	0,13	0,375	18	0,3	44
Mn (mg/L)	316	277	0,0004	0,0004	0,003	0,014	0,05	2,4	0,05	73
* LD : limite de détection										

Tableau 1.4: Dépassements des maximum acceptables (CMA) des échantillons collectés dans le cadre du PACES-SLSJ (Règlement québécois sur la qualité de l'eau potable; tiré de CERM-PACES, 2013).

Paramètre	N	N détection	L.D	Min.	25%	Médiane	75%	Max.	CMA	N dépassements
Ba (mg/L)	316	298	0,002	0,002	0,016	0,039	0,090	1,2	1,00	1
F (mg/L)	316	222	0,1	0,1	0,2	0,600	1,5	4,9	1,50	52

Roy et al. (2011) suggèrent trois types d'eau d'infiltration à l'origine de l'eau souterraine dans la région : l'eau météoritique, l'eau marine (datant de la mer de Laflamme et de l'océan ordovicien) et l'eau sous-glaciaire. À partir de leur zone de recharge, ces eaux d'infiltration sont amenées à évoluer dans le temps et dans l'espace, et à imprimer en leur sein la signature géochimique des milieux géologiques qui les

contiennent. Les groupes d'eau identifiés dans le cadre du PACES-SLSJ et des études antérieures tirent peut-être leurs caractéristiques du mélange de ces eaux d'infiltration à des stades différents de leur évolution respective.

Les travaux de recherche présentés précédemment mettent en évidence la nécessité d'un travail scientifique de fond portant sur le fonctionnement hydrogéochimique régional, considérant la complexité des paramètres chimiques des eaux souterraines, de leur distribution et de leurs interactions entre elles et avec le milieu qui les contient. Ainsi, le projet proposé s'intéresse à la compréhension des mécanismes d'acquisition et d'évolution temporelle de la signature géochimique des eaux souterraines du SLSJ, à la détermination de pôles compositionnels hydrogéochimiques régionaux et à leur empreinte géochimique héritée des mécanismes d'interaction eau-roche[1]. Les conclusions permettent d'expliquer la présence de certains paramètres chimiques ainsi que la variabilité spatiale de la qualité de l'eau souterraine et pourraient ultimement permettre de prédire son évolution future, si des études subséquentes étaient menées.

1.2.2 HYPOTHÈSES DE RECHERCHE

Pour donner naissance aux eaux souterraines présentes sur le territoire du SLSJ, les eaux d'infiltration ont évolué dans le temps (augmentation du temps de résidence accompagnée d'une augmentation de la salinité) et dans l'espace (variabilité des

[1] Le terme *interaction eau-roche* désigne l'interaction entre l'eau et tout matériel solide en contact, qu'il soit de type granulaire, cohésif ou rocheux.

propriétés chimiques et hydrauliques des milieux réservoirs). Ainsi, 5 hypothèses de recherche appuient cette thèse.

1. La composition géochimique de l'eau au moment de l'infiltration et au stade d'évolution le plus avancé constitue des pôles compositionnels hydrogéochimiques régionaux. Toute l'eau souterraine de la région tire son origine de l'un des 3 types d'eau d'infiltration suivants (i.e. pôle compositionnel initial) :
    - Eau météoritique
    - Eau marine
    - Eau sous-glaciaire (non abordé dans cette thèse)

et éventuellement d'un quatrième type d'eau correspondant à un pôle «eau de formations» pré-glaciation présent en profondeur et de nature saumurée.

2. L'eau infiltrée évolue au contact avec les réservoirs régionaux qui sont distingués sur la base des unités lithologiques régionales et de leur composition chimique globale. Trois groupes sont définis et le nombre total de réservoirs qui peut être considéré est de 7 :
    - Groupe des roches cristallines :
        - Granite (1)
        - Anorthosite (2)
        - Carbonatite de Saint-Honoré (3)
    - Groupe des roches calcaires :
        - Calcaires de Trenton (4)

- Shale de Pointe Bleue (5)

- Groupe des sédiments meubles :
  - Argiles silteuses de la mer de Laflamme (6)
  - Sédiments granulaires (sables et graviers) (7)

Dans cette thèse, par manque de données quantitatives (analyses chimiques de la matrice solide des réservoirs présumés), les réservoirs sont regroupés en 2 grands groupes : a) le roc fracturé (roches ignées, métamorphiques et sédimentaires) et b) les dépôts granulaires d'âge quaternaire (sédiments meubles);

3. Chaque groupe de réservoirs présente une composition chimique (éléments majeurs, traces et isotopiques) qui lui est propre et qui est susceptible d'être léguée à l'eau qu'il contient (i.e. traceurs géochimiques intrinsèques);

4. Plus le temps de transit augmente, plus le contenu en ions dissous augmente (modèle de Tóth, 1999) et plus le groupe considéré imprime sa signature géochimique à l'eau souterraine et tend vers une composition de pôles hydrogéochimiques régionaux. L'eau de pluie à l'origine de l'infiltration correspond aussi à un pôle compositionnel régional;

5. La signature géochimique des eaux souterraines prélevées à partir de la surface dans des puits ouverts (cas des échantillons du PACES-SLSJ) peut reflèter le mélange de

plusieurs pôles hydrogéochimiques régionaux qu'il faudrait pouvoir préciser afin d'en déterminer l'importance relative;

1.3 OBJECTIFS

Le premier objectif de ce projet vise à conceptualiser stratigraphiquement les principaux réservoirs d'eau souterraine présents sur le territoire d'étude. (Abordé au chapitre 2);

Le second objectif de ce projet consiste à appliquer des méthodes statistiques multivariées sur une base de données hydrogéochimiques pour définir des pôles hydrogéochimiques régionaux de l'interaction eau-roche. (Abordé aux chapitres 3 et 4);

Le troisième objectif consiste à établir et comparer les pôles hydrogéochimiques régionaux identifiés avec des eaux de références dont l'origine est connue. (Abordé au chapitre 4);

Le quatrième objectif vise à décrire l'enrichissement ou l'appauvrissement de l'eau souterraine en certaines espèces chimiques dissoutes, notamment en éléments indésirables tels que les fluorures, le fer et le manganèse, au cours de l'évolution chimique naturelle de l'eau souterraine vers l'un ou l'autre des pôles identifiés. (Abordé au chapitre 4);

Le cinquième objectif vise à proposer des ions ou des groupements d'ions dissous caractéristiques de l'évolution naturelle de l'eau souterraine vers l'un ou l'autre des pôles hydrogéochimiques régionaux identifiés. (Abordé aux chapitres 3 et 4)

1.4 METHODOLOGIE

1.4.1 BASE DE DONNÉES HYDROGÉOCHIMIQUES EXISTANTES ET STATISTIQUES UNIVARIÉES

Dans le cadre du PACES-SLSJ, les résultats de l'analyse chimique d'environ 40 paramètres de chimie inorganique (Tableau 1.5) réalisée sur 321 échantillons fournissent une première série de teneurs de fonds géochimiques de l'eau souterraine dans différents types d'aquifères présents dans la région du SLSJ (CERM-PACES, 2013).

En première approche, les statistiques descriptives nous permettent de bien faire ressortir les principales différences qui existent entre les groupes d'échantillons construits à partir de la combinaison entre le type d'eau et le type de milieu aquifère. Cette étude statistique inclut la comparaison du nombre de détection enregistré pour chaque paramètre chimique, des valeurs médianes, moyennes, maximales, minimales, du 1er et 3^{e} quartiles. L'étude des statistiques descriptives conduit à la réduction du jeu de données initial. La réduction du nombre d'échantillons est réalisée dans le but de permettre une utilisation optimale de techniques statistiques plus poussées et de tenir compte dans nos investigations des éléments traces indésirables identifiés dans l'eau souterraine du territoire d'étude (fluor, fer et manganèse).

Tableau 1.5: Liste des paramètres analysés lors des campagnes d'échantillonnage des eaux souterraines collectées dans le cadre du PACES-SLSJ et leur technique d'analyse

Analyse par ICP-MS		Analyses spécifiques	
Aluminium (Al)	Bore (B)	Alcalinité totale (en $CaCO_3$) à pH 4.5	1
Antimoine (Sb)	Fer (Fe)	Azote ammoniacal (N-NH3)	2
Argent (Ag)	Magnésium (Mg)	Bromure (Br-)	3
Arsenic (As)	Lithium (Li)	Chlorures (Cl)	3
Baryum (Ba)	Potassium (K)	Fluorure (F)	2
Cadmium (Cd)	Sélénium (Se)	Nitrate (N) et Nitrite (N)	3
Chrome (Cr)	Strontium (Sr)	Phosphore inorganique	2
Cobalt (Co)	Etain (Sn)	Sulfates (SO4)	3
Cuivre (Cu)	Titane (Ti)	Sulfures (S)	3
Manganèse (Mn)	Vanadium (V)	1-Titration 2-Sonde spécifique 3- Chromatographie ionique	
Molybdène (Mo)	Béryllium (Be)		
Nickel (Ni)	Bismuth (Bi)		
Sodium (Na)	Calcium (Ca)		
Zinc (Zn)	Silicium (Si) (soluble dans HNO_3)		
Plomb (Pb)	Uranium (U)		

1.4.2 ANALYSES STATISTIQUES MULTI-VARIÉES ET PÔLES COMPOSITIONNELS RÉGIONAUX

Les concentrations en éléments dans les eaux souterraines n'évoluent pas de façon indépendante les unes des autres. L'équilibre électrique devant être respecté, toute augmentation de la concentration d'un cation dans l'eau sera balancée par celle d'un anion, et vice-versa. L'existence de ces corrélations justifie certaines méthodes de traitements statistiques fondées sur le calcul de corrélations (Blum et al, 2003). Des techniques dites multi-variables, sont disponibles et sont fréquemment employées dans les études hydrogéochimiques (Coutier et al., 2008; Hitchon et al., 1971; Davis, 1986; Güler et Thyne, 2004). Les plus usuelles sont l'analyse en grappe (HCA), l'analyse en composante principale (ACP), l'analyse factorielle (AF), ou la combinaison de certaines de ces méthodes (Cloutier et al., 2008; Belkhiri et al., 2010; Montcoudiol et al., 2014). L'HCA est basée sur les similarités entre les échantillons (Ji et al., 1995; Cloutier et al., 2008;

Templ et al., 2008). L'ACP est basée sur la variance chimique d'un jeu de données permettant d'évaluer les inter-relations entre les variables et entre les échantillons (Razack et Dazy, 1990; Mencio et al., 2012), et de déduire des composantes principales ou des facteurs principaux influençant un jeu de données. L'AF permet de définir de nouvelles variables (appelés *facteurs*) qui rendent compte de la co-variance d'un jeu de données (Brown, 1998).

À partir des résultats d'analyses chimiques des 40 paramètres physico-chimiques des 321 échantillons considérés, l'analyse multi-variée appliquée sur le jeu de données nous permet de définir des groupes d'eau souterraine contenant des échantillons avec une affinité chimique intra-groupe considérés des pôles compositionnels régionaux de l'interaction eau-roche.

1.4.3 REPRÉSENTATIONS GRAPHIQUES

Ces groupes d'eau ainsi définis sont comparés entre eux à l'aide de divers types de graphiques mettant en jeu différents ions. L'origine d'un ion peut être testée à l'aide de diagrammes binaires lorsque les équations régissant la mise en solution de cet ion sont connues. En effet, les ions impliqués dans ces processus sont liés par la stœchiométrie des réactions chimiques. C'est le cas par exemple du calcium et du strontium qui peuvent être utilisés pour identifier l'altération des plagioclases (Beaucaire et Michard, 1982; Stober et Bucher, 1999) ou de la calcite (Clow et al., 1997; Blum et al, 1998). Par ailleurs, le potassium et le magnésium (Gascoyne et Kamineni, 1994), ou le bore et le lithium

(Edmunds et al., 1984) peuvent traduire l'altération de certains micas. Finalement, les mélanges d'eau de mer sont fréquemment identifiés dans l'eau souterraine à partir des graphiques binaires faisant intervenir le contenu de l'eau en ions chlorures (Frape et al., 1984; Cloutier et al., 2008; Ghesquière et al., 2015). Sinon, les diagrammes binaires sont aussi utilisés pour distinguer différents groupes d'échantillons sur la base de leur proportion relative en certains ions, comme par exemple le calcium et le sodium, deux cations majeurs retrouvés dans l'eau souterraine. Certains graphiques combinent même l'ensemble des ions majeurs pour permettre la détermination du faciès hydrogéochimique des échantillons (Diagrammes de Schoeller, Piper et Durov). Dans cette étude, le diagramme de Piper (1944) nous permet de suggérer certains mécanismes physico-chimiques de l'évolution de l'eau souterraine.

1.4.4 MÉTHODE NORMATIVE ET MODÈLE D'ÉVOLUTION

Les pôles compositionnels régionaux de l'évolution chimique naturelle de l'eau souterraine sont comparés à des eaux de références inédites ou compilées à partir de la littérature. Dans cette thèse, nous présentons une compilation de données hydrogéochimiques extraites de la littérature scientifique portant sur les saumures continentales en milieu de roches cristallines précambriennes (Bouclier canadien). Nous présentons aussi une signature moyenne de l'eau de pluie calculée à partir de quatre échantillons prélevés dans le cadre de ce projet doctoral et d'une compilation d'une partie de la littérature existante sur le sujet. Pour décrire l'évolution chimique temporelle de

l'eau souterraine, nous proposons la détermination d'un indice de maturation obtenu à partir d'une méthode de normalisation faisant intervenir les pôles compositionnels régionaux et une eau de référence. Cette méthode s'inspire de la technique de normalisation au manteau primitif des *Mid Oceanic Ridge Basalt* (MORB) ou d'autres techniques de normalisation communément employés en géochimie (Rock, 1987).

1.5 FORMAT DE LA THÈSE

La présente thèse de doctorat en Sciences de la Terre et de l'atmosphère est présentée sous la forme d'un recueil de trois manuscrits d'articles scientifiques dont le premier auteur est l'auteur de cette thèse. Les articles sont rédigés en anglais et au moment de la rédaction de cette thèse sont soumis et/ou publiés dans des revues spécialisées internationales avec comité d'évaluation par les pairs.

Le premier article est publié dans la revue *Canadian Water Ressources Journal / Revue canadienne des ressources hydriques* depuis avril 2018 et a pour titre : « Characterization of general and singular features of major aquifer systems in the Saguenay-Lac-Saint-Jean region ». Cet article présente les faits saillants de la cartographie hydrogéologique qui a été réalisée au Saguenay-Lac-Saint-Jean, territoire d'étude de ce projet de recherche doctoral, et décrit l'éventail de projets de recherche qui en découlent. Il sert à établir le cadre stratigraphique (objectif 1) requis pour les travaux subséquents. Dans le cadre du projet PACES, j'ai agi comme chargé principal de projet. À ce titre, j'ai supervisé tous les volets du projet, j'ai participé, souvent directement, à l'encadrement du

personnel et j'ai été impliqué dans les discussions sur la collecte, le traitement des données et leur présentation finale.

Le second article a été publié dans la revue *Journal of Hydrology: Regional Studies* en septembre 2017 et a pour titre : « The influence of water/rock – water/clay interactions and mixing in the salinization processes of groundwater ». Cet article porte spécifiquement sur l'identification de pôles géochimiques de l'évolution naturelle de l'eau souterraine, en combinant les résultats d'une analyse statistique multivariée réalisée sur les échantillons d'eau souterraine et l'interprétation de divers types de représentations graphiques. Il répond donc principalement à l'objectif 2 de la thèse.

Le troisième article a été soumis au journal *Geofluids* le 30 décembre 2017, et a pour titre: « Chemical element pathfinders for the natural evolution of groundwater toward brackish end-members in Precambrian bedrock Aquifers and Pleistocene Granular aquifers ». Ce troisième article présente un modèle conceptuel de l'évolution naturelle de l'eau souterraine vers les deux principaux pôles hydrogéochimiques de cette étude, ce qui nous conduit aussi à proposer des traceurs géochimiques hérités de l'interaction eau-roche à l'origine de cette évolution. Il aborde donc les autres objectifs de la thèse.

Cette thèse contient six chapitres : une introduction (Chapitre 1) qui présente les aspects de la problématique, les objectifs et la méthode du projet doctoral; les 3 articles scientifiques constituant chacun un chapitre, et qui ont été soumis ou publiés dans des

revues internationales spécialisées avec comité d'évaluation par les pairs (Chapitre 2 à 4); une discussion (Chapitre 5) et une conclusion (Chapitre 6).

1.6 RÉFÉRENCES

Adiaffi, B., Marlin, C., Oga, Y. M. S., Pichon, R., and Biemi, J.; 2012. *Approche semi-quantitative de la minéralisation des aquifères schisteux en zone Équatoriale de transition: Cas de la région Sikensi-Agboville (Côte d'Ivoire)*: International Journal of Biological and Chemical Sciences, v. 6, no. 5, p. 2228-2240.

Babuska, V., and Plomerova, J.; 2003. *Seismic experiment searches for active magmatic source in deep lithosphere, central Europe*: Eos, Transactions American Geophysical Union, v. 84, no. 40, p. 409.

Beaucaire, C., and Michard, G.; 1982. *Origin of dissolved minor elements (Li, Rb, Sr, Ba) in superificial waters in a granitic area*: Geochemical Journal, v. 16, no. 5, p. 247-258.

Belkhiri, L., Boudoukha, A., Mouni, L., and Baouz, T.; 2010. *Application of multivariate statistical methods and inverse geochemical modeling for characterization of groundwaters - A case study: Ain Azel plain (Algeria)*: Geoderma, v. 159, no. 3, p. 390-398.

Blum, J. D., Gazis, C. A., Jacobson, A. D., and Chamberlain, C. P.; 1998. *Carbonate versus silicate weathering in the Raikhot watershed within the High Himalayan Crystalline Series*: Geology, v. 26, no. 5, p. 411-414.

Bouchard, R., Dion, D. J., and Tavenas, F.; 1983. *Origine de la préconsolidation des argiles du Saguenay, Québec*: Canadian Geotechnical Journal, v. 20, no. 2, p. 315-328.

Brown, C. E., 1998. *Applied multivariate statistics in geohydrology and related sciences*, Springer Berlin.

Casanova, J., Négrel, P., Petelet-giraud, E., Brach, M., Bourguignon, A., and Millot, R.; 2004. *Projet PALÉOHYD II Paléohydrologie et géoprospective: modèles conceptuels et processus d'acquisition de la chimie des eaux dans les massifs granitiques*: BRGM, Rapport BRGM/RP-53469-FR. 124 p. 98 ill.

CERM-PACES; 2013. *Résultats du programme d'acquisition de connaissances sur les eaux souterraines du Saguenay-Lac-Saint-Jean*: Centre d'études sur les ressources minérales, Université du Québec à Chicoutimi. p.248; 3 annexes; 29 cartes.

Chebotarev; 1955. *Metamorphism of natural waters in the crust of weathering 1-2-3*: Geochimica et Cosmochimica Acta, v. 8, no. 1, p. 22-48.

Cloutier, V., Lefebvre, R., Therrien, R., and Savard, M. M.; 2008. *Multivariate statistical analysis of geochemical data as indicative of the hydrogeochemical evolution of groundwater in a sedimentary rock aquifer system*: Journal of Hydrology, v. 353, no. 3, p. 294-313.

Clow, D. W., Mast, M. A., Bullen, T. D., and Turk, J. T.; 1997. *Strontium 87/strontium 86 as a tracer of mineral weathering reactions and calcium sources in an alpine/subalpine watershed, Loch Vale, Colorado*: Water Resources Research, v. 33, no. 6, p. 1335-1351.

Davis, J.; 1986. *Statistics and data analysis in geology*: John Wiley & Sons, New York.

Derron; 2004. *Géochimie des eaux de sources et interaction eau-roche dans les Alpes*, *in* Quanterra short course, Lausanne, p. 18.

Desbiens, S., and Lespérance, P. J.; 1989. *Stratigraphy of the Ordovician of the Lac Saint-Jean and Chicoutimi outliers, Quebec*: Canadian Journal of Earth Sciences, v. 26, no. 6, p. 1185-1202.

Dessureault, R.; 1975. *Hydrogéologie du Lac Saint-Jean, partie nord-est*, Québec: Ministère des richesses naturelles, Direction générale des eaux, Service des eaux souterraines.

Edmunds, W. M., Andrews, J. N., Burgess, W. G., Kay, R. L. F., and Lee, D. J.; 1984. *The evolution of saline and thermal groundwaters in the Carnmenellis granite*: Mineralogical Magazine, v. 48, no. 348, p. 407-424.

Frape, S. K., Fritz, P., and McNutt, R. H. t.; 1984. *Water-rock interaction and chemistry of groundwaters from the Canadian Shield*: Geochimica et Cosmochimica Acta, v. 48, no. 8, p. 1617-1627.

Fritz, P.; 1997. *Saline groundwater and brines in crystalline rocks: the contributions of John Andrews and Jean-Charles Fontes to the solution of a hydrogeological and geochemical problem*: Applied geochemistry, v. 12, no. 6, p. 851-856.

Fritz, P., and Frape, S. K.; 1987. *Saline water and gases in crystalline rocks*, Geological Assn of Canada.

Gascoyne, M., and Kamineni, D. C., 1994. *The hydrogeochemistry of fractured plutonic rocks in the Canadian Shield*: Applied Hydrogeology, v. 2, no. 2, p. 43-49.

Ghesquière, O., Walter, J., Chesnaux, R., Rouleau, A., 2015. Scenarios of groundwater chemical evolution in a region of the Canadian Shield based on multivariate statistical analysis. J. Hydrol.: Regional Studies 4: 246-266.

Güler, C., and Thyne, G. D.; 2004. *Hydrologic and geologic factors controlling surface and groundwater chemistry in Indian Wells-Owens Valley area, southeastern California, USA*: Journal of Hydrology, v. 285, no. 1, p. 177-198.

Hébert, C., and Lacoste, P.; 1998. *Géologie de la région de Jonquière-Chicoutimi (SNRC 22D)*: [Québec]: Hitchon, B., Billings, G. K., and Klovan, J. E.; 1971. *Geochemistry and origin of formation waters in the western Canada sedimentary basine - III. Factors controlling chemical composition*: Geochimica et Cosmochimica Acta, v. 35, no. 6, p. 567-598.

Ji, H., Zhu, Y., and Wu, X.; 1995. *Correspondence cluster analysis and its application in exploration geochemistry*: Journal of geochemical Exploration, v. 55, no. 1, p. 137-144.

Kumarapeli, P. S.; 1985. *Vestiges of lapetan rifting in the craton west of the northern Appalachians*: Geoscience Canada, v. 12, no. 2.

Laaksoharju, M., Smellie, J., Nilsson, A.-C., and Skarman, C.; 1995. *Groundwater sampling and chemical characterisation of the Laxemar deep borehole KLX02*: Swedish Nuclear Fuel and Waste Management Company.

Lodemann, M., Fritz, P., Wolf, M., Ivanovich, M., Hansen, B. T., and Nolte, E.; 1997. *On the origin of saline fluids in the KTB (continental deep drilling project of Germany)*: Applied geochemistry, v. 12, no. 6, p. 831-849.

MDDEFP, Règlement sur la qualité de l'eau potable c. Q-2, r.40 :

http://www2.publicationsduquebec.gouv.qc.ca/dynamicSearch/telecharge.php?type=2&file=//Q_2/Q2R40.htm , Consulté le 15 janvier 2014.

Mencio, A., Folch, A., and Mas-Pla, J.; 2012. *Identifying key parameters to differentiate groundwater flow systems using multifactorial analysis*: Journal of Hydrology, v. 472-473, p. 301 -313.

Montcoudiol, N., Molson, J., Lemieux, J.-M., 2014. Groundwater geochemistry of the Outaouais Region (Québec, Canada): a regional-scale study. Hydrogeology Journal, 23(2): 377-396.

Rock, N.M.S., 1987. The need for standardization of normalized multi-element diagrams in geochemistry: a comment. Geochemical Journal, 21(2): 75-84.

Piper, A. M.; 1944, *A graphic procedure in the geochemical interpretation of water-analyses*: Transactions, American Geophysical Union, v. 25, p. 914-928.

Comité fédéral provincial territorial sur l'eau potable (CFPTEP), Recommandations pour la qualité de l'eau potable au Canada: tableau sommaire : http://www.hc-sc.gc.ca/ewh-semt/pubs/water-eau/2012-sum_guide-res_recom/index-fra.php , consulté le 15 janvier, 2014.

Razack, M., and Dazy, J.; 1990. *Hydrochemical characterization of groundwater mixing in sedimentary and metamorphic reservoirs with combined use of Piper's principle and factor analysis*: Journal of Hydrology, v. 114, no. 3, p. 371-393.

Rivers, T., Martignole, J., Gower, C. F., and Davidson, A.; 1989. *New tectonic divisions of the Grenville Province, southeast Canadian Shield*: Tectonics, v. 8, no. 1, p. 63-84.

Rouleau, A., Walter, J., Daigneault, R., Chesnaux, R., Roy, D. W., Germaneau, D., Lambert, M., Moisan, A., and Noël, D.; 2011. *Un aperçu de la diversité hydrogéologique du territoire du Saguenay-Lac-Saint-Jean (Québec), in* Proceedings of GeoHydro 2011, Joint Meeting of the Canadian Quaternary Association and the Canadian Chapter of the International Association of Hydrogeologists.

Roy, D. W., Beaudoin, G., Leduc, É., Rouleau, A., Walter, J., Chesnaux, R., and Cousineau, P.; 2011. *Isostasie postglaciaire différentielle au lac-Saint-Jean (Québec) et implications sur la qualité de l'eau souterraine, in* Proceedings of GeoHydro 2011, Joint Meeting of the Canadian Quaternary Association and the Canadian Chapter of the International Association of Hydrogeologists.

Roy, D. W., Schmitt, L., Woussen, G., and DuBerger, R.; 1993. *Lineaments from airborne SAR images and the 1988 Saguenay earthquake, Quebec, Canada*: Photogrammetric engineering and remote sensing, v. 59, p. 1299-1305.

Simard, G., and Des Rosiers, R.; 1979. *Qualité des eaux souterraines du Québec*: Ministere des richesses naturelles, Direction generale des eaux, Service des eaux souterraines, H.G.-13. 161p.

Stober, I., and Bucher, K.; 1999. *Deep groundwater in the crystalline basement of the Black Forest region*: Applied geochemistry, v. 14, no. 2, p. 237-254.

Templ, M., Filzmoser, P., and Reimann, C.; 2008. *Cluster analysis applied to regional geochemical data: Problems and possibilities*: Applied Geochemistry, v. 23, no. 8, p. 2198-2213.

Tòth, J.; 1985. *Role of Regional Gravity Flow in the Chemical and Thermal Evolution of Ground Water*, *in* First Canadian/American Conference on Hydrogeology: Practical Applications of Ground Water Geochemistry June 22-26, 1984, Banff, Alberta. 1985. p 3-39, 45 fig, 8 tab, 68 ref.

Tòth, J.; 1999. *Groundwater as a geologic agent: an overview of the causes, processes, and manifestations*: Hydrogeology Journal, v. 7, no. 1, p. 1-14.

Walter, J.; 2010. *Les eaux souterraines à salinité élevée autour du lac Saint-Jean, Québec : origines et incidences*: M.Sc. Université du Québec à Chicoutimi, ix, 177 f. p.

Walter, J., Rouleau, A., Roy, D. W., and Daigneault, R.; 2011. *Hydrogéochimie des eaux souterraines de la région du Saguenay-Lac-Saint-Jean: résultats préliminaires, in* Proceedings of GeoHydro 2011, Joint Meeting of the Canadian Quaternary Association and the Canadian Chapter of the International Association of Hydrogeologists.

CHAPITRE 2

CHARACTERIZATION OF GENERAL AND SINGULAR FEATURES OF MAJOR AQUIFER SYSTEMS IN THE SAGUENAY-LAC-SAINT-JEAN REGION

Julien Walter, Alain Rouleau, Romain Chesnaux,

Mélanie Lambert, Réal Daigneault

Centre d'études sur les ressources minérales, Université du Québec à Chicoutimi, Chicoutimi, Québec, G7H 2B1

Canadian Water Resources Journal (2018)

2.1 MISE EN CONTEXTE

Dans l'article qui suit, nous répondons à l'objectif 1 de cette thèse en établissant le modèle conceptuel stratigraphique du territoire à l'étude à partir de l'inventaire des résultats de travaux de recherche en lien avec le programme d'acquisition des connaissances hydrogéologiques (PACES). L'état d'avancement des connaissances quant à la qualité naturelle de l'eau souterraine est aussi présenté. De plus, nous discutons des défis importants pour maintenir à jour les résultats des travaux de cartographie à l'échelle régionale à jour et assurer leur utilisation par les acteurs du milieu dans une optique de développement durable. La valorisation de tels travaux par le biais de projet de recherche de la nature de cette thèse répond en partie à ces défis.

2.2 ABSTRACT:

The hydrogeology of the municipalized territory (13,210 km^2) of the Saguenay-Lac-Saint-Jean region (SLSJ) has been studied as part of the groundwater knowledge acquisition program entitled *Programme d'acquisition de connaissances sur les eaux souterraines* (PACES) launched in 2008 by the Government of Quebec, Canada. This study involved the collaboration of numerous contributors (municipal policymakers, government agencies, watershed organizations and universities) to meet the program's multiple and wide-ranging requirements. The key deliverables included a numerical geodatabase, 38 regional-scale maps and a scientific report, all elaborated after four years of data gathering and compilation, fieldwork and information synthesis. In addition,

numerous collateral research projects were undertaken by undergraduate and graduate students. The results of the SLSJ-PACES project provided new insights into regional groundwater resources and led to a generalized conceptual model of regional hydrostratigraphic features and groundwater quality. This paper summarizes the particular aspects of the major aquifers in the SLSJ region as uncovered by PACES, and presents the emerging challenges for updating and improving the region's hydrogeological knowledge and ensuring the sustainable management of regional groundwater resources.

2.3 INTRODUCTION

Over the years, large amounts of data have been collected for many portions of the aquifer systems of the Saguenay-Lac-Saint-Jean (SLSJ) region, located in the central portion of Quebec, north of the St-Lawrence River (Figure 2.1). Discrete elements of hydrogeological data (from well logs, hydrogeological studies, etc.) acquired in the past and stored by various public and private organizations can remain largely underused and even lost unless they are collated and formatted into a database, making them accessible for hydrogeologists as well as water and land-use managers. Effective management of groundwater resources is hindered when limited access to usable data contributes to a poor understanding of existing hydrogeological features, related knowledge remains fragmented and available information is inadequate. Aware of these limitations, Ogunba (2012) recommended that water suppliers should consistently carry out comprehensive and sustained studies of groundwater.

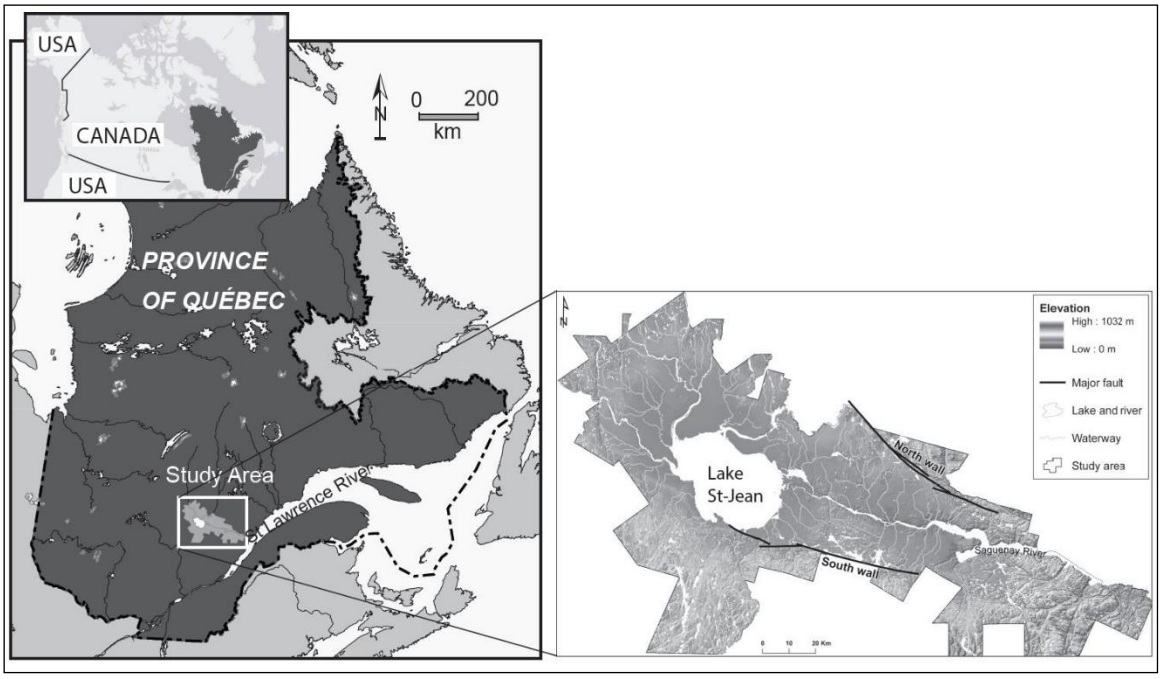

Figure 2.1 : Location of the Saguenay-Lac-Saint-Jean region and its principal physiographic features. The delineation of the study area is based on municipal boundaries.

Developing a groundwater database was the main objective of a project conducted from 2009 to 2013 across the municipalized territory (13,210 km^2) of the Saguenay-Lac-Saint-Jean region (SLSJ). Part of the *Programme d'acquisition de connaissances sur les eaux souterraines* (PACES) launched in 2008 by the Government of Quebec, Canada, the project was carried out by the *Centre d'études sur les ressources minérales* (CERM) of the *Université du Québec à Chicoutimi* (UQAC). Preliminary results of the PACES-SLSJ project were reported by Rouleau et al. (2011) and the overall results were described in CERM-PACES (2013).

The PACES-SLSJ project produced many collateral research projects related to aquifer characterization, groundwater quality and protection at the local and regional scale. In the SLSJ area, the wide diversity of geological units having specific hydrogeological properties is reflected by an equally diverse range of aquifer systems with contrasting characteristics. This paper presents a summary of the main results of the PACES-SLSJ project and the related research projects. Topics dealing with groundwater resources and groundwater management that require further research and application are also identified. This paper summarizes the singular aspects of the hydrogeological features of the SLSJ region, and provides an overview of the comprehensive database in a geographic information system (GIS) and a conceptual regional-scale hydrogeological model. The presented results are derived from both the bedrock units and the surficial deposits, which cover much of the lowland area of the region. Interconnections between aquifers and a synthesis of the groundwater quality in the region are also highlighted. The discussion focuses on recommendations that have emerged from the PACES-SLSJ project that aim to enhance regional hydrogeological knowledge and to improve the sustainable management of groundwater resources. As with other PACES projects (MDDELCC 2017b), the comprehensive database and all deliverables of the PACES-SLSJ project have been transferred to the Quebec Ministry of Sustainable Development, Environment and the Fight against Climate Change (*Ministère du Développement durable, de l'Environnement et de la Lutte contre les changements climatiques* - MDDELCC) and to regional partners.

2.4 METHODOLOGY

The PACES-SLSJ project included three phases: (1) collection and digitization of existing data, (2) field work and data acquisition, and (3) synthesis of the results in the form of a numerical geodatabase, 38 regional-scale maps and a final scientific report. The project lasted four years (2009–2013).

The initial phase led to the compilation and digitization of existing data from 1200 borehole logs, 261 hydrochemical analyses, 548 grading curves, 63 piezometric maps, 11 geophysical surveys, 39 direct-push stratigraphic soundings, 74 permeability tests, 171 pumping tests and 50 stratigraphic cross-sections.

Numerous approaches were used for the project's second phase (CERM-PACES 2013). Using various geophysical techniques, 31,701 m was surveyed using ground penetrating radar, 7565 m was surveyed using the time domain electromagnetic technique (TDEM) and 1750 m were surveyed using the resistivity technique. A detailed survey and analysis of fractures was conducted over a selected area that presented a high density of crystalline rock outcrops (n = 224) in the centre of the SLSJ region. Geophysical logging (caliper, fluid temperature, rock and fluid resistivity, gamma radiation, acoustic televiewer) was conducted in 12 boreholes. A total of 345 stratigraphic profiles were mapped in gravel pits or along river banks. At 30 locations, direct-push stratigraphic sounding of surficial deposits was carried out to a maximum depth of 40 m. Piezometers (1" diameter) were installed at ten of these locations. Destructive drilling carried out in

five other locations led to the installation of 13 more piezometers (2–6” diameter). Short-duration permeability tests were conducted at 165 boreholes pumped for groundwater sampling. A total of 161 groundwater samples were collected from fractured-rock aquifers and 193 samples were collected from granular aquifers, mostly private wells; the samples were analyzed for 40 hydrogeochemical parameters.

A GIS-based comprehensive database was created. It includes all previously existing data and all data acquired by the PACES-SLSJ project. All data were then interpreted to address specific research questions and to produce PACES-SLSJ deliverables. The major findings of the project are presented in this paper.

Geographic information system database

A major output of the PACES-SLSJ project was the development of a comprehensive groundwater database generated through (1) the gathering of relevant sources of information related to groundwater, and (2) the application of a quality control process to screen the data for accuracy and quality (Chesnaux et al. 2011a). This hydrogeological database was implemented within a geographic information system (GIS) framework coupled to a relational database management system (RDBMS) as a *file geodatabase* using GIS (ESRI format) technology (Chesnaux et al. 2011a). Stratigraphic data stored within the spatial database was used for constructing 3D subsurface hydro-structural models that supported the elaboration of many PACES project deliverables and provided a sound basis

for a variety of subregional, geology-related projects (e.g. Rouleau et al. 2011; Chesnaux 2013; Richard et al. 2016a; Hudon-Gagnon et al. 2015; Foulon et al. 2016; Chesnaux et al. 2017).

2.5 THE SLSJ HYDROGEOLOGICAL FRAMEWORK

Another significant output of the PACES-SLSJ project was the creation of a schematic conceptual model of the main hydrogeological systems present in the SLSJ region (Figure 2.2). This model was derived from existing data that were integrated during the first year of the project. Regional physiography is strongly influenced by the Saguenay Graben that has protected parts of the Paleozoic sedimentary rock units from erosion and has controlled the formation of major granular deposits in the lowland areas. Aquifer systems in the SLSJ region are composed of geological units and structures ranging from Proterozoic to Quaternary in age (Rouleau et al. 2015). These include: (1) a Precambrian crystalline basement belonging to the Grenville Province, (2) the Saguenay Graben, a significant topographic E-W trending depression, (3) remnants of Ordovician sedimentary cover located in the lowlands, (4) Holocene glacial and proglacial deposits, and (5) marine, littoral and deltaic sediments related to the Laflamme Sea that inundated the lowlands at the end of the last glaciation, between 11,000 and 7000 years BP. Regional geomorphology and the graben (Figure 2.2) structure a drainage system from the highlands located to the north and south, toward the central surface water bodies and the surrounding lowlands, which include Lake Saint-Jean and the Saguenay plains, the main inhabited parts of the

region. From a conceptual point of view, groundwater in the highlands infiltrates into a network of interconnected fractures and faults within the igneous and metamorphic rocks. In the lowlands, the groundwater discharges and flows dominantly into the permeable sediments. Lake Saint-Jean and the Saguenay River are the primary terminal discharge zones of the two regional groundwater flow systems (Figure 2.2).

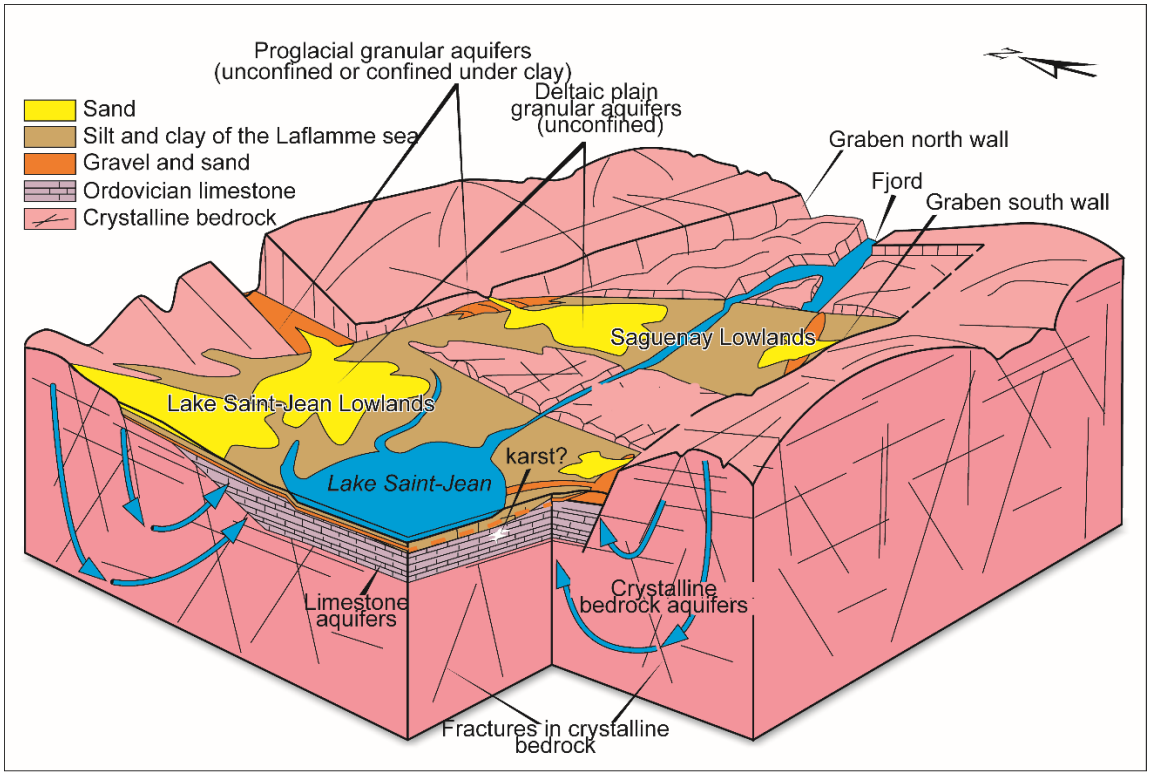

Figure 2.2 : Schematic block diagram of aquifer types identified in the Saguenay-Lac-Saint-Jean region (modified from Rouleau et al., 2011).

2.6 BEDROCK AQUIFERS

Fractured-rock aquifers are mostly present within the crystalline Precambrian basement and the Ordovician sedimentary rock units (Figure 2.3) and are detailed below.

2.6.1 PRECAMBRIAN ROCKS

As outlined by Rouleau et al. (2013), the Grenville Province (Rivers et al. 1989; Hocq 1994; Davidson 1998) is the latest Precambrian geological province accreted to the south-eastern portion of the Canadian Shield. In the SLSJ region, rock units are mostly composed of amphibolite to granulite gneissic rocks intruded by AMCG (anorthosite, mangerite, charnockite, granite) suites of plutonic rocks. The Lac Saint-Jean anorthosite is the major mafic intrusion present in the area.

A large amount of oxide minerals such as magnetite and ilmenite are present in the Grenvillian bedrock, especially in association with gabbroic phases. These minerals are also present in the Quaternary units deposited downstream by the ice sheet. The presence of magnetite can interfere with the use of the magnetic resonance sounding (MRS), an approach that has a proven track record in hydrogeology (Legchenko et al. 2002; Roy and Lubczynski 2003). MRS is very efficient in supplying highly relevant information related to the storage and flow properties of geological formations. As described by Roy et al. (2008, 2011a) and Menier et al. (2009), the wide distribution of magnetite constitutes a challenge when using the MRS technique in the Grenville Province.

2.6.2 ORDOVICIAN SEDIMENTARY ROCK UNITS

Large remnants of mid-Ordovician sedimentary rock units, comprised of limestone and shale, uncomformably overlie the Precambrian bedrock. Two of these units are

recognized: the 100 km^2 Saint-Honoré and the 400 km^2 Lac-Saint-Jean remnants. These units form a series of stratified sedimentary rocks, including siliciclastic strata, micritic limestones and highly fossiliferous alternating limestones and shales (Desbiens and Lespérance 1989). In the Saguenay area, the Ordovician sequence has a maximum thickness of 110 m in PACES-SLSJ boreholes (CERM-PACES 2013). These boreholes also revealed the presence of shale and limestone covered in places by 60 m of overburden. This new data doubles the known surface area of the Lac Saint-Jean remnant currently found on regional geological maps (Avramtchev 1993) that cover the areas to the north of Lake Saint-Jean (Figure 2.3). The calcareous units constitute an important exploitable aquifer, at least locally where karstic structures are observed, making this groundwater very vulnerable to contamination. However, results from a few hydraulic tests in Ordovician limestone aquifers (presumably in non-karstic zones) indicate only a slightly higher average transmissivity value ($9.5x10^{-5}$ m^2/s) than that of Precambrian rocks ($4.3x10^{-5}$ m^2/s; Richard et al. 2011a, b).

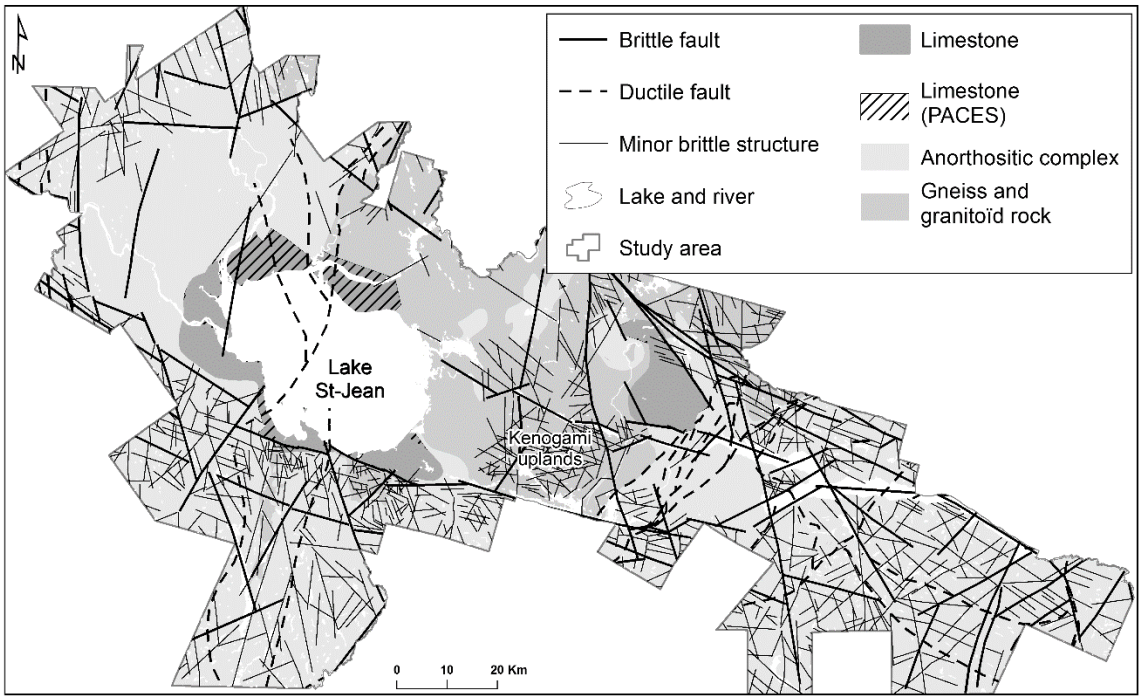

Figure 2.3 : Bedrock geology of the Saguenay-Lac-Saint-Jean region, showing important structural features (brittle and ductile main structures), as the major faults delimiting the graben and the local uplands within the graben.

2.6.3 FAULTS AND FRACTURES NETWORK WITHIN THE BEDROCK

Crystalline rocks are usually marked by a low matrix permeability, however the locally well-developed fracture systems in the SLSJ region (Rouleau et al. 2013) present higher flow property values. The fault and fracture pattern shown in Figure 2.3 is interpreted from existing geological maps (Hébert and Lacoste 1995) and is mostly related to the formation of the graben. The main brittle fracture set in the region trends WNW-ESE; this set delineates the highlands to the north and south starting from the central lowlands. A second NNW-SSE fracture set is also recognized.

The Grenvillian deformation is responsible for ductile NE trending shear zones and dominant rock fabrics (Hébert and Lacoste 1995) within the area. This dominant structural trend was reactivated locally during later brittle events and generated a strong anisotropic behaviour that influences underground water flow paths. The NE trending Saint-Fulgence deformation zone is a good example of this highly anisotropic area.

Brittle structures, such as faults and joints, increase the aquifer potential of the bedrock across the region. This factor was assessed in a structural hydrogeology study conducted in the Kenogami Uplands. These uplands offer a high density of outcrops, mostly constituted of anorthosite. This structure separates the Lake Saint-Jean Lowlands to the west from the Saguenay Lowlands to the east (Pino et al. 2011; Pino 2012). The orientations of both main subvertical fracture sets identified in this outcrop-scale study are similar to the brittle fractures identified at the above-mentioned regional scale. The general trend of these fractures (NW-SE) is approximately normal to the major compressional component (σ_1, oriented NE) of the current regional stress field in eastern Canada, based on the literature review by Pino (2012). This factor may imply that the fractures of the two main sets would tend to close and be poorer water conductors due to the action of the current stress field, while the fractures of secondary sets, including a subhorizontal set, would tend to remain open. The effects of permeable structures at depth have also been demonstrated by geophysical logging in seven boreholes in the SLSJ region (Roy et al. 2011b). Nevertheless, a study based on piezometric data and an analytical model (Chesnaux 2013) suggested that groundwater recharge in the crystalline

bedrock aquifer is quite low (about 3.5 mm/yr) although higher recharge values may occur locally around fault systems.

The PACES-SLSJ study showed that the mean transmissivity (*T*) values for the bedrock aquifers were generally low with mean *T* values ranging from $3.9x10^{-5}$ m^2/s to $9.3x10^{-5}$ m^2/s depending on rock type (Richard et al. 2011a,b; Richard et al. 2012a,b; Richard et al. 2016a), although much higher values (up to 10^{-2} m^2/s) have been observed (Figure 2.4). These estimates are based on specific capacity data from 1305 wells in bedrock aquifers recorded within the Quebec hydrogeological information system (MDDELCC 2017c).

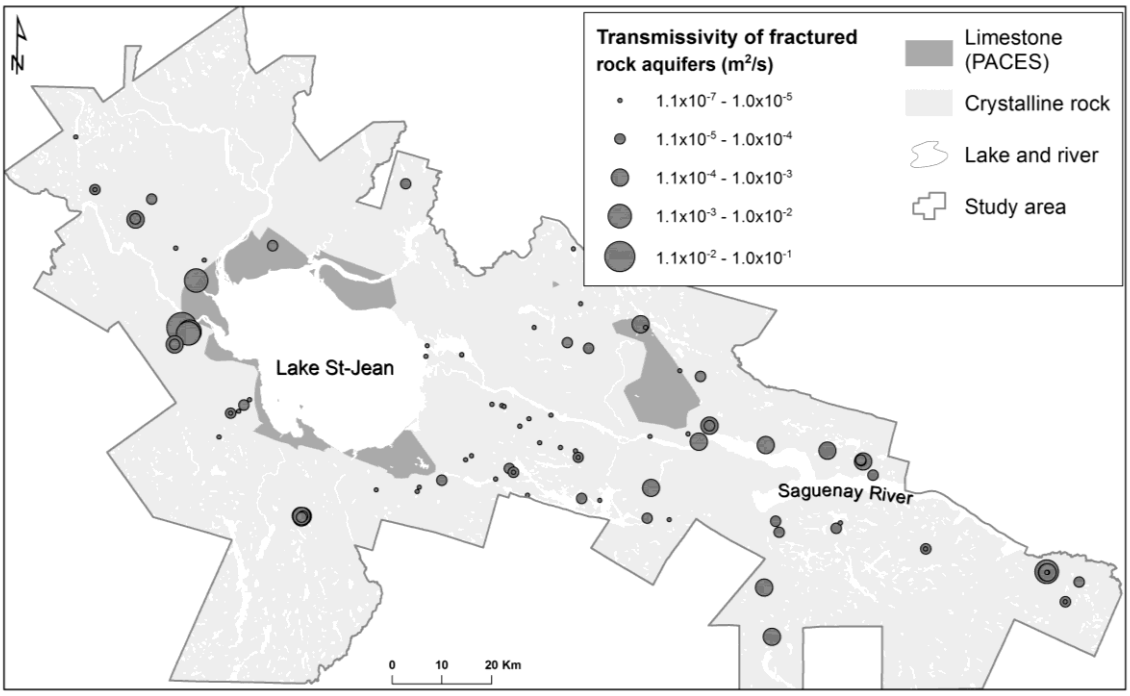

Figure 2.4 : Compiled and calculated Transmissivity in the fractured rock aquifers (adapted from CERM-PACES 2013).

2.6.4 MAPPING OF BEDROCK TOPOGRAPHY

The PACES-SLSJ project produced a map of the bedrock topography over the entire territory. This map is of hydrogeological interest, particularly in areas where thick surficial deposits cover the bedrock, as it provides valuable information on the thickness of granular aquifers, and may indicate the presence of buried valleys—some perhaps previously undetected—that are now filled up by granular aquifer material. Bedrock topography and the thickness of overlying layers of surficial deposits were determined through a large number (134) of stratigraphic cross-sections, distributed regularly over the territory, that were constructed from boreholes and sounding data (Figure 2.5a). An example of stratigraphic cross-sections is presented in Figure 2.5b. An original approach was developed for modeling complex bedrock topography, based on virtual data points along cross-sections that are added between boreholes where the stratigraphy has been observed (Chesnaux et al. 2017). This methodology is comprised of five steps: (1) gathering the maximum amount of relevant surface and subsurface data (from observation points), (2) determining the location of the stratigraphic sections to be constructed for interpreting bedrock topography, (3) selecting the most appropriate technique for interpolating the observed bedrock elevations that will be added into the dataset to be modeled, (4) increasing the quantity of modeling data by adding data elements based on geological interpretations of cross-sections, thus creating virtual boreholes that are inserted into the model alongside the original data, and (5) 3D

numerical modeling of the bedrock topography with the use of the triangulated irregular network (*TIN*) interpolation method.

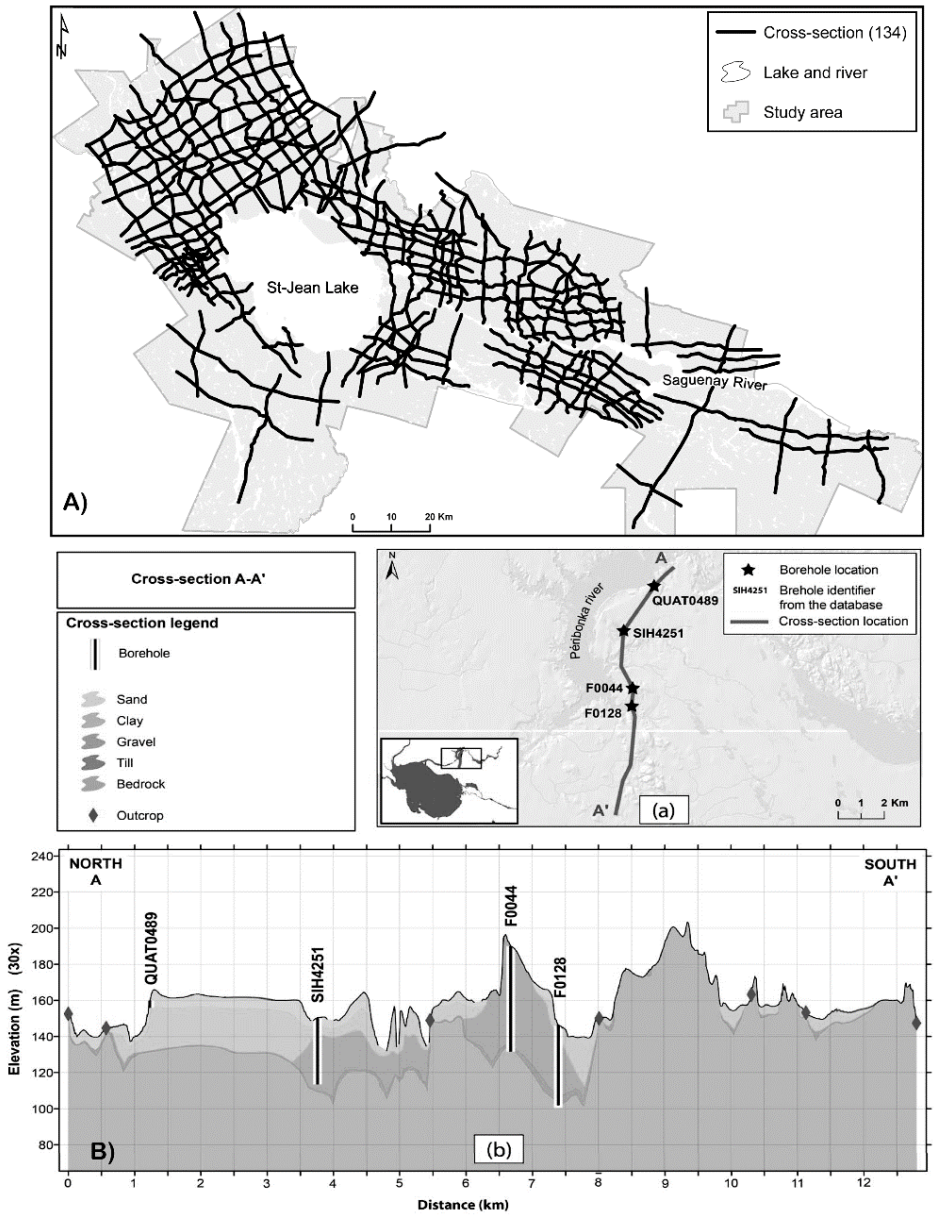

Figure 2.5 : (A) Position of the 134 cross-sections developed by interpreting local stratigraphic logs from boreholes and soundings. (B) An example of cross section: a) cross section location; b) cross section interpretation (Figure from Chesnaux et al. 2017).

The second step is the most critical for achieving relevant results as the quality of the interpretation conducted at this stage will greatly influence the results of the interpolation of the rock topography. Many quasi-regularly distributed data points are required to ensure a reliable model of bedrock topography using interpolation methods.

2.7 GRANULAR AQUIFERS

2.7.1 SURFACE TOPOGRAPHY AND QUATERNARY GRANULAR DEPOSITS

The regional physiography (Figure 2.1) is strongly influenced by the Saguenay Graben that has controlled the emplacement and the accumulation of Quaternary deposits (sand, gravel, clay-silt), which can reach up to 180 m in thickness in the central lowlands (CERM-PACES 2013; Figure 2.2), where the most populated areas are located. The map of surficial deposits is based on data from LaSalle and Tremblay (1978), updated by Daigneault et al. (2011).

The Quaternary granular deposits include glacial, glaciofluvial and post-glacial prograding alluvial and delta plains sediments. These sediments are deposited across the lowlands and on the bedrock uplands and plateaus. In glaciofluvial deposits, such as eskers and kames, in many places the fine particles have been washed out during the sedimentation process, resulting in permeable granular aquifers. In some locations, these granular units are unconfined whereas in other sites they are confined by extensive units of Laflamme Sea marine silt or clay. The Laflamme Sea deposited a clay-silt layer that is

thickest in its central part, with sandy material around its edges. Rivers that discharged into the Laflamme Sea formed deltas and deltaic plains, which are today partly covered by more recent alluvium. These deposits are present on both sides of the graben, as rivers were then flowing both from the north and south toward the Laflamme Sea.

The deposits making up the granular aquifers present generally complex and heterogeneous internal structures due to sedimentation processes that were highly variable in space and time. The determination of hydrofacies provides a valuable approach to this complexity problem. Hydrofacies are defined as homogeneous sedimentological units, formed under characteristic conditions that lead to particular hydraulic properties (Anderson 1989; Klingbeil et al. 1999). This approach has proven relevant to the hydrogeological characterization of the Saint-Honoré granular aquifer system (Boumaiza 2008; Boumaiza et al. 2017). It was also useful for developing a conceptual hydrostratigraphic model that provided accurate numerical groundwater flow simulations over selected portions of the region (Hudon-Gagnon et al. 2011; Hudon-Gagnon et al. 2015).

2.7.2 QUATERNARY AQUIFERS AND MUNICIPAL GROUNDWATER SUPPLY

Most municipalities (about 40) in the study region that use groundwater for their drinking water supply are pumping water from wells drilled into Quaternary granular aquifers. The Quaternary units presenting the highest aquifer potential include (1) proglacial deposits left behind during the retreat of the Wisconsinan ice sheet, and (2)

post-glacial deposits within deltas and deltaic plains that were formed along the coast of the Laflamme Sea. These permeable granular deposits also facilitate groundwater recharge, increasing groundwater flux within underlying bedrock aquifers; this type of indirect recharge is suggested by observed cases of interconnection between fractured bedrock and granular aquifers.

The proglacial sediments presenting the highest aquifer potential were deposited through glaciofluvial processes, forming structures such as eskers, kames and lateral moraines. Figure 2.6 shows that large glaciofluvial deposits (shown in orange) are located along the normal faults delineating the graben to the north and south. In many locations, these earlier Quaternary deposits are covered by more recent layers of post-glacial marine clay-silt or sandy deltaic deposits. In Figure 2.6 such superposing layers, including the areas where a glaciofluvial aquifer is confined by a clay-silt upper layer, are indicated by a hatched pattern. The presence as well as the extent of such confined aquifers is better known thanks to the creation of several stratigraphic sections (Figure 2.5). The proglacial aquifers are characterized by T values averaging between 1.5×10^{-4} and 1.8×10^{-3} m^2/s (Richard et al. 2016a), depending on test type and duration, as estimated from the results of 244 tests including data obtained prior to and during PACES.

Post-glacial granular sediments constitute relatively productive unconfined aquifers. The Saint-Honoré aquifer described by Tremblay (2005), Tremblay and Rouleau (2004), and Boumaiza (2008) is an example of a paleodeltaic aquifer that was created by a

south-flowing river that discharged into the Laflamme Sea. Deltaic and shore deposits compose the major regional water table aquifers and exhibit variable *T* values ranging from 10^{-5} m^2/s to 10^{-2} m^2/s (Chesnaux et al. 2011b; CERM-PACES 2013) as represented in Figure 2.6.

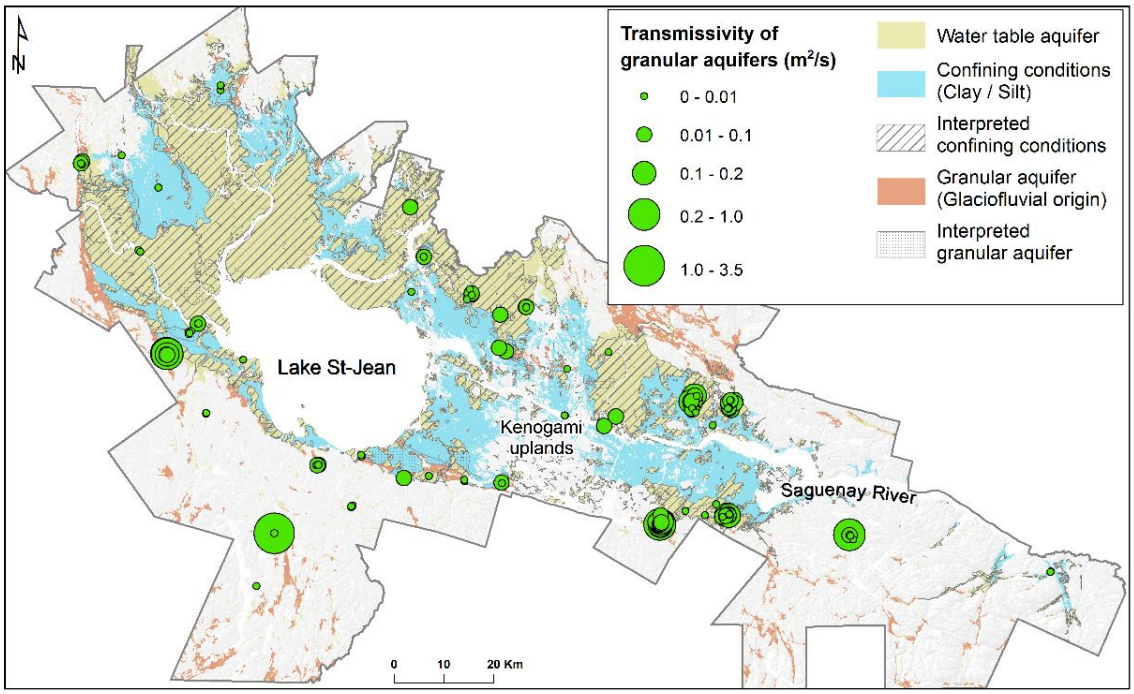

Figure 2.6 : Compiled and calculated transmissivity in the granular aquifers (adapted from CERM-PACES 2013). Main granular aquifers in the Saguenay-Lac-Saint-Jean region, forming either free-surface aquifers shown in yellow and orange, or confined aquifers indicated by hatching.

2.8 INTERCONNECTION BETWEEN FRACTURED BEDROCK AND GRANULAR AQUIFERS

The superposition of granular aquifers over bedrock may lead to a natural groundwater flux between aquifers and to wells pumping water simultaneously from both types of aquifer (Chesnaux and Elliott 2011). These two factors are often not considered in groundwater studies although they may affect significantly groundwater quality and resource assessment. Cases of hydraulic interconnection between fractured bedrock and overlying granular aquifers have been observed in numerous boreholes throughout the SLSJ region. These connections could be natural and related to the presence of fractures in the top layer of the bedrock (Chesnaux and Elliott 2011), or they could be due to defective borehole seals at the interface between the bedrock and the granular aquifer (Richard et al. 2013; Richard et al. 2014).

One of the bedrock sites investigated by Richard et al. (2014) presented a natural hydraulic connection with the overlying granular aquifer caused by the weathered surface of the uppermost bedrock. Another site presented an artificial hydraulic connection between the bedrock and the granular aquifer created by an improperly sealed casing (Chesnaux and Richard 2015; Richard et al. 2016b). These connections present a risk of cross-contamination between aquifer units as demonstrated by Chesnaux et al. (2012) who used numerical simulations motivated by PACES-SLSJ observations. Moreover, a regional analysis has shown that all types of hydraulic connections lead to erroneous interpretations of the hydraulic properties of the individual components of the aquifer

system. Indeed, a significant proportion of the individual hydraulic tests results are influenced by other aquifer units beyond the unit being tested, a factor generally not identified and therefore not considered in the characterization of aquifer systems. This has implications for the assessment and protection of groundwater resources, and may result in the inaccurate definition of well-capture areas and contamination risk. The hydraulic and chemical consequences of hydraulic connections were also investigated numerically by Chesnaux et al. (2012).

Along the flow lines from the highlands to discharge areas, a portion of the groundwater crosses from one type of aquifer to another. This includes the transfer of groundwater from fractured bedrock to granular aquifers (Richard et al. 2014) during which multiple sequences of geochemical processes affect the composition, properties and quality of the groundwater.

2.9 GROUNDWATER GEOCHEMISTRY

The geochemical characteristics of groundwater were investigated by analyzing 354 samples collected the summer of 2010 and 2011, from mostly private-use water wells for single homes (Walter et al. 2011; Walter et al. 2013; CERM-PACES 2013; Walter et al. 2014). The sampled wells were uniformly distributed over the study region (Figure 2.8). Among the samples, 161 were collected from Quaternary granular aquifers and 193 were obtained from fractured bedrock aquifers. Combining aquifer types and the two identified water types ((Na-Ca)-HCO_3; (Na-Ca)-Cl) yielded four groups of samples. The number of

samples considered in each group (Table 2.1) excluded samples that failed an ionic balance validity test. At a regional scale, there was no clear association identified between the regional geology and groundwater chemistry (Walter et al. 2017).

Groundwater in the SLSJ region is generally lightly mineralized and of good quality. However, Table 2.2 shows that the conductivity of water can vary from very low values (4 µS/cm) to values suggesting a brackish end-member (10,140 µS/cm). Samples having a higher conductivity mostly correspond to (Na-Ca)-Cl-type groundwater (Table 2.1).

Table 2.1 : Number of groundwater samples by aquifer and water type

Aquifer type	Water type	No of samples
Fractured bedrock	(Na-Ca)-HCO_3	127
Fractured bedrock	(Na-Ca)-Cl	26
Quaternary granular	(Na-Ca)-HCO_3	144
Quaternary granular	(Na-Ca)-Cl	19

According to Dessureault (1975), the regional marine clay aquitard is responsible for the presence of brackish groundwater in the confined Quaternary sediments. This observation was later supported by Roy et al. (2011c). Walter (2010) also identified brackish groundwater in the bedrock at shallow depths (<100 m), but suggested that the region's graben morphology was responsible for the long residence time of the regional-

scale flow system that converges toward Lake Saint-Jean and the Saguenay River. These observations agree with the Tóth (1999) model, in which the salinity of groundwater increases with the scale of the flow system (i.e. fresh groundwater in a local-scale system, fresh to brackish in an intermediate-scale system, and brackish to brine in a regional-scale system).

Table 2.2: Descriptive statistics for groundwater chemistry

Parameters	D.L (mg/L)	N	Min.	Q1- 25%	Median	Q3- 75%	Max.
pH*	-	316	4,4	6,5	7,6	8,1	10,1
Temperature (Celcius)*	-	316	1,7	6,9	7,5	8,6	17,5
Dissolved oxygen (mg/L)*	-	316	0	0	1,1	4,5	43,7
Redox potential (mV)*	-	316	-156	-31,5	70,5	101,0	195,2
Conductivity. (uS/cm)	-	316	4	134	278	470	10140
Bicarbonates*****	1	316	2	52,25	110	170	620
Silicium**	0.1	316	0,1	4,8	5,6	7,1	16
Sodium**	0.1	315	0,89	3,25	11	45,5	1800
Calcium**	0.1	314	0,12	9,5	23	50	1500
Potassium**	0.1	313	0,12	0,96	1,8	3,6	55
Chloride***	0.05	312	0,14	1,87	8,7	36,25	4200
Magnesium**	0.01	312	0,02	1,47	3,85	8,13	140
Strontium**	0.002	312	0,003	0,06	0,18	0,5	37
Sulfates***	0.5	311	0,2	4,5	10	17	420
Barium**		298	0,0025	0,0163	0,0395	0,0898	1,2
Aluminium**	0.001	285	0,001	0,004	0,007	0,016	0,230
Manganese**	0.0004	277	0,0004	0,0029	0,014	0,053	2,40
Zinc**	0.005	262	0,0016	0,0082	0,015	0,03	0,71
Amonium****	0.02	252	0,02	0,04	0,07	0,21	3
Boron**	0.005	234	0,005	0,011	0,032	0,100	0,75
Lead**	0.0001	225	0,0001	0,0002	0,0003	0,0006	0,0073
Fluoride****	0.1	222	0,1	0,2	0,6	1,5	4,9
Copper**	0.0005	220	0,0005	0,0016	0,0045	0,0130	0,35
Molybdene**	0.0005	189	0,0005	0,0010	0,0018	0,0031	0,0240
Nitrate***	0.1	154	0,02	0,10	0,30	1,08	8,60
Iron**	0.1	142	0,03	0,06	0,13	0,38	18
Silver**	0.0001	95	0,0001	0,0001	0,0002	0,0003	0,009
Nickel**	0.001	78	0,001	0,001	0,001	0,003	0,02
Uranium**	0.001	66	0,001	0,001	0,002	0,003	0,02
Chromium**	0.0005	48	0,0005	0,0007	0,0010	0,0016	0,011
Bromide***	0.1	42	0,1	0,4	1,5	6,1	45,0
Lithium**	0.01	35	0,01	0,01	0,01	0,02	0,57
Inorganic phosphorus****	0.03	22	0,04	0,05	0,07	0,10	0,50
Vanadium**	0.002	22	0,002	0,002	0,003	0,003	0,012
Cobalt**	0.0005	17	0,0006	0,0010	0,0013	0,0025	0,0066
Sulfures (mg/l)	0.02	15	0,02	0,05	0,16	0,55	16,00
Cadmium**	0.0002	9	0,0002	0,0003	0,0003	0,0007	0,0007
Antimony**	0.001	9	0,001	0,001	0,001	0,002	0,005
Tin**	0.001	4	0,001	0,001	0,001	0,002	0,003
Titanium**	0.001	3	0,001	0,001	0,001	0,002	0,004
Beryllium**	0.0005	2	0,0008	0,0017	0,0026	0,0035	0,0044
Bismuth**	0.00025	1	0,00070	0,00070	0,00070	0,00070	0,00070
Selenium**	0.001	1	0,001	0,001	0,001	0,001	0,001

ANALYTICAL METHODS

* multiparameter probe (in situ)

**Inductively Coupled Plasma Mass Spectrometry

*** Ionic chromatography

**** Specific probe

***** Titration

25 and 75 header = the first and the third quantiles

TDS is calculated using the software Aquachem v.5.0

Walter et al. (2017) proposed two processes to explain the evolution of groundwater chemistry in the SLSJ region (Figure 2.7): (1) evolution due to water/rock

interactions, and (2) evolution of recharge groundwater due to water/clay interactions and groundwater mixing. The first process is specific to fractured-rock aquifers. Water/clay interactions account for a combination of processes, namely ion exchange and/or the leaching of saltwater trapped in the regional aquitard (Walter et al. 2017). A mixing with fossil seawater present in the aquifer might also increase groundwater salinity.

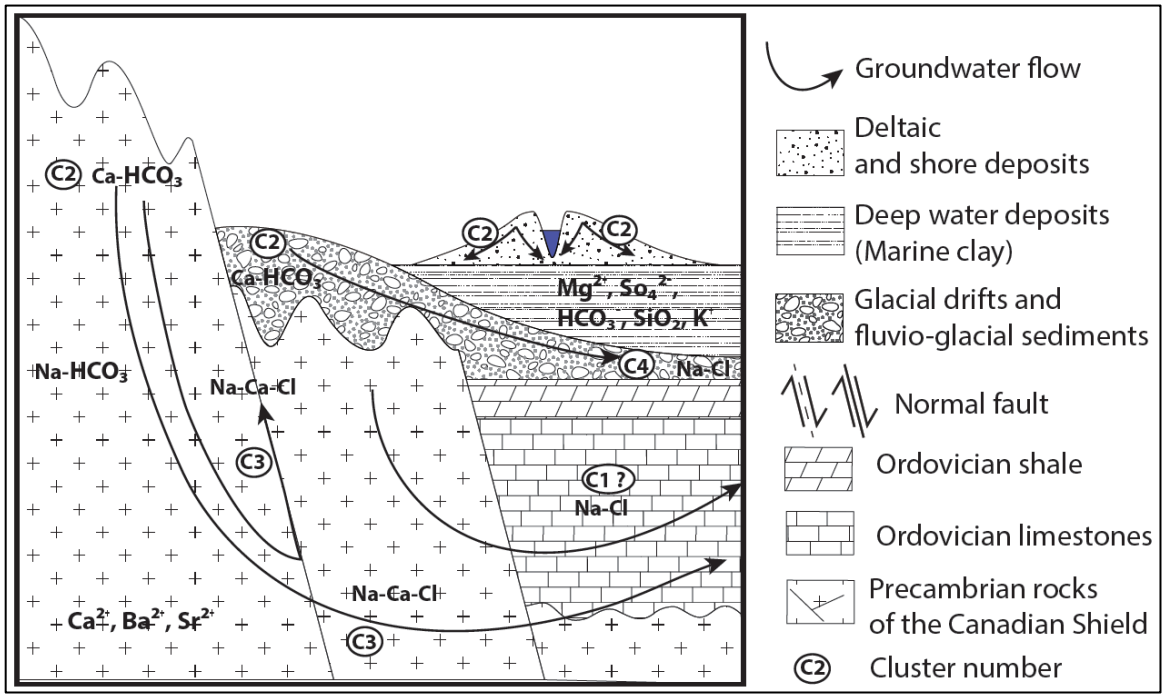

Figure 2.7 : Generalized cross-section showing the different salinization pathways occurring in the SLSJ region. Bedrock groundwater evolves from Ca,Na-HCO3 in unconfined environments to Ca,Na-Cl (Cluster 3) in rock-dominated environments due to interactions with basement fluids (water-rock interactions) along the graben fault system (groundwater flow line). The groundwater in the granular aquifers evolves from the recharge groundwater (Ca-HCO3) by Ca^{2+}water-Na^{+}mineral ion exchange process in a confined environment (Na-HCO3) and through possible mixing with the Laflamme seawater end-member (Na-Cl). This latter evolution might also be observed in bedrock aquifers where confining conditions prevail (Figure from Walter et al. 2017).

In some wells, the concentrations for some elements fell beyond the limits of provincial requirements (Quebec Government 2017) or federal guidelines (Health Canada 2014) on drinking water quality: fluoride (>1.5 mg/L), barium (>1 mg/L), manganese (>0.05 mg/L), iron (>0.3 mg/L) and aluminum (>0.1 mg/L) (CERM-PACES 2013) (Table 2.2).

Approximately 20% of the sampled wells had groundwater fluoride levels above World Health Organization (WHO 2004) standards (Walter 2011; CERM-PACES 2013). Exposure to excessive levels of fluoride can cause fluorosis, a very dangerous and often deadly condition (Edmunds and Smedley 2013). In the study area, the source of fluoride has not yet been identified, but preliminary observations indicate that groundwater with a high fluoride content is collected more often in fractured-rock aquifers than in granular aquifers.

2.10 DISCUSSION

Through the PACES program, the Government of Quebec, has mandated the regional scientific community to provide scientific background data to policymakers responsible for ensuring the protection of groundwater and the sustainability of its supply (Chesnaux et al. 2011a). To this end, the PACES-SLSJ project has characterized the hydrogeological systems across the large 13,210 km^2 municipalized portion of the region. Multiple actions must now be taken to ensure that groundwater is truly considered in water and land management policies. Most of the points addressed in this discussion relate to the updating and transfer of knowledge from the scientists producing the data

(hydrogeologists, various experts and researchers) to the various end-users, including municipal policymakers, governmental agencies, watershed agencies and consultants. Achieving the full benefit of the PACES project requires action, including a continual updating of the database, an on-going monitoring of groundwater quality, an assurance of proper protection to vulnerable aquifers and a development of the capacity of land-use and water managers to make full use of the groundwater database.

2.10.1 DATABASE UPDATING

The PACES project in the SLSJ region has yielded a very comprehensive database detailing the regional aquifer systems and groundwater. This database is designed to answer the needs of groundwater management at the regional level. The high density of data observation points also makes the database useful for local or subregional applications. These applications may be required to address geotechnical or groundwater-related problems (Foulon et al. 2016), and include field activities such as borehole drilling, geotechnical sounding and geophysical surveys. The resultant data from these activities must be integrated into the database, to maintain its relevance for future use and to provide solutions to a variety of problems involving groundwater quality, its management and its protection.

2.10.2 GROUNDWATER QUALITY

The geochemical data obtained by the PACES-SLSJ project revealed that water in a significant proportion of private wells had concentrations for some elements that approached or exceeded threshold levels for drinking water quality. This was particularly true for fluoride and manganese. Moreover, resampling from selected wells has shown cases where the water content of regulated substances, such as fluoride, can fall below drinking water standards one year, then fall above drinking water standards the following year (CERM-PACES 2013). More extensive groundwater sampling of private wells would yield a more valid baseline of groundwater quality. This baseline could then be used in health-related studies and to identify wells that should be sampled on a regular basis to ensure a better monitoring of groundwater chemical conditions.

2.10.3 GROUNDWATER PROTECTION

Some of the major aquifers composed of proglacial or glaciofluvial granular deposits are currently being pumped for private or municipal water supply. The exploitation of these aquifers for public drinking water supply indirectly provides these wells and the groundwater they produce with statutory protection against contamination (MDDELCC 2017a, b, c). However, this protection is only local, limited to the capture zones of the pumping wells. Larger portions of these granular aquifers are not contained within the capture zones of existing pumping wells and are therefore not legally protected, even in areas where the aquifer is exposed at the surface and the groundwater is deemed to be

vulnerable to contamination. This lack of protection of highly valuable aquifers may jeopardize future water supplies. The database constructed by the PACES-SLSJ project represents a good starting point to define the extent of the regional aquifers that require protection even if they are not currently exploited for water supply. These groundwater reservoirs are important components of the regional natural ecosystems and are vital resources for future human generations.

2.10.4 GROUNDWATER FLOW IN A GRABEN ENVIRONMENT

The graben morphology controlled the incursion of the Laflamme Sea after the retreat of the Laurentide Ice Sheet. Thick accumulations of marine sediment across the lowlands act as a confining layer for some underlying aquifers. Groundwater in the southern portion of the region has a greater calcium content, while groundwater in the northern portion is dominated by sodium (Figure 2.8). This observation is true for both fractured-rock (Figure 2.8a) and granular aquifers (Figure 2.8b). The dissolution of calcite and/or Ca-plagioclase minerals controls the chemical background of recharge groundwater in the region and explains its calcium content (Walter et al. 2017). Ca^{2+}_{water}-$Na^{+}_{mineral}$ ion exchange results in the transformation of Ca-HCO_3 to Na-HCO_3 due to a salinization path within the confined aquifers that are in contact with the regional aquitard and that possibly undergo groundwater mixing with the Laflamme Sea end-member (Walter et al. 2017). The seawater could be trapped in the regional aquitard

(solute diffusion) or may be stagnant (mixing) in some portions of the aquifer (Cloutier et al. 2010).

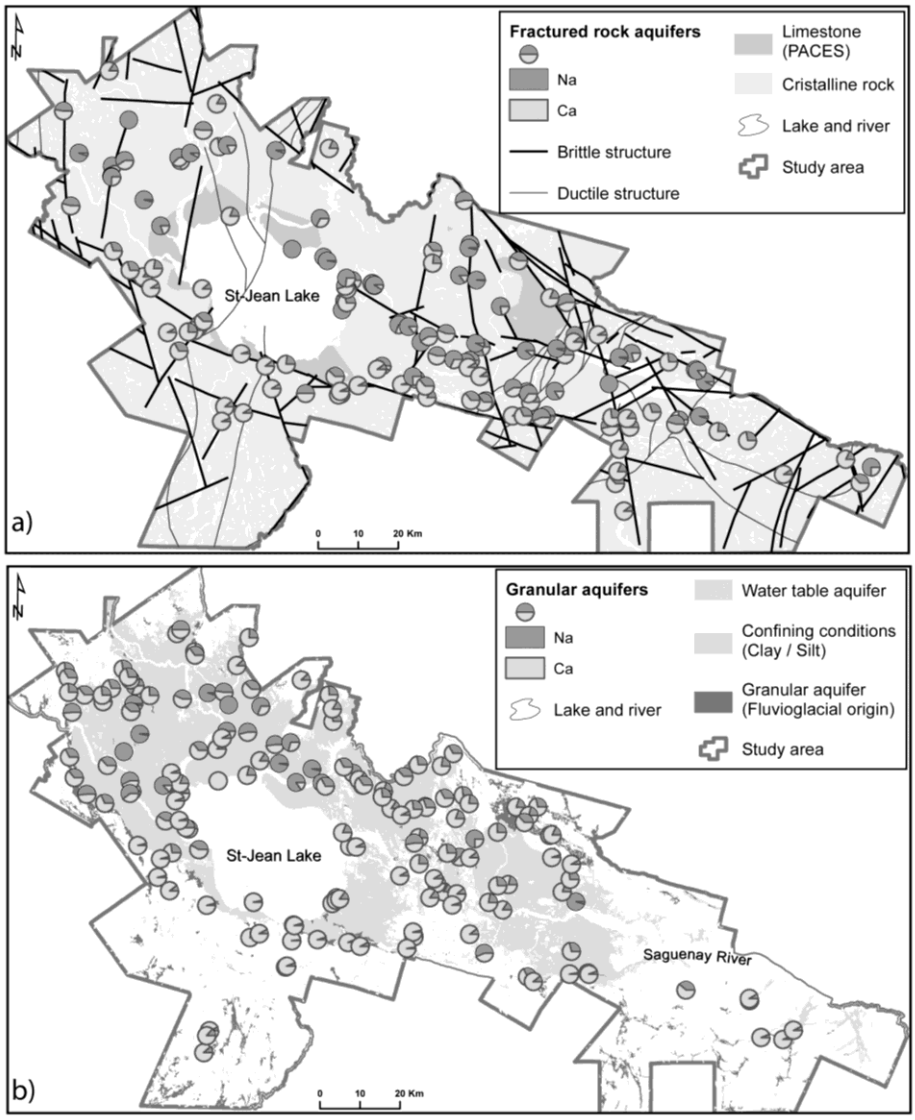

Figure 2.8 : Relative proportion of the major cations (calcium and sodium) in the collected groundwater in (a) the bedrock aquifers, and (b) the granular aquifers.

Consequently, Figure 2.8 suggests that in the SLSJ region, the transit time from recharge to discharge areas is shorter in the south than in the north. This suggests that the

southern fault of the graben might be sufficiently permeable to allow only minor changes in the chemical content of groundwater and might cause a rapid discharge of groundwater from the bedrock to the major proglacial aquifers located at the foot of the southern wall of the graben.

2.10.5 EXPERTISE REQUIRED OF GROUNDWATER DATABASE USERS

The database developed by the PACES-SLSJ project has been transferred to the Quebec *Ministère du Développement durable, de l'Environnement et de la Lutte contre les changements climatiques* (MDDELCC 2017a) and to regional partners, as requested for all PACES projects (MDDELCC 2017b). The maximal exploitation of the database requires users having an adequate expertise in hydrogeology and GIS. These skilled users will not only allow for the database to be fully exploited and refined, yet will offer a means of training future hydrogeologists. The database represents not only a resource to be used by territorial managers and government, but also serves as an important and continually evolving link between the scientific community, government, regional and municipal authorities and, ultimately, the population that relies upon groundwater resources.

2.11 CONCLUSION

The complex geological history of the SLSJ region explains the spatial heterogeneity observed in the regional hydrogeology. Confined and unconfined aquifers located in both fractured-rock and Quaternary deposits combine locally to form multilayered aquifers.

Glaciofluvial sediments are characterized by a transmissivity (*T*) of 10^{-4} to 10^{-3} m^2/s and, as a consequence, are favoured as sources of municipal water supply. These reservoirs are frequently covered by a marine clay-silt aquitard, but are also occasionally unconfined at higher elevations that were not inundated by the Laflamme Sea. Deltaic and shore deposits exhibit variable *T* values ranging from 10^{-5} m^2/s to 10^{-2} m^2/s and constitute the major regional water table aquifers. Fractured-rock aquifers exhibit relatively low *T* values (10^{-6} to 10^{-2} m^2/s). The regional-scale deformation zones can give rise to local maximum *T* values of 10^{-3} m^2/s.

The chemical composition of groundwater varies markedly across the study area. Although groundwater in the SLSJ area is largely of good quality, there are areas of brackish groundwater and water containing trace element concentrations, such as fluoride (>1.5 mg/L), barium (>1 mg/L), manganese (>0.05 mg/L), iron (>0.3 mg/L) and aluminum (>0.1 mg/L) that are above provincial and federal drinking water quality standards

The PACES-SLSJ project revealed the presence of a limestone unit scattered across the region that offers a new target for potential water supply. Furthermore, numerous unexplored, confined glaciofluvial aquifers were identified through the compilation and construction of stratigraphic cross-sections developed in the framework of the PACES-SLSJ project. These aquifers may represent major groundwater reservoirs.

The PACES-SLSJ project highlighted the regional consequences of graben morphology on groundwater resources. The configuration of the Saguenay Graben exerted a major control over the accumulation profiles of granular deposits, thereby impacting the presence of confined and/or unconfined porous aquifers in the lowlands. These multilayered deposits may be unconnected or highly interconnected. Graben morphology is also responsible for the degradation of groundwater quality by increasing groundwater salinity along a regional-scale flow system that converges toward Lake Saint-Jean and the Saguenay River. This may also be the origin of the brackish groundwater found in some confined granular aquifers. On the other hand, in some locations of the study area, brittle structures associated with the graben are sufficiently permeable to allow only a slight modification of the chemical content of groundwater and may cause a rapid discharge of groundwater from the bedrock to the proglacial aquifers located at the foot of the graben faults in the lowlands.

The PACES-SLSJ project produced a conceptual model of regional hydrogeology. This model can serve as a solid basis for future hydrogeological investigations at a local or regional scale. Across the SLSJ region, new, relevant and accurate data (well drilling, pumping tests, groundwater quality tests, etc.) are constantly being generated by consulting firms, government agencies and others. These data should improve the accuracy of this generalized regional hydrostratigraphic model. These data must also continue to be incorporated into the regional geodatabase to ensure that this important

output of the PACES-SLSJ project remains current and relevant for future projects involving regional water resources.

The results of the PACES-SLSJ project should support land-use planning efforts that consider the protection and sustainable development of groundwater resources. Much work remains to ensure a sustainable management of Quebec's groundwater resources. The protection of water resources starts with an efficient transfer of knowledge to decision- and policymakers. This is particularly so in a context of climate change that will have a significant impact on regional hydrological systems (Trainer et al. 2010).

2.12 ACKNOWLEDGEMENTS

This project was made possible by financial support from the Quebec Ministère du Développement durable, de l'Environnement, de la Faune et des Parcs (MDDEFP), as well as the Conférence régionale des Élus du Saguenay-Lac-Saint-Jean (CRÉ-SLSJ), the City of Saguenay, the Pekuakamiulnuatsh band council, as well as the following regional county municipalities (MRC): Domaine-du-Roy, Fjord-du-Saguenay, Lac-Saint-Jean-Est and Maria-Chapdelaine. A preliminary project (2008–2009) focusing on a portrait of regional groundwater resources was financed by these same regional organizations and by the regional office of the following Quebec ministries: Ressources naturelles (MRN), Affaires municipales, des Régions et de l'Occupation du territoire (MAMROT), Agriculture, Pêcheries et Alimentation (MAPAQ), and l'Agence régionale de la Santé et des Services sociaux (ASSS). The authors acknowledge the input of numerous collaborators (colleagues,

assistants and students) during the data acquisition and analysis phases of the project. We are also grateful for the constructive comments of two anonymous reviewers.

2.13 REFERENCES

Anderson, M. P. 1989. Hydrogeological facies models to delineate large-scale spatial trends in glacial and glaciofluvial sediments. *Geological Society of America Bulletin* 101: 501–511.

Avramtchev, L. 1993. *Carte minérale de la région du Saguenay-Lac-Saint-Jean*. Ministère de l'énergie et des ressources du Québec, 1 map. PRO9307.

CERM-PACES. 2013. *Résultats du programme d'acquisition de connaissances sur les eaux souterraines de la région Saguenay-Lac-Saint-Jean*. Chicoutimi: Centre d'études sur les ressources minérales, Université du Québec à Chicoutimi, 308 pp.

Boumaiza, L. 2008. *Caractérisation hydrogéologique des hydrofaciès dans le paléodelta de la rivière Valin au Saguenay*. Master's thesis, Université du Québec à Chicoutimi.

Boumaiza, L., A. Rouleau, and P. A. Cousineau. 2017. Determining hydrofacies in granular deposits of the Valin River paleodelta in the Saguenay region, Quebec. (In Proceedings of the 70th Canadian Geotechnical Conference and 12th Joint CGS/IAH-CNC Groundwater Conference, Ottawa, 7 pp).

Chesnaux, R., and A.-P. Elliott. 2011. Demonstrating evidence of hydraulic connections between granular aquifers and fractured rock aquifers. (In Proceedings of GeoHydro 2011, Joint Meeting of the Canadian Quaternary Association and the Canadian Chapter of the International Association of Hydrogeologists, August 28–31, 2011, Quebec City, 8 pp).

Chesnaux, R., M. Lambert, J. Walter, U. Fillastre, M. B. Hay, A. Rouleau, R. Daigneault, A. Moisan, and D. Germaneau. 2011a. Building a geodatabase for mapping hydrogeological features and 3D modeling of groundwater systems: Application to the Saguenay-Lac-St-Jean Region, Canada. *Computers & Geosciences* 37(11): 1870–1882.

Chesnaux, R., C. Baudement, and M. Hay. 2011b. Assessing and comparing the hydraulic properties of granular aquifers on three different scales. (In Proceedings of

GeoHydro 2011, Joint Meeting of the Canadian Quaternary Association and the Canadian Chapter of the International Association of Hydrogeologists, August 28–31, 2011, Quebec City, 8 pp).

Chesnaux, R., S. Rafini, and A.-P. Elliott. 2012. A Numerical investigation to illustrate the consequences of hydraulic connections between granular and fractured-rock aquifers, *Hydrogeology Journal* 20(8): 1669–1680.

Chesnaux, R. 2013. Regional recharge assessment in the crystalline bedrock aquifer of the Kenogami uplands, Canada. *Hydrogeological Sciences Journal* 58(2): 421–436.

Chesnaux, R., and S. K. Richard. 2015. Consequences of a defective seal into a bedrock aquifer: field site example and numerical study. (In International Association of Hydrogeologists IAH, 42nd IAH International Congress – Aqua 2015, Rome).

Chesnaux, R., M. Lambert, J. Walter, V. Dugrain, A. Rouleau, and R. Daigneault. 2017. A simplified geographical information system (GIS)-based methodology for modeling the topography of bedrock: Illustration using the Canadian Shield. *Journal of Applied Geomatics*, DOI 10.1007/s12518-017-0183-1.

Cloutier, V., R. Lefebvre, M. M. Savard, and R. Therrien. 2010. Desalination of a sedimentary rock aquifer system invaded by Pleistocene Champlain Seawater and processes controlling groundwater geochemistry. *Environmental Earth Sciences* 59: 977–994.

Daigneault, R., P. A. Cousineau, E. Leduc, G. Beaudoin, S. Millette, N. Horth, D. W. Roy, M. Lamothe, and G. Allard. 2011. *Rapport final sur les travaux de cartographie des formations superficielles réalisés dans le territoire municipalisé du Saguenay-Lac-Saint-Jean*. Ministère des Ressources naturelles et de la Faune du Québec.

Davidson, A., 1998. An overview of Grenville Province geology. Chap. 3 in *Geology of the Superior and Grenville Provinces and Precambrian Fossils in North America*, ed. S. B. Lucas and M. R. St-Onge. 205–270. Geology of Canada, no.7, Geological Survey of Canada; and Geology of North America, vol. C-1, Geological Society of America.

Desbiens, S., and P. J. Lespérance. 1989. Stratigraphy of the Ordovician of the Lac Saint-Jean and Chicoutimi outliers, Quebec. *Canadian Journal of Earth Sciences* 26: 1185–1202.

Dessureault, R., 1975. *Hydrogéologie du Lac Saint-Jean, partie nord-est*. Québec: Ministère des richesses naturelles, Direction générale des eaux, Service des eaux souterraines.

Edmunds, W. M., and P. L. Smedley. 2013. Fluoride in natural waters. In *Essentials of Medical Geology*, ed. O. Selinus. 311–336. Dordrecht, The Netherlands: Springer.

Foulon T., A. Saeidi, R. Chesnaux, A. Rouleau, and M. Nastev. 2016. Modélisation des dépôts meubles, un élément du risque sismique sur le territoire de la Ville de Saguenay. (In GeoVancouver 2016, Proceedings of the Canadian Geotechnical Society Annual Meeting, 7 pp.)

Gascoyne, M., and D. C. Kamineni. 1994. The hydrogeochemistry of fractured plutonic rocks in the Canadian Shield. *Applied Hydrogeology* 2(2): 43–49.

Health Canada, 2014. *Guidelines for Canadian drinking water quality: summary table*. Federal–Provincial–Territorial Committee on Drinking Water, http://www.hc-sc.gc.ca/ewh-semt/pubs/water-eau/sum_guide-res_recom/index-eng.php (accessed July 2015)

Hébert, C., and P. Lacoste. 1995. *Compilation géoscientifique, géologie du Saguenay Lac Saint-Jean*. Ministère des Ressources naturelles, Système d'information géominière du Québec, 8 maps. 1:50 000.

Hocq, M. 1994. La province de Grenville. In *Géologie du Québec*, ed. M. Hocq. 75–94. Québec: Les Publications du Québec.

Hudon-Gagnon, E., R. Chesnaux, P. A. Cousineau, and A. Rouleau. 2015. A hydrostratigraphic simplification approach to build 3D groundwater flow numerical models: example of a Quaternary deltaic deposit aquifer. *Environmental Earth Sciences* 74: 4671–4683.

Klingbeil, R., S. Kleineidam, U. Asprion, T. Aigner, and G. Teutsch. 1999. Relating lithofaciès to hydrofacies: outcrop-based hydrogeological characterization of quaternary gravel deposits. *Sedimentary Geology* 129 (3-4): 299–310.

LaSalle, P., and G. Tremblay. 1978. *Dépôts meubles, Saguenay - Lac St- Jean*. Ministère des Richesses naturelles du Québec, Geology Report 191, 61 pp.

Legchenko, A., J. M. Baltassat, A. Beauce, and J. Bernard. 2002. Nuclear magnetic resonance as a geophysical tool for hydrogeologists. *Journal of Applied Geophysics* 50: 21–46.

MDDELCC. 2017a. *Système d'Information Hydrogéologique*. Quebec, Ministère du Développement durable, de l'Environnement et de la Lutte aux changements climatiques. http://www.mddelcc.gouv.qc.ca/eau/souterraines/sih/index.htm (Accessed September 2017).

MDDELCC. 2017b. *Programme d'acquisition de connaissances sur les eaux souterraines*. Ministère du Développement durable, de l'Environnement et de la Lutte aux changements climatiques. http://www.mddelcc.gouv.qc.ca/eau/souterraines/programmes/acquisition-connaissance.htm. (Accessed February 2017)

MDDELCC. 2017c. *Water Withdrawal and Protection Regulation*. Ministère du Développement durable, de l'Environnement et de la Lutte aux changements climatiques. http://www.mddelcc.gouv.qc.ca/eau/prelevements/reglement-prelevement-protection/index-en.htm (Accessed February 2017)

Menier, J., J. Roy, and A. Rouleau.2009. Field and laboratory investigation in support of the application of the magnetic resonance sounding method in granular aquifers in the Grenville Province. (In Proceedings of the 62nd Canadian Geotechnical Conference and 10thJoint CGS/IAH-CNC Groundwater Conference, Halifax, September 20–24, 1593–1599).

Ogunba, A., 2012. Threats to groundwater: lessons from Canada and selected jurisdictions. *Journal of Energy & Natural Resources Law* 30(2): 159–184.

Pino, D.S. 2012. *Structural hydrogeology in the Kenogami uplands, Quebec, Canada.* Master's thesis, Université du Québec à Chicoutimi. http://constellation.uqac.ca/2572/

Pino, D.S., A. Rouleau, D. W. Roy, and R. Daigneault. 2011. Analysis of the joint system in the Kenogami uplands bedrock aquifer: methodology and preliminary results. (In Proceedings of GeoHydro 2011, Joint Meeting of the Canadian Quaternary Association and the Canadian Chapter of the International Association of Hydrogeologists, August 28–31, 2011, Quebec City).

Quebec Government. 2017. *Regulation respecting the quality of drinking water*. Environment Quality Act, Chapter Q-2, r. 40. http://legisquebec.gouv.qc.ca/en/ShowDoc/cr/Q-2,%20r.%2040 (accessed October 2017)

Richard, S. K., R. Chesnaux, and A. Rouleau. 2011a. Estimating the hydraulic properties of aquifers from specific capacity data: Saguenay-Lac-Saint-Jean, Quebec. (In Proceedings of GeoHydro 2011, Joint Meeting of the Canadian Quaternary Association and the Canadian Chapter of the International Association of Hydrogeologists, August 28–31, 2011, Quebec City, 8 pp).

Richard, S. K., R. Chesnaux, and A. Rouleau. 2011b. Evaluación de la transmisividad a partir del caudal específico enlos acuiferos de la región de Saguenay-Lac-St-Jean, Québec, Canada. (In Proceedings of VII Congreso Argentino de Hidrogeología, October 18–21 2011, Salta, Argentina, 8 pp.).

Richard, S. K., R. Chesnaux, and A. Rouleau. 2012a. From calculating transmissivity to understanding its origin in the fractured-rock aquifers. (In Proceedings of International Conference on Groundwater in Fractured Rocks, May 21–24, 2012, Prague, Czech Republic).

Richard, S. K., R. Chesnaux, and A. Rouleau. 2012b. Hydraulic factors controlling groundwater flow in the fractured rock aquifers of the Saguenay-Lac-Saint-Jean region, Quebec, Canada. (In 39th IAH International Conference, September 17–21, 2012, Niagara Falls, Canada).

Richard, S. K., R. Chesnaux, and A. Rouleau. 2013. Detecting preferential seepage along casing installed in fractured rock aquifers: Examples from the Saguenay-Lac-Saint-Jean region, Canada. (In GeoMontreal 2013, the 66th Canadian Geotechnical Conference and the 11th Joint CGS/IAH-CNC Groundwater Conference, September 29–October 3, 2013, Montreal, Quebec).

Richard, S. K., R. Chesnaux, A. Rouleau, R. Morin, J. Walter, and S. Rafini. 2014. Field evidence of hydraulic connections between bedrock aquifers and overlying granular aquifers: examples from the Grenville Province of the Canadian Shield. *Hydrogeology Journal* 22(8): 1889–1904.

Richard, S. K., R. Chesnaux, A. Rouleau, and R. H. Coupe. 2016a. Estimating the reliability of aquifer transmissivity values obtained from specific capacity tests: examples from the Saguenay-Lac-Saint-Jean aquifers, Canada. *Hydrological Sciences Journal* 61(1): 173–185.

Richard, S. K., R. Chesnaux, and A. Rouleau. 2016b. Detecting a defective casing seal at the top of a bedrock aquifer. *Groundwater* 54(2): 296–303.

Rivers, T., J. Martignole, C. F. Gower, and T. Davidson.1989. New tectonic divisions for the Grenville province, southeast Canadian Shield; *Tectonics* 8: 63–84.

Rouleau, A., J. Walter, R. Daigneault, D. Germaneau, D. W. Roy, M. Lambert, R. Chesnaux, A. Moisan, and D. Noël. 2011. La diversité hydrogéologique du territoire du Saguenay-Lac-Saint-Jean (Québec). (In Proceedings of GeoHydro 2011, Joint Meeting of the Canadian Quaternary Association and the Canadian Chapter of the International Association of Hydrogeologists, August 28–31, 2011, Quebec City).

Rouleau, A., I. D. Clark, D. J. Bottomley, and D. W. Roy. 2013. Precambrian Shield. Chap 11 in *Canada`s Groundwater Resources*, ed. A. Rivera. 415–442. Markham: Fitzhenry & Whiteside.

Rouleau, A., J. Walter, R. Chesnaux, V. Cloutier, and I. D. Clark. 2015. An overview of the hydrogeology of the Canadian Shield with emphasis on the Saguenay-Lac-St-Jean area, (In Vingtième journée du comité français d'hydrogéologie de l'association international des hydrogéologues, "Aquifères de socle: le point sur les concepts et les applications opérationnelles," La Roche-sur-Yon, France, June 11–13, 2015).

Roy, J., and M. Lubczynski. 2003. The magnetic resonance sounding technique and its use for groundwater investigations. *Hydrogeology Journal* 11: 455–465.

Roy, J., A. Rouleau, M. Chouteau, and M. Bureau. 2008. Widespread occurrence of aquifers currently undetectable with the MRS technique in the Grenville geological Province, Canada. *Journal of Applied Geophysics* 66(3–4): 82–93.

Roy, J., A. Legchenko, A. Rouleau, M. Bureau, M. Chouteau, J. Menier, Y. Leblanc, D. Richard, E. Gloaguen, and Y. Benhouhou. 2011a. In-situ ^{1}H NMR to map groundwater non-invasively: problems and prospects in the Grenville. (In Proceedings of GeoHydro 2011, Joint Meeting of the Canadian Quaternary Association and the Canadian Chapter of the International Association of Hydrogeologists, August 28–31, 2011, Quebec City).

Roy, J., R. Morin, R. Chesnaux, S. Richard, D. Pino, A. Rouleau, D. W. Roy, J. Walter, and D. Noël. 2011b. Hydrogeological insight from geophysical water-well logging in hard rocks in the Saguenay region, Québec. (In Proceedings of GeoHydro 2011, Joint Meeting of the Canadian Quaternary Association and the Canadian Chapter of the International Association of Hydrogeologists, August 28–31, 2011, Quebec City).

Roy, D.W., G. Beaudoin, E. Leduc, A. Rouleau, J. Walter, R. Chesnaux, and P. A. Cousineau. 2011c. Post glacial differential isostasy in the Lac-St.-Jean area (Quebec, Canada) and implications for the quality of groundwater. (In Proceedings of GeoHydro 2011, Joint Meeting of the Canadian Quaternary Association and the Canadian Chapter of the

International Association of Hydrogeologists, August 28–31, 2011, Quebec City, 8 pp.).

Tóth, J. 1999. Groundwater as a geologic agent: An overview of the causes, processes, and manifestations, *Hydrogeology Journal* 7*(1):* 1–14.

Trainer, M. A., P. Baveye, and G. Syme. 2010. Goals, gaps and governance: The holy grail in preserving Canada's hidden liquid gold. *Journal of Hydrology* 380(1): 1–3.

Tremblay, P. 2005. Étude hydrogéologique de l'aquifère de Saint-Honoré avec emphase sur son bilan hydrique. Master's thesis, Université du Québec à Chicoutimi, Chicoutimi.

Tremblay, P., and A. Rouleau. 2004. Water budget analysis of the paleo-deltaic Saint-Honoré aquifer in the Saguenay lowlands. (In Proceedings of the Fifth Joint Annual Conference, Canadian Geotechnical Society & Canadian Chapter of the International Association of Hydrogeologists, Québec, Québec, October 23–27, 2004, 8 pp.).

Walter, J. 2010. Les eaux souterraines à salinité élevée autour du lac Saint-Jean, Québec: origines et incidences. Master's thesis, Université du Québec à Chicoutimi, Chicoutimi.

Walter, J., A. Rouleau, D. W. Roy, and R. Daigneault.2011. Hydrogéochimie des eaux souterraines de la région du Saguenay-Lac-Saint-Jean: résultats préliminaires. (In Proceedings of GeoHydro 2011, Joint Meeting of the Canadian Quaternary Association and the Canadian Chapter of the International Association of Hydrogeologists, August 28–31, 2011, Quebec City, 6 pp.).

Walter, J., A. Rouleau, and R. Chesnaux. 2013. Regional assessment of composite groundwater parameters, illustrated by the Saguenay-Lac-Saint-Jean region, including methods and limitations. (In GeoMontreal 2013, the 66th Canadian Geotechnical Conference and the 11th Joint CGS/IAH-CNC Groundwater Conference, September 29–October 3, 2013, Montreal, Quebec, Canada).

Walter, J., R. Chesnaux, D. Gaboury, and V. Cloutier. 2014. Multivariate analysis of hydrochemical data to assess the geochemical processes controlling the groundwater geochemistry of the Saguenay-Lac-St-Jean region, Quebec, Canada. (In International Association of Hydrogeologists IAH, the Moroccan Chapter, 41st IAH International Congress "Groundwater: Challenges and Strategies", Marrakech, September, 15–19, 2014).

Walter, J., R. Chesnaux, and V. Cloutier. 2015. Groundwater evolution trends and natural salinization processes in Canadian Shield rocks and Pleistocene deposit aquifers systems. (In International Association of Hydrogeologists IAH, 42nd IAH International Congress – Aqua 2015, Rome).

Walter, J., R. Chesnaux, V. Cloutier, and D. Gaboury. 2017. The influence of water/rock − water/clay interactions and mixing in the salinization processes of groundwater. *Journal of Hydrology: Regional Studies* 13 (2017) 168–188.

World Health Organization. 2004. *Guidelines for drinking-water quality: recommendations, (Vol. 1)*. World Health Organization. http://www.who.int/water_sanitation_health/publications/gdwq3rev/en/ (accessed October 2017).

CHAPITRE 3

THE INFLUENCE OF WATER/ROCK – WATER/CLAY INTERACTIONS AND MIXING IN THE SALINIZATION PROCESSES OF GROUNDWATER

Julien Walter[1], Romain Chesnaux[1],
Vincent Cloutier[2], Damien Gaboury[1]

[1]Centre d'études sur les ressources minérales, Université du Québec à Chicoutimi, Chicoutimi, Québec, G7H 2B1

[2]Groundwater Research Group, Institut de recherche en mines et en environnement, Université du Québec en Abitibi-Témiscamingue, Campus d'Amos, Amos, Québec, Canada.

Journal of Hydrology: Regional Studies, 2017, Vol. 13, pp 168-188

3.1 MISE EN CONTEXTE

Dans l'article qui suit, nous répondons principalement à l'objectif 2 de cette thèse et partiellement à l'objectif 4. L'application des statistiques multivariées, du type analyse hiérarchique en grappe, sur le jeu de données constitué de 321 échantillons d'eau souterraine nous permet de définir une première série de pôles hydrogéochimiques régionaux, à savoir un pôle d'eau de recharge et deux pôles salins distincts en fonction du type de milieu aquifère (roc fracturé ou dépôts granulaires). L'application subséquente d'une analyse en composante principale sur le même jeu de données nous conduit à proposer les ions Ca^{2+}, Sr^{2+}, Ba^{2+} comme étant fortement corrélés au pôle salin collecté dans les milieux rocheux fracturés et les ions Mg^{2+}, SiO_2, K^+, SO_4^{2-} and HCO_3^- plutôt corrélés au pôle salin collecté dans les milieux granulaires.

3.2 ABSTRACT

Study region: Groundwater from the Precambrian Shield rock and Pleistocene deposit aquifers in Saguenay-Lac-Saint-Jean region (>13 000 km^2) in the province of Quebec, Canada.

Study focus: Interpretations are based on the combination of *hierarchical cluster analysis* (HCA) results, *principal component analysis* (PCA), binary plots investigations ([Na^+, Ca^{2+}, Br^-] *vs.* Cl^-; Ca^{2+} *vs.* HCO_3^-; Ca^{2+} *vs.* Na^+) and Piper diagram investigations. The HCA and PCA was applied on 321 samples to specifically enable the identification of two very distinct salinization paths that produce the brackish groundwater in the study area.

New hydrological insights for the region: The results show that each of the two salinization paths exerts a major and different influence on the chemical signature of groundwater. Groundwater present in the crystalline bedrock naturally evolve from a recharge-type groundwater (Ca-HCO_3-dominant) to a type of brackish groundwater (Ca-(Na)-Cl-dominant) due to water/rock interactions (plagioclase weathering and mixing with deep basement fluids). Groundwater evolution in confined aquifers is dominated by water/clay interactions. The term water/clay interactions was introduced in this paper to account for a combination of processes: ion exchange and/or leaching of salt water trapped in the regional aquitard. Mixing with fossil seawater might also increase the groundwater salinity. PCA revealed that Ca^{2+}, Sr^{2+}, Ba^{2+} are highly correlated with groundwater from bedrock aquifers, while Mg^{2+}, SiO_2, K^+, $SO_4^{2-}$and HCO_3^- are more representative of the regional confining conditions.

Keywords: hydrogeochemistry; groundwater salinization; Precambrian Shield; granular deposits; multivariate analysis

3.3 INTRODUCTION

Deep groundwater in crystalline basement is typically highly mineralized, as indicated by numerous studies (Edmunds et al., 1984; Frape and Fritz, 1987; Fritz et al., 1994; Gascoyne and Kamineni, 1994; Lodemann et al., 1997; Bucher and Stober, 2010). Saline to brine waters are systematically encountered deep in the crust by 1) nuclear waste disposal programs in various countries, particularly in Canada (Gascoyne et al., 1995), Sweden (Nordstrom et al., 1989), Finland (Lahermo and Lampen, 1987), and Switzerland (Pekdeger and Balderer, 1987); in continental deep drilling programs (Russia: Kola island well; Germany: KTB); and in geothermal energy programs (France: Soultz-sous-Forêts; Switzerland: Urach; U.K.: Cornwall; USA: Los Alamos). Brackish to highly saline brines have been detected at depths down to several kilometers in many mines in crystalline rocks, particularly in the Canadian Shield (Fritz and Frape, 1982; Frape and Fritz, 1987) and in oil field sedimentary basins around the world (Fyfe et al., 1978; Kharaka and Hanor, 2003). Overall, the water from basement rocks is systematically contaminated with brines at depths of less than 5 km (Pauwels et al., 1993; Bucher and Stober, 2010).

New chemical and isotopic data have yielded several hypotheses to explain the occurrence of saline groundwater deep in the crust. Total dissolved solids (TDS) generally increase with depth, and chlorides are the common salts. According to Bucher and Stober (2010), this chlorinity probably has a common global source because it is present at depth in all continental basement units worldwide. The main theories about the origins of the

brines in Precambrian Shields include: 1) modified Paleozoic seawater (Bottomley et al., 1994) or basinal brines (Guha and Kanwar, 1987); 2) leaching of saline fluid inclusions in crystalline rocks (Nordstrom and Olsson, 1987); and 3) intense water/rock interactions (Frape and Fritz, 1987; Gascoyne et al., 1987; Kamineni, 1987; Bucher and Stober, 2010). More recently, studies on glaciation effects have demonstrated that glacial meltwater infiltrating bedrock aquifers has a major impact on groundwater chemistry (Lemieux et al., 2008; Aquilina et al., 2015; McIntosh et al., 2011). Clearly, a combination of several different physicochemical processes rather than a single process appears responsible for the generation of basement water (Douglas et al., 2000; Frape et al., 2003; Bucher et al., 2012). Studies of the origin and evolution of fluids in crystalline rocks are ongoing and are constantly being supplemented by new data contrasting geochemical conditions at different study sites.

Brackish groundwater have been identified at shallow depths (<100 m) in fractured rock aquifers and in Pleistocene granular aquifers in the Saguenay-Lac-Saint-Jean region (SLSJ) in the province of Quebec, Canada (Figure 3.1) by Dessureault (1975) and Walter (2010). In the study area, bedrock mainly consists of a variety of igneous and metamorphic Precambrian Shield rocks and some Ordovician remnants of several units of sedimentary rocks (shale, limestone and siltstone). The rocks of the basement are cut by a Phanerozoic faulted graben that defines the limits between the highlands and lowlands. Based on the specific morphology of the graben in the SLSJ region, a discharging regional gravity-driven flow system according to the Tóth model (Tóth, 1999) would explain the

natural contamination by salt of lower fresh groundwater systems in the lowlands (Walter, 2010). The lowlands are covered by highly heterogeneous surficial Pleistocene deposits that include a semi-continuous regional aquitard of marine origin left behind by the retreat of seawater approximately 10,000 years ago (Lasalle and Tremblay, 1978). The leaching of trapped salt in the regional marine clay confining layer would explain the presence of brackish groundwater in some confined Pleistocene aquifers in the SLSJ region (Dessureault, 1975).

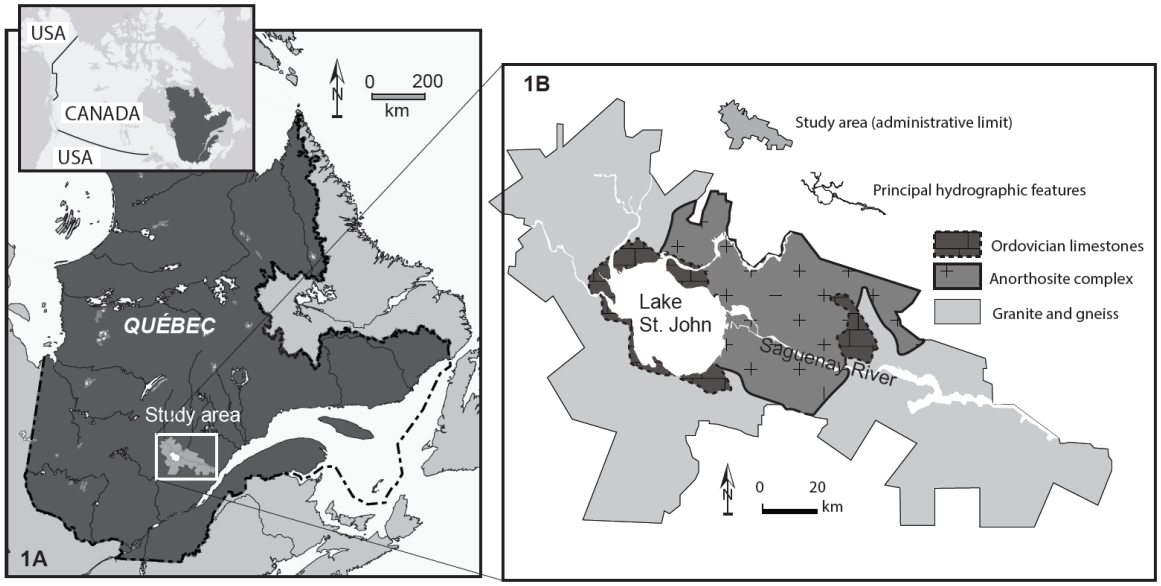

Figure 3.1 : A. Location of the study area and B, conceptual model of the geological features (adapted from CERM-PACES, 2013).

Groundwater quality has major implications for drinking water and other groundwater uses, such as agriculture and manufacturing. The SLSJ region is a perfect laboratory field for testing the hypotheses of groundwater salinization for the following

reasons: 1) a large hydrogeological database, including hydrogeochemical data, covering the entire region is available; 2) the graben topography implies that all surficial waters are drained toward the lowlands, thus defining a single watershed; 3) various aquifer types are known.

This study is based on a regional-scale dataset of 321 samples. The initial purpose of the sampling was to characterize the groundwater quality and the possible exposition of the local population to natural and/or anthropic contaminants (CERM-PACES, 2013). Therefore, sampling was conducted on existing private wells, usually used for drinking water supply. The physical characteristics of the sampling wells (location of the well screen, geology of the aquifer, casing depth) are poorly documented. Based on this regional database, this paper is a first attempt to statistically characterize groundwater chemistry in the SLSJ region with the goal of deciphering the possible geochemical evolution of groundwater controlled by the process of salinization. Another objective is to test whether this evolution is similar within two different types of aquifers: fractured rock and porous granular sediments.

Multivariate analyses are performed on the regional-scale dataset of 321 samples and the results are discussed by means of graphical representations (log-log plot, Piper plot). Based on the existing literature, chemical reactions are proposed to explain the chemical trends observed in the data. In the SLSJ region, the groundwater dynamic appears to be largely influenced by the topography of the graben that is responsible for

influencing the local discharge of contaminated groundwater (brines) from the deep crust involving natural cross-contamination issues.

3.4 GEOLOGY OF THE STUDY AREA

The study area in the SLSJ region in the province of Quebec, Canada (Figure 3.1A) covers 13,210 km^2, is oriented WNW-ESE and contains two important water bodies: Lake St. John (1,200 km^2) and the Saguenay River (Figure 3.1B), which is the main outlet of Lake St. John and is a tributary of the St. Lawrence River.

The following are the main geological features in the study area in chronological order:

1) Precambrian rocks of the Canadian Shield;
2) Ordovician limestone;
3) Pleistocene glacial drifts and fluvioglacial sediments;
4) Deep Pleistocene seawater deposits;
5) Pleistocene deltaic and shore deposits.

These features are described according to their chronostratigraphy in the following section.

3.4.1 FRACTURED ROCKS

The SLSJ region is located in the Allochthonous Polycyclic Belt (Rivers et al., 1989) in the Grenville Province of the Canadian Precambrian Shield (Laurin and Sharma, 1975).

The main Precambrian lithologies are plutonic rocks that range in composition from felsic to intermediate and consist of a gneissic complex of orthogneiss and paragneiss (Hébert and Lacoste, 1998). One major event was the emplacement of the enormous Lac-Saint-Jean anorthosite complex and other intrusions between 1157 and 1142 Ma, covering an area of approximately 20,000 km^2 (Woussen et al., 1988; Hervet et al., 1994; Higgins and van Breemen, 1996) (Figure 3.1B).

A few remnants of an Ordovician platform composed of sedimentary rocks are found in the Lake St. John and Saguenay lowlands. These remnants form a series of stratified sedimentary rocks, including siliciclastic strata, micritic limestones and highly fossiliferous alternating limestones and shales (Desbiens and Lespérance, 1989). A maximum thickness of 110 m has been recorded in the Ordovician sequence by drilling in the Saguenay area (CERM-PACES, 2013). The limestones (Figure 3.1B) occur along the northern, western and southern shores of the lake and are separated from the Saguenay outcrops by approximately 45 km of Precambrian rocks (Kénogami uplands).

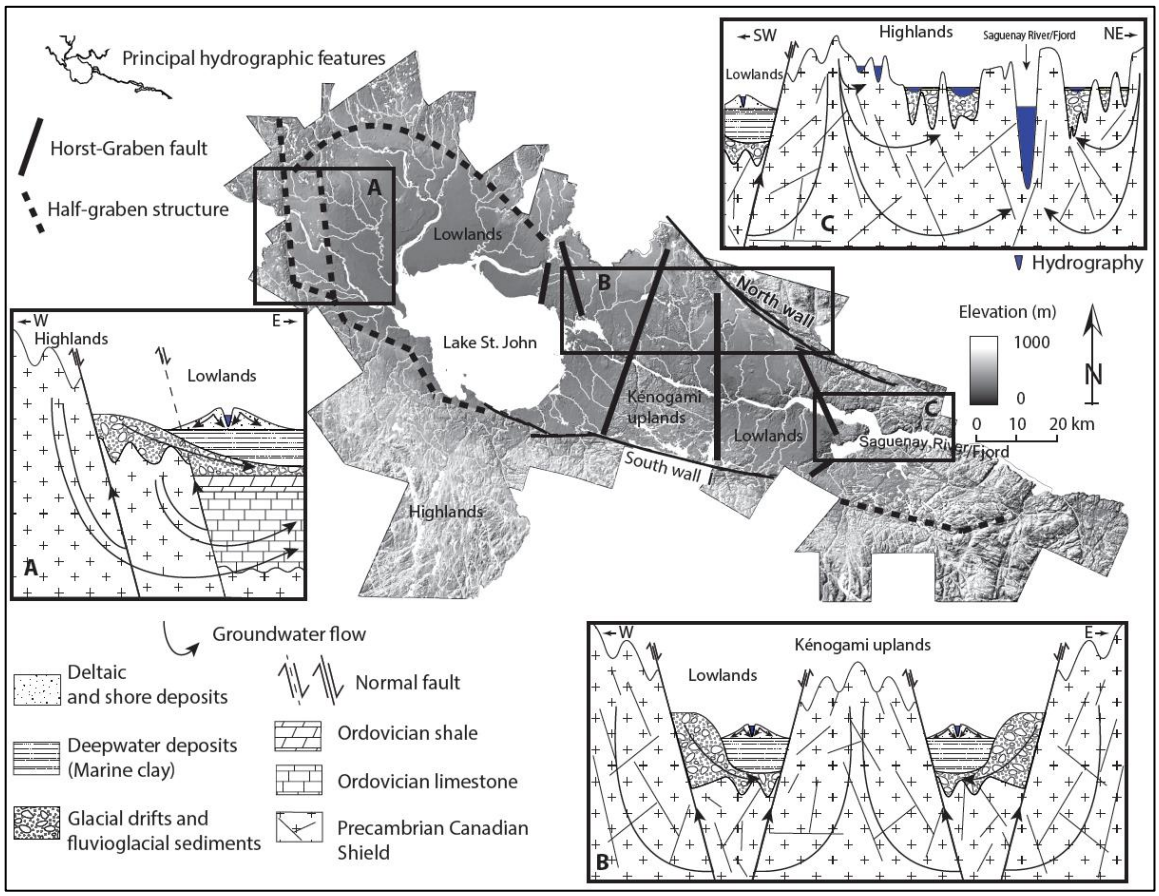

Figure 3.2 : Schematic of regional A, graben topography, B, major hydrogeological features and C, general flow lines.

3.4.2 BEDROCK TOPOGRAPHY

The bedrock that controls the topography is cut by the Phanerozoic Saguenay Graben that is approximately 30 km wide and is crossed by a NNE-SSW rise in the elevation of the bedrock (*Kénogami uplands*; Figure 3.2, model B). The northern and southern walls of the Saguenay Graben are bounded by WNW fault systems (Du Berger et al., 1991) that mark the limits between the lowlands (from 0 m to approximately 200 m above the sea level) and the highlands (up to 1000 m above sea level). Outcrops with

rugged terrain dominate the highlands (Figure 3.2, model C), whereas the topography of the lowlands is relatively flat due to the important local accumulations of Pleistocene deposits having a thickness of up to 180 m (CERM-PACES, 2013; Figure 3.2, model A).

The geological structures along the western side of the study area are oriented NNW-SSE (Figure 3.2; model A). In the northwestern portion of the study area, the delimitation between the highlands and the lowlands is not clear, thus giving an asymmetrical shape to the topography from north to south (half graben system, Figure 3.2). Remnants of Ordovician limestone units have been identified principally in the lowlands (Figure 3.2, model A), mostly at the border of the Lake St. John. Limestones are generally covered by sequences of Pleistocene deposits.

3.4.3 PLEISTOCENE DEPOSITS

In North America, the last glaciation began approximately 85,000 years ago during the early stage of the Wisconsinan period and ended approximately 7,000 years ago (Parent and Occhietti, 1988). During its retreat toward the west-northwest (orientation of the graben), the last glacier covering the region left a discontinuous and heterogeneous layer of till, several terminal moraines, glaciolacustrine deposits and important fluvioglacial esker deposits (Daigneault et al., 2011; Lasalle and Tremblay, 1978). The morphology of the graben in the study area controlled the local accumulation of up to 50 m of interbedded sand and coarse grain fluvioglacial sediments (CERM-PACES, 2013; Figure 3.2, models A, B and C).

After the retreat of the glacier, the lowlands in the area were invaded approximately 10,000 years ago by the Laflamme Sea (Dionne and Laverdière, 1969). This invasion resulted in a semi-continuous extensive layer of deep-water sediments consisting of laminated argillaceous silt and grey silty clay (Tremblay, 1971; Lasalle and Tremblay, 1978). The fine-grained sea deposits contain salty interstitial water (Bouchard et al., 1983) and are relatively abundant, with a thickness of up to 100 m in some areas within the limits of the graben (Dessureault, 1975; Figure 3.2, models A, B and C). The regional aquitard represents a confining layer for the underlying aquifers (Dessureault, 1975; CERM-PACES, 2013).

The isostatic uplift in response to the long-term subsidence of the region due to the weight of ice-forced the retreat of the Laflamme Sea (Lasalle et Tremblay, 1978; Bouchard et al., 1983). At that time, various facies of deltaic, littoral and pre-littoral sediments were emplaced on the top of the sedimentary sequences (Figure 3.2, models A, B and C). These sediments are laminated with a highly heterogeneous stratigraphy, layers with particle sizes ranging from silt to gravel (Daigneault et al., 2011), and a thickness of up to 100 m (CERM-PACES, 2013).

3.5 HYDROGEOLOGICAL BACKGROUND

During the complex geological history of the SLSJ region, several hydrogeological environments have been created. Confined and/or unconfined aquifers occur in the fractured rock and Pleistocene deposits and combine locally to form multilayered aquifers

(CERM-PACES, 2013), some of which are unconnected and some of which are interconnected (Chesnaux et al., 2012; Richard et al., 2014). Fluvioglacial sediments are the most productive regional aquifers. These aquifers are characterized by a hydraulic transmissivity (T) of 10^{-4} to 10^{-3} m^2/s and are consequently favored as a source of municipal drinkable water (CERM-PACES, 2013). These reservoirs are frequently covered by the regional marine clay aquitard (Dessureault, 1975; CERM-PACES, 2013) but can also be unconfined, particularly in the major valleys in the highlands that were not covered by the invading Laflamme Sea (Figure 3.2, model C). Deltaic and shore deposits exhibit variable T values ranging from 10^{-5} m^2/s to 10^{-2} m^2/s. These sediments constitute the major regional water-table aquifers (CERM-PACES, 2013).

Fractured rock aquifers exhibit relatively low values of T (10^{-6} to 10^{-5} m^2/s), with local maximum values of 10^{-3} m^2/s attributed to regional-scale deformation zones (Hébert and van Breemen, 2004; CERM-PACES, 2013). To date, no clear distinctions have been made between the hydraulic properties of Ordovician limestone and Precambrian rocks.

The regional hydrogeological flow systems can be divided into two major systems that characterize other graben topography (Meinken and Stober, 1997). In the highlands, groundwater infiltrates into a network of interconnected fractures and faults within igneous and metamorphic rocks (Figure 3.2, model A, B and C). In contrast, the regional water table in the lowlands replicates the topography (Figure 3.2, model A, B and C). Lake

St. John and the Saguenay River are the primary terminal discharge zones of the two regional groundwater flow systems.

3.5.1 HYDROGEOCHEMICAL BACKGROUND

The groundwater in the study area exhibits a wide range of chemical compositions (Dessureault, 1975; Simard and Des Rosiers, 1979; Walter et al., 2006; Walter, 2010; Rouleau et al., 2011; Roy et al., 2011; Walter et al., 2011; CERM-PACES, 2013). Although the groundwater in the SLSJ area is largely of good quality, brackish groundwater and water with excessive trace element concentrations relative to Canadian drinking water quality guidelines (Health Canada, 2014), such as fluoride (>1.5 mg/L), barium (>1 mg/L), manganese (>0.05 mg/L), iron (>0.3 mg/L) and aluminum (>0.1 mg/L), have recently been identified (CERM-PACES, 2013).

Simard and Des Rosiers (1979) presented an overview of several aquifers in the southern portion of Quebec. Among the 20 samples collected from the Precambrian bedrock in the SLSJ region, two occurrences of excessive fluoride content (>1.5 mg/L), one excessive chloride concentration (>250 mg/L), and one significant salinity value (>1000 mg/L) were observed. According to Dessureault (1975), the marine clay regional aquitard is responsible for the presence of brackish groundwater in the confined Pleistocene sediments. Moreover, Walter (2010) identified brackish groundwater in the bedrock at shallow depths (<100 m).

Walter (2010) suggests that the graben morphology of this region is responsible for the long residence time of the regional-scale flow system that discharges around Lake St. John (Figure 3.2). The observations of Walter (2010) agree with the Tóth (1999) model, in which the salinity of groundwater increases with the scale of the flow system (i.e., local-scale (fresh groundwater), intermediate-scale (fresh to brackish groundwater), or regional-scale (brackish groundwater to brine)).

3.6 METHODOLOGY

3.6.1 SAMPLING SITES AND GROUNDWATER SAMPLING LOCATION

In this study, 363 samples were collected from private and municipal wells as part of two hydrogeochemical mapping campaigns in the SLSJ region. The first campaign was conducted in 2004 and 2005 and focused on brackish groundwater in the bedrock (Walter, 2010). The second campaign was conducted in 2010 and 2011 to establish an overview of the groundwater quality of the fractured rock and granular aquifers (CERM-PACES, 2013).

A conventional and recognized protocol was used to collect and preserve the samples (Cloutier et al., 2006; Walter, 2010; Montcoudiol et al., 2013; Ghesquière et al., 2015). The chemical analyses were performed in certified laboratories using standard methods (Table 3.1). The sampling protocol included follow-up of selected physicochemical parameters when purging the wells (temperature; redox potential, Eh; pH; dissolved oxygen; and electrical conductivity; Table 3.1). Purging was complete when

the physicochemical parameters stabilized. The sampled water was filtered through a 0.45 µm filter and analyzed for major, minor and trace levels of 38 inorganic constituents (Table 3.1).

Table 3.1 : Summary statistical data for the 321 samples.

	N	Mean	Median	Min	Max	25	75	% det	Multivariate
TDS (mg/L)	321	611.8	280.4	12.1	8266.6	153.5	467.9	100%	
Temperature (Celcius)*	317	8.1	7.6	4.0	15.6	7.0	8.8	99%	
Redox potential (mV)*	283	49.0	82.9	-375.6	743.9	-21.2	108.4	88%	
pH*	318	7.7	7.5	4.4	10.8	6.5	8.1	99%	
Dissolved oxygen (mg/L)*	275	2.8	0.7	0.0	90.0	0.0	4.1	86%	
Bicarbonates**	***321***	***162.3***	***146.4***	***6.1***	***695.4***	***76.3***	***219.6***	***100%***	***x***
Silicium*	***321***	***6.2***	***5.7***	***0.220***	***16.0***	***4.8***	***7.3***	***100%***	***x***
Sodium*	***320***	***116.7***	***14.0***	***0.870***	***2500.0***	***3.7***	***74.8***	***100%***	***x***
Calcium*	***319***	***62.0***	***26.0***	***0.040***	***1500.0***	***10.0***	***58.0***	***99%***	***x***
Potassium*	***318***	***4.6***	***2.1***	***0.120***	***82.0***	***1.0***	***4.3***	***99%***	***x***
Magnesium*	***317***	***10.5***	***4.3***	***0.021***	***220.0***	***1.7***	***9.7***	***99%***	***x***
Chloride**	***317***	***212.9***	***10.0***	***0.160***	***4200.0***	***2.3***	***64.5***	***99%***	***x***
Strontium*	***317***	***1.5***	***0.2***	***0.003***	***37.0***	***0.1***	***0.7***	***99%***	***x***
Sulfates**	***316***	***31.2***	***11.0***	***0.200***	***530.0***	***4.8***	***20.0***	***98%***	***x***
Barium*	***303***	***0.103***	***0.041***	***0.003***	***2.800***	***0.018***	***0.090***	***94%***	***x***
Aluminium*	***292***	***0.014***	***0.007***	***0.001***	***0.230***	***0.004***	***0.014***	***91%***	***x***
Manganese*	***285***	***0.079***	***0.017***	***0.000***	***2.400***	***0.004***	***0.064***	***89%***	***x***
Zinc**	**260**	**0.035**	**0.014**	**0.002**	**0.710**	**0.008**	**0.031**	**81%**	***x***
Boron**	**250**	**0.150**	**0.046**	**0.004**	**3.400**	**0.013**	**0.180**	**78%**	***x***
Fluoride*****	234	0.923	0.700	0.060	4.900	0.300	1.500	73%	
Amonium*****	227	0.253	0.080	0.020	5.700	0.040	0.230	71%	
Copper**	213	0.014	0.004	0.001	0.350	0.002	0.013	66%	
Lead**	203	0.001	0.000	0.000	0.010	0.000	0.001	63%	
Iron**	173	1.051	0.120	0.002	35	0.048	0.370	54%	
Molybdene**	171	0.003	0.002	0.001	0.024	0.001	0.003	53%	
Nitrate***	136	0.896	0.300	0.020	8.600	0.100	1.075	42%	
Silver**	85	0.0004	0.0002	0.0001	0.0090	0.0001	0.0003	26%	
Nickel**	82	0.003	0.002	0.001	0.020	0.001	0.003	26%	
Bromide***	75	6.565	2.500	0.100	45.000	0.700	11.000	23%	
Lithium**	72	0.038	0.015	0.001	0.570	0.010	0.036	22%	
Uranium**	59	0.004	0.002	0.001	0.020	0.001	0.004	18%	
Chromium**	46	0.001	0.001	0.001	0.011	0.001	0.001	14%	
Vanadium**	18	0.003	0.003	0.002	0.007	0.002	0.003	6%	
Inorganic phosphorus*****	16	0.154	0.070	0.040	0.500	0.050	0.260	5%	
Cobalt**	15	0.002	0.001	0.001	0.007	0.001	0.003	5%	
Antimony**	9	0.002	0.002	0.001	0.005	0.001	0.003	3%	
Cadmium**	9	0.000	0.000	0.000	0.001	0.000	0.001	3%	
Tin**	3	0.002	0.002	0.001	0.003	0.001	-	1%	
Titanium**	3	0.002	0.001	0.001	0.004	0.001	-	1%	
Beryllium**	2	0.003	0.003	0.001	0.004	0.001	-	1%	
Selenium**	1	0.042	0.042	0.042	0.042	0.042	0.042	0%	
Bismuth**	1	0.001	0.001	0.001	0.001	0.001	0.001	0%	

ANALYTICAL METHODS
* multiparameter probe (in situ)
**Inductively Coupled Plasma Mass Spectrometry
*** Ionic chromatography
**** Specific probe
***** Titration
25 and 75 header = the first and the third quantiles
TDS is calculated using the software Aquachem v.5.0

For major, minor and trace elements, data are given in mg/L
For the physical parameters, N = number of mesured data
For the lab analysed parameters, N = Number of detected values
If N = 1 or 2: data are underlined
If N = 1: unique measured value is presented
If N = 2: mean value is presented

Multivariate header = parameters used in the multivariate analysis

Among the 363 samples, 42 groundwater samples with an electro-neutrality beyond ±10% were rejected (Hounslow, 1995; Appelo and Postma, 2005). Figure 3.3 shows the locations of the remaining 321 groundwater sample sites used in this study. Among these samples, 170 and 151 samples were collected from bedrock and granular deposit aquifers, respectively.

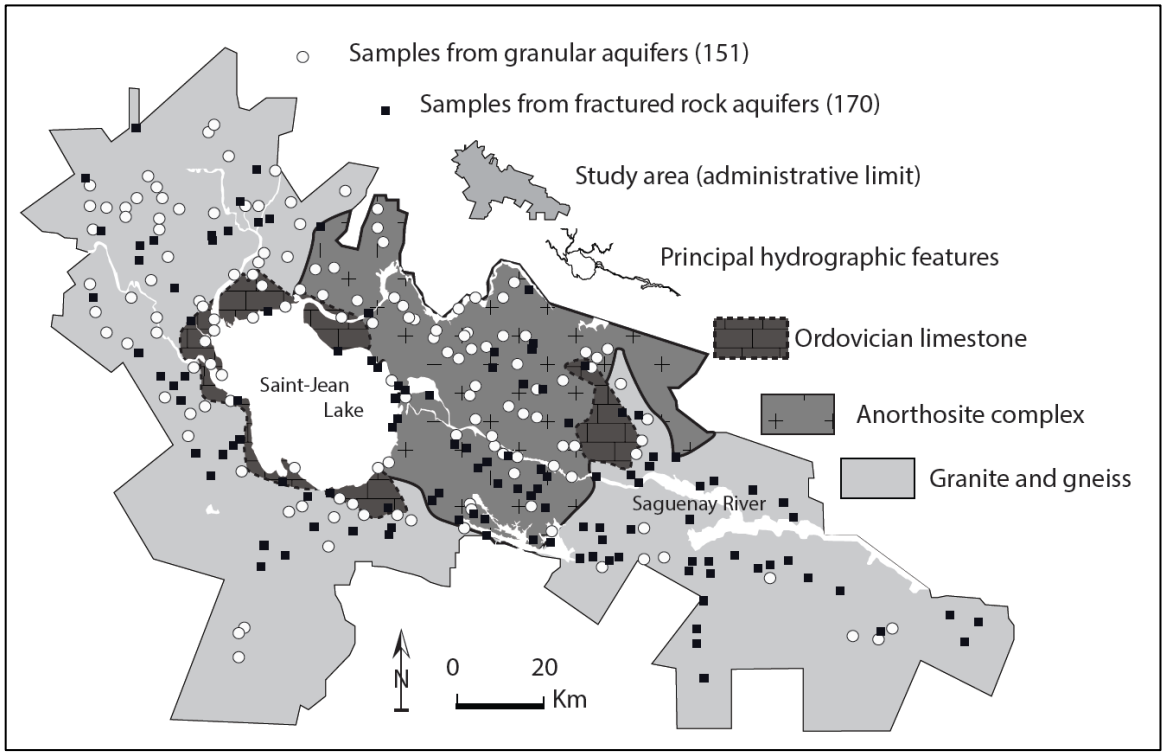

Figure 3.3 : Location of the 321 groundwater sample sites in this study.

3.6.2 Data processing

The proposed approach relies on a combination of: *hierarchical cluster analysis* (HCA), *principal component analysis* (PCA), binary plot investigations ([Na^+, Ca^{2+}, Br^-] *vs.* Cl^- ; Ca^{2+} *vs.* HCO_3^-; Ca^{2+} *vs.* Na^+) and Piper diagram interpretations. HCA is applied with the

objective of grouping end-member samples according to their chemical similarities. PCA is next applied to the same subset to reveal details relating to end-member chemistry. All samples from the regional dataset are plotted on binary plots and a Piper diagram to highlight groundwater chemical evolution. The data processing methods used to determine the geochemical characteristics of the samples and the evolution of the water are presented in the following sections as steps 1 through 3.

3.6.2.1 STEP 1: SELECTION OF THE CHEMICAL ELEMENTS USED IN MULTIVARIATE ANALYSIS

Censored data are not appropriate for many multivariate statistical techniques (Güler et al., 2002). Therefore, the non-detected, less-than, and greater-than values must be replaced by unqualified values (Farnham et al., 2002). When dealing with below detection limit (DL) or DL values for a given dataset, Farnham et al., (2002) showed that substitution with DL/2 gave better results than using DL or 0. Therefore, to prevent sample exclusion, we replaced DL concentrations by half the value of the detection limit (DL/2).

Irrelevant performances of all substitution methods have been obtained when the number of '<DL' values exceeded approximately 25% of the dataset (Farnham et al., 2002). For this reason, chemical parameters were selected with the aim of having less than 25% censored data.

3.6.2.2 STEP 2: MULTIVARIATE STATISTICAL ANALYSIS

Multivariate analyses are designed to highlight the linear correlations between variables and they assume that the values of the variables satisfy a normal statistical distribution (Brown, 1998). The Box-Cox power transformation was applied to the regional data set to represent the data as a normal distribution (Box and Cox, 1964; ArandaCirerol et al., 2006). Each of the selected variables (in major, minor and trace elements) were then standardized to unit variance. The standardized data were obtained for each element by subtracting the mean concentration of the element from each concentration and dividing by the standard deviation of the distribution (Davis, 2002). At that point, the values for each element were measured in standard deviation units, and the multivariate analysis could be performed. The software Statistica version 6.1 (Statsoft Inc., Ok, USA; 2013) was used to perform the multivariate statistical analysis.

Hierarchical cluster analysis

Hierarchical cluster analysis (HCA) is used to identify the optimal clustering in which the groundwater samples within each cluster are geochemically similar and the different clusters are geochemically dissimilar (Alvin, 2002). When applying HCA to the regional data set, the clusters that are obtained correspond to samples exhibiting similar geochemical characteristics. Consequently, the HCA produced different cluster samples, each characterized by particular chemical contents. In this manner, HCA helps to define chemical end-members of different origins within the study area. Specifically, the

Euclidian distance as a distance measure of similarities and Ward's method as a linkage rule are the best combination for producing the most distinctive groups when applied to groundwater chemical analysis (Güler et al., 2002; Cloutier et al., 2008; Templ et al., 2008).

Principal Component Analysis

Principal component analysis (PCA) was used with the aim of reducing and deciphering patterns within the large set of water chemistry data into principal components (PC). PC are expressed as linear functions of the chemical elements and the emphasis is on explaining the total variance of the subset of samples. We present PCA results on two different plots commonly referred to as *correspondence circle graphs*. In one graph, PCA values plot chemical element loadings while the second plots the sample scores.

3.6.2.3 STEP 3: GRAPHICAL REPRESENTATIONS OF THE INVESTIGATIONS

Binary diagrams

Investigations of salinization processes typically rely on log-log plots of Na^+, Ca^{2+} and Br^- concentrations *vs.* Cl^- concentrations. Chloride (Cl^-) plays a predominant role in groundwater salinization (Chebotarev, 1955; Tóth, 1985; Cloutier et al., 2010). Because seawater is the major source of Cl^- on Earth, the composition of groundwater is frequently compared with the composition of seawater to discuss the origin of salinity and, more

specifically, the possibility of mixing between dilute freshwater and a seawater end-member (Frape and Fritz, 1987). Moreover, many authors used this comparison to discuss the water/rock interaction control of saltwater chemistry (Frape and Fritz, 1987; Beaucaire et al., 1999; Walter, 2010). Geochemically conservative elements such as bromide (Br^-) are particularly relevant and useful for investigating salinization processes (Edmunds et al., 1985; Bottomley et al., 1999; Cloutier et al., 2010).

Piper diagram

As most of the interpretations presented in this paper are based on the major chemical elements of groundwater (Ca^{2+}, Na^+, Cl^-, HCO_3^-), the chemical results can be plotted on a Piper diagram (Piper, 1944) to interpret general geochemical evolution pathways of groundwater in the study area. Piper diagrams are widely used in the literature to illustrate trends in the chemical evolution of groundwater based on chemical facies.

3.7 RESULTS

Summary statistics regarding the chemical contents of the regional data set are presented in Table 3.1. The chemistry of the individual 321 samples is presented in the Supplementary Material (see the electronic appendix). Table 3.1 presents the number of analyses with values above the detection limit (*N*), the mean, the median, the first (*25*) and third (*75*) quartiles, the maximum (*Max)* and the minimum (*Min*) values. The

frequency of detection is calculated for each physicochemical parameters and is presented in Table 3.1 (% value). The frequency of detection corresponds to the percentage of *N* over the 321 samples of the dataset (% value = (*N*/321) × 100)). The chemical parameters for which the frequency of detection was >75% were used to perform the multivariate analyses. The selected parameters are marked in Table 3.1 using bold characters and checked in Table 3.1 (column *Multivariate*).

3.7.1 Hierarchical cluster analysis

HCA determined the levels of similarity for samples and presented the results in a dendrogram (Figure 3.4). The number of clusters increases when the position of the Phenon line is moved from top to bottom on the dendrogram. Owing to this subjective evaluation, HCA is a semi-objective method (Güler et al., 2002). For this study, four clusters provided the most satisfactory result. Descriptive statistics, the water and aquifer types for each cluster are presented in Table 3.2.

The largest cluster is Cluster 2 (N=274) mainly composed of Ca(Na)-HCO_3 samples (251/274). Almost half of these samples come from unconfined environments (127/274), and for around 25% of the Cluster 2 samples, the hydrogeological context is unknown (67/274). The median depth for Cluster 2 is 36 m, the shallowest median depth of all clusters. Chloride waters (calcium and sodium type) are also found in Cluster 2. The chloride waters could not be clustered from the bicarbonate waters by moving downward the Phenon line on the dendrogram. In comparison to the other clusters, Cluster 2

represents a freshwater end-member. Cluster 2 also presents some samples representative of intermediate chlorinated facies situated between Cluster 2 and the other clusters (Clusters 1, 3 and 4) dominated by chloride.

Cluster 1 is mainly composed of Na(Ca)-Cl waters (25/30). The bicarbonate type samples of Cluster 1 dominate the other samples of Cluster 1 (5/30). Cluster 3 is exclusively composed of Ca(Na)-Cl (12/12) type samples, with a large predominance of Ca-Cl waters (10/12). Cluster 4 is the smallest cluster with only five samples (over the 321 samples of this study) which all are of Na-Cl type. Confined conditions dominate in Clusters 1, 3 and 4. The median depth for Cluster 1 is 59 m.

Cluster 4 shows the highest mean TDS value (median value = 6 301 mg/L as well as the highest minimum and maximum TDS values (respectively 5573 ppm and 8267 ppm). The median depth for Cluster 4 is 69 m. In Cluster 4, 3 samples were collected in bedrock aquifers and 2 samples were collected in granular aquifers. Confining conditions dominate Cluster 4. The TDS values are decreasing from Cluster 4 to Cluster 2 (Cluster 2 median value = 233 ppm). The mean TDS value of Cluster 3 (median = 2860 ppm) is almost the double as the one of Cluster 1 (Median = 1670 ppm). All the samples in Cluster 3 were collected in fractured rock aquifers. Cluster 3 has the greatest median depth value (106 m). Fractured rock aquifers also dominate in Cluster 1 (22/30). It must be underlined that this study does not address the issue of distinguishing water chemistry from Ordovician limestone and from the crystalline basement.

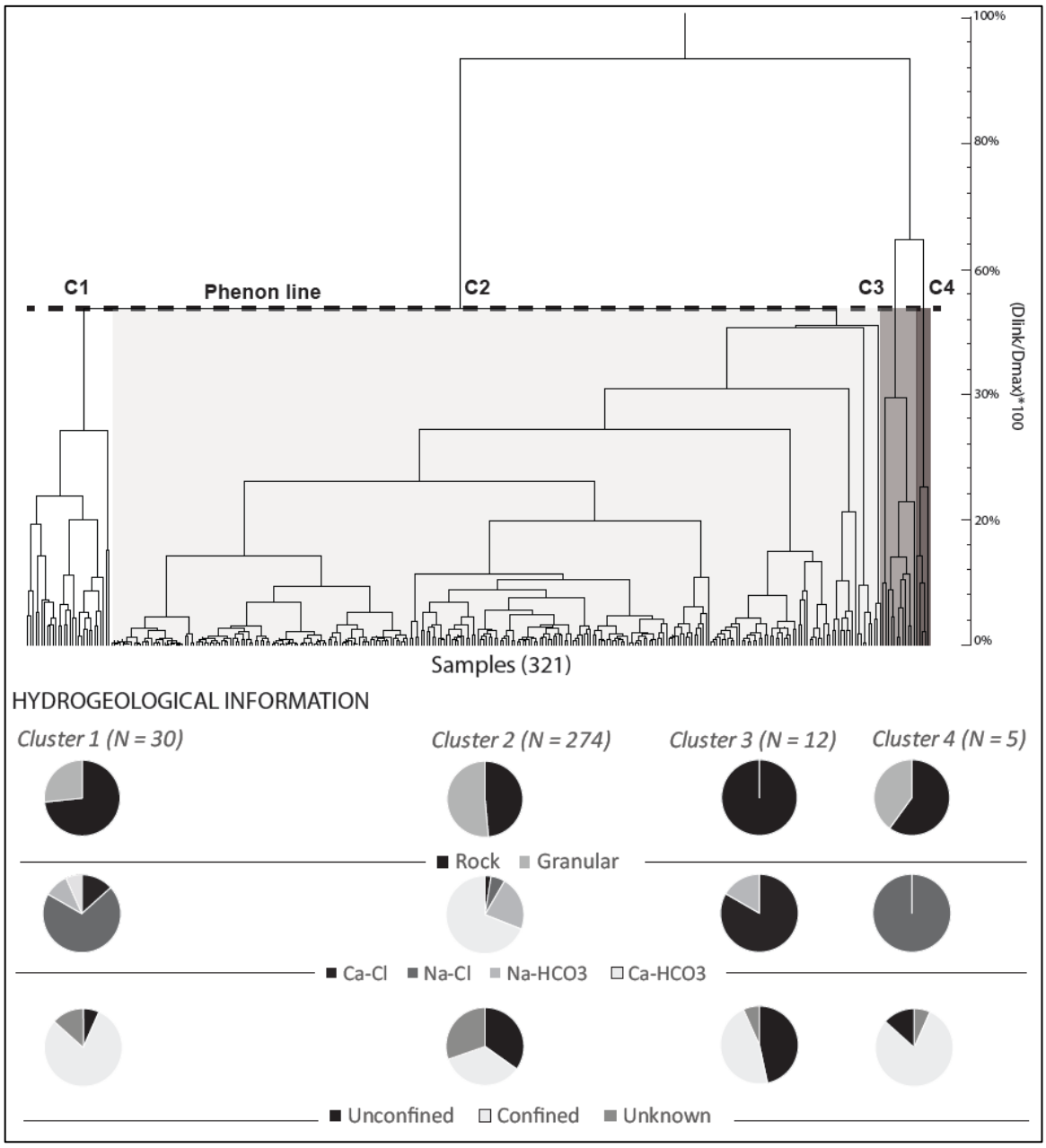

Figure 3.4 : Dendrogram produced from hierarchical cluster analysis. When Dlink is <60% of Dmax (i.e., position of the Phenon line), the samples are divided into four clusters (C1 to C4).

Table 3.2 : Water type, aquifer type, median depth of the sample wells and chemical content (median) of the four clusters obtained by hierarchical cluster analysis (HCA).

	Cluster 1 (N = 30)			Cluster 2 (N=274)			Cluster 3 (N=12)			Cluster 4 (N=5)		
Water type	Na-Cl (21) / Ca-Cl (4) Na-HCO3 (3) / Ca-HCO3 (2)			Na-Cl (16) / Ca-Cl (7) Na-HCO3 (62) / Ca-HCO3 (189)			Na-Cl (2) / Ca-Cl (10) Na-HCO3 (0) / Ca-HCO3 (0)			Na-Cl (5) / Ca-Cl (0) Na-HCO3 (0) / Ca-HCO3 (0)		
Aquifer type	Rock (22) / Granular (8)			Rock (133) / Granular (141)			Rock (12) / Granular (0)			Rock (3) / Granular (2)		
Hydrogeological Context*	UnC (2) / C (24) / UnK (4)			UnC (127) / C (77) / UnK (67)			UnC (4) / C (7) / UnK (1)			UnC (1) / C (4) / UnK (0)		
PARAMETER	**Min**	**Med**	**Max**	**Min**	**Med**	**Max**	**Min**	**Med**	**Max**	**Min**	**Med**	**Max**
Depth (m)	0	59	127	0	36	198	64	106	153	8	69	105
TDS (mg/L)	575	1670	4197	12	233	1237	2113	2860	5228	5573	6301	8267
Temperature (Celcius)**	5.8	7.7	13.3	4.0	7.7	15.6	6.1	7.4	9.2	4.9	7.5	7.8
Redox potential (mV) **	-375.6	-22.1	108.2	-314.1	90.8	743.9	-258.5	-17.0	108.4	-100.0	-21.8	27.9
pH **	5.5	7.7	10.1	4.2	7.5	10.8	5.2	7.6	8.6	6.5	7.2	7.6
Dissolved oxygen (mg/l)**	0.0	0.0	9.9	0.0	1.2	90.0	0.0	0.1	0.4	0.0	0.0	1.8
Sodium	**20**	**430**	**1400**	**1**	**9**	**410**	**180**	**335**	**790**	**1600**	**1900**	**2500**
Magnesium	**0.04**	**15.80**	**79.00**	**0.02**	**3.60**	**26.00**	**3.00**	**47.00**	**96.00**	**100.00**	**160.00**	**220.00**
Potassium	**0.54**	**14.00**	**34.00**	**0.12**	**1.80**	**20.00**	**1.60**	**4.05**	**14.00**	**16.00**	**64.00**	**82.00**
Calcium	**0**	**58**	**310**	**0**	**23**	**170**	**210**	**665**	**1500**	**60**	**120**	**520**
Bicarbonates	**87**	**295**	**683**	**6**	**134**	**438**	**6**	**106**	**232**	**134**	**464**	**695**
Chloride	**29**	**590**	**2400**	**0**	**8**	**560**	**1000**	**1650**	**3000**	**2700**	**3200**	**4200**
Sulfates	**1**	**70**	**400**	**0**	**10**	**110**	**1**	**76**	**300**	**330**	**420**	**530**
Barium	**0.01**	**0.07**	**0.76**	**0.00**	**0.04**	**1.20**	**0.04**	**0.17**	**2.80**	**0.02**	**0.04**	**0.20**
Boron	**0.03**	**0.36**	**3.40**	**0.00**	**0.03**	**0.75**	**0.05**	**0.30**	**0.81**	**0.46**	**0.66**	**0.82**
Strontium	**0.003**	**1.550**	**9.100**	**0.014**	**0.170**	**4.300**	**11.000**	**18.500**	**37.000**	**1.400**	**3.700**	**27.000**
Silicium	**0.22**	**6.80**	**11.00**	**1.30**	**5.70**	**16.00**	**1.30**	**4.80**	**6.50**	**4.80**	**9.60**	**13.00**
Manganese	**0.0003**	**0.0355**	**0.1900**	**0.0004**	**0.0130**	**2.4000**	**0.0180**	**0.0855**	**0.7100**	**0.0430**	**0.0890**	**0.6100**
Fluoride	0.60	1.60	4.90	0.10	0.50	2.90	0.06	1.35	2.40	0.80	1.10	1.20
Aluminium	**0.002**	**0.007**	**0.087**	**0.001**	**0.007**	**0.230**	**0.004**	**0.010**	**0.026**	**0.005**	**0.009**	**0.020**
Bromide	0.43	2.93	19.44	0.10	0.51	5.96	13.82	19.23	45.00	10.00	12.00	19.00
Iron	0.005	0.150	3.100	0.002	0.115	35.000	0.008	0.093	17.000	0.190	1.000	1.300
Lithium	0.003	0.020	0.180	0.001	0.012	0.021	0.003	0.070	0.570	0.018	0.037	0.120
Zinc	**0.004**	**0.011**	**0.150**	**0.002**	**0.015**	**0.710**	**0.003**	**0.010**	**0.064**	**0.010**	**0.044**	**0.100**
Lead	0.0001	0.0002	0.0080	0.0001	0.0003	0.0073	0.0006	0.0080	0.0100	0.0080	0.0080	0.0080
Amonium	0.05	0.69	1.80	0.02	0.07	1.10	0.12	1.50	5.70	2.20	2.60	3.00
Copper	0.0008	0.0018	0.0070	0.0005	0.0050	0.3500	0.0006	0.0028	0.0220	0.0030	0.0030	0.0030
Molybdenium	0.0006	0.0033	0.0240	0.0005	0.0017	0.0180	0.0017	0.0059	0.0065	0.0014	0.0015	0.0150
Nickel	0.0009	0.0020	0.0098	0.0010	0.0018	0.0200	0.0009	0.0020	0.0020	0.0016	0.0018	0.0020
Silver	0.0001	0.0003	0.0090	0.0001	0.0002	0.0019	0.0002	0.0002	0.0002	0.0002	0.0002	0.0002
Uranium	0.0011	0.0019	0.0024	0.0010	0.0023	0.0200	*<DL*	*<DL*	*<DL*	0.0012	0.0016	0.0018
Chromium	0.0005	0.0008	0.0010	0.0005	0.0010	0.0110	0.0010	0.0010	0.0010	0.0005	0.0015	0.0024
Nitrate	0.40	0.43	0.46	0.02	0.30	8.60	*<DL*	*<DL*	*<DL*	*<DL*	*<DL*	*<DL*
Cobalt	*<DL*	*<DL*	*<DL*	0.0006	0.0014	0.0066	*<DL*	*<DL*	*<DL*	*<DL*	*<DL*	*<DL*
Inorganic phosphorus	0.05	0.08	0.11	0.04	0.14	0.50	0.06	0.06	0.06	0.04	0.04	0.04
Vanadium	*<DL*	*<DL*	*<DL*	0.0020	0.0026	0.0069	*<DL*	*<DL*	*<DL*	*<DL*	*<DL*	*<DL*
Antimony	*<DL*	*<DL*	*<DL*	0.0010	0.0016	0.0052	*<DL*	*<DL*	*<DL*	*<DL*	*<DL*	*<DL*
Cadmium	*<DL*	*<DL*	*<DL*	0.0002	0.0003	0.0007	*<DL*	*<DL*	*<DL*	*<DL*	*<DL*	*<DL*
Selenium	*<DL*	*<DL*	*<DL*	0.0420	0.0420	0.0420	*<DL*	*<DL*	*<DL*	*<DL*	*<DL*	*<DL*
Tin	0.003	0.003	0.003	0.0011	0.0016	0.0021	*<DL*	*<DL*	*<DL*	*<DL*	*<DL*	*<DL*
Titanium	*<DL*	*<DL*	*<DL*	0.0010	0.0013	0.0044	*<DL*	*<DL*	*<DL*	*<DL*	*<DL*	*<DL*
Beryllium	*<DL*	*<DL*	*<DL*	0.0008	0.0026	0.0044	*<DL*	*<DL*	*<DL*	*<DL*	*<DL*	*<DL*
Bismuth	*<DL*	*<DL*	*<DL*	0.0007	0.0007	0.0007	*<DL*	*<DL*	*<DL*	*<DL*	*<DL*	*<DL*

* Unconfined (UnC); Confined (C); Unknown (UnK)
** multiparameter probe (in situ); TDS is calculated using the software Aquachem v.5.0
For major, minor and trace elements, data are given in mg/L
Under Detection Limit (<DL)
Non Applicable (NA)
Parameters presented in bold characters have been selected for multivariate treatment

In Clusters 2 and 4, the numbers of samples from granular aquifers and the number of samples from fractured rock aquifers are almost the same. Based on HCA fundamentals, this observation suggests that brackish groundwater samples grouped in Cluster 3 and collected in the bedrock aquifers are chemically distinct from the brackish groundwater samples that are grouped in Clusters 1, 2 and 4.

3.7.2 Principal component analysis

To investigate the similarities/dissimilarities between clusters, the samples were plotted on the PCA correspondence circle according to the cluster to which they belong (Figure 3.5A). The horizontal axis of the correspondence circle corresponds to the first principal component (Component 1; 38.3% of the total variance of the data set) and the vertical axis corresponds to the second principal component (Component 2; 14.3% of the total variance of the data set).

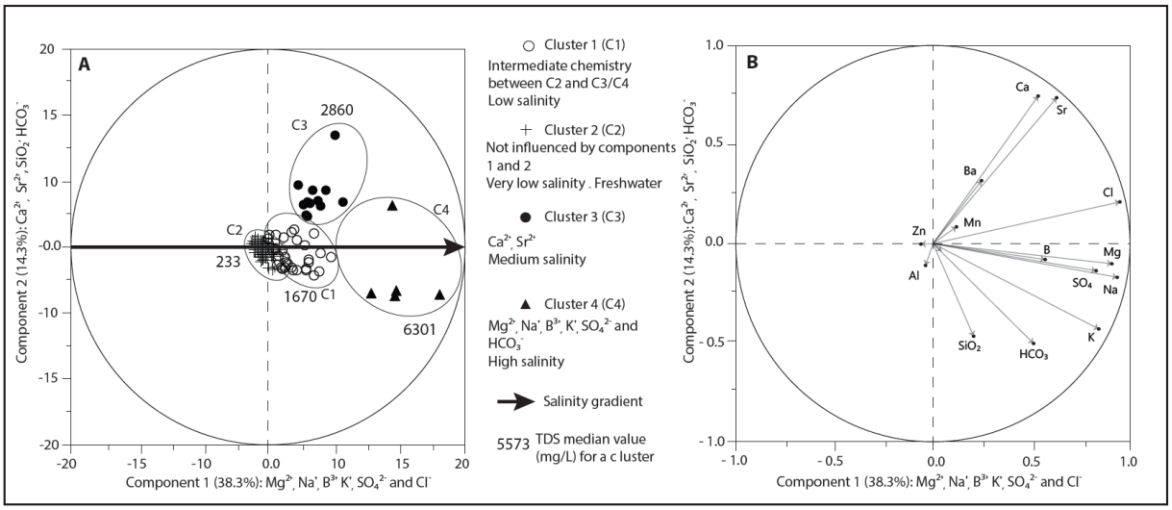

Figure 3.5 : Graphical presentation of the first two components derived from principal component analysis (PCA). Component 1(K^+, Na^+, Mg^{2+}, SO_4^{2-} and Cl^-) explained 38.3% of the total variance of the data set while Component 2 and the vertical axis corresponds to the second principal component (Sr^{2+}, Ca^{2+}) explained 14.3%. A, PCA diagram of samples classified by cluster membership. B, PCA presenting the chemical element loadings.

The samples of Cluster 2 are located on the middle left part of the graph. The samples of Cluster 1 are located at an intermediate position between the samples of

Cluster 2 and Clusters 3 and 4. From left to right along Component 1, TDS increases and groundwater samples evolve gradually from bicarbonate (Clusters 2; Table 3.2) to brackish (Clusters 1, 3 and 4; Table 3.2) types. Component 1 is thus defined as representing an increasing salinity gradient from left to right on Figure 3.5A.

Chemical element loadings are presented in Table 3.3. Table 3.3 reveals that Component 1 loadings are dominated by Cl^- (0.947) and that positive and negative loadings for Component 2 constrain chemical elements in two distinct groups: Group 1 (positive load): Ca^{2+}, Ba^{2+}, Sr^{2+}, and Mn^{2+} and Group 2 (negative load): Mg^{2+}, Na^+, B^{3+}, SiO_2, K^+, SO_4^{2-}, and HCO_3^-. Chemical element loadings for Components 1 and 2 are plotted in the correspondence circle in Figure 3.5B. The distribution for Group 1 fits with the distribution of samples for Cluster 3, and the distribution for Group 2 fits with the distribution of samples for Cluster 4. Clusters 3 samples and one sample for Cluster 4 are in the upper right quadrant of the correspondence circle. This distribution is due to Component 2 scores that are positive for Cluster 3 samples and negative for Cluster 4 samples. Cluster 3 correspond exclusively to brackish groundwater collected in the bedrock aquifers (Table 3.2), their distribution in Figure 3.5A suggests that chemical elements in Group 1 (Ca^{2+}, Ba^{2+}, Sr^{2+}, and Mn^{2+}) characterize samples in Cluster 3 and that chemical elements in Group 2 (Mg^{2+}, Na^+, B^{3+}, SiO_2, K^+, SO_4^{2-}, and HCO_3^-) preferentially characterize samples in Cluster 4. Moreover, it also suggests that an increase of the salinity enhances the fingerprint of the rock type aquifer on the groundwater chemistry.

Table 3.3 : Chemical element loadings for Components 1 and 2 and the explained variance as obtained by principal component analysis (PCA).

Parameter	Component 1	Component 2
K^+	0.839	-0.434
Na^+	0.933	-0.172
Ca^{2+}	0.533	0.742
Mg^{2+}	0.909	-0.107
Mn^{2+}	0.121	0.081
B^{3+}	0.561	-0.087
Zn^{2+}	-0.063	-0.008
Cl^-	0.947	0.206
Sr^{2+}	0.626	0.733
SO_4^{2-}	0.830	-0.138
Ba^{2+}	0.248	0.313
Al2+	-0.041	-0.112
SiO_2	0.207	-0.486
HCO_3^-	0.505	-0.506
Explained variance	7.155	0.024
Explained variance (%)	38.3	14.3
Cumulative % of variance	38.3	52.6

3.7.3 Geographical distribution of clusters

Figure 3.6 presents the geographical distribution of clusters according to the principal rock type units (anorthosite complex, limestones, granite and gneiss). The samples from Cluster 1 are predominately distributed near limestone units (24/30 samples) and a pair of Cluster 1 samples are in the highlands. The distribution of Cluster 2 samples is uniform over the region. The Cluster 3 samples are located close to the major geological structures of the graben (fault) and 8 of 12 Cluster 3 samples are located within the anorthosite complex. The samples of Cluster 4 are near limestone and 4 of 5 of them are located around the Lake St. John area.

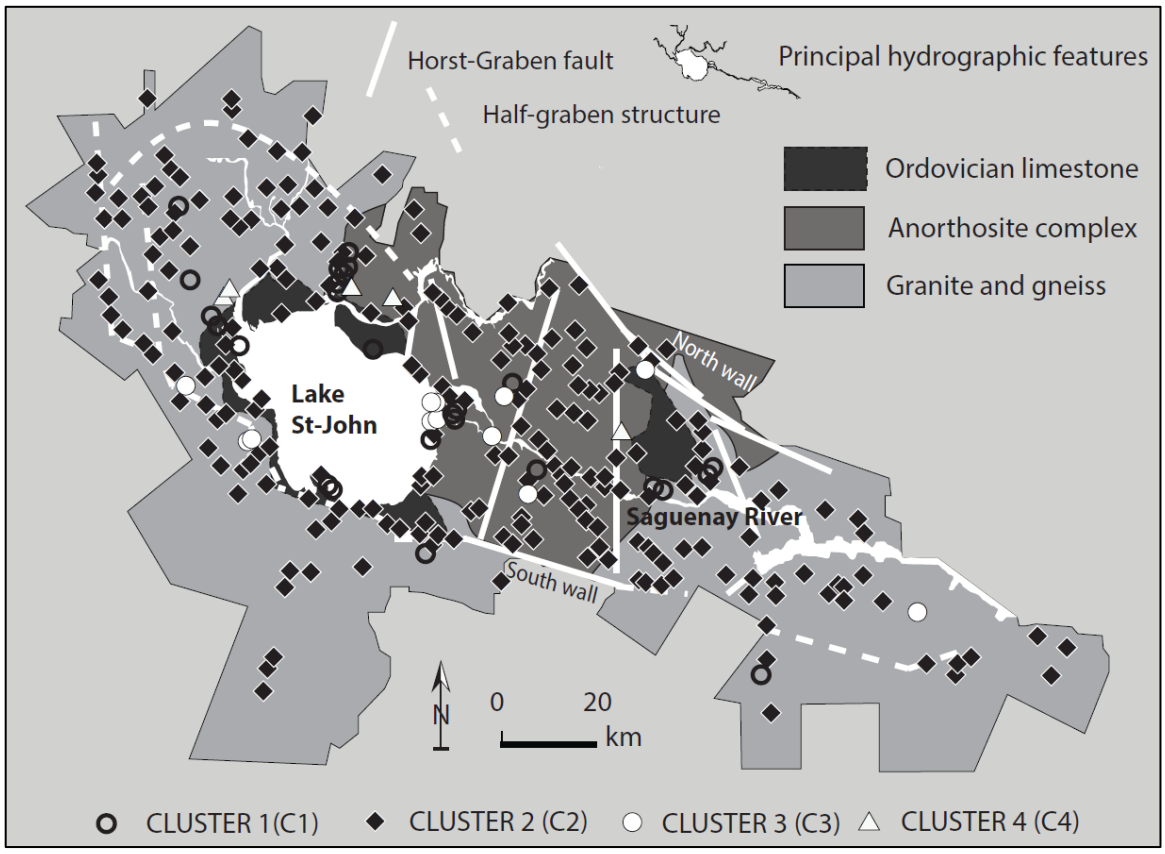

Figure 3.6 : The simplified geological map of the study area used to locate the 321 groundwater samples according to their belonging cluster. The distribution of Cluster 2 samples is uniform over the region. The samples from Cluster 1 are predominately distributed near limestone units. The Cluster 3 samples are located close to the major geological structures of the graben (fault) and 8 of 12 Cluster 3 samples are located within the anorthosite complex. The samples of Cluster 4 are located around the Lake St. John area.

3.8 DISCUSSION

In the following graphs, the samples are represented with respect to their membership in an HCA cluster. Seawater dilution lines were defined using seawater ratios from Goldberg (1971).

3.8.1 Recharge groundwater and water/rock interactions – Ca^{2+} VS HCO_3^-

The log-log plot of Ca^{2+} *vs.* HCO_3^- (Figure 3.7) indicates the strong positive linear correlation between Ca^{2+} and HCO_3^-, particularly for samples in which the Ca^{2+} concentrations remain unchanged with increasing Cl^- concentrations. The correlation between the $Ca^{2+}$and HCO_3^- concentrations in Figure 3.7 follows the calcite and plagioclase dissolution/precipitation trends (Figure 3.7; $[Ca^{2+}] = 2[HCO_3^-]$):

$$3H_2O + 2CO_2 + CaAl_2Si_2O_8 \Leftrightarrow Al_2Si_2O_5(OH)_4 + Ca^{2+} + 2HCO_3^- \quad \text{(Eq. 1)}$$
(Anorthite) (Kaolinite)

$$CaCO_3 + H_2O + CO_2 \Leftrightarrow Ca^{2+} + 2HCO_3^- \quad \text{(Eq. 2)}$$
(Calcite)

This observation strengthens the hypothesis that most of the samples of Cluster 2 correspond principally to recharge groundwater, primarily in unconfined hydrogeological environments (Table 3.2). This observation also implies that the dissolution of calcite and/or anorthite minerals is a fundamental process for inducing the initial geochemical footprint at the beginning of the chemical evolution of groundwater, i.e., in recharge areas.

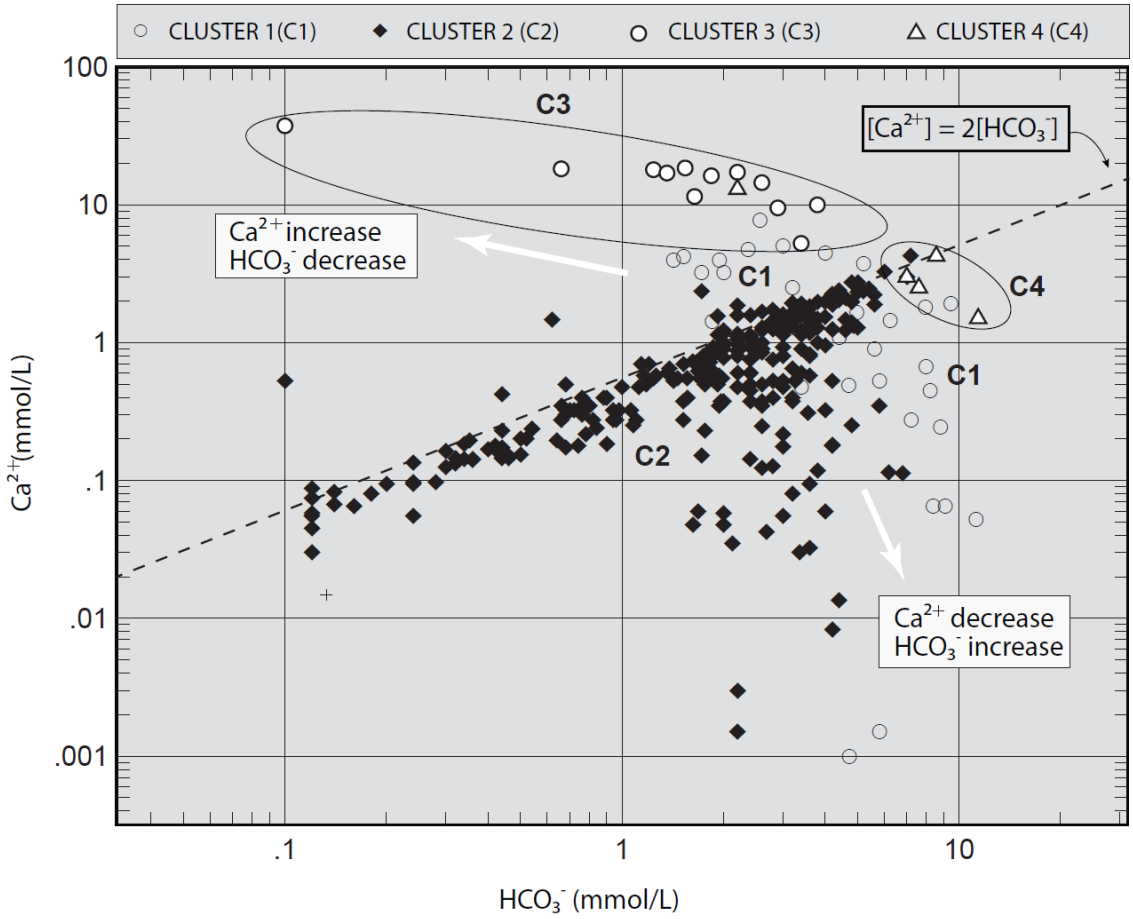

Figure 3.7 : Log-log plot of bicarbonate versus calcium concentrations (in mmol/L) plotted against to the dissolution trends of calcite ($[Ca^{2+}] = 2[HCO_3^-]$) and anorthite plagioclase ($[Ca^{2+}] = 3[HCO_3^-]$).

Another set of reactions leading to the same conclusion is the dissolution of labradorite, a common mineral of the anorthosite complex of the region:

$$2NaCaAl_3Si_5O_{16} + 9H_2O + 6CO_2 \Leftrightarrow 3\ Al_2Si_2O_5(OH)_4 + 4\ SiO_2aq + 2\ Na^+ + 2\ Ca^{2+} + 6HCO_3^-$$
(Labradorite) (Kaolinite)

(Eq. 3)

$$2NaCaAl_3Si_5O_{16} + 6H_2O + 6CO_2 \Leftrightarrow 2Al_2Si_2O_5(OH)_4 + 2NaAlSi_3O_8 + 2\ Ca^{2+} + 4HCO_3^-$$
(Labradorite) (Kaolinite) (Albite)

(Eq. 4)

Thus, the weathering of labradorite (anorthosite) produces clay, albite (albitization of labradorite) and a Ca-HCO_3 water.

The samples in Cluster 4 exhibit a slight increase in HCO_3^- content that is accompanied by a decrease in Ca^{2+} content. PCA results confirm the influence of HCO_3^- on the chemistry of Cluster 4 samples (Figure 3.5).

Ca^{2+} may result from incongruent reactions of magnesian carbonates and having various relationships with HCO_3^-. Incongruent dolomite and limestone dissolution is caused by the difference in solubility products of the two minerals. When water is saturated for calcite, it remains undersaturated for dolomite (or any magnesian limestone) and dissolution of the magnesian minerals will continue and resulting in the precipitation of Ca^{2+} and CO_3^{2-} ions to conserve the equilibrium for calcite (Wigley, 1973; Aquilina et al., 2003). However, these reactions are mostly observed in karst systems (Aquilina et al., 2003) and karst systems are sparse in the study area.

According to Equation 4, the HCO_3^- content is attributable to the dissociation of water molecules in the presence of CO_2:

$$H_2O + CO_2 \Leftrightarrow H_2CO_3^- \Leftrightarrow H^+ + HCO_3^- \qquad \text{(Eq. 5)}$$

The excess of HCO_3^- in Cluster 4 samples relative to the dissolution of calcite/anorthite can be interpreted as the result of any reaction that produces CO_2

(organic matter degradation, sulfate reduction/calcite-dolomite dissolution, etc.). Adding HCO_3^- results in calcite precipitation—according to Equation 3 in reverse—and thus the removal of dissolved Ca^{2+} from the solution and a decrease in the Ca^{2+} concentration.

The diminishing HCO_3^- concentrations in the Cluster 3 samples is accompanied by an increase in Ca^{2+} content (Figure 3.7). This agrees with the PCA results that showed the predominant role of Ca^{2+} in the chemistry of the samples of Cluster 3 (Table 3.2 and Figure 3.5). When groundwater reaches calcite saturation in the presence of CO_2, Ca^{2+} precipitates as secondary calcite (Eq. 5; Stober and Bucher, 1999). This process is evident in the minerals observed in the fractures, veins and cavities of the Canadian Shield rocks (Gascoyne and Kamineni, 1994). With the consumption of all available CO_2, no more HCO_3^- is available in solution. However, Ca^{2+} will continue to be released during anorthite plagioclase alteration according to Equation 6 (Stober and Bucher, 1999), in which the CO_2 in Equation 1 is replaced by H^+ ions.

$$\underset{\text{(Anorthite)}}{CaAl_2Si_2O_8} + 2H_2O + CO_2 \rightarrow \underset{\text{(Kaolinite)}}{Al_2Si_2O_5(OH)_4} + \underset{\text{(Calcite)}}{CaCO_3} \qquad \text{(Eq. 6)}$$

$$\underset{\text{(Anorthite)}}{CaAl_2Si_2O_8} + 2H^+ + H_2O \rightarrow Ca^{2+} + \underset{\text{(Kaolinite)}}{Al_2Si_2O_5(OH)_4} \qquad \text{(Eq. 7)}$$

The control of the plagioclase weathering process on the chemical evolution of groundwater within fractured rock aquifers is also suggested by the PCA results. Ba^{2+} and Sr^{2+} are commonly incorporated as trace elements in the crystalline structure of feldspar

plagioclase minerals (Beaucaire et al., 1982; Hem, 1986). In Figure 3.5, these two chemical elements, in particular, characterize the chemistry Cluster 3 samples.

3.8.2 Salinization processes

The Cl^-/Br^- ratios (based on ppm) are often used to provide insight into the marine origin of salinity in groundwater (Carpenter, 1978; Frape et al., 1984; Montcoudiol et al., 2014). In comparing ratios with seawater ratios (Cl^-/Br^- = 288; Stober and Bucher, 1999), groundwater Cl^-/Br^- ratios can indicate if a brine has undergone Br^- enrichment or Cl^- depletion (relative to seawater). For comparison, water derived from dissolved Tertiary halite deposits of the East African Rift System (EARS) has a Cl^-/Br^- ratio of 2400 while the average Cl^-/Br^- ratio for crystalline rocks is below Cl^-/Br^- = 100 (Stober and Bucher, 1999).

In Figure 3.8C, Br^- enrichment (or Cl^- depletion) relative to seawater is apparent for Cluster 3 samples, whereas the samples of Cluster 4 tend to follow the seawater dilution line. Cluster 4 waters have a Cl^-/Br^- ratio = 266 (Cl^-/Br^- seawater = 283; Goldberg, 1971). Cluster 3 waters have a Cl^-/Br^- ratio around 88, close to that of crystalline rocks (Stober and Bucher, 1999) suggesting a basement origin for chloride in Cluster 3. Many Cluster 2 samples also have low Cl^-/Br^- ratios (~85) suggesting that salinization is related to basement fluids for these samples as well.

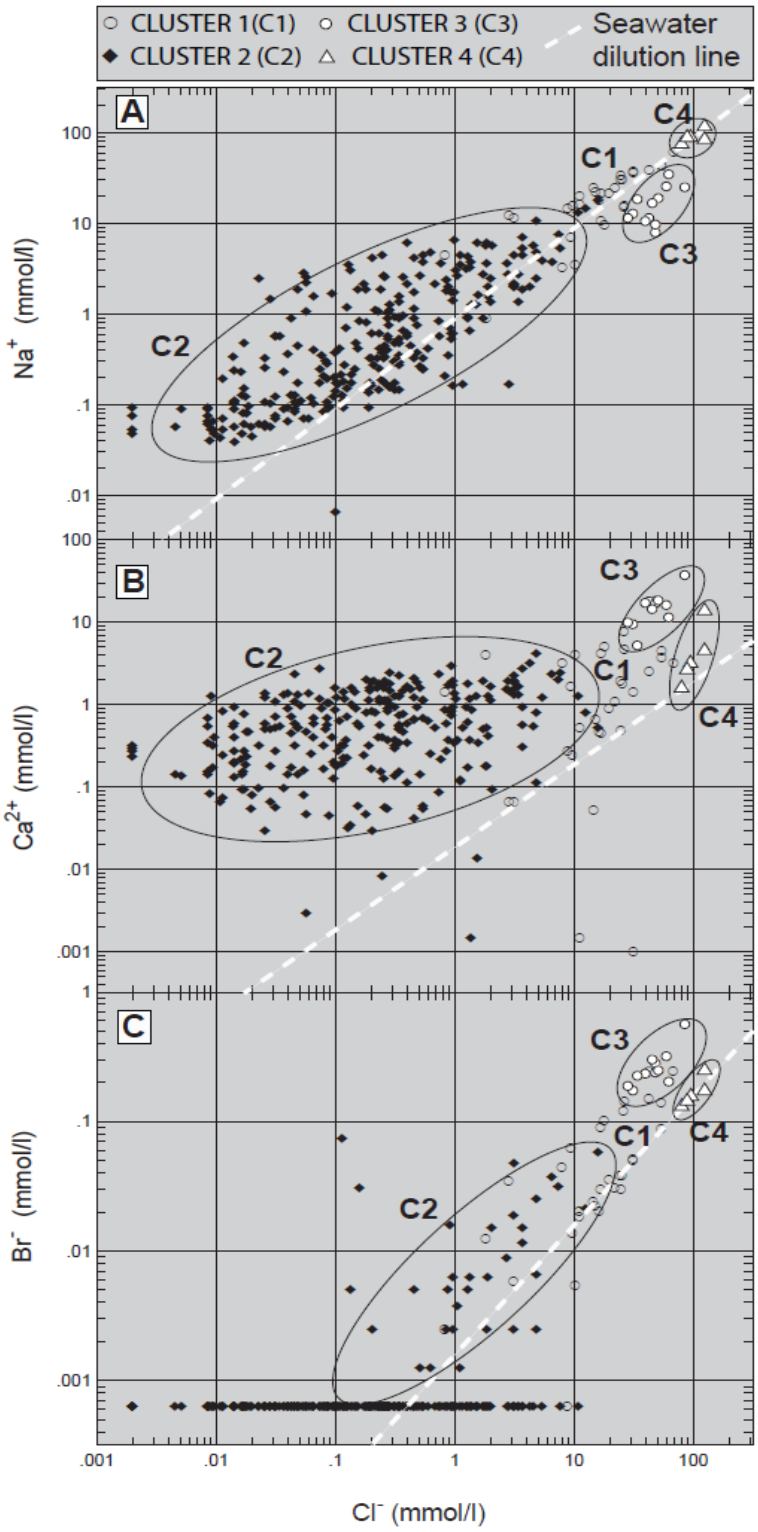

Figure 3.8 : Log-log plots of A, Na^+ versus Cl^- concentrations (in mg/L) and B, Ca^{2+} versus Cl^- concentrations (in mg/L); and C: Br^- versus Cl^- concentrations (in mg/L). Seawater (SW) dilution lines were defined using seawater ratios from Goldberg (1971).

The Na^+/Cl^- ratios for Cluster 3 are slightly depleted in Na^+ relative to those of seawater (Figure 3.8A). Na^+/Cl^- ratios lower than those in seawater have been observed in saline groundwater in granitic rocks in the United Kingdom (Edmunds et al., 1984) and France (Beaucaire et al., 1999). In both studies, the low Na^+/Cl^- ratios relative to seawater are attributed to equilibration with secondary aluminosilicates and thus a predominance of water/rock interaction processes. Cluster 3 samples follow this trend. The Na^+/Cl^- ratios for Cluster 4 samples are slightly enriched in Na^+ and are very similar to the Na^+/Cl^- ratios of seawater.

Enrichment relative to seawater was also observed for the Ca^{2+}/ Cl^- ratios (Figure 3.8B), particularly for the Cluster 3 samples relative to the Cluster 4 samples. In this figure, the linear relationship between Ca^{2+} and Cl^- is striking. Calcium exhibits a strong positive linear correlation with Cl^- in deep saline groundwaters in the Canadian Shield (Frape et al., 1984; Frape and Fritz, 1987; Bottomley, 1996).

The Ca^{2+}/Na^+ ratios for the Cluster 4 samples are very similar to those of seawater (Figure 3.9). The Cluster 4 samples tend to reach the seawater dilution line (Figure 3.9). For these samples, the salinization process might then correspond to the mixing between a seawater end-member (Na-Cl of Cluster 4) and more diluted water containing (Ca, Na)-HCO_3 (Clusters 1 and 2) (Salinization path 2; Figure 3.9).

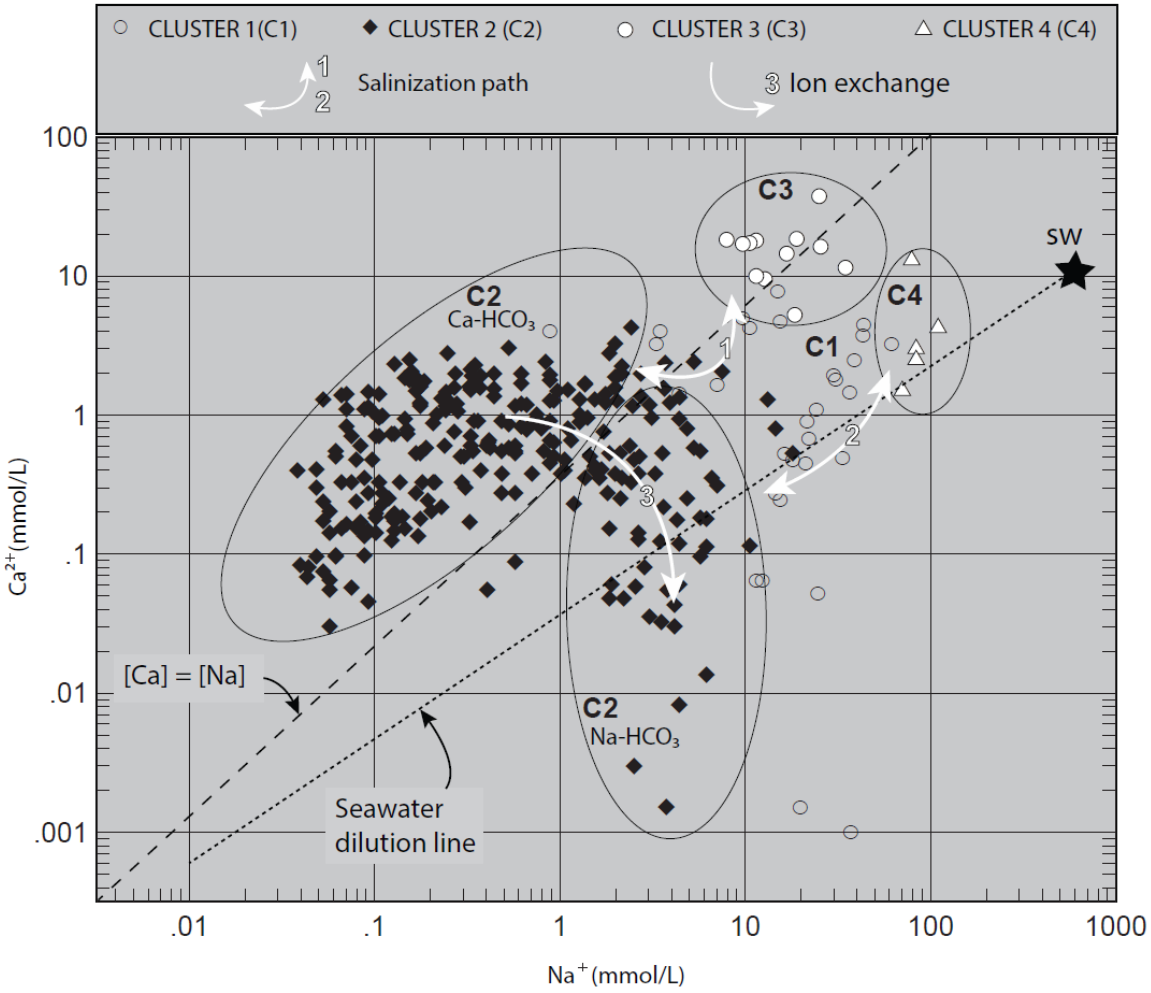

Figure 3.9 : Log-log plots of Na^+ versus Ca^{2+} concentrations (in mmol/L). The seawater (SW) dilution line was defined using the seawater ratios from Goldberg (1971). Salinization path 1 corresponds to the geochemical evolution from Cluster 2 ($Ca\text{-}HCO_3$) to Cluster 3 (Ca-(Na)-Cl) groundwater samples. Salinization path 2 corresponds to the mixing between a seawater end-member (Na-Cl of Cluster 4) and more diluted water containing (Ca, Na)-HCO_3 (Cluster 2). Salinization path 3 corresponds to groundwater evolution under Ca^{2+}_{WATER}-$Na^+_{MINERAL}$ ion exchange process.

Gascoyne and Kamineni (1994) presented a model for different types of crystalline rocks in the Canadian Shield, in which the near surface groundwater ($Ca\text{-}HCO_3$ in composition) evolves into slightly more mature groundwater ($Na\text{-}HCO_3$ in composition) as

it moves along the flow paths and increases with depth (~250 m). At greater depths (>1000 m), all groundwaters tend toward a (Ca-Na)-Cl composition. For samples of Cluster 3, the salinization process corresponds to the geochemical evolution from Cluster 2 (Ca-HCO_3) to Cluster 3 (Ca-(Na)-Cl) groundwater (Salinization path 1; Figure 3.9).

Cluster 1 samples stand in an intermediate position between both Clusters 2 and 3 and between Clusters 2 and 4 (Figure 3.9). Cluster 1 as well as some Cluster 2 samples within the field of Cluster 1 samples correspond to groundwater that may have undergone mixing and dilution between fresh and brackish groundwater that evolved along Salinization paths 1 or 2.

3.8.3 CA^{2+}_{WATER}-$NA^{+}_{MINERAL}$ ion exchange

Ion exchange reactions in these confining layers may underlie the desorption of Na^+ from the Na-Cl-rich seawater according to Equation 8 (where $X_{(s)}$ represents the solid matter of the confining layer, which plays the role of cation exchanger):

$$Ca^{2+} + 2Na\text{-}X_{(s)} \Leftrightarrow 2Na^{+} + Ca\text{-}X_{(s)} \quad \text{(Eq. 8)}$$

When freshwater (Ca-HCO_3 in composition) infiltrates and circulates in confined granular deposits and contacts the confining layers, Ca^{2+} is taken up from the freshwater to replace Na^+, which is released from the cation exchanger in the groundwater (Eq. 8).

This process is known to occur in coastal aquifers (Appelo and Postma, 2005) and has been observed within the Basses-Laurentides aquifer. In the Basses-Laurentides aquifer system, granular aquifers are confined by marine Pleistocene clays deposited during the Champlain Sea episode (Cloutier et al., 2010). In this case, clays play the role of cation exchanger liberating Na^+ in groundwater.

Samples in Cluster 4 are all Na-Cl type reflecting a marine origin. Cluster 4 samples are the closest samples to the seawater end-member in Figure 3.9 and most Cluster 4 samples plot near the seawater dilution line. Some of the samples for Cluster 1 plot in an intermediate position between Na-HCO_3 samples in Clusters 2 and 4 and are aligned along the seawater dilution line. Path 2 in Figure 3.9 corresponds to the salinization process that brings Na-HCO_3 groundwater to a Na-Cl water type. Cluster 4 then represents an end-member of the mixing trend between a seawater end-member and the more diluted water that prevails in confined aquifers within the study area.

The combination of reactions 3 and 4 for the plagioclase dissolution shows that 2 $Na^+ = Ca^{2+}$. A gradually changing Na^+/Ca^{2+} ratio of the groundwater may then be related to the dissolution/precipitation kinetics of feldspars. In Figure 3.9, samples that follow Salinization path 3 correspond to groundwater evolving from a Ca-HCO_3 facies to a Na-HCO_3 facies according to this kinetic process.

3.8.4 Microcline weathering

Mineralogical analyses performed on deep marine deposits in some areas of the SLSJ region showed that microcline and illite represent 41% and 21% of the argillaceous fraction of clay, respectively (Gravel; 1974). K-feldspar (microcline) transformation into the clay mineral (illite), is represented by:

$$3KAlSi_3O_8 + 2H^+ \rightarrow 2K^+ + 6SiO_2 + KAl_3Si_3O_{10}(OH)_2 \quad \text{(Eq. 9)}$$
(Microcline) (Illite)

According to the PCA results (Figure 5), SiO_2 and K^+ are related to samples in Cluster 4. The influence of SiO_2 and K^+ on the chemistry of Cluster 4 results from the chemical breakdown of microcline and it confirms that the weathering of silicate minerals occurs more efficiently within the regional aquitard than in the bedrock.

3.8.5 General geochemical evolution path in the SLSJ aquifer systems

The combination of HCA, PCA and binary graphs demonstrates that the occurrence of two distinct salinization paths depends on the hydrogeological context. Based on the content of major elements, the general geochemical evolution paths of groundwater within the SLSJ aquifer systems are presented in the Piper diagram in Figure 3.10. The samples are presented according to the HCA cluster to which they belong.

Cluster 2 samples (Ca,Na-HCO3) reflect the first stage of groundwater evolution as the cation composition changes from Ca^{2+} dominant to Na^+ dominant, which is explained

by ion exchange processes in the presence of the marine clay aquitard and further explained by the feldspar dissolution/precipitation kinetics in the bedrock. Then, the evolution of groundwater follows two possible paths.

The first path occurs as groundwater flows through the crystalline bedrock aquifers, which induces a change in the anion composition from HCO_3^- -dominant (Clusters 2) to Cl^- -dominant end-members (Clusters 3 and 4). According to the first path (Path 1), groundwater tends to evolve by water/rock interactions toward a Ca-Cl end-member. This evolution is accompanied by the simultaneous increase of the Ca^{2+}, Sr^{2+} and Ba^{2+} contents of groundwater.

The second path begins with Ca^{2+}_{water}-Na^+mineral ion exchange and results in the transformation of the samples from Ca-HCO_3 to Na-HCO_3 (Figure 10; Path 2). Path 2 represents the evolution of groundwater due to a salinization path within the confined aquifers that are in contact with the regional aquitard and possible groundwater mixing with the Pleistocene Laflamme Sea end-member. The seawater could be trapped in the regional aquitard (solute diffusion) or may be stagnant (mixing) in some part of the aquifer (Cloutier et al., 2010). This latter combination of processes (cation exchange and/or leaching of saltwater trapped in the regional aquitard) is grouped in this study under the term “water/clay interactions”.

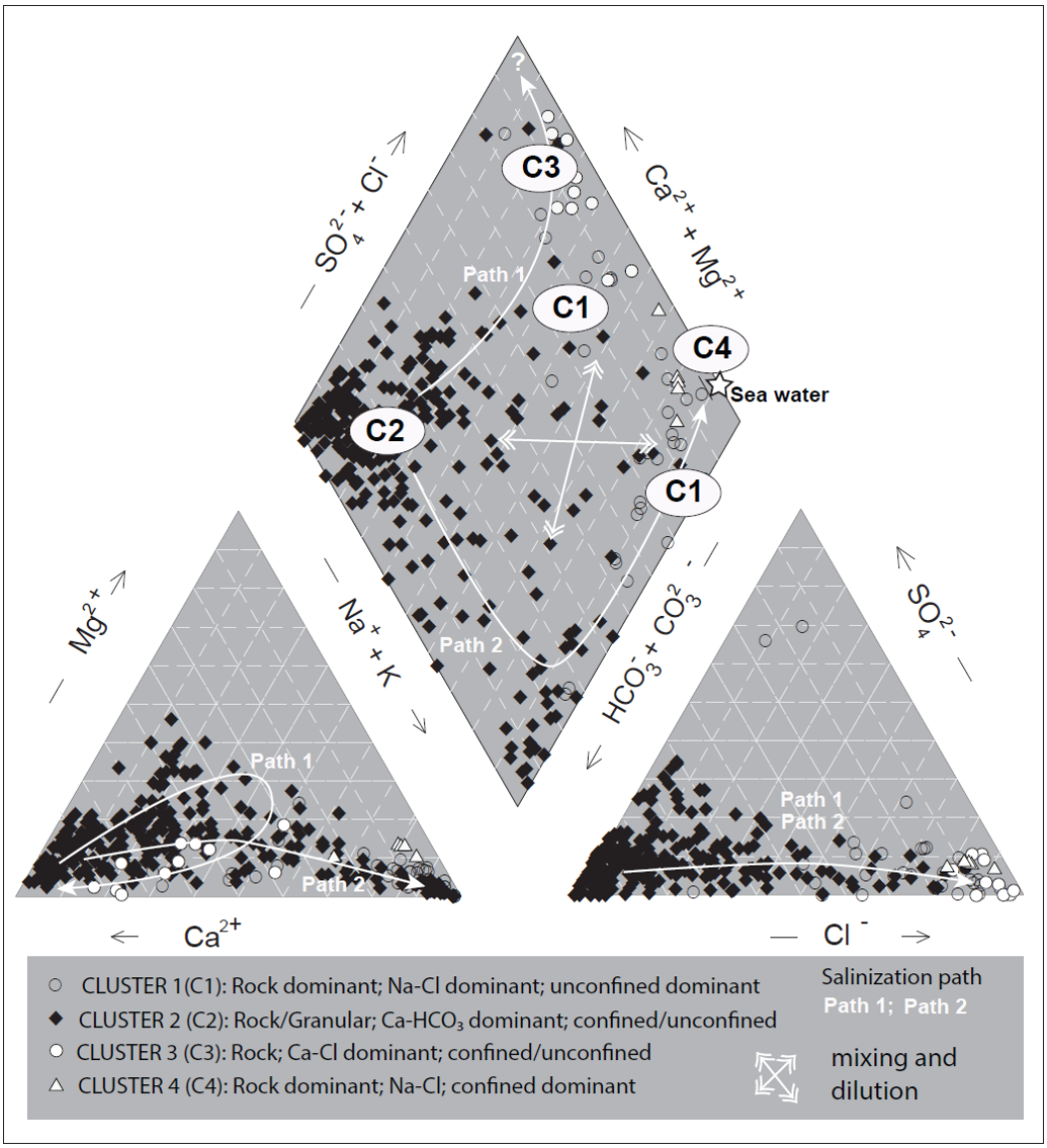

Figure 3.10 : Piper diagram of the general evolution pathways of groundwater within the Saguenay-Lac-Saint-Jean aquifer systems. Mixing and dilution occur at different rates during the evolution of groundwater having different origins (mixing and dilution zones). From the recharge area, the evolution of groundwater follows two possible paths. The first (Path 1) occurs as groundwater flows through crystalline bedrock aquifers, which induces a change in the anion composition from HCO_3^- -dominant (Cluster 2) to Cl^- -dominant (Cluster 3). In this path, groundwater evolves by water/rock interactions toward a Ca-Cl end-member. The second path begins with the weathering of feldspath and results in the movement of the samples from Ca-HCO_3 to Na-HCO_3. Ca^{2+}_{water}-Na^+ mineral ion exchange, solute diffusion from the Laflamme Sea clay aquitard and/or mixing with Laflamme seawater provoke the evolution of recharge Ca-HCO_3 groundwater (Cluster 2) to Na-HCO_3 groundwater and brackish groundwater (Na-Cl in composition, Cluster 4).

Ion exchange, solute diffusion from the Laflamme Sea clay aquitard and/or mixing with Laflamme seawater cause the evolution of Cluster 2 (recharge Ca-HCO_3 groundwater to Na-HCO_3 groundwater) to Cluster 4 (brackish groundwater Na-Cl in composition). Following this latter trend, the chemistry of the groundwater tends to evolve toward an end-member having a composition that is like that of present seawater, i.e., Na-Cl-rich. According to the PCA, this evolution is accompanied by a simultaneous increase of the Mg^{2+}, SiO_2, K^+ and SO_4^{2-} contents of groundwater.

Figure 3.11 is a generalized cross-section showing the different salinization pathways occurring in the SLSJ area. The topography caused by a graben structure (>1000 m) displays a connection between water composition and groundwater flow driven by the topographic gradient. Bedrock groundwater evolves from Cluster 2 (Ca,Na-HCO_3, unconfined environment) to Cluster 3 (Ca,Na-Cl; rock dominated) by interactions with basement fluids (water-rock interactions, e.g. Cl^-/Br^- mass ratios of 88 derived from Figure 3.8) coming up along the graben fault system. The distribution of Cluster 3 samples along major faults in Figure 3.6 also suggests the upwelling of basement fluids toward the surface. In the crystalline basement, the dissolution/precipitation kinetics of feldspars induce a gradual changing of the chemical facies from Ca-HCO_3 to Na-HCO_3 (Cluster 2).

Confining conditions dominate Cluster 4 (Figure 3.4; Table 3.2). The groundwater in the granular aquifers exhibits an evolution from the recharge groundwater of Cluster 2 by ion exchange (Cluster 2 Na-HCO_3) in a confined environment and possible mixing with the

Laflamme seawater end-member (e.g., Cl^-/Br^- mass ratios of 266 derived from Figure 3.8; Cluster 4). This latter evolution might also be observed in bedrock aquifers where confining conditions prevail.

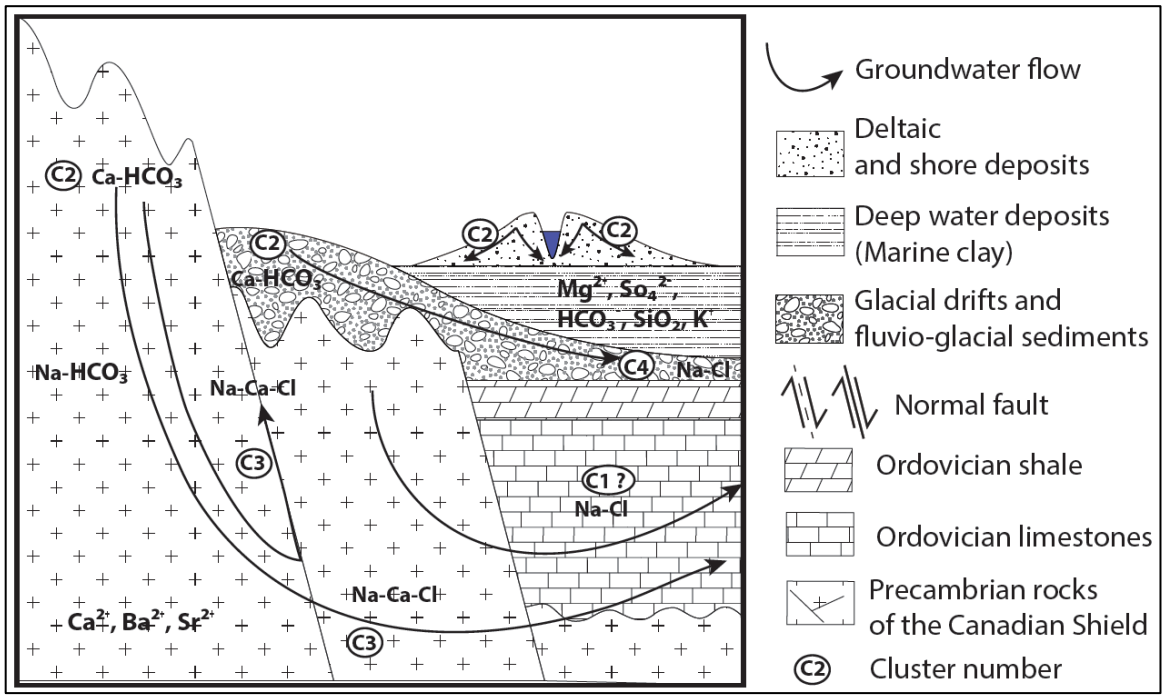

Figure 3.11 : Generalized cross-section showing the different salinization pathways occurring in the SLSJ area. Bedrock groundwater evolves from Cluster 2 (Ca,Na-HCO_3, unconfined environment) to Cluster 3 (Ca,Na-Cl; rock dominated) by interactions with basement fluids (water-rock interactions) coming up along the graben fault system (groundwater flow line). The distribution of Cluster 1 close by Limestone units (Figure 6) and the hydrogeological information related to Cluster 1 (Figure 4: Na-Cl type in confined bedrock aquifers) suggest that Cluster 1 represent a seawater end-member of groundwater evolving in contact with the Ordovician limestone. The groundwater in the granular aquifers exhibits an evolution from the recharge groundwater (Ca-HCO_3) by Ca^{2+}_{water}-$Na^{+}_{mineral}$ ion exchange process in a confined environment (Na-HCO_3; Cluster 2) and possible mixing with the Laflamme seawater end-member (Na-Cl; Cluster 4). This latter evolution might also be observed in bedrock aquifers where confining conditions prevail.

Cluster 1 samples are dominated by Na-Cl waters from confined bedrock aquifers (Figure 3.4). The samples from Cluster 1 are predominately distributed near limestone units (24/30 samples) (Figure 3.6) and may then represent a seawater end-member of groundwater evolving in contact within the confined Ordovician limestone.

The end-members of the salinization paths, represented by Clusters 3 and 4, are thus identified and can be distinguished based on the relative concentrations of the following trace elements: Ca^{2+}, Sr^{2+}, Ba^{2+} for Cluster 3 and Mg^{2+}, SiO_2, K^+, SO_4^{2-}, and HCO_3^- for Cluster 4 (Figure 3.5). Mixing and dilution (Figure 3.10) occur at different rates during the evolution of groundwater having different origins in response to the specific hydrogeological context prevailing locally in the region.

3.9 SUMMARY AND CONCLUSION

In this paper, groundwater evolution paths that account for the chemical characteristics of a large dataset obtained from groundwater analyses in a regional-scale study has been described. The dissolution of calcite and/or plagioclase minerals controls the chemical background of recharge groundwater. Anorthite plagioclase weathering is more effective in bedrock aquifers, and the Ca^{2+}_{water}-$Na^{+}_{mineral}$ ion exchange process is dominant in confined aquifers. In addition, there is mixing with a seawater end-member where confining conditions by the regional aquitard are prevailing. In the crystalline bedrock, mixing with deep brackish groundwater by topographically driven groundwater flow appears to be a possibility in the Lake St. John area.

The combination of HCA, PCA and binary graphs identifies two distinct salinization paths occur: 1) an evolution by water/rock interactions; and 2) an evolution from the recharge groundwater by water/clay interactions and groundwater mixing. The first evolution path is specific to fractured rock aquifers. The term water/clay interactions was introduced in this paper to account for a combination of processes, namely: ion exchange and/or leaching of salt water trapped in the regional aquitard. Mixing with fossil seawater present in the aquifer might also increase the groundwater salinity.

Based on the results obtained using PCA, clusters can be distinguished according to the relative concentrations of the following trace elements: Ca^{2+}, Sr^{2+} and Ba^{2+} for Cluster 3 (water/rock interactions) and HCO_3^-, Mg^{2+}, SiO_2, K^+ and SO_4^{2-} for Cluster 4 (water/clay interactions). One of the main processes controlling the groundwater chemistry in confined aquifers is believed to be the degradation of organic matter and/or any other reaction that produces CO_2. Another process could be the silicate alteration process, more specifically microcline plagioclase weathering.

The percentage of cumulative variance obtained via PC 1 and 2 is 52.6%. This suggests that 50% of the variance of the dataset cannot be explained by the first two components (salinity). Other components need to be investigated to establish a more global portrait of regional hydrogeochemistry. Further work should also focus on identifying reliable tracers of the two salinization paths using Factorial Analysis (FA). In contrast to PCA, the emphasis of FA is explaining covariances instead of the total variance

of a dataset. Thus, FA could be used to highlight highly correlated chemical parameters within the dataset and shed new light on the chemical nature of the samples.

Next steps should prioritize an improved knowledge of the different rock types and their geochemical properties. Compilation of the existing geochemical data on rocks and sediments should be coupled with the sampling of outcrops to investigate the mineralogical assemblages of the various regional rocks (via thin section analysis). Leaching experiments should also be performed to obtain different specific ionic ratios, as for instance the Cl^-/Br^- ratio. Finally, a new sampling campaign focused on isotopic data (^{18}O, ^{2}H, ^{13}C, etc.) and residence time constraints could contribute to deciphering the data set, especially the origins of the saline end-members.

This study—derived from a routine chemical analysis of water quality—provides a new understanding of the chemical evolution of groundwater that is of interest in conceptualizing the dynamics of groundwater, such as flow patterns and hydraulic connectivity between aquifers. With a better understanding of the chemical characteristics of the salinization paths, the major, minor and trace element chemistry of groundwater becomes a relevant tool for investigating groundwater dynamics, such as the interconnectivity of aquifer systems or groundwater flow dynamics according to gravity-driven flow processes. With a better knowledge of the geochemistry of the porous and the fractured matrix of regional aquifers, as well as of the geochemistry of aquitards present in the SLSJ region, this study may leads to discussions on the spatial and temporal

evolution of groundwater quality with respect to the prevailing geochemical paths (water/rock and/or water/clay interactions).

3.10 ACKNOWLEDGEMENTS

This project was funded by the Natural Sciences and Engineering Research Council of Canada (NSERC), the Fonds de recherche du Québec – Nature et technologies (FRQNT), the Fondation de l'université du Québec à Chicoutimi (FUQAC), Rio Tinto Alcan (RTA), and the Programme d'acquisition de connaissances sur les eaux souterraines of Quebec (PACES), with contributions from the Quebec Ministère du Développement durable, de l'Environnement, de la Faune et des Parcs (MDDEFP), and the five county municipalities of the SLSJ region (Domaine-du-Roy, Du-Fjord-Du-Saguenay, Lac-Saint-Jean-Est; Maria-Chapdelaine and the City of Saguenay). The authors wish to acknowledge the anonymous reviewers for their meaningful input, Professor Philippe Page from the University du Quebec à Chicoutimi (UQAC) who gave us the benefit of his extensive experience in geochemistry, technician David Noël for his multiple skills in field hydrogeology, all the students involved in the project as field assistants and, finally, the research assistants M. Lambert, A. Moisan, M.L. Tremblay and D. Germaneau for their help with the PACES project. In addition, the authors wish to thank the well owners who graciously provided access to their groundwater intakes for sampling.

3.11 REFERENCES

Alvin, C.R., 2002. Methods of multivariate analysis. Wiley Interscience.

Aquilina, L., Ladouche, B., Doerfliger, N., Bakalowicz, M., 2003. Deep water circulation, residence time, and chemistry in a karst complex. Ground Water, 41(6): 790-805.

Aquilina, L. et al., 2015. Impact of climate changes during the last 5 million years on groundwater in basement aquifers. Sci. Rep. 5.

Appelo, C.A.J., Postma, D., 2005. Geochemistry, Groundwater, Pollution. AA Balkema Publishers, Amsterdam.

ArandaCirerol, N., Herrera-Silveira, J.A., Comín, F.A., 2006. Nutrient water quality in a tropical coastal zone with groundwater discharge, northwest Yucatan, Mexico. Estuar., Coast. and Shelf Sci., 68: 445-454.

Beaucaire, C., Gassama, N., Tresonne, N., Louvat, D., 1999. Saline groundwaters in the hercynian granites (Chardon Mine, France): geochemical evidence for the salinity origin. Appl. Geochemistry, 14: 67-84.

Beaucaire, C., Michard, G., 1982. Origin of dissolved minor elements (Li, Rb, Sr, Ba) in superficial waters in a granitic area. Appl. Geochemstry, 16: 247-258.

Bottomley, D.J., Conrad Gregoire, D., Raven, K.G., 1994. Saline ground waters and brines in the Canadian Shield: Geochemical and isotopic evidence for a residual evaporite brine component. Geochim. Cosmochim. Acta, 58: 1483-1498.

Bottomley, D.J. et al., 1999. The origin and evolution of Canadian Shield brines: evaporation or freezing of seawater? New lithium isotope and geochemical evidence from the Slave craton. Chem. Geol., 155: 295-320.

Bouchard, R., Dion, D.J., Tavenas, F., 1983. Origine de la préconsolidation des argiles du Saguenay, Qc. Can. Geotech. J., 20: 315-328.

Box, G.E., Cox, D.R., 1964. An analysis of transformations. Journal of the Royal Statistical Society. Series B (Methodological): 211-252.

Brown, C.E., 1998. Applied multivariate statistics in geohydrology and related sciences. Springer Berlin.

Bucher, K., Stober, I., 2010. Fluids in the upper continental crust. Geofluids, 10: 241-253.

Bucher, K., Stober, I., Seelig, U., 2012. Water deep inside the mountains: Unique water samples from the Gotthard rail base tunnel, Switzerland. Chem. Geol., 334: 240-253.

Carpenter, A.B., 1978. Origin and chemical evolution of brines in sedimentary basins, SPE Annual Fall Technical Conference and Exhibition. Soc. of Petroleum Eng.

CERM-PACES, 2013. Résultats du programme d'acquisition de connaissances sur les eaux souterraines du Saguenay-Lac-Saint-Jean, Centre d'étude sur les ressources Minérales de l'Université du Québec à Chicoutimi.

Chebotarev, I.I., 1955. Metamorphism of natural waters in the crust of weathering 1-2-3. Geochim. Cosmochim. Acta, 8: 22-48.

Chesnaux, R. et al., 2011. Building a geodatabase for mapping hydrogeological features and 3D modeling of groundwater systems: Application to the Saguenay–Lac-St.-Jean region, Canada. Comput. Geosci., 37: 1870-1882.

Chesnaux, R., Rafini, S., Elliott, A.-P., 2012. A numerical investigation to illustrate the consequences of hydraulic connections between granular and fractured-rock aquifers. Hydrogeol. J., 20: 1669-1680.

Cloutier, V., Lefebvre, R., Savard, M.M., Bourque, É., Therrien, R., 2006. Hydrogeochemistry and groundwater origin of the Basses-Laurentides sedimentary rock aquifer system, St. Lawrence Lowlands, Quebec, Canada. Hydrogeol. J., 14: 573-590.

Cloutier, V., Lefebvre, R., Savard, M.M., Therrien, R., 2010. Desalination of a sedimentary rock aquifer system invaded by Pleistocene Champlain Seawater and processes controlling groundwater geochemistry. Environ. Earth Sci., 59: 977-994.

Cloutier, V., Lefebvre, R., Therrien, R., Savard, M.M., 2008. Multivariate statistical analysis of geochemical data as indicative of the hydrogeochemical evolution of groundwater in a sedimentary rock aquifer system. J. Hydrol., 353: 294-313.

Daigneault, R. et al., 2011. Rapport final sur les travaux de cartographie des formations superficielles réalisés dans le territoire municipalisé du Saguenay-Lac-Saint-Jean (Québec) entre 2009 et 2011. Govern. Report MRNF (Qc).

Davis, J., 2002. Statistics and data analysis in geology. John Wiley & Sons, New York.

Desbiens, S., Lespérance, P.J., 1989. Stratigraphy of the Ordovician of the Lac Saint-Jean and Chicoutimi outliers, Quebec. Can. J. Earth Sci., 26: 1185-1202.

Dessureault, R., 1975. Hydrogéologie du Lac Saint-Jean, partie nord-est. Québec: MRN, Dir. Gen. Eaux, Service des eaux souterraines.

Dionne, J., Laverdière, C., 1969. Sites fossilifères du golfe de Laflamme. Rev. Géogr. Montréal, 23: 259-270.

Douglas, M., Clark, I., Raven, K., Bottomley, D., 2000. Groundwater mixing dynamics at a Canadian Shield mine. Journal of Hydrology, 235(1): 88-103.

Du Berger, R. et al., 1991. The Saguenay (Quebec) earthquake of November 25, 1988: seismologic data and geologic setting. Tectonophysics, 186: 59-74.

Durov, S., 1948. Natural waters and graphic representation of their composition, Dokl Akad Nauk SSSR, pp. 87-90.

Edmunds, W., Kay, R., McCartney, R., 1985. Origin of saline groundwaters in the Carnmenellis granite (Cornwall, England): natural processes and reaction during hot dry rock reservoir circulation. Chem. Geol., 49: 287-301.

Edmunds, W.M., Andrews, J.N., Burgess, W.G., Kay, R.L.F., Lee, D.J., 1984. The evolution of saline and thermal groundwaters in the Carnmenellis granite. Mineral. Mag., 48: 407-424.

Farnham, I.M., Singh, A.K., Stetzenbach, K.J., Johannesson, K.H., 2002. Treatment of nondetects in multivariate analysis of groundwater geochemistry data. Chemometrics and Intelligent Laboratory Systems, 60(1): 265-281.

Farnham, I.M., Johannesson, K.H., Singh, A.K., Hodge, V.F., Stetzenbach, K.J., 2003. Factor analytical approaches for evaluating groundwater trace element chemistry data. Anal. Chem. Acta, 490: 123-138.

Frape, S., Blyth, A., Blomqvist, R., McNutt, R., Gascoyne, M., 2003. Deep fluids in the continents: II. Crystalline rocks. Treatise on Geochemistry, 5: 541-580.

Frape, S., Fritz, P., 1987. Geochemical trends for groundwaters from the Canadian Shield. Saline water and gases in crystalline rocks. Geol. Assoc. Can., 33: 19-38.

Frape, S.K., Fritz, P., McNutt, R.H.t., 1984. Water-rock interaction and chemistry of groundwaters from the Canadian Shield. Geochim. Cosmochim. Acta, 48: 1617-1627.

Fritz, P., Frape, S.K., 1982. Saline groundwaters in the Canadian Shield — A first overview. Chem. Geol., 36: 179-190.

Fritz, P., Frape, S.K., Drimmie, R.J., Appleyard, E.C., Hattori, K., 1994. Sulfate in brines in the crystalline rocks of the Canadian shield. Geochim. Cosmochim. Acta, 58: 57-65.

Fyfe, W.S., Price, N.J., Thompson, A.B., 1978. Fluids in the Earth's crust, 383. Elsevier Amsterdam.

Gascoyne, M., Davison, C.C., Ross, J., Pearson, R., 1987. Saline groundwaters and brines in plutons in the Canadian Shield, Saline water and gases in crystalline rocks. Geol. Assoc. Can.: 53-68.

Gascoyne, M., Kamineni, D.C., 1994. The hydrogeochemistry of fractured plutonic rocks in the Canadian Shield. Appl. Hydrogeol., 2: 43-49.

Gascoyne, M., Stroes-Gascoyne, S., Sargent, F., 1995. Geochemical influences on the design, construction and operation of a nuclear waste vault. Appl. Geochemistry, 10: 657-671.

Ghesquière, O., Walter, J., Chesnaux, R., Rouleau, A., 2015. Scenarios of groundwater chemical evolution in a region of the Canadian Shield based on multivariate statistical analysis. J. Hydrol.: Regional Studies 4: 246-266.

Goldberg, E., Broecker, W., Gross, M., Turekian, K., 1971. Radioactivity in the marine environment. National Academy of Science, Washington, DC: 137.

Guha, J., Kanwar, R., 1987. Vug brines-fluid inclusions: A key to the understanding of secondary gold enrichment processes, the evolution of deep brines in the Canadian

Shield. Saline water and gases in crystalline rocks. Geol. Assoc. Can., Ottawa: Geol. Assoc. Can. Spec. Pap. 33: 95-101.

Güler, C., Thyne, G. D., McCray, J. E., Turner, K. A., 2002. Evaluation of graphical and multivariate statistical methods for classification of water chemistry data. Hydrogeol. J. 10: 455-474.

Hébert, C., Lacoste, P., 1998. Géologie de la région de Jonquière-Chicoutimi (SNRC 22D), Qc. MRN Sect. Mines.

Hébert, C., Van Breemen, O., 2004. Mesoproterozoic basement of the Lac St. Jean Anorthosite Suite and younger Grenvillian intrusions in the Saguenay region, Québec: Structural relationships and U-Pb geochronology. Geol. Soc. Am. Mem. 197: 65-79.

Health Canada, 2007. Guidelines for Canadian drinking water quality: summary table. Federal–Provincial–Territorial Committee on Drinking Water, July 2015. http://www.hc-sc.gc.ca/ewh-semt/pubs/water-eau/sum_guide-res_recom/index-eng.php

Hervet, M., Van Breemen, O., Higgins, M., 1994. U–Pb crystallisation ages of intrusive rocks near the southeast margin of the Lac-St-Jean anorthosite complex, Grenville Province, Quebec. Radiogen. Age Isot. Stud., Rep. 8: 115-124.

Higgins, M. D., Van Breemen, O., 1996. Three generations of anorthosite-mangerite-charnockite-granite (AMCG) magmatism, contact metamorphism and tectonism in the Saguenay-Lac-Saint-Jean region of the Grenville Province, Canada. Precamb. Res. 79: 327-346.

Hounslow, A., 1995. Water quality data: analysis and interpretation, CRC press.

Kamineni, D. C., 1987. Halogen-bearing minerals in plutonic rocks: a possible source of chlorine in saline groundwater in the Canadian Shield. Saline water and gases in crystalline rocks. Geol. Assoc. Can. Spec. Pap. 33: 69-79.

Kharaka, Y., Hanor, J., 2003. Deep fluids in the continents: I. Sedimentary basins. Treatise on Geochemistry 5: 499-540.

Lahermo, P., Lampen, P., 1987. Brackish and saline groundwaters in Finland. Saline water and gases in crystalline rocks. Geol. Assoc. Can. Spec. Pap. 33: 103-109.

LaSalle, P., Tremblay, G., 1978. Dépôts meubles: Saguenay Lac Saint-Jean, MRN, Dir. gén.

Laurin, A. F., Sharma, K. N. M., 1975. Région des rivières Mistassini, Péribonca, Saguenay: Mistassini, Péribonca, Saguenay Rivers area: Grenville 1965-1967, MRN, Dir. gén.

Lemieux, J.M., Sudicky, E., Peltier, W., Tarasov, L., 2008. Dynamics of groundwater recharge and seepage over the Canadian landscape during the Wisconsinian glaciation. J. of Geophys. Research: Earth Surface, vol. 113. No F1

Lodemann, M., Fritz, P., Wolf, M., Ivanovich, M., Hansen, B. T., Nolte, E., 1997. On the origin of saline fluids in the KTB (continental deep drilling project of Germany). Appl. Geochemistry 12: 831-849.

McIntosh, J., Garven, G., Hanor, J., 2011. Impacts of Pleistocene glaciation on large-scale groundwater flow and salinity in the Michigan Basin. Geofluids, 11(1): 18-33.

Meinken, W., Stober, I., 1997. Permeability distribution in the Quaternary of the Upper Rhine glacio-fluvial aquifer. Terra nova, 9(3): 113-116.

Montcoudiol, N., Molson, J., Lemieux, J.-M., 2014. Groundwater geochemistry of the Outaouais Region (Québec, Canada): a regional-scale study. Hydrogeol. J. 23: 377-396.

Nordstrom, D. K., Ball, J. W., Donahoe, R. J., Whittemore, D., 1989. Groundwater chemistry and water-rock interactions at Stripa. Geochim. Cosmochim. Acta 53: 1727-1740.

Nordstrom, D. K., Olsson, T., 1987. Fluid inclusions as a source of dissolved salts in deep granitic groundwaters. Saline water and gases in crystalline rocks. Geol. Assoc. Can. 33: 111-119.

Parent, M., Occhietti, S., 1988. Late Wisconsinan deglaciation and Champlain sea invasion in the St. Lawrence valley, Québec. Géogr. Phys. et Quat. 42: 215-246.

Pauwels, H., Fouillac, C., Fouillac, A.-M., 1993. Chemistry and isotopes of deep geothermal saline fluids in the Upper Rhine Graben: Origin of compounds and water-rock interactions. Geochim. Cosmochim. Acta 57(12): 2737-2749.

Pekdeger, A., Balderer, W., 1987. The occurrence of saline groundwaters and gases in the crystalline rocks of Northern Switzerland. Saline water and gases in crystalline rocks. Geol. Assoc. Can. 33: 127-143.

Piper, A. M., 1944. A graphic procedure in the geochemical interpretation of water-analyses. Transactions, Am. Geophys. Union 25: 914-928.

Richard, S. K., Chesnaux, R., Rouleau, A., Morin, R., Walter, J., Rafini, S., 2014. Field evidence of hydraulic connections between bedrock aquifers and overlying granular aquifers: examples from the Grenville Province of the Canadian Shield. Hydrogeol. J. 22: 1889-1904.

Rivers, T., Martignole, J., Gower, C. F., Davidson, A., 1989. New tectonic divisions of the Grenville Province, southeast Canadian Shield. Tectonics 8: 63-84.

Rouleau, A., Walter, J., Daigneault, R., Chesnaux, R., Roy, D. W., Germaneau, D., Lambert, M., Moisan, A., Noël, D., 2011. Un aperçu de la diversité hydrogéologique du territoire du Saguenay-Lac-Saint-Jean (Qc). Proceedings of GeoHydro 2011, Joint Meeting of the Can. Quat. Association, IAH Can. Chapter.

Roy, D. W., Beaudoin, G., Leduc, É., Rouleau, A., Walter, J., Chesnaux, R., Cousineau, P., 2011. Post glacial differential isostasy in the Lac-Saint-Jean area (Qc) and implications for the quality of groundwater. Proceedings of GeoHydro 2011, Joint Meeting of the Can. Quat. Association, IAH Can. Chapter.

Simard, G., Des Rosiers, R., 1979. Qualité des eaux souterraines du Québec, MRN, Dir. Gén. Eaux: 161p.

Statsoft, Inc., 2013. STATISTICA (Data Analysis software System), Version 12.

Stober, I., Bucher, K., 1999. Deep groundwater in the crystalline basement of the Black Forest region. Applied geochemistry, 14(2): 237-254.

Stober, I., Bucher, K., 1999. Origin of salinity of deep groundwater in crystalline rocks. Terra Nova-Oxford, 11(4): 181-185.

Templ, M., Filzmoser, P., Reimann, C., 2008. Cluster analysis applied to regional geochemical data: Problems and possibilities. Appl. Geochemistry 23: 2198-2213.

Tóth, J., 1985. Role of Regional Gravity Flow in the Chemical and Thermal Evolution of Ground Water. First Can./Am. Conf. on Hydrogeology: Practical Applications of Ground Water Geochemistry.

Tóth, J., 1999. Groundwater as a geologic agent: an overview of the causes, processes, and manifestations. Hydrogeol. J. 7: 1-14.

Tremblay, G., 1971. Glaciation et déglaciation dans la région Saguenay-Lac-Saint-Jean, Québec, Canada. Cahiers de géographie du Québec 15: 467-494.

Walter, J., 2010. Les eaux souterraines à salinité élevée autour du lac Saint-Jean, Québec : origines et incidences. Chicoutimi, Université du Québec à Chicoutimi: ix, 177 p.

Walter, J., Rouleau, A., Clark, I. D., Guha, J., 2006. A first investigation of groundwater geochemistry in the crystalline bedrock around lake Saint-Jean, Québec. IAH Can. Chapter.

Walter, J., Rouleau, A., Roy, D. W., Daigneault, R., 2011. Hydrogéochimie des eaux souterraines de la région du Saguenay-Lac-Saint-Jean: résultats préliminaires. Proceedings of GeoHydro 2011, Joint Meeting of the Can. Quat. Association, IAH Can. Chapter.

Wigley, T., 1973. The incongruent solution of dolomite. Geochim. Cosmochim. Acta, 37(5): 1397-1402.

Woussen, G., Martignole, J., Nantel, S., 1988. The Lac-St-Jean anorthosite in the St-Henri-de-Taillon area (Grenville Province): a relic of a layered complex. Can. Mineral. 26: 1013-1025.

Yu, Z., Zhang, L., Jiang, P., Papelis, C., Li, Y., 2015. Study on Water-Rock Interactions of Trace Elements in Groundwater with Leaching Experiments. Groundwater 53: 95-102.

CHAPITRE 4

CHEMICAL PATHFINDERS FOR THE NATURAL EVOLUTION OF GROUNDWATER TOWARD BRACKISH END-MEMBERS IN PRECAMBRIAN BEDROCK AQUIFERS AND PLEISTOCENE GRANULAR AQUIFERS

Julien Walter[1], Romain Chesnaux[1],
Vincent Cloutier[2], Damien Gaboury[1]

[1]Centre d'études sur les ressources minérales, Université du Québec à Chicoutimi, Chicoutimi, Québec, G7H 2B1

[2]Groundwater Research Group, Institut de recherche en mines et en environnement, Université du Québec en Abitibi-Témiscamingue, Campus d'Amos, Amos, Québec, Canada.

Geofluids

(soumis le 30 décembre 2017)

4.1 MISE EN CONTEXTE

Dans l'article qui suit, nous répondons principalement aux objectifs 3, 4 et 5 de cette thèse, en plus de présenter schématiquement le modèle conceptuel final de l'évolution naturelle des faciès hydrogéochimiques identifiés. L'originalité de cet article repose sur l'application d'une méthodologie particulière visant le rehaussement du signal hydrogéochimique contenu dans le jeu de données (321 échantillons) avec comme objectif d'inclure certains paramètres chimiques en traces, tels que le fluor et le manganèse, dans le traitement statistique multivarié. La méthodologie décrite dans les grandes lignes est discutée de manière plus approfondie au chapitre 5 de cette thèse. Elle conduit à la création d'une sous base de données de 51 échantillons parmi les quels sont définis un pôle d'eau de recharge, un pôle d'eau de recharge évoluée et deux pôles salins différentiables sur la base de la provenance des échantillons (roc fracturé ou dépôts granulaires). Le jeu de données réduit est soumis à une analyse factorielle (dérivée de l'analyse en composante principale) pour permettre l'identification de nouveaux traceurs. Les résultats concordent avec ceux obtenus au chapitre précédent mais vont plus loin. Ils permettent entre autre de proposer différentes hypothèses pour expliquer la présence sous forme dissoute d'un plus large spectre d'ions, incluant le fer et le manganèse. De plus, nous introduisons dans cet article un indice de maturation de l'évolution de l'eau souterraine permettant de discuter de manière quantitative l'évolution de l'eau souterraine pour l'ensemble des paramètres chimiques considérés dans le cadre de cette thèse.

4.2 ABSTRACT

Fingerprinting of chemical elements is used to identify processes of natural groundwater salinization. This approach relies on a normative method defining the "maturation index", a parameter that describes the degree of chemical evolution of groundwater. For a region of the Canadian Shield, we analyzed the chemical content of 51 samples, selected from an original regional-scale dataset of 321 samples. Maturation index calculations, factor analysis, and the relationship between elements showed that: a) K^+, HCO_3^-, Mg^{2+}, SiO_2, NH_4^+, CO_2, HS^- and SO_4^{2-}characterize a seawater Na-Cl end-member in confined granular aquifers; b) dissolved F^- can be generated either from the interaction of groundwater with marine clays or from the mixing of different groundwaters within bedrock aquifers and fluoride is preferentially added to groundwater in Na(Ca)-HCO_3 type of groundwater; c) Bromide and lithium particularly characterize groundwater evolving toward a CaCl end-member similar to that of Precambrian Shield Brines (PSB) and a mass ratio $Ca^{2+}/Sr^{2+} \approx 40$ is proposed to identify *PSB-like* groundwater; d) rainwater is enriched in Al^{3+} and Pb^{2+} suggesting atmospheric contamination; and e) Copper, iron and nitrate are likely to be chemical pathfinders for early processes of the recharge event. Based on these results, we propose a conceptual model of groundwater chemical evolution.

Keywords: Geochemistry, geochemical pathfinders, brackish groundwater, multivariate statistics, Precambrian shield brines.

4.3 INTRODUCTION

The chemical content of groundwater is continually modified through space and time along its flow path through underground systems. As water moves through the subsurface, its initial chemical content evolves in response to different chemical environments through which it flows [1, 2]. The chemical composition of groundwater thus reflects dynamic coupled mineral-water chemical reactions and the rate and mechanisms of groundwater flow and transport [3, 4]. Chemical interactions and flow occur simultaneously at all space and time scales from the surface to the deepest portions of the continental crust [5, 6].

Hydrochemical data are useful for tracing groundwater flow [7]. The chemical evolution of groundwater can be characterized by considering the water types that are typically found in different zones of groundwater flow systems [3, 8, 9]. Rainwater is the most diluted form of liquid water infiltrating the soil surface. From this starting point, groundwater will tend to increase its content in dissolved minerals. This mineralization usually corresponds to a process of salinization as the increased residence time of water in the aquifer enhances the dilution of salt minerals contained in the solid fraction of the porous or fractured medium. Due to weathering, ion exchange, salt dissolution, and/or mixing with seawater, groundwater evolves from a dilute calcium bicarbonate type in recharge areas, toward a more concentrated sodium chloride or calcium chloride type along its flow path [3]. Experimental studies of trace elements at the aquifer rock/water

interface provide valuable information regarding the source and evolution of groundwater [11]. One of the major problems in the trace element analysis of groundwater is that salinization processes of groundwater are still poorly understood at the regional scale.

Recently, Walter et al. [11] studied 321 groundwater samples from a region of the Canadian Precambrian Shield, the Saguenay-lac-Saint-Jean area (SLSJ), located in the Province of Quebec in Eastern Canada (Figure 4.1A). Two processes are proposed to explain the evolution of groundwater chemistry in this region: (1) evolution due to water/rock interactions, and (2) evolution of recharge groundwater due to water/clay interactions and groundwater mixing. The first process is specific to fractured-rock aquifers. Water/clay interactions account for a combination of processes, namely ion exchange and/or the leaching of saltwater trapped in the regional aquitard. The results show that each of the two salinization paths exerts a major and distinct influence on the chemical signature of groundwater. Groundwater quality in the SLSJ area is generally good, although some brackish groundwater is present, as well as some minor and trace element concentrations that exceed World Health Organization (WHO) standards [12] for barium, manganese, iron and aluminum [13–18]. Moreover, approximately 20% of the wells sampled for this study produced groundwater fluoride levels exceeding World Health Organization standards [12]. Exposure to excessive levels of fluoride can exert negative effects on human health (Edmunds and Smedley, 2013).

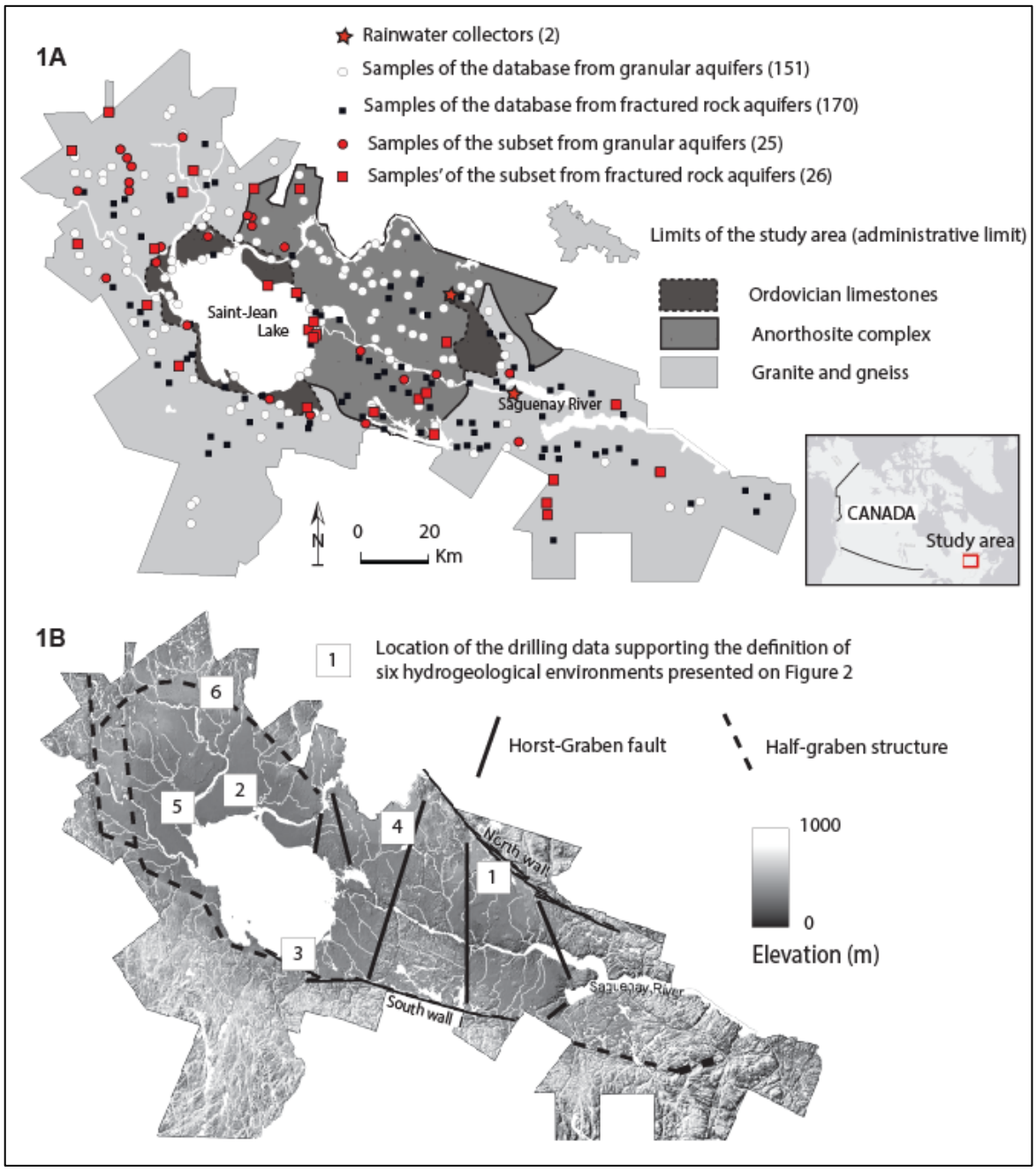

Figure 4.1 : A) The study area is located in the Province of Quebec, Canada. The regional-scale dataset is composed of 321 groundwater samples, among which 170 were collected from bedrock aquifers and 151 were collected from granular deposits. 51 samples were selected from this dataset to form the subset which was subjected to the multivariate (factorial) analysis performed in this study. Two rain collectors were installed to collect and analyse rainwater in the framework of this study. This figure is modified after Water et al. (2017). B) **Schematic of regional graben topography and**

location of the six principal stratigraphic assemblages according to drilling data and presented in Figure 4.2.

This paper aims to discuss the possible origin and evolution of groundwater based on a study of its chemical characteristics acquired during (1) water/rock interactions and (2) water/clay interactions and groundwater mixing [11], with special emphasis on certain elements that are locally present in concentrations that exceed the limits established by Canadian governmental policy for groundwater quality. The proposed approach relies on a combination of sample classifications, *hierarchical cluster analysis* (HCA), *factorial analysis* (FA) and binary plot investigations, with the objective of identifying reliable chemical pathfinders of the two aforementioned salinization processes. We aimed to establish a benchmark for discussing the chemical differences of groundwater given its evolutionary stage (from rainwater to brackish groundwater). A conceptual model of groundwater chemical evolution is proposed for the study area, based on a simple normative method.

4.4 STUDY AREA

The Saguenay-Lac-Saint-Jean (SLSJ) region of Quebec, Canada covers 13,210 km^2 and contains two important surface water features: Lake Saint-Jean (surface 1200 km^2) and the Saguenay River (Figure 4.1). Regional topography is controlled by the Phanerozoic Saguenay Graben (180 Ma), which is approximately 30 km wide. The northern and southern walls of the Saguenay Graben are bounded by WNW fault systems [19] that mark the limits between the highlands (up to 1000 m asl) and the lowlands (0 to ca. 200 m asl) (Figure 4.1B). The regional physiography deeply affected by the Saguenay graben has

controlled the emplacement and the formation of large accumulations of Quaternary deposits (sand, gravel, clay-silt) to a thickness of up to 180 m in the central lowlands [15], where the most populated areas are located. The highlands are characterized by rugged terrain dominated by thin glacial drift (till) deposits and outcropping areas.

A simplified representation of the basement geology of the SLSJ area is shown in Figure 4.1A. The basement is made up of plutonic rocks belonging to the Precambrian Canadian Shield [20]. Around Lake Saint-Jean and in the lowlands, there are several remnants of an Ordovician platform composed of a series of stratified sedimentary rocks, including siliciclastic strata, micritic limestones, and highly fossiliferous alternating limestones and shales [21]. The Ordovician sequence has a maximum thickness of 110 m [15].

The principal hydrogeological contexts encountered in the study area are presented in a conceptual cross-section in Figure 4.2A. The most recent glaciation left behind a discontinuous and heterogeneous layer of till, several terminal moraines and important esker deposits [22, 23] (*fluvio-glacial sediments*; Figure 4.2A). When the glaciers retreated approximately 10,000 years ago, the lowlands were invaded by the Laflamme Sea [24]. This marine incursion deposited a semi-continuous extensive layer of deep water sediments consisting of laminated clayey silt and grey silty clay [23, 25] (*Deep water sediments*; Figure 4.2A). Various facies of deltaic, littoral and pre-littoral sediments were

deposited during the phase of isostatic rebound that forced the retreat of the Laflamme Sea [23, 26] (*Deltaic and shore deposits*; Figure 4.2A).

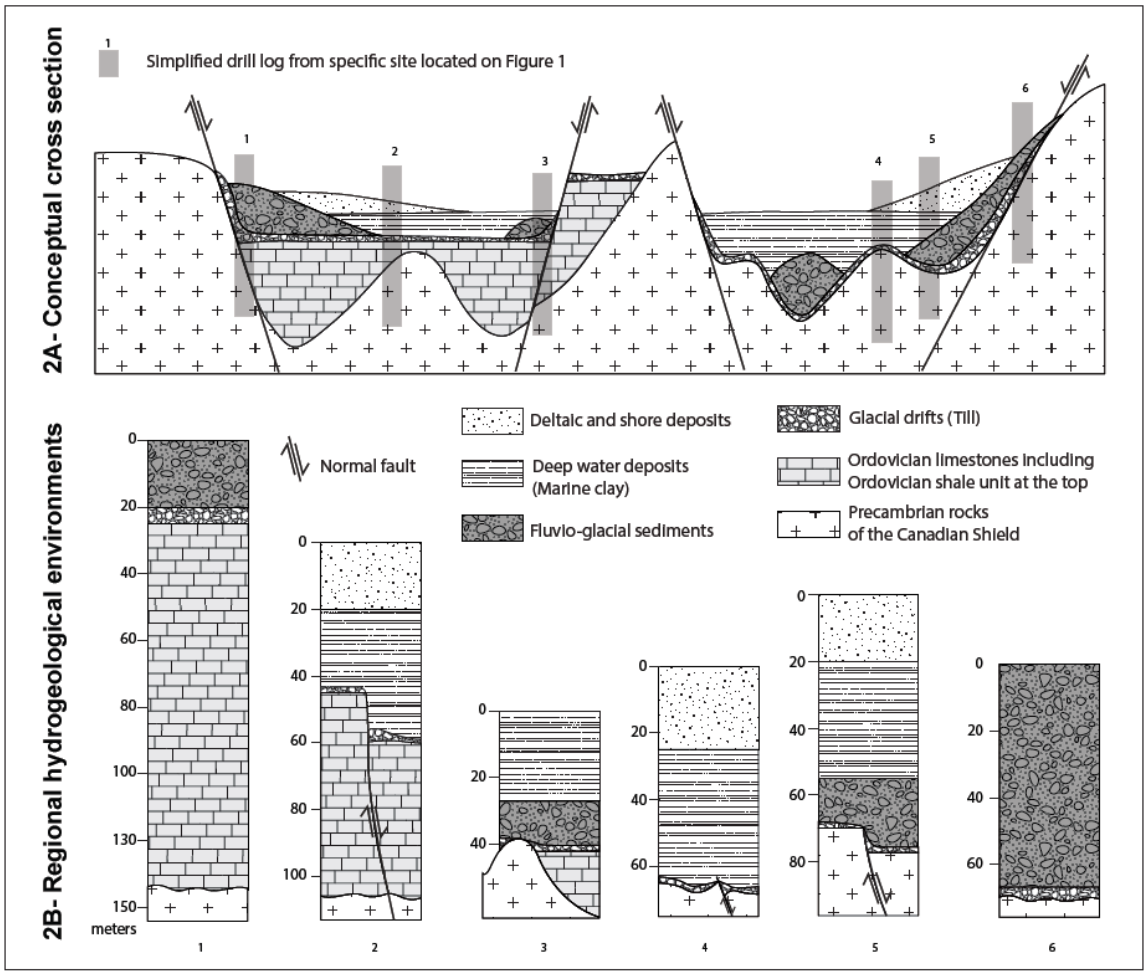

Figure 4.2 : A) Conceptual cross-section of the principal hydrogeological contexts encountered in the study area. B) Drilling data for the six principal regional hydrogeological environments reported on the conceptual cross-section presented in Figure 2A.

The geological history of the SLSJ region has created several hydrogeological environments that can be simplified into six principal stratigraphic assemblages (Figure

2B). The definition of the six hydrogeological environments was based on drilling data obtained at different locations over the study area (Figure 4.1B). Confined and/or unconfined aquifers occur in the Pleistocene deposits and combine locally to form multilayered aquifers [15] that can be either disconnected from or interconnected with Ordovician and/or Precambrian bedrock aquifers [27, 28]. Fluvio-glacial sediments are the most productive regional aquifers; they are frequently covered by the regional marine clay aquitard [13, 15]. Deltaic and shore deposits constitute the other main aquifer type [15].

4.5 METHODOLOGY

4.5.1 REGIONAL GROUNDWATER SAMPLING

Groundwater samples were collected from private wells [11]. The sampling protocol included the recording of temperature (T), redox potential (Eh), pH, dissolved oxygen (DO) and electrical conductivity (EC) while purging the wells. In situ parameters were measured using a Hanna Instruments HI 9828 multi-parameter probe. Purging was completed and samples were collected after the field parameters were stabilized. The sampled water was filtered in the field through a 0.45 µm membrane filter prior to the analysis of metallic ions. Nitric acid stabilized the samples for determining major cation and trace element concentrations. Zinc acetate was applied to determine sulphides. Samples were kept at 4 °C until they were sent to an accredited commercial laboratory for all chemical analyses including major, minor and trace levels of 38 inorganic constituents. Trace elements were analyzed by ICP-MS and total alkalinity was determined by titration

(final pH 4.5). Ion exchange chromatography measured chloride, bromide, sulphate, sulphide, and nitrate levels whereas ammonium, fluoride and inorganic phosphorous were determined using a specific probe. The threshold for ionic balance for all the selected samples was set at less ±10% [29, 30]; samples exceeding this threshold were discarded from the chemical sample dataset. The original dataset contains 321 samples: 170 samples from bedrock aquifers and 151 samples from granular deposits (Figure 4.1A).

4.5.2 CLASSIFICATION OF SAMPLES

Walter et al. [15] proposed that the chemistry of groundwater found in bedrock is chemically different from groundwater found in granular aquifers. Generally speaking, bicarbonate groundwater evolves towards a chloride endmember. Considering this fact, the database was divided into four groups depending on the permutations of 2 water types (HCO_3^- or Cl^-) combined with 2 aquifer types (bedrock or granular aquifer). The 2 groundwater types were identified using a Durov plot based on the relative concentrations of the major elements of chloride (Cl^-) and bicarbonate (HCO_3^-) as expressed in milliequivalent per liter (meq/L). The Durov classification [31] provides a means of identifying a dominant cation, for instance, calcium (Ca^{2+}) or sodium (Na^+). Information on aquifers making it possible to divide them into 2 types were obtained from the owners of the wells. No distinction was made between limestone aquifers and crystalline bedrock aquifers, due to a lack of information.

4.5.3 PREPARATION FOR MULTIVARIATE ANALYSIS: DEFINING THE SUBSET OF DATA

Farnham et al. [32] performed data experiments to determine the best constant to use for substitution of analytical values below the detection limit (<DL) in statistical multivariate processing. The simulation experiments showed that substitution of <DL values with DL/2 was superior to substitution with 0 or DL. Results also showed that the performance for all substitution methods in statistical multivariate processing was weakened when the number of analytical values <DL exceeded approximately 30% of the dataset. Including these analytical values in the multivariate study would add substantial noise to the analysis [32]. In this study, chemical parameters with a number of analytical values <DL exceeding 25% were discarded.

In some cases, the chemical parameter to be discarded was a key parameter considered in this study (for instance, fluoride or iron). A key parameter corresponded to a chemical parameter for which concentration exceeded the limits for groundwater quality established by Canadian policy. To ensure that at least one of the key chemical parameters were included in the statistical multivariate processing, samples in which the key parameter was not detected (analytical value <DL) were withdrawn from the database. As a first step, sample selection was made by screening (using *Excel* software) analytical values > or <DL for each of the 38 chemical parameters. The screening of the data is completed when the number of analytical data >DL (i.e., valid data) for the key parameters reaches (or exceeds) 75% of the new set of data.

The screening step is iterative. It can be repeated with more than one *screened chemical parameter*. The choice of *screened parameter* is subjective and may vary depending on the group of groundwater (brackish or fresh groundwater; bedrock or the granular aquifers). In this study, correlation matrices constructed for each group of groundwater (supplementary material; Appendix 1[2]) support the choice of the *screened chemical parameters* in each group of groundwater samples. The screening of the data reduced the total number of samples which could then be subjected to statistical multivariate processing. In this study, the number of screened samples varied between 10 and 15 samples per sub-group, for a total number of samples varying between 40 and 60 samples. The newly formed set of data is called *the 51-sample subset*.

4.5.4 HIERARCHICAL CLUSTER ANALYSIS AND FACTORIAL ANALYSIS

The Box-Cox power transformation was applied to the 51 samples of the subset to ensure a normal distribution [33] for the data. The variables (major, minor, and trace elements) were standardized by subtracting the mean concentration of a given element from each measured concentration and dividing by the standard deviation of the distribution [34]. The Statistica software version 6.1 [35] was used to perform multivariate statistical analyses. Euclidian distance was used as a distance measure of similarities and Ward's method was applied as a linkage rule.

[2] Annexes disponibles en annexe de la thèse

Factorial analysis (FA) was then applied to the subset. FA attempts to explain covariances [36] expressed as linear combinations of a small number of highly correlated variables (i.e., the chemical elements). The combinations of variables are called factors. Normalized Varimax rotation was applied to the factors [34, 36, 37]. The Kaiser criterion [34, 38] helps to determine the number of factors to be retained; finally, only those components with loadings greater than 1 were retained [35].

4.5.5 RAINWATER SAMPLING AND COMPILATION

Existing data for rainwater composition, primarily extracted from the National Atmospheric Chemistry Database (NatChem database) [39] were initially compiled. In addition, four samples were collected from two stations (two from each) where handmade rain collectors had been installed (Figure 1A). The samples were sent to a commercial lab for analysis, for the same chemical parameters as for groundwater. Rainwater chemistry used in this study is presented in Table 4.1.

Table 4.1 : Rainwater compositions compiled and sampled in this study.

Detection Limit (mg/L)	0.03	0.01	0.1	0.05	2	0.5	2	0.001	0.001	0.0001	0.001	0.0002	0.001	0.001	0.001	0.0001	0.001	0.001	0.002
Sample	**Na (mg/L)**	**Mg (mg/L)**	**K (mg/L)**	**Ca (mg/L)**	**HCO3 (mg/L)**	**Cl (mg/L)**	**SO4 (mg/L)**	**Al (mg/L)**	**Sb (mg/L)**	**Ag (mg/L)**	**Ba (mg/L)**	**Cd (mg/L)**	**Cr (mg/L)**	**Co (mg/L)**	**Cu (mg/L)**	**Mn (mg/L)**	**Mo (mg/L)**	**Ni (mg/L)**	**Zn (mg/L)**
Compilation average*	0.07	0.02	0.02	0.11	*1*	0.13	1.18	0.05	*0.0005*	*0.0001*	*0.0005*	*0.0001*	0.0006	*0.0005*	0.0009	0.008	*0.0005*	*0.0005*	0.074
1	0.16	0.05	0.21	0.40	*1*	*0.25*	1.50	0.02	*0.0005*	*0.0001*	*0.0005*	*0.0001*	*0.0005*	*0.0005*	0.0019	0.004	*0.0005*	*0.0005*	0.019
2	0.05	0.05	0.05	0.15	*1*	*0.25*	1.50	0.04	*0.0005*	*0.0001*	*0.0005*	*0.0001*	0.0016	*0.0005*	0.0150	0.001	*0.0005*	*0.0005*	0.042
3	2.00	0.05	1.10	0.95	*1*	*0.25*	10.00	0.02	*0.0005*	*0.0001*	*0.0005*	*0.0001*	*0.0005*	*0.0005*	0.0010	0.002	*0.0005*	*0.0005*	0.010
4	1.50	0.05	0.81	0.90	*1*	*0.25*	11.00	0.01	*0.0005*	*0.0001*	*0.0005*	*0.0001*	*0.0005*	*0.0005*	0.0009	0.001	*0.0005*	*0.0005*	0.031
Mean	**0.76**	**0.04**	**0.44**	**0.50**	**1**	**0.23**	**5.04**	**0.02**	**0.0005**	**0.0001**	**0.0005**	**0.0001**	**0.0007**	**0.0005**	**0.0039**	**0.003**	**0.0005**	**0.0005**	**0.035**

Half of the detection limit in italic character

Table 2 (continue):

Detection Limit (mg/L)	0.004	0.001	0.01	0.01	0.002	0.001	0.001	0.002	0.001	0.001	0.1	0.0001	0.001	0.02	0.1	0.1	0.1	0.04
Sample	**B (mg/L)**	**Fe (mg/L)**	**Li (mg/L)**	**Se (mg/L)**	**Sr (mg/L)**	**Sn (mg/L)**	**Ti (mg/L)**	**V (mg/L)**	**Be (mg/L)**	**Bi (mg/L)**	**Si (mg/L)**	**Pb (mg/L)**	**U (mg/L)**	**NH4 (mg/L)**	**Br (mg/L)**	**F (mg/L)**	**NO3 (mg/L)**	**P (mg/L)**
Compilation average*	*0.002*	0.033	*0.005*	*0.005*	0.002	0.0017	*0.0005*	*0.001*	*0.0005*	*0.0005*	0.10	0.0034	*0.0005*	*0.01*	*0.05*	*0.05*	1.19	*0.02*
1	*0.002*	*0.005*	*0.005*	*0.005*	0.003	0.0017	*0.0005*	*0.001*	*0.0005*	*0.0005*	*0.05*	0.0015	*0.0005*	*0.01*	*0.05*	*0.05*	*0.05*	*0.02*
2	*0.002*	*0.005*	*0.005*	*0.005*	*0.001*	*0.0005*	*0.0005*	*0.001*	*0.0005*	*0.0005*	*0.05*	0.0070	*0.0005*	*0.01*	*0.05*	*0.05*	0.10	*0.02*
3	*0.002*	*0.005*	*0.005*	*0.005*	*0.001*	*0.0005*	*0.0005*	*0.001*	*0.0005*	*0.0005*	*0.05*	0.0003	*0.0005*	1.50	*0.05*	*0.05*	0.10	*0.02*
4	*0.002*	*0.005*	*0.005*	*0.005*	*0.001*	*0.0005*	*0.0005*	*0.001*	*0.0005*	*0.0005*	*0.05*	0.0003	*0.0005*	0.72	*0.05*	*0.05*	0.10	*0.02*
Mean	**0.002**	**0.011**	**0.005**	**0.005**	**0.002**	**0.0010**	**0.0005**	**0.001**	**0.0005**	**0.0005**	**0.06**	**0.0025**	**0.0005**	**0.45**	**0.05**	**0.05**	**0.31**	**0.02**

Half of the detection limit in italic character

*Compiled data: Canadian Air and Precipitation Monitoring Network (CAPMoN; Environment Canada, 2015); Réseau d'échantillonnage des precipitations du Québec (REPQ; MDDELCC, 2015); Blanchette et al. (2011); Losno (1989); Jaffrezo (1987); Jickells et al. (1984); Ross (1987); Boutron (1979); Cambray et al. (1975); The MAP3S/RAINE Research Community, (1982).

4.5.6 STANDARDIZATION TECHNIQUE

The degree of enrichment and/or depletion of an element is calculated by dividing the concentration of an element found in a sample by the concentration of the same element found in a selected reference water sample. The gain or the loss of one or a combination of chemical elements during the process of evolution is interpreted to be a consequence of the interaction of the groundwater with its environment — in this case the "environment" is a combination of aquifer type and hydrogeological context. Another possible explanation for the increase of chemical content in groundwater during its evolution over time could be the mixing of several different groundwaters having different origins.

Standardization gives rise to the maturation index (MI) expressed as:

$$MI = \frac{[X]_{Step\ y+n}}{[X]_{Step\ y}}$$ (Equation 1)

where $[X]_{Step\ y}$ is the mean concentration of the chemical element *X* of the water that characterizes the step of evolution y, and $[X]_{Step\ y+n}$ is the mean concentration of the chemical element *X* of the water of reference that characterizes a more advanced stage of evolution (+ n). A value of one denotes no enrichment nor depletion during the process of evolution. A value of *MI* greater than 1 indicates that the chemical element *X* is gained in groundwater from the environment. A value of *MI* lower than 1 suggests the loss of the chemical element from groundwater (i.e., precipitation/adsorption) or by mixing with groundwater whose content in the chemical element has been depleted.

4.5.7 COMPILATION OF CANADIAN SHIELD BRINE DATA

Chemical data for brines found at depth in the Canadian Shield were compiled from the existing literature so as to investigate the geochemical origin of the end-members in this study. A total of 137 chemical analyses (i.e. samples) from five studies were included: Frape and Fritz [40], 33 samples; Bottomley et al. [41], 24 samples; Frape and Fritz [42], 36 samples; Frape et al. [43], 35 samples; and Gascoyne and Kamineni [44], 17 samples. The compiled data are presented as supplementary material (Appendix 2).

4.6 RESULTS

4.6.1 DATABASE *VERSUS* SUBSET

By combining the 2 groundwater types (HCO_3^- or Cl^-) and the 2 aquifer types (bedrock or granular aquifer) considered in this study, the 321-sample dataset was divided into four groundwater groups: Group 1: bicarbonate groundwater from granular aquifers (*Ca*(*Na)-HCO$_3$_ GranAq*; 132 samples); Group 2: chloride groundwater from granular aquifers (*Na(Ca)-Cl_GranAq*; 19 samples); Group 3: bicarbonate groundwater from bedrock aquifers ((*NaCa)-HCO$_3$_RockAq*; 124 samples); Group 4: chloride groundwater from bedrock aquifers ((*NaCa)-Cl_RockAq*; 46 samples). For each group, values above the detection limit (*N*), the median, the first (*25*) and third (*75*) quartiles, the maximum (*Max)* and the minimum (*Min*) are presented in supplementary material (Appendix 3). Conventional statistics calculated for the entire database are also presented and described in Walter et al. [11].

Figure 4.3 presents the frequencies of detection of the chemical elements for each of the four groundwater groups. Along the X-axis, ionic species are sorted in descending order of abundance for Group 1 (*Ca*(*Na)-HCO$_3$_ GranAq*). Depending on the type of groundwater (HCO_3^- or Cl^-) and the type of aquifer (bedrock or granular aquifer), each chemical element presented a different number of valid data units. For instance, boron (B^{3+}) and molybdenum (Mo^{6+}) are commonly detected in groundwater from bedrock aquifers; lithium (Li^+) and bromide (Br^-) were frequently detected in brackish groundwater,

particularly in bedrock aquifers; and copper (Cu^{2+}), lead (Pb^{2+}) and nitrate (NO_3^-) were more commonly detected in bicarbonate groundwater, particularly in granular aquifers. These observations suggest that the salinization path of bicarbonate groundwater toward a chloride endmember is characterized by several different chemical fingerprints inherited from the aquifer matrix (bedrock or granular aquifer).

Figure 4.3 also shows that only 10 chemical parameters (K^+, HCO_3^-, Mg^{2+}, SiO_2, Na^+, Ca^{2+}, Ba^{2+}, Sr^{2+}, SO_4^{2-}, and Mn^{2+}) presented less than 25% of valid data and can be directly used in multivariate statistical process of the dataset (c.f. *3.3 Preparation for multivariate purposes: the subset*). On the contrary, more than 25% of the bicarbonated water (Group 1 and 3) showed fluoride and iron contents to be <DL. Again for iron, more than 25% of the chloride groundwater from granular aquifers (Group 2) was <DL. To include fluoride and iron in the multivariate processing, a subset of samples was defined (c.f. *3.3 Preparation for multivariate purposes: the subset*). The subset included samples that were screened in each of the four groups of groundwater: 16 samples were screened in group 1 (bicarbonate groundwater from granular aquifers – (*Ca*N*a)-HCO$_3$_ GranAq*); 9 samples were screened in group 2 (chloride groundwater from granular aquifers – (*CaNa)-Cl_GranAq*); 16 samples were screened in group 3 (bicarbonate groundwater from bedrock aquifers – (*CaNa)-HCO$_3$_RockAq*); and 10 samples were screened in group 4 (chloride groundwater from bedrock aquifers – (*CaNa)-Cl_RockAq*).

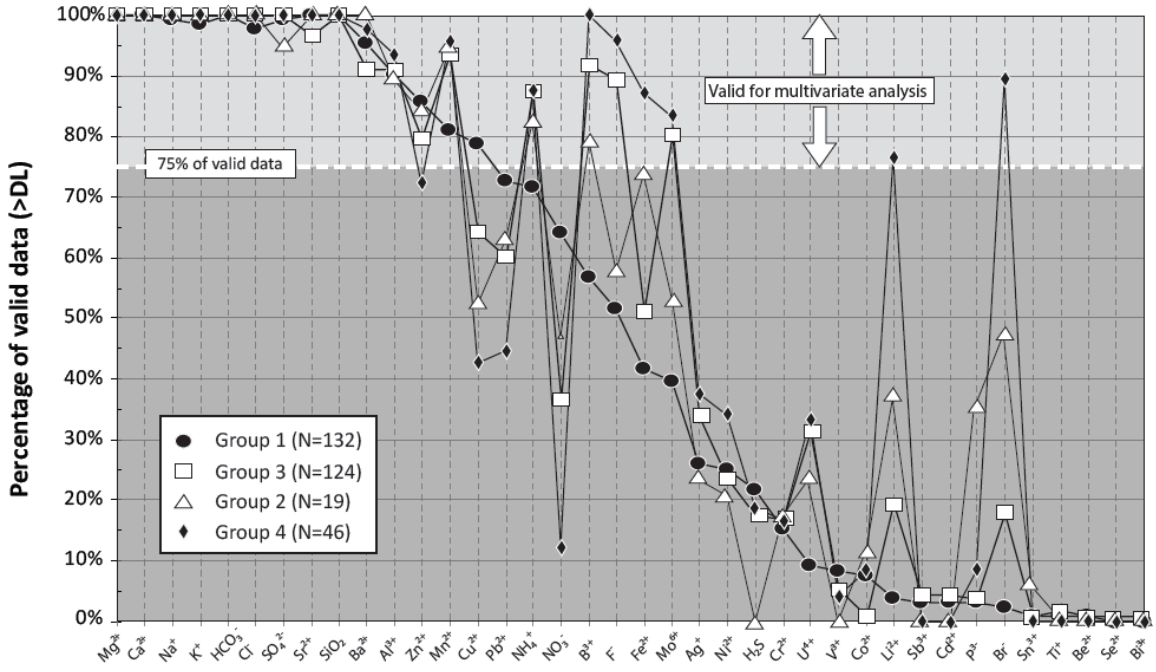

Figure 4.3 : Line graph of the percentage of valid data (i.e., above the detection limit) for each groundwater group (Group 1: *Ca(Na)-HCO_3_ GranAq;* Group 2*: Na(Ca)-Cl_GranAq;* Group *3:* (*NaCa)-HCO_3_RockAq;* and Group 4: (*NaCa)-Cl_RockAq group).* Depending on the type of groundwater (HCO_3^- or Cl^-) and the type of aquifer (bedrock or granular), for each chemical element presented, there were varying numbers of valid data. Ten chemical parameters (K^+, HCO_3^-, Mg^{2+}, SiO_2, Na^+, Ca^{2+}, Ba^{2+}, Sr^{2+}, SO_4^{2-}, and Mn^{2+}) presented less than 25% of valid data and could be directly used in multivariate statistical processing. For each group, values above the detection limit (*N*), the median, the first (*25*) and third (*75*) quartiles, the maximum (*Max)* and the minimum (*Min*) are presented in supplementary material (Appendix 3).

Table 4.2 presents the descriptive statistics (values above the detection limit - *N*; the median, the first - *25*; and third - *75* quartiles, the maximum – *Max;* and the minimum - *Min*) for the 51-sample subset. The physical and chemical data for the 51 samples are presented in Table 4.3. The distribution of the 51 samples over the study area is presented in Figure 4.1A. Some of the samples were taken from wells that followed the general

orientation of the major fault delimitating the South and the West wall of the graben, and the other sampled wells were generally located around Lake Saint-Jean and along the Saguenay River. The 51 samples represent a good distribution over the study area.

Figure 4.4 shows the comparison between the frequencies of detection of the chemical elements for the 321-sample dataset and the 51-sample subset. Along the X-axis, ionic species are sorted in descending order of abundance for the database. A total of four new chemical elements showed a number of analytical data >DL (i.e., valid data) exceeding 75% of the 51-sample subset (fluoride, ammonium, iron and molybdenum) and can now be rigorously used in statistical multivariate processing. The 51-sample subset also presented more manganese, barium, zinc, boron, ammonium, molybdenum, nitrate, silver, nickel, bromide, lithium, uranium and phosphorus. Only the number of detection for aluminium slightly decreased. Figure 4.5 shows the comparison between the median concentration in ppm for each chemical parameter of the database and the subset on a log scale (Y axis). Chemical parameters (X axis) are sorted in descending order of differences between median concentrations for the 321-sample database and the 51-sample subset (Δ m.c) expressed in ppm.

Table 4.2 : Statistical data for the 51 sample subset.

	N	%Detect	Median	25	75	Min	Max	Multivariate
TDS (mg/L)	51	100%	427.2	238.3	1359.6	72.0	7291.4	
Temperature (Celcius)*	50	98%	7.66	7.13	8.56	5.97	15.60	
Redox potential (mV)*	47	92%	79.4	-27.1	101	-245.7	524.9	
pH*	50	98%	7.63	7.23	8.09	4.49	10.06	
Dissolved oxygen (mg/L)*	38	75%	0.17	0.00	1.82	0.00	8.63	
Sodium**	***51***	***100%***	***40.00***	***7.50***	***350.00***	***1.50***	***1900.00***	x
Magnesium**	***51***	***100%***	***8.70***	***3.90***	***15.00***	***1.50***	***160.00***	x
Potassium**	***51***	***100%***	***3.50***	***2.40***	***7.50***	***0.54***	***64.00***	x
Calcium**	***51***	***100%***	***55.00***	***21.00***	***81.00***	***2.10***	***1500.00***	x
Bicarbonates*****	***51***	***100%***	***207.40***	***118.34***	***280.60***	***6.10***	***695.40***	x
Chloride***	***50***	***98%***	***37.00***	***6.40***	***510.00***	***0.40***	***4200.00***	
Sulfates***	***51***	***100%***	***18.00***	***9.20***	***63.00***	***1.00***	***430.00***	x
Barium**	***50***	***98%***	***0.055***	***0.027***	***0.110***	***0.006***	***0.320***	x
Boron**	***47***	***92%***	***0.120***	***0.016***	***0.320***	***0.006***	***0.750***	x
Strontium**	***51***	***100%***	***0.400***	***0.180***	***1.900***	***0.033***	***37.000***	x
Silicium**	***51***	***100%***	***6.500***	***5.400***	***8.100***	***0.220***	***13.000***	x
Manganese**	***50***	***98%***	***0.031***	***0.011***	***0.067***	***0.001***	***0.900***	x
Fluoride****	***48***	***94%***	***0.800***	***0.300***	***1.300***	***0.100***	***2.400***	x
Aluminium**	***44***	***86%***	***0.007***	***0.005***	***0.013***	***0.002***	***0.087***	
Bromide***	21	41%	3.5000	1.6000	11.0000	0.1000	45.0000	
Iron**	***41***	***80%***	***0.1500***	***0.0900***	***0.3600***	***0.0320***	***3.4000***	x
Lithium**	22	43%	0.0180	0.0120	0.0370	0.0050	0.5700	
Zinc**	***44***	***86%***	***0.0145***	***0.0077***	***0.0375***	***0.0016***	***0.1500***	
Lead**	33	65%	0.0004	0.0002	0.0006	0.0001	0.0024	
Amonium****	***46***	***90%***	***0.2300***	***0.0600***	***0.5100***	***0.0200***	***3.0000***	x
Copper**	33	65%	0.0027	0.0014	0.0110	0.0006	0.0350	
Molybdene**	***45***	***88%***	***0.0018***	***0.0014***	***0.0029***	***0.0006***	***0.0150***	x
Nickel**	19	37%	0.0019	0.0011	0.0039	0.0010	0.0110	
Silver**	21	41%	0.0002	0.0002	0.0003	0.0001	0.0090	
Uranium**	17	33%	0.0018	0.0011	0.0054	0.0010	0.0096	
Chromium**	6	12%	0.0013	0.0007	0.0018	0.0005	0.0024	
Nitrate***	28	55%	0.3000	0.1000	0.7500	0.0200	6.3000	
Cobalt**	2	4%	0.0023	0.0019	0.0026	0.0019	0.0026	
Inorganic phosphorus****	9	18%	0.0500	0.0443	0.0600	0.0400	0.0900	
Vanadium**	3	6%	0.0023	0.0023	0.0069	0.0023	0.0069	
Antimony**	2	4%	0.0017	0.0014	0.0020	0.0014	0.0020	
Cadmium**	2	4%	0.0007	0.0006	0.0007	0.0006	0.0007	
Selenium**	0	0%	-	-	-	-	-	
Tin**	1	2%	0.0034	-	-	-	-	
Titanium**	0	0%	-	-	-	-	-	
Beryllium**	0	0%	-	-	-	-	-	
Bismuth**	0	0%	-	-	-	-	-	

ANALYTICAL METHODS
* multiparameter probe (in situ)
**Inductively Coupled Plasma Mass Spectrometry
*** Ionic chromatography
**** Specific probe
***** Titration
25 and 75 header = the first and the third quantiles
TDS is calculated using the software Aquachem v.5.0

For major, minor and trace elements, data are given in mg/L
For the physical parameters, N = number of mesured data
For the lab analysed parameters, N = Number of detected values
If N = 1 or 2: data are underlined
If N = 1: unique measured value is presented
If N = 2: mean value is presented

Multivariate header = parameters used in the multivariate analysis

By screening the samples, the ionic content of the 51-sample subset increased, although the m.c of some chemical elements remained unchanged or decreased (Figure 4.5). Variations of the median of the 2 datasets calculated in percentages are presented in supplementary material (Appendix 4). Chemical parameters with decreasing content were vanadium (88% the m.c of the 321-sample database), uranium (86% the m.c of the 321-

sample database), phosphate (71% the m.c in the 321-sample database) and copper (63% the m.c of the 321-sample database). Selenium, beryllium, titanium and bismuth were all <DL in the 51-sample subset. For silver, nitrate and nickel, the m.c for the 51-sample subset was equal to the m.c for the 321-sample database. The most significant increase is for chloride (370% the m.c of the 321-sample database) and ammonium, (288% the m.c of the 321-sample database). The correlation matrices for the subset and the database (supplementary material; Appendix 5) showed that ammonium was highly correlated to major elements (K^+, HCO_3^-, Mg^{2+}, Na^+, Ca^{2+}, Cl^- and SO_4^{2-}), as well as some minor elements (Ba^{2+}, Sr^{2+} and B^{3+}) and some trace elements (Li^{2+}, Br^- and Pb^{2+}).

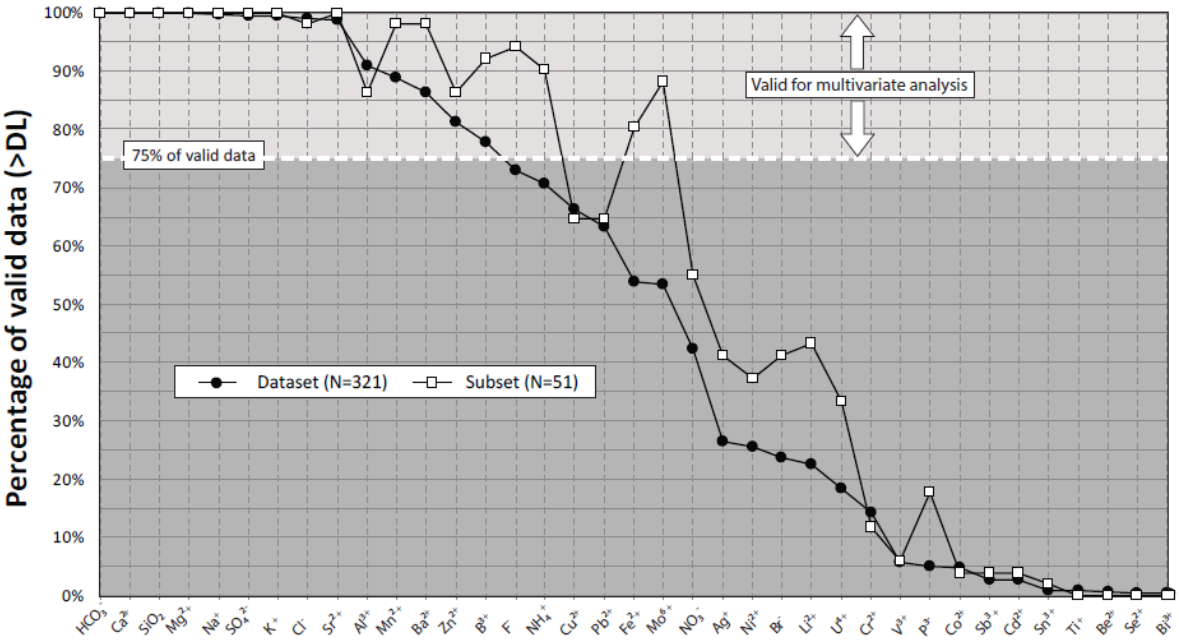

Figure 4.4: Comparison between the frequencies of detection of the chemical elements for the 321-sample dataset and the 51-sample subset. Compared to Figure 4.3, four additional chemical elements showed a number of analytical data >DL (i.e., valid data) exceeding 75% (F^-, NH_4^+, Fe^{2+} and Mo^{6+}). A total of 14 chemicals could be justifiably included in statistical multivariate treatment (valid data exceeding 75%).

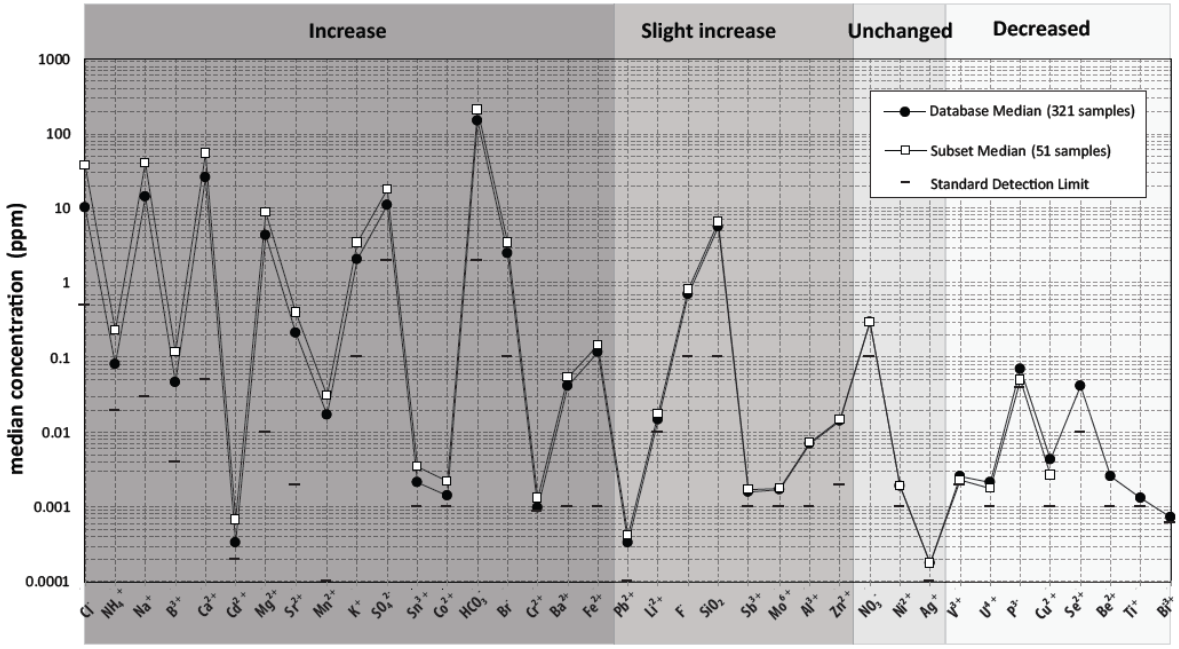

Figure 4.5 : Comparison between the median concentration in ppm for each chemical parameter of the database and the subset on a log scale (Y axis). Chemical parameters (X axis) are sorted in descending order of differences between median concentrations for the 321-sample database and the 51-sample subset expressed in ppm. Compared to the 321-sample dataset, the ionic content of the 51-sample subset increased although the m.c. of some chemical elements remained unchanged or decreased. Variations for the median of the 2 datasets calculated in percentage are presented in supplementary material (Appendix 4).

In conclusion, compared to the original 321-sample dataset, the 51-sample subset contains concentrated samples for major (cation and anion), minor and some trace metallic elements, and is depleted for only few ultra-trace elements (selenium, beryllium, titanium and bismuth).

Table 4.3 : Physical and chemical data for the 51 samples of the subset.

Sample	Cluster Number	Aquifer Type	Water Type	TDS	T	Eh	pH	O.D	Sodium	Magnesium	Potassium	Calcium	Bicarbonate	Chloride	Sulfate	Aluminium	Antimony	Silver	Baryum	Cadmium	Chromium	Cobalt
				(mg/L)		(mV)		(mg/L)	(mg/L)	(mg/L)	(mg/L)	(mg/L)	(mg/L)	(mg/L)	(mg/L)	(mg/L)	(mg/L)	(mg/L)	(mg/L)	(mg/L)	(mg/L)	(mg/L)
				Detection Limit (DL)					0.03	0.01	0.1	0.05	2	0.5	2	0.001	0.001	0.0001	0.001	0.0002	0.001	0.001
1	1	Rock	Ca-HCO3	125.5	11	133.5	4.7	Unk	4.3	2.1	2.5	23	70.76	3	4.8	0.0076	-	-	0.022	-	-	-
2	1	Rock	Ca-HCO3	72.0	7.9	100.5	4.49	Unk	2.1	1.5	0.92	11	40.26	-	4	0.0095	-	0.00041	0.018	-	-	-
3	1	Rock	Ca-HCO3	153.6	6	524.9	8.06	0.22	5.4	4.3	1	24	104.92	0.5	1.1	0.007	-	-	0.015	-	-	-
4	1	Rock	Ca-HCO3	322.8	8.8	UnK	7.44	5.59	5.5	7.5	2.9	58	219.6	5.1	13	0.0048	0.002	-	0.12	-	-	-
5	1	Rock	Ca-HCO3	162.6	7.8	101.5	6.19	6.46	7.5	3.9	1.5	28	69.54	19	13	0.0092	-	-	0.047	0.00073	-	-
6	1	Rock	Ca-HCO3	93.0	7.1	101	7.83	0.9	2.5	2.8	2.1	11	50.02	0.5	6.3	0.0067	-	-	0.018	-	-	-
7	1	Granular	Ca-HCO3	326.5	6.3	55.7	6.29	Unk	4.2	3.5	2.7	70	207.4	8.6	11	0.0075	-	0.00015	0.026	-	-	-
8	1	Granular	Ca-HCO3	229.6	11	5.63	41.8	Unk	9.3	11	3.3	24	146.4	5.4	9.4	-	-	0.00018	0.02	-	-	-
9	1	Granular	Ca-HCO3	84.7	7	64.5	5.56	Unk	4.4	2.1	1.3	9.6	51.24	0.4	3.3	0.0095	-	0.00018	0.0055	-	0.0018	-
10	1	Granular	Ca-HCO3	427.2	6.9	90.6	7.73	1.7	3.6	11	3.9	81	268.4	6.4	41	0.003	-	-	0.14	-	-	-
11	1	Granular	Ca-HCO3	335.4	6.6	90.2	8.01	8.63	4	6.1	2.5	64	219.6	4.8	25	-	-	-	0.08	-	-	-
12	1	Granular	Ca-HCO3	396.7	7.1	120.4	7.39	3.33	7.6	10	2.4	76	256.2	9.1	23	0.022	-	0.0001	0.027	-	-	-
13	1	Granular	Ca-HCO3	200.1	7.7	116.4	7.63	2.85	9.5	9.7	3.6	23	118.34	8.3	10	0.0088	-	-	0.017	-	-	-
14	1	Granular	Ca-HCO3	311.6	8.1	97.8	7.49	0.77	13	8.2	3.5	46	207.4	9.6	7	0.0053	-	-	0.055	-	-	-
15	1	Granular	Ca-HCO3	238.3	9.1	UnK	7.67	2.45	1.5	3	0.77	55	170.8	1.4	5.8	0.002	-	-	0.058	-	0.00071	-
16	2	Rock	Ca-HCO3	372.2	7.9	95.2	5.58	Unk	25	7.2	2.8	60	231.8	10	26	0.0096	-	0.00029	0.16	-	-	-
17	2	Rock	Ca-HCO3	229.1	6.6	42.5	6.02	Unk	21	6.3	2.4	25	102.48	45	12	0.023	-	0.00021	0.087	-	0.0017	-
18	2	Rock	Ca-HCO3	393.0	6.3	-182	7.55	0	20	6.7	2.8	71	207.4	45	25	0.0072	-	0.00018	0.11	0.00061	-	-
19	2	Rock	Na-HCO3	474.5	7.7	93	8.64	0	110	3	3	10	292.8	22	18	0.017	-	-	0.037	-	-	-
20	2	Rock	Na-HCO3	512.4	7.3	111.5	8.01	0	140	2.6	3.3	7.1	256.2	65	24	0.0078	-	-	0.03	-	-	-
21	2	Rock	Ca-HCO3	304.9	7.2	307.2	7.53	4.73	8.4	6.8	1.8	63	207.4	3.5	14	-	-	0.00016	0.13	-	-	-
22	2	Rock	Ca-HCO3	508.6	UnK	UnK	UnK	Unk	47	12	3.7	77	195.2	110	45	0.058	-	-	0.065	-	-	-
23	2	Rock	Ca-HCO3	207.7	7.3	-98.9	8.21	1.18	20	5.7	1.4	26	111.02	16	15	0.0054	-	-	0.24	-	-	-
24	2	Rock	Na-HCO3	497.4	8.6	UnK	8.06	0	130	3	5.3	7.3	256.2	64	16	0.02	-	-	0.015	-	-	-
25	2	Rock	Na-HCO3	401.0	7.7	58.1	8.54	0.87	100	1.9	4.4	4.7	231.8	39	3.3	-	-	-	-	-	-	-
26	2	Granular	Na-HCO3	403.8	13	43.1	5.64	Unk	48	15	5.9	21	256.2	24	18	0.0097	-	0.00016	0.043	-	-	-
27	2	Granular	Ca-HCO3	459.4	7.6	79.4	8.04	0	40	11	3.1	56	292.8	35	2.1	0.036	0.0014	0.00069	0.055	-	-	-
28	2	Granular	Na-HCO3	217.4	9.8	88.7	8.22	0	16	8.7	7.1	15	146.4	4.3	3.5	0.0022	-	-	0.05	-	-	-
29	2	Granular	Ca-HCO3	247.9	6.8	98.9	7.57	8.48	13	14	4.8	21	170.8	1.1	5	0.0039	-	0.0001	0.031	-	-	-
30	2	Granular	Ca-HCO3	228.6	6	91.6	8.33	0	13	11	5.6	24	134.2	14	9.2	0.0044	-	0.00012	0.078	-	-	-
31	2	Granular	Ca-HCO3	454.7	9.1	-75	6.93	0.72	7.5	15	5.6	84	280.6	16	30	0.0063	-	0.00014	0.06	-	-	0.0026
32	2	Granular	Ca-HCO3	463.9	16	6.4	6.84	1.57	5.6	4	7.5	110	305	2.6	12	0.022	-	-	0.094	-	-	0.0019
33	2	Rock	Ca-Cl	391.3	6.7	129.6	7.54	7.55	45	3.9	0.65	62	117.12	110	40	-	-	-	0.018	-	-	-
34	2	Rock	Na-Cl	1794.8	7.3	102.5	10.1	0	560	12	20	2.1	683.2	510	1	0.0048	-	0.009	0.012	-	-	-
35	2	Granular	Na-Cl	1679.6	7.6	-147	7.41	0	490	20	34	36	341.6	690	68	0.087	-	-	0.094	-	-	-
36	3	Rock	Na-Cl	499.0	7.3	-29.9	7.62	Unk	110	7.8	3.2	32	134.2	170	25	0.0029	-	0.0012	0.32	-	-	-
37	3	Rock	Ca-Cl	630.0	6.6	-27.1	7.72	Unk	75	3.3	0.54	130	104.92	280	9.5	0.0028	-	-	0.22	-	-	-
38	3	Rock	Ca-Cl	5227.9	8.5	-246	8.6	0	570	3	1.6	1500	6.1	3000	53	0.0035	-	-	0.26	-	-	-
39	3	Rock	Ca-Cl	2113.4	9.2	82.9	7.78	0	260	60	4.5	400	231.8	1000	110	0.026	-	0.0002	0.16	-	-	-
40	3	Rock	Ca-Cl	590.7	7.4	91.1	8.53	0	84	17	1.6	94	104.92	230	45	0.0037	-	-	0.054	-	-	-
41	3	Rock	Ca-Cl	2857.2	8.4	-102	7.82	0	380	54	3.6	580	158.6	1600	81	0.0072	-	-	0.18	-	-	-
42	3	Rock	Na-Cl	7291.4	7.8	-21.8	7.59	1.82	1800	140	16	520	134.2	4200	420	0.0091	-	0.00015	0.2	-	0.0024	-
43	3	Granular	Na-Cl	1352.8	7.8	104.9	8.1	0	220	15	11	200	183	630	63	0.02	-	-	0.07	-	-	-
44	4	Rock	Na-Cl	6301.0	7.2	-100	7.23	0	1900	160	64	120	427	3200	430	-	-	-	0.024	-	-	-
45	4	Granular	Na-Cl	5573.4	7.5	27.9	6.47	Unk	1600	100	55	60	695.4	2700	330	0.0046	-	0.00016	0.039	-	-	-
46	4	Granular	Na-Cl	1359.6	9.5	-21.2	7.31	Unk	350	13	13	9.8	536.8	340	79	0.012	-	0.00028	0.029	-	0.00098	-
47	4	Granular	Na-Cl	3576.0	7.8	-132	7.61	0.73	980	52	21	150	317.2	1900	120	0.0021	-	0.00033	0.25	-	-	-
48	4	Granular	Na-Cl	1387.7	7.5	107.5	8.71	0	410	18	14	19	207.4	570	130	0.013	-	-	0.053	-	-	-
49	4	Granular	Na-Cl	6107.6	7.6	-97.9	7.2	0	1900	160	64	100	463.6	3000	420	-	-	-	0.064	-	0.00052	-
50	4	Granular	Na-Cl	2709.1	9.4	-8.3	8.09	0	830	33	31	58	380.64	1100	250	0.007	-	-	0.06	-	-	-
51	4	Granular	Na-Cl	1283.2	9.4	-75.3	8.47	0.11	370	13.4	15	21	353.8	390	100	0.007	-	-	0.043	-	-	-

-: undetected
UnK: unknown

Table 4.3 (continued)

Sample	0.001	0.0001	0.001	0.001	0.002	0.004	0.001	0.01	0.01	0.002	0.001	0.001	0.002	0.001	0.001	0.1	0.0001	0.001	0.02	0.1	0.1	0.1	0.04
	Copper	Manganese	Molybdenum	Nickel	Zinc	Boron	Iron	Lithium	Selenium	Strontium	Tin	Titan	Vanadium	Berillium	Bismuth	Silicium	Lead	Uranium	Amonium	Bromide	Fluoride	Nitrate	Phosphorus
	(mg/L)	(mg/L)	(mg/L)	(mg/L)	(mg/L)	(mg/L)	(mg/L)	(mg/L)	(mg/L)	(mg/L)	(mg/L)	(mg/L)	(mg/L)	(mg/L)	(mg/L)	(mg/L)	(mg/L)	(mg/L)	(mg/L)	(mg/L)	(mg/L)	(mg/L)	(mg/L)
1	0.026	0.0025	-	-	0.052	-	0.046	-	-	0.068	-	-	-	-	-	5.6	0.001	-	0.03	-	0.1	3.5	-
2	0.035	0.0094	-	-	0.038	0.0086	0.12	-	-	0.18	-	-	-	-	-	5.6	0.00042	-	0.32	-	0.2	0.1	-
3	0.0034	0.048	0.008	0.0012	0.036	0.021	0.032	-	-	0.23	-	-	-	-	-	5.5	0.00041	0.0013	0.05	-	0.9	-	-
4	0.0098	0.0019	-	-	0.0081	-	0.071	-	-	0.43	-	-	-	-	-	4.9	0.00047	-	0.03	-	-	0.7	-
5	0.01	0.0043	-	0.0011	0.037	-	0.033	-	-	0.18	-	-	-	-	-	8.3	0.00055	-	-	-	-	3.2	-
6	0.002	0.0041	0.002	-	0.012	0.011	0.043	-	-	0.041	-	-	0.0023	-	-	8.5	0.00029	-	0.04	-	0.4	0.2	-
7	0.0007	0.062	0.0006	-	0.0073	-	0.062	-	-	0.19	-	-	-	-	-	6.2	0.00031	-	0.05	-	-	6.3	-
8	0.012	0.014	0.0006	-	0.058	0.01	0.14	0.013	-	0.21	-	-	-	-	-	9.6	0.00022	-	0.06	-	0.2	0.9	-
9	0.0092	0.00089	0.00087	-	0.055	0.011	-	-	-	0.033	-	-	0.0023	-	-	5.7	0.0014	-	0.04	-	0.6	0.2	-
10	0.0027	0.039	0.0018	0.0029	0.0052	0.0055	1.1	-	-	0.2	-	-	-	-	-	5.1	0.00049	-	0.02	-	0.2	-	-
11	-	0.015	0.0013	0.0021	-	0.011	0.11	-	-	0.17	-	-	-	-	-	4.4	-	-	-	-	0.1	0.1	-
12	0.0059	0.03	0.0015	0.0019	0.017	0.014	-	-	-	0.21	-	-	-	-	-	5.7	0.00023	-	0.05	-	0.1	0.51	-
13	0.0019	0.0024	0.00075	-	0.024	0.0072	0.3	-	-	0.16	-	-	-	-	-	8.1	-	-	0.07	-	0.1	0.8	-
14	0.015	0.032	0.0021	0.0016	0.026	0.015	3.4	-	-	0.14	-	-	-	-	-	6.3	-	0.0011	-	-	0.3	0.3	-
15	0.0012	0.094	0.00083	-	-	0.02	2.4	-	-	0.14	-	-	-	-	-	5.7	-	-	0.05	-	0.2	0.02	-
16	0.029	0.0087	0.00099	0.0012	0.0086	0.12	-	-	-	1.2	-	-	-	-	-	3.4	0.00067	-	0.06	-	0.8	0.21	-
17	0.0049	0.038	0.002	0.0011	0.014	0.024	0.09	-	-	0.33	-	-	-	-	-	6.8	0.00045	-	0.09	-	0.6	-	-
18	0.028	0.015	0.0011	0.0039	0.028	0.03	0.32	-	-	0.72	-	-	-	-	-	6.7	0.00032	-	0.08	-	0.4	-	-
19	-	0.013	0.0015	-	-	0.18	0.12	-	-	0.4	-	-	-	-	-	6.1	-	0.0054	0.29	0.1	2.3	0.02	0.05
20	-	0.0035	0.0027	-	-	0.14	0.032	-	-	0.28	-	-	-	-	-	5.3	0.0024	0.0089	0.06	0.2	2.3	0.5	-
21	0.0025	0.013	0.0029	-	0.011	0.022	-	-	-	2	-	-	-	-	-	6.1	0.00088	0.0054	0.05	-	1.7	1.7	-
22	0.002	0.065	0.0018	0.0021	0.02	0.057	0.36	-	-	1.6	-	-	-	-	-	7.1	0.00043	-	0.11	-	1	-	-
23	0.014	0.009	0.0012	0.0058	0.032	0.042	-	-	-	2.2	-	-	-	-	-	4.5	0.002	-	0.16	-	0.8	0.1	-
24	0.0014	0.013	0.0029	0.0039	0.011	0.3	-	-	-	0.16	-	-	-	-	-	6.7	0.00058	0.0055	0.23	-	1.3	0.1	-
25	-	0.015	0.00065	-	0.13	0.46	0.19	0.011	-	0.077	-	-	-	-	-	6.5	-	-	0.45	-	1.2	0.4	-
26	0.011	0.00081	0.0031	-	0.012	0.068	-	-	-	0.27	-	-	-	-	-	7.1	0.00041	0.001	0.08	-	0.7	0.3	-
27	0.0009	0.042	-	-	0.004	0.13	0.78	0.018	-	0.96	-	-	-	-	-	8.1	0.00016	-	0.51	-	0.4	-	-
28	-	0.021	0.003	-	0.0021	0.011	0.13	-	-	0.14	-	-	-	-	-	7.7	0.00014	-	0.28	-	0.3	0.02	-
29	0.016	0.011	0.0017	0.011	0.015	0.015	-	-	-	0.16	-	-	-	-	-	8.6	0.00051	-	0.07	-	0.2	0.5	-
30	0.0009	0.033	0.0029	-	0.0023	0.016	0.081	-	-	0.35	-	-	-	-	-	8	0.00022	-	0.23	-	0.8	-	-
31	0.0006	0.9	0.0022	0.0031	0.09	0.017	2	-	-	0.31	-	-	-	-	-	6.1	0.0002	-	0.34	-	0.1	-	-
32	0.0035	0.66	-	0.0042	0.072	0.025	0.21	-	-	0.46	-	-	0.0069	-	-	6.5	0.00015	-	0.4	-	0.1	2.1	-
33	-	-	0.0015	-	0.0041	0.037	-	0.021	-	0.69	-	-	-	-	-	5.4	-	0.0096	-	0.2	0.7	0.11	-
34	0.0012	0.0092	0.006	0.001	0.0067	0.35	0.15	0.01	-	0.22	-	-	-	-	-	0.22	-	-	1.8	1.9	1.6	-	-
35	-	0.15	0.00056	-	0.0092	0.29	3.1	0.017	-	0.49	-	-	-	-	-	9.2	-	-	0.46	2.8	0.7	-	0.09
36	-	0.025	0.0016	-	-	0.25	0.066	0.013	-	1.4	-	-	-	-	-	5.6	0.00019	-	0.51	2	1	-	-
37	-	0.19	0.0078	-	0.0041	0.22	0.15	0.07	-	4.1	-	-	-	-	-	8.2	-	0.0019	-	3.5	1.9	-	-
38	0.0015	0.11	0.0065	-	0.012	0.14	0.7	0.57	-	37	-	-	-	-	-	4.5	-	-	0.12	45	1.3	-	-
39	0.0006	0.046	0.0017	0.001	0.0029	0.32	0.1	0.084	-	18	-	-	-	-	-	5.2	0.0015	-	1.7	15	1.3	-	0.06
40	-	0.081	0.0036	-	0.0016	0.15	0.13	0.014	-	2.3	-	-	-	-	-	3.4	0.00011	0.0036	0.07	3	1.6	-	-
41	0.0026	0.077	0.0059	-	0.064	0.75	-	0.082	-	22	-	-	-	-	-	5	0.00062	-	1.3	24	2.4	-	-
42	-	0.61	0.015	-	0.1	0.46	0.27	0.12	-	27	-	-	-	-	-	4.8	-	-	3	19	0.8	-	0.04
43	-	0.061	0.0028	-	0.0066	0.17	0.29	0.012	-	7.8	-	-	-	-	-	6.5	-	0.0011	0.41	8	1	-	-
44	-	0.089	0.0014	-	-	0.68	1.3	0.037	-	3.7	-	-	-	-	-	11	-	0.0016	2.8	12	1.1	-	-
45	-	0.071	0.0015	0.0016	0.044	0.57	0.19	0.018	-	1.4	-	-	-	-	-	8.8	-	0.0018	2.2	10	0.9	-	-
46	0.0011	0.031	0.0044	-	0.026	0.36	0.13	-	-	0.19	0.0034	-	-	-	-	6.9	0.00021	0.0021	0.47	1.1	1.8	-	0.07
47	-	0.055	0.0016	0.0011	0.015	0.38	1	0.031	-	5.8	-	-	-	-	-	9.1	0.00019	-	1.4	7	1.7	-	0.05
48	-	0.011	0.0055	-	0.15	0.19	0.19	-	-	0.71	-	-	-	-	-	6.7	0.0001	-	0.81	1.6	1.7	0.46	-
49	-	0.098	0.0015	-	-	0.66	1.3	0.03	-	2.9	-	-	-	-	-	13	-	0.0012	2.4	11	1.1	-	0.04
50	0.002	0.067	-	-	0.014	0.6	0.19	0.02	-	1.9	-	-	-	-	-	9.1	-	LD	LD	4.105	1.3	LD	LD
51	-	0.018	-	-	0.011	0.36	0.047	0.009	-	0.98	-	-	-	-	-	7.7	-	LD	LD	1.477	1.6	LD	LD

4.6.2 HIERARCHICAL CLUSTER ANALYSIS

Hierarchical cluster analysis (HCA) is a semi-objective method [45], where the number of clusters of similar samples is determined by the position of the phenon line that cuts across the resulting dendrogram (Figure 4.6A). In our HCA, the distance linkage (Dlink) of the samples is expressed as a percentage of the maximum distance (Dmax) between the most dissimilar samples ([Dlink/Dmax]*100). At this scale, 100% linkage (Dlink = Dmax) would indicate that all samples are grouped into a single cluster that corresponds to the 51-sample subset. For this study, four clusters (Dlink <30% of Dmax) provided the most satisfactory result and fulfilled the objectives of our classification method (Figure 4.6A). Major cation and anion concentrations for the 4 clusters were projected on a log-scale spider diagram in ppm on Figure 6B. Chloride, sulfate and sodium dominated clusters 3 and 4. Calcium dominated cluster 3. Except for calcium, cluster 4 is enriched in major elements when compared to cluster 1, 2 and 3. Clusters 1 and 2 correspond to more diluted groundwater where bicarbonate ion dominated.

The HCA clusters showed some similarities with the classification of the 321 samples from the database (c.f. *3.2 Classification of samples*), particularly for clusters 3 and 4. For each cluster, Table 4.4 shows the median concentrations for the physical and the analytical parameters and presents the water type, the aquifer type and the hydrogeological context. The HCA results for brackish groundwater clearly distinguish bedrock (cluster 3: 7/8 samples) from granular groundwater (cluster 4: 7/8 samples). The chemistry of these two latter clusters appears related to the nature of the porous

matrix of aquifers with samples containing Na-Cl (cluster 4) mainly found in confined environments. Cluster 1 samples (Ca-HCO_3) originated mainly from unconfined environments.

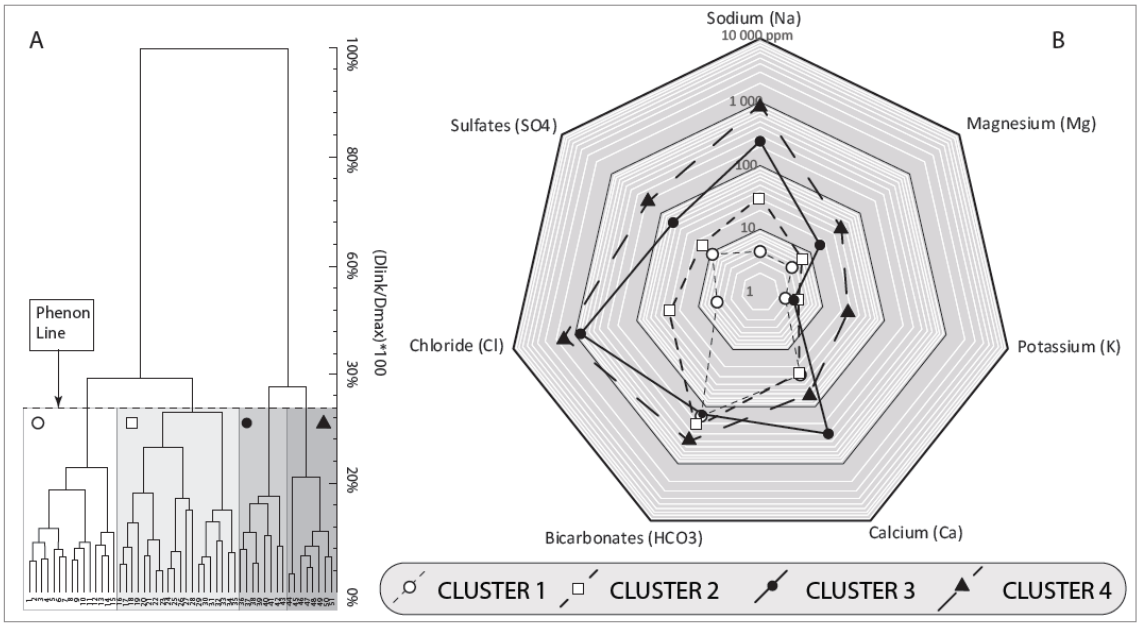

Figure 4.6 : A) Dendrogram of the hierarchical cluster analysis: when Dlink is <30% of Dmax (i.e., position of the Phenon Line), the subset is divided into 4 clusters (C1 to C4). B) Log-scale spider diagram of major cation and anion concentrations for the 4 Clusters. Clusters 1 and 2 correspond to more diluted groundwater where bicarbonate ion dominates, Cluster 4 is enriched in major elements when compared to Cluster 1, 2 and 3, and calcium dominates Cluster 3.

Cluster 2 samples (Ca(Na)-HCO_3) originated equally from both confined and unconfined environments. Clusters 1 and 2 are largely composed of bicarbonate waters (32/35 samples) while clusters 3 and 4 are composed of chloride waters (16/16; Table 4). All cluster 1 samples are composed of Ca^{2+}-dominant groundwater, whereas cluster 2 samples are primarily composed of Ca-HCO3 (11/20) and Na-HCO_3 (6/20) groundwater with a limited number of Ca-Cl (1/20) and Na-Cl (2/20) groundwater samples. Cluster 4

is exclusively a Na-Cl type groundwater and cluster 3 is a mixture of Na^+ (3/8) and Ca^{2+} (5/8) chloride groundwater.

Consequently, the key finding of the HCA is that the subset brackish groundwater samples collected from the bedrock aquifers (cluster 3) are chemically distinct from the subset brackish groundwater samples collected in the granular aquifers (cluster 4).

Table 4.4 : Water type, aquifer type and chemical content (median) of the 4 clusters obtained by Hierarchical Cluster analysis.

	Cluster 1 (N = 15)	Cluster 2 (N=20)	Cluster 3 (N=8)	Cluster 4 (N=8)
Water type	Na-Cl (0) / Ca-Cl (0) Na-HCO3 (0) / Ca-HCO3 (**15**)	Na-Cl (**2**) / Ca-Cl (**1**) Na-HCO3 (**6**) / Ca-HCO3 (**11**)	Na-Cl (**3**) / Ca-Cl (**5**) Na-HCO3 (0) / Ca-HCO3 (0)	Na-Cl (**8**) / Ca-Cl (0) Na-HCO3 (0) / Ca-HCO3 (0)
Aquifer type	Rock (**6**) / Granular (**9**)	Rock (**12**) / Granular (**8**)	Rock (**7**) / Granular (**1**)	Rock (**1**) / Granular (**7**)
Hydrogeological Context*	UnC (10) / C (0) / UnK (6)	UnC (6) / C (7) / UnK (7)	UnC (5) / C (0) / UnK (3)	UnC (1) / C (6) / UnK (1)
	Median	**Median**	**Median**	**Median**
TDS (mg/L)	229.6	402.4	1733.1	3142.6
Temperature (Celcius)**	7.68	7.58	7.77	7.69
Redox potential (mV) **	100.5	84.05	-24.45	-48.25
pH **	7.49	7.57	7.80	7.46
Dissolved oxygen (mg/l)**	2.65	0.00	0.00	0.00
Sodium	**4.40**	**32.50**	**240.00**	**905.00**
Magnesium	**4.30**	**7.00**	**16.00**	**42.50**
Potassium	**2.50**	**4.05**	**3.40**	**26.00**
Calcium	**28.00**	**25.50**	**300.00**	**59.00**
Bicarbonates	**146.40**	**231.80**	**134.20**	**403.82**
Chloride	**5.10**	**29.50**	**815.00**	**1500.00**
Sulfates	**9.40**	**15.50**	**58.00**	**190.00**
Barium	**0.026**	**0.058**	**0.190**	**0.048**
Boron	**0.010**	**0.050**	**0.235**	**0.475**
Strontium	**0.180**	**0.375**	**12.900**	**1.650**
Silicium	**5.700**	**6.600**	**5.100**	**8.950**
Manganese	**0.014**	**0.014**	**0.079**	**0.061**
Fluoride	**0.200**	**0.750**	**1.300**	**1.450**
Aluminium	**0.007**	**0.008**	**0.005**	**0.006**
Bromide	*<DL*	*<DL*	11.500	5.553
Iron	**0.071**	**0.105**	**0.140**	**0.190**
Lithium	*<DL*	*<DL*	0.076	0.019
Zinc	**0.0240**	**0.0110**	**0.005**	**0.015**
Lead	*<DL*	*<DL*	*<DL*	*<DL*
Amonium	**0.040**	**0.195**	**0.460**	**1.282**
Copper	0.006	0.001	*<<DL*	*<DL*
Molybdenium	**0.001**	**0.002**	**0.0048**	**0.002**
Nickel	*<DL*	0.001	*<<DL*	*<DL*
Silver	*<DL*	0.0001	*<DL*	*<DL*
Uranium	*<DL*	*<DL*	*<DL*	0.001
Chromium	*<DL*	*<DL*	*<DL*	*<DL*
Nitrate	0.300	0.060	*<DL*	*<DL*
Sulfide	*NA*	*NA*	*<DL*	*<DL*
Cobalt	*<DL*	*<DL*	*<DL*	*<DL*
Inorganic phosphorus	*<DL*	*<DL*	*<DL*	0.042
Vanadium	*<DL*	*<DL*	*<DL*	*<DL*
Antimony	*<DL*	*<DL*	*<DL*	*<DL*
Cadmium	*<DL*	*<DL*	*<DL*	*<DL*
Selenium	*<DL*	*<DL*	*<DL*	*<DL*
Tin	*<DL*	*<DL*	*<DL*	*<DL*
Titanium	*<DL*	*<DL*	*<DL*	*<DL*
Beryllium	*<DL*	*<DL*	*<DL*	*<DL*
Bismuth	*<DL*	*<DL*	*<DL*	*<DL*

* Unconfined (UnC); Confined (C); Unknown (UnK)
** multiparameter probe (in situ); TDS is calculated using the software Aquachem v.5.0
For major, minor and trace elements, data are given in mg/L
Under Detection Limit (<DL)
Non Applicable (NA)
Parameters presented in bold characters have been selected for multivariate treatment

4.6.3 FACTOR ANALYSIS

Factors were calculated on the symmetrical correlation matrix computed for 16 variables (K^+, HCO_3^-, Mg^{2+}, SiO_2, NH_4^+, F^-, B^{3+}, Mo^{6+}, Na^+, Ca^{2+}, Ba^{2+}, Sr^{2+}, SO_4^{2-}, Fe^{2+} and Mn^{2+}). Chloride has been consciously discarded from the factorial analysis after observation of the correlation matrix (supplementary material; Appendix 5) as Cl^- was highly correlated with all the other major elements and some trace elements and would induce a redundancy [53]. The correlation matrix for the 51-sample subset also revealed that aluminium and zinc had no significant correlation with other chemical elements. To prevent noise introduction in the multivariate statistical treatment, aluminium and zinc have been discarded too.

The first four factors present loadings (*i.e.* explained variance; Table 4.5) greater than 1 and account for 78.8% of the total variance of the subset. The first factor (25.1% of the total variance) is characterized by high loadings for K^+, HCO_3, Mg^{2+}, SiO_2, NH_4^+, and SO_4^{2-}. Loadings for F^-, B^{3+}, Mo^{6+}, and Na^+ explain the second factor (22.2% of the total variance). Loadings for the third factor (20.6% of the total variance of the subset) are dominated by Ca^{2+}, Ba^{2+}, Sr^{2+}, and SO_4^{2-}. Finally, the fourth factor (10.8% of the total variance of the subset) is strongly influenced by Fe^{2+} and Mn^{2+}.

Table 4.5 : Factor analysis loadings and explained variance after applying a varimax rotation.

Parameter	Factor 1	Factor 2	Factor 3	Factor 4
Potassium	***0.87***	0.21	-0.03	0.24
Bicarbonates	***0.71***	0.24	-0.22	0.22
Magnesium	***0.70***	0.22	0.45	0.15
Silicium	***0.67***	-0.34	0.08	0.00
Amonium	***0.64***	0.49	0.05	0.28
Fluoride	0.16	***0.90***	0.07	-0.12
Boron	0.50	***0.78***	0.15	0.10
Molybdenum	-0.12	***0.77***	0.20	0.04
Sodium	0.60	***0.70***	0.23	0.03
Calcium	0.02	-0.05	***0.93***	0.20
Barium	-0.11	0.15	***0.83***	0.15
Strontium	0.21	0.47	***0.79***	0.09
Sulfates	***0.61***	0.22	***0.62***	-0.03
Iron	0.26	-0.14	0.08	***0.82***
Manganese	0.14	0.16	0.40	***0.80***
Explained variance	3.77	3.33	3.10	1.63
Explained variance (%)	25.1	22.2	20.6	10.8
Cumulative % of variance	25.1	47.3	68.0	78.8

4.7 DISCUSSION

4.7.1 EVOLUTION OF RECHARGE GROUNDWATER (CLUSTERS 1 AND 2; FACTOR 4)

Clusters 1 and 2 appear to belong to a “recharge” type groundwater. The fourth factor explains only 10.8% of the total variance of the data set and thus characterizes only a few samples among the 51-sample subset. In Figures 4.7(c), 4.7(e), and 4.7(f), sample scores for the fourth factor are projected onto the Y-axis. This factor presents high loadings for Fe^{2+} and Mn^{2+} (Table 4.5). These are redox sensitive species [46, 47] and thus, their concentrations in groundwater are primarily influenced by the amount of available dissolved oxygen [48]. In the presence of dissolved oxygen, principally near surface environments, Fe^{2+} and Mn^{2+} will be solubilized by oxidizing and acidic

conditions that tend to increase the Fe^{2+} and Mn^{2+} content in groundwater. This may explain why Factor 4 predominantly influences (CaNa)-HCO_3 groundwater (clusters 1 and 2; Figures 4.7(c), 4.7(e), and 4.7(f)).

Negative values for the fourth factor can be interpreted as a lack of correlation between the two chemical elements. Based on the Eh-pH diagram (Supplementary material; Appendix-6), the range of stability for dissolved Fe^{2+} differs from that of Mn^{2+}. Depending on the Eh-pH conditions, Fe^{2+} and Mn^{2+} may not coexist in the soluble form. This might be at the origin of the negative values obtained for the fourth factor in Figures 4.7(c), (e), and (f). For instance, negative values are recorded in the recharge type of groundwater (predominantly cluster 2) that follows the freshwater influx vector interpreted at the bottom left quarter in Figures 4.7(c), (e), and (f).

4.7.2 FINGERPRINT OF THE LAFLAMME SEAWATER (CLUSTER 4; FACTOR 1)

Positive scores for the first factor are recorded for samples from cluster 4 (Figures 4.7(a) – 4.7(c)) highlighting the influence of the first factor on cluster 4 samples. The first factor is characterized by high loadings of K^+, HCO_3^-, SiO_2, NH_4^+, SO_4^{2-}, and Mg^{2+} (Table 4.5).

Wang et al. [49] argued recently that dissolved NH_4^+ found in groundwater originates from overlying marine clay aquitards. The aquitard plays a role of a strong anaerobic environment favorable for mineralization of sedimentary organic matter. Degradation of organic matter would produce CO_2 gas and favor the formation of HCO_3^-.

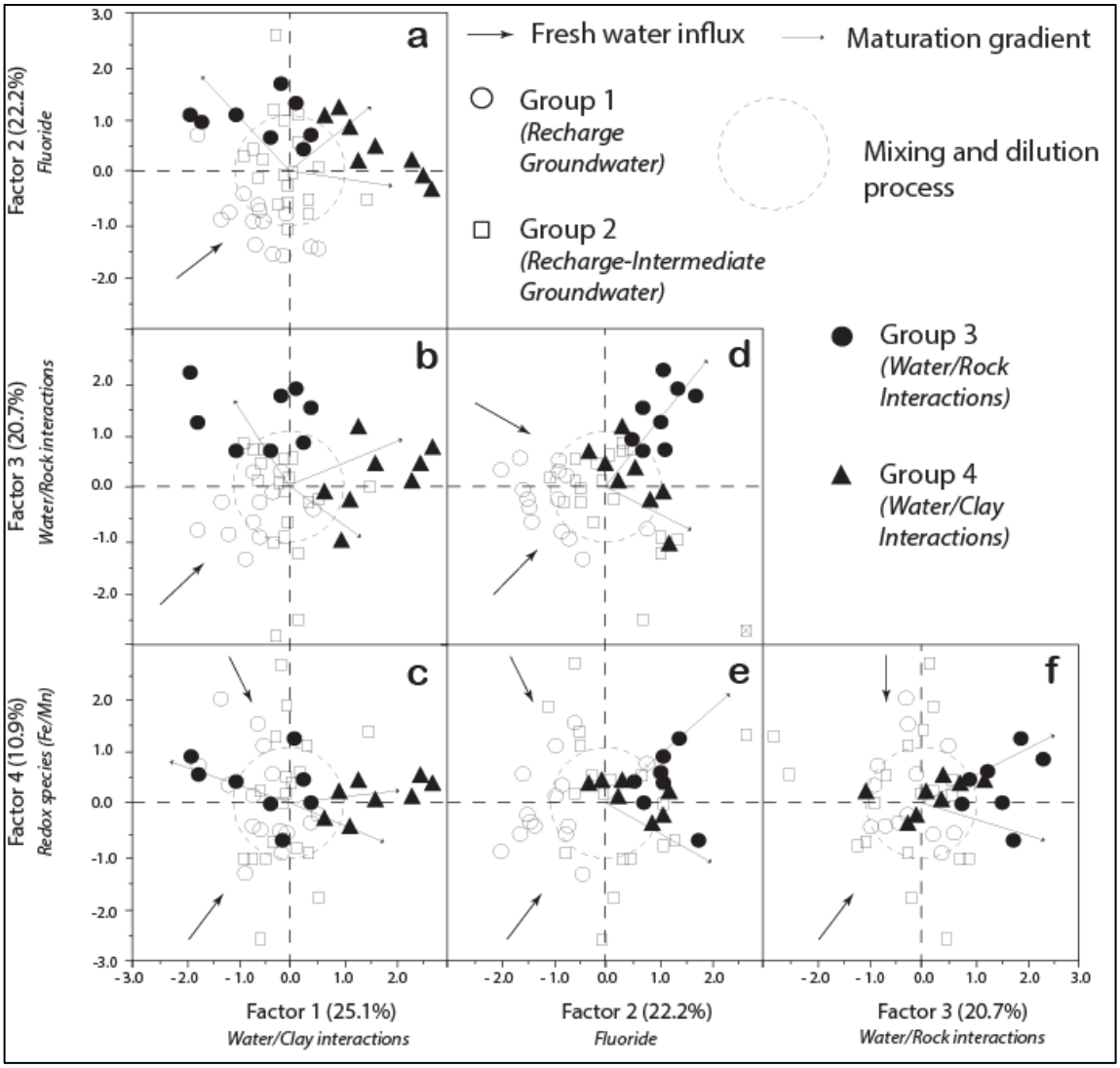

Figure 4.7 : Graphical representation of the sample scores calculated for each factors obtained during the factorial analysis procedure. The different combinations of factors lead to the construction of six binary diagrams: Fig. 6a: Factor 1 vs. Factor 2; Fig. 6b: Factor 1 vs. Factor 3; Fig. 6c: Factor 1 vs. Factor 4; Fig. 6d: Factor 2 vs. Factor 3; Fig. 6e: Factor 2 vs. Factor 4; Fig. 6f: Factor 3 vs. Factor 4. Samples are represented with symbols corresponding to the cluster number of the samples for the subset. Mixing and dilution zones defined in the center of the binary diagrams contain samples that are weakly influenced by the factors (scores <1). Two series of vectors represent the evolution of groundwater: one set of vectors represent the evolution of the recharge groundwater (fresh water influx) and the second set of vectors corresponds to the evolution of groundwater from the mixing and dilution zones toward the brackish groundwater (maturation gradient).

As a result, NH_4^+ preferentially characterizes groundwater in cluster 4 and is correlated to HCO_3^- in this cluster. Sulfate reduction also produces CO_2. If SO_4^{2-} reduction enhances the production of HCO_3^- by the dissociation of water molecules in the presence of CO_2, this reaction is accompanied by the production of aqueous HS^- gas [50]. The general form of the reaction is given as:

$$SO_4^{2-} + 9H^+ + 8e^- \rightarrow HS^- + 4H_2O \qquad \text{(Equation 2)}$$

The regional chemical characterization of groundwater showed that sulfide gas was preferentially detected in granular confined environments where handmade piezometers were installed for private water supply [51]. For cluster 4, SO_4^{2-} might have a marine origin (i.e., seawater trapped in the marine aquitard). Sulfide isotopes would help to test this hypothesis.

Based on mineralogical analyses performed on deep marine deposits from some areas in the SLSJ region [52], the chemical breakdown of silicate minerals, for instance microcline, was at the origin of SiO_2 and K^+ in groundwater (Equation 7; [11]). This assumption is reinforced by FA results obtained in this study.

$$3KAlSi_3O_8 + 2H^+ \rightarrow 2K^+ + 6SiO_2 + KAl_3Si_3O_{10}(OH)_2 \qquad \text{(Equation 3)}$$
(microcline) (illite)

Variations of the chemical elements for Factor 1 (K^+, HCO_3^-, SiO_2, NH_4^+, and SO_4^{2-}) is believe to characterize groundwater from a confined environment due to the presence of the regional marine aquitard (Water-clay interactions; [11]). The first factor

characterizes the tendency of groundwater to evolve toward an end-member with a composition similar to that of the present seawater (i.e., Na-Cl-rich in composition). Cluster 4 belongs to a “seawater” type of groundwater.

4.7.3 FINGERPRINTING OF THE PRECAMBRIAN SHIELD BRINES (CLUSTER 3; FACTOR 3)

In Figures 4.7(b), 4.7(d), and 4.7(f), samples from cluster 3 are predominantly influenced by the third factor with loadings dominated by Ca^{2+}, Ba^{2+}, Sr^{2+}, and SO_4^{2-} (Table 4.5). Log-log plots of [Ca^{2+}, Ba^{2+}, Sr^{2+}, and SO_4^{2-}] vs. Cl^- concentrations (Figures 4.8(a)–8(d)) for the subset of samples in this study were coupled with the data from other Canadian Shield brines.

Frape et al. [43] determined that the geochemistry of Ca^{2+} plays a major role in controlling the chemistry of mineralized groundwater in the crystalline bedrock of the Canadian Shield. Frape et al. [43] described very old stagnant groundwater that may have undergone prolonged chemical alteration since its original emplacement. The similar Ca^{2+}/Cl^- trend for the cluster 3 and the Precambrian Shield brines (PSB) (Figure 4.8(a)) suggest a common origin for Ca^{2+} and Cl^-. In Figures 4.8(a) and 4.8(d), Ca^{2+} and Sr^{2+} concentrations for clusters 3 and 4 show similar trends. This suggests a common origin for Sr^{2+} and Ca^{2+} in cluster 3. For Sr^{2+}, as well as Ba^{2+}, it is commonly found incorporated as a trace element in the crystalline structure of feldspar plagioclase minerals, [53, 54]. In Figure 4.8(b), the trend for Ba^{2+} is different than that of Sr^{2+} and Ca^{2+}. Edmunds and Smedley [61] showed that barite solubility controls Ba^{2+} concentration and that Ba^{2+} quickly reaches saturation or supersaturation in recharge

groundwater. In Figure 4.8(b), Ba^{2+} concentrations for clusters 1 and 2 reach levels similar to the concentrations for clusters 3 and 4. Which suggest that maximal Ba^{2+} concentrations are attained in "recharge" groundwater. Unlike Ba^{2+}, Sr^{2+} is not limited in terms of solubility [55]. Some of the Sr^{2+} may be added by the dissolution of anhydrite or gypsum. However, SO_4^{2-} vs Cl^- (Figure 4.8(c)) shows a different trend than Sr^{2+} vs Cl^- (Figure 8(d)) that refutes this possibility. According to Gascoyne and Kamineni [44], most of the added Cl^- and some SO_4^{2-} in groundwater collected in selected granitic, gabbroic, and gneissic plutons in the Canadian Shield are derived from the rock matrix. Ions are present either as soluble salts in fluid inclusions and on grain surfaces [56] or as structurally bound elements in micas and amphiboles [57]. Sulphate may then be more derived from the oxidation of sulphide minerals in the rock matrix rather than due to the presence of gypsum-infilling minerals in the fractures.

For cluster 3 samples, the strong relationship of [Ca^{2+}, Sr^{2+}] vs. Cl^- concentrations, the Ba^{2+} content for recharge groundwater and the similar trends with the Precambrian Shield brines (*PSB*), all suggest that cluster 3 corresponds to some diluted end-members with a composition like that of the *PSB* compiled in this study. Cluster 3 thus belongs to a "PSB" type of groundwater.

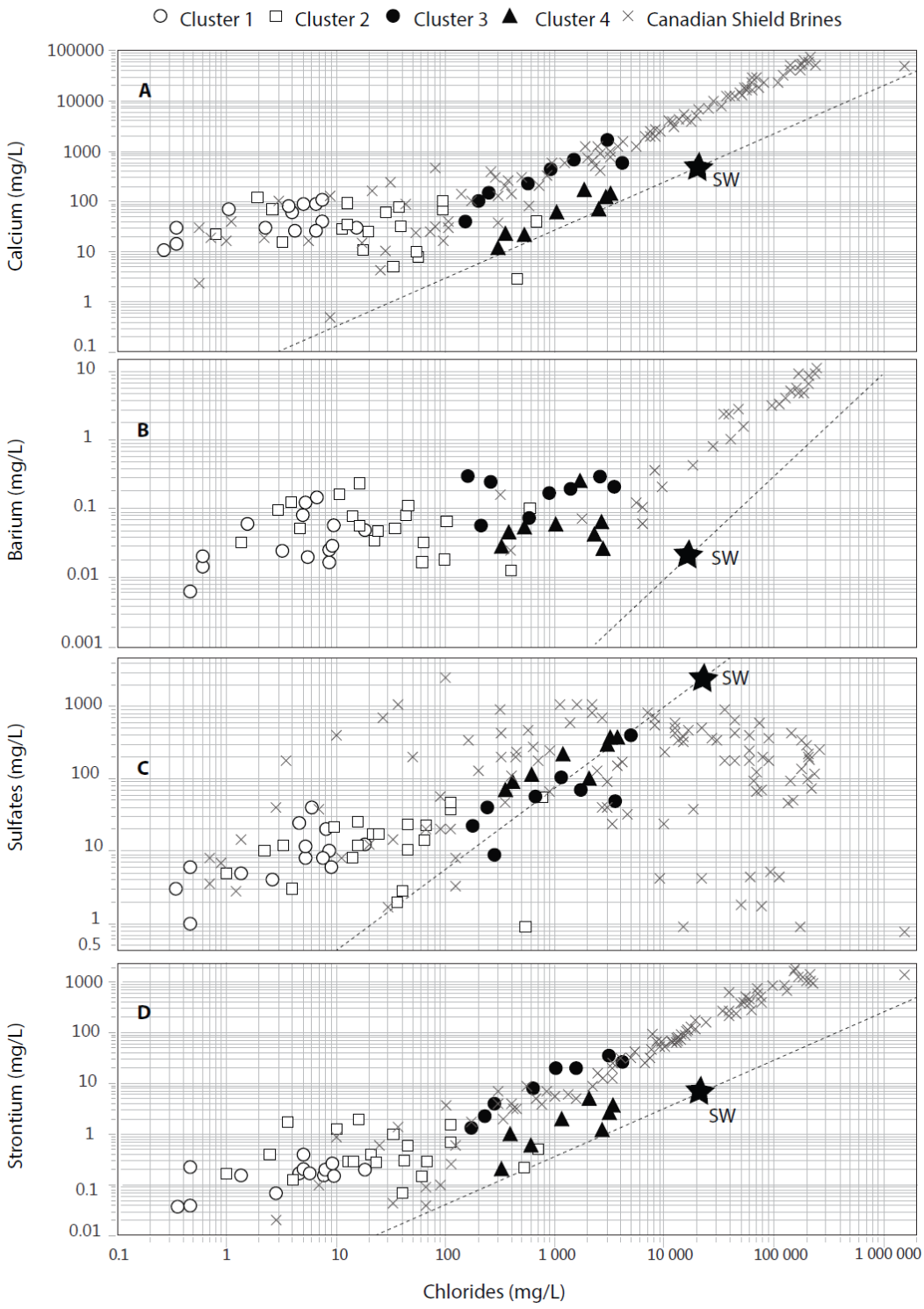

Figure 4.8 : Log-log plots of Ca^{2+} vs. Cl^- concentrations in mg/L (Fig. 8A); Ba^{2+} vs. Cl^- concentrations in mg/L (Fig. 8B); SO_4^{2-} vs. Cl concentrations in mg/L (Fig. 8C), and Sr^{2+} vs. Cl^- concentrations in mg/L (Fig. 8D) . Seawater (SW) dilution lines were defined using seawater ratios from Goldberg (1971). The strong linear correlation between calcium, strontium and chloride in PSB groundwater suggests a mass ratio Ca^{2+}/Sr^{2+} ≈ 40 for salinization related to basement fluids.

4.7.4 THE SOURCE OF DISSOLVED FLUORIDE IN GROUNDWATER (FACTOR 2)

The second factor requires investigation as it may provide clues as to the origin of dissolved fluoride in groundwater. Factor 2 is characterized by high loadings of F^-, B^{3+}, Mo^{6+}, and Na^+ (Table 4.5). In the study area, F^- concentrations of 20% of the sampled wells [15] exceed both the Canadian drinking water quality guidelines [58] and the WHO standards [12]. Sample scores for Factor 2 are projected on the X-axis in Figures 4.7(d) and 4.7(e) and on the Y-axis in Figure 4.7(a). Factor 2 influences groundwater from cluster 2, 3, and 4. The source of F^- is ambiguous since more than one group is influenced by the second factor. The co-variations of the chemical elements that compose Factor 2 suggest multiple processes of interaction between groundwater and the solid matrix of aquifers or aquitards at the origin of fluoride in groundwater.

Boron (B^{3+}) and Mo^{6+} are found incorporated in the crystalline structure of tourmaline and molybdenite, two very common minerals in pegmatite of the Grenville Province [59] that constitute some of the Precambrain rock of the study area. Despite the low solubility of these minerals, the long-term interaction between groundwater and granitic rocks could account their source, hence explaining the co-variations of B^{3+}, Mo^{6+}, and F^-. On the other hand, B^{3+} has been described in the SLSJ region where shales are present [17]. Mo^{6+} is also frequently found in fossil fuels [54]. Occurrences of gas and oil in shale and limestone have been identified in the study area [51]. The combination of B^{3+} and Mo^{6+} could indicate that F^- originates from the groundwater

interaction with sedimentary rocks present in the region. Investigations on a local scale would help to test this hypothesis.

Recent studies showed that micas in granitic rocks are the main source of dissolved fluoride in groundwater [60-62]. Experiments with regional rocks should be performed in order to test if this hypothesis applies to the study area. Chae et al. [62] experimentally explained that the geochemical behavior and concentration of fluorine in groundwater are controlled by the existence of Ca-bearing minerals and by the fluorite precipitation as a function of the absolute concentration of Ca^{2+} ions in water. In the study region, Walter et al. [11] suggested that the Ca^{2+}_{water}-$Na^{+}_{mineral}$ ion exchange processes may lead to a decrease in the groundwater Ca^{2+} content. As fluorite (CaF_2) equilibrium controls F^- and Ca^{2+} concentrations [30], it is expected that the removal of Ca^{2+} from the water in exchange for Na^+ will increase the fluoride (F^-) concentration in presence of fluorite. A slight increase in F^- is observed in Table 4 between cluster 1 and 2 (*Recharge-like*) and would suggest the presence of fluorite in the system. The Ca^{2+}_{water}-$Na^{+}_{mineral}$ ion exchange processes also support the linear correlation of Na^+ and F^- in Factor 2. Ion exchange is believed to occur early in the evolution of groundwater in bedrock aquifers [43], but also particularly characterizes groundwater from confined aquifers [11]. The second factor influenced samples from cluster 4 (seawater type of groundwater), as indicated by the evolution vector pointing toward the South-East quadrant in Figure 4.7(d).

Based on these observations, dissolved F^- can be generated either from the interaction of groundwater with marine clay or from the interaction of groundwater with bedrock aquifers in the early stage of evolution of recharge type of groundwater. This also means that a perfect environment for generating and maintaining dissolved fluoride in groundwater would be found in crystalline bedrock aquifers confined by marine clay aquitard.

4.8 CONCEPTUAL MODEL OF THE GROUNDWATER CHEMICAL EVOLUTION IN THE STUDY AREA

4.8.1 THE GRAVITY-DRIVEN FLOW MODEL

Two conceptual cross-sections of the chronostratigraphic units are presented in Figures 4.9(a) and (b). In both Figures, model A represents the regional rock formations that consist of two main units: Precambrian rocks of the Canadian Shield and Ordovician limestones and shale. A schematic vertical fault marks the discordant contact between Ordovician rocks and Precambrian rocks and represents the limits between the highlands and lowlands (Saguenay Graben). Model B represents the regional Pleistocene units simplified into three main units: Pleistocene glacial drift and fluvio-glacial sediments, deep Pleistocene seawater deposits, and Pleistocene deltaic and shore deposits. Parts of or the complete sequence of Pleistocene units presented in Model B may also be present at the surface of bedrock in Model A.

Clusters identified in this study are shown in Figure 4.9(a). As discussed above

(*5.1 Evolution of Recharge Groundwater*), cluster 1 and cluster 2 belong to a recharge type of groundwater (RGW) in the bedrock and granular aquifers. Cluster 3 belongs to a Precambrian Shield Brine (PSB) type of groundwater which can locally mix with Limestone Brines (LB) and cluster 4 belongs to a diluted seawater (SW) type of groundwater originating from the mixing of RGW with fossil SW. Dilution is also believed to occur in the bedrock as basement fluids upwelling toward the surface along the graben fault system encounter RGW [11]. Based on the principles of the gravity-driven flow model, flow lines in Figure 4.9 conceptualize the evolution of groundwater. The groundwater chemical content will tend to increase as the length of flow line increases [5]. Mixing of the flow lines is believed to occur at different sites in the study area as confined and unconfined aquifers may exist in the fractured rock and the Pleistocene deposits; these combine locally to form multilayered aquifers [15]. When present, multilayered aquifers can be either disconnected or interconnected [27, 28]. Mixing of the flow lines is potentially enhanced by pumping groundwater in either bedrock wells or granular deposit wells. The mechanical mixing of the flow lines in the well presented in Figure 4.9 will lead to the mixing of groundwaters that have differing ages and chemistries. In this case, samples pumped to the surface correspond to a mixture of different groundwater endmembers (combination of RGW+PSB+LB+SW). A standardized approach is proposed in the following lines with the attempt to identify chemical pathfinders of groundwater endmembers illustrated in Figure 4.9(a).

4.8.2 GROUNDWATER CHEMICAL FACIES AND CHEMICAL PATHFINDERS

The maturation index (MI) is introduced here to testify to the contribution of the natural environment to the chemistry of groundwater at different hypothetical steps of groundwater evolution (clusters 1 to 4). Such values attest to the chemical enrichment/depletion of groundwater as it interacts with its environment (i.e., physicochemical conditions of groundwater). The maturation index is calculated for each analyzed chemical (Figures 4.10(a)– 4.10(c)). Each figure represents one of three steps in groundwater evolution in the study area. Shadowed boxes in Figure 4.10(a) to 4.10(c) highlight chemical elements belonging to Factors 1 to 4 produced by factorial analysis. Factorial analysis results and MI calculations showed that groundwater chemical facies are modified through the hypothetical steps of groundwater evolution toward groundwater endmembers (cluster 1 to 4). The process of evolution was accompanied by the releasing of certain trace elements which were considered as chemical pathfinders of groundwater's endmembers. Evolution of groundwater chemical facies and chemical pathfinders of groundwater chemical speciation along the proposed process of evolution (Step 1 to Step 3) are presented in Figure 4.9b.

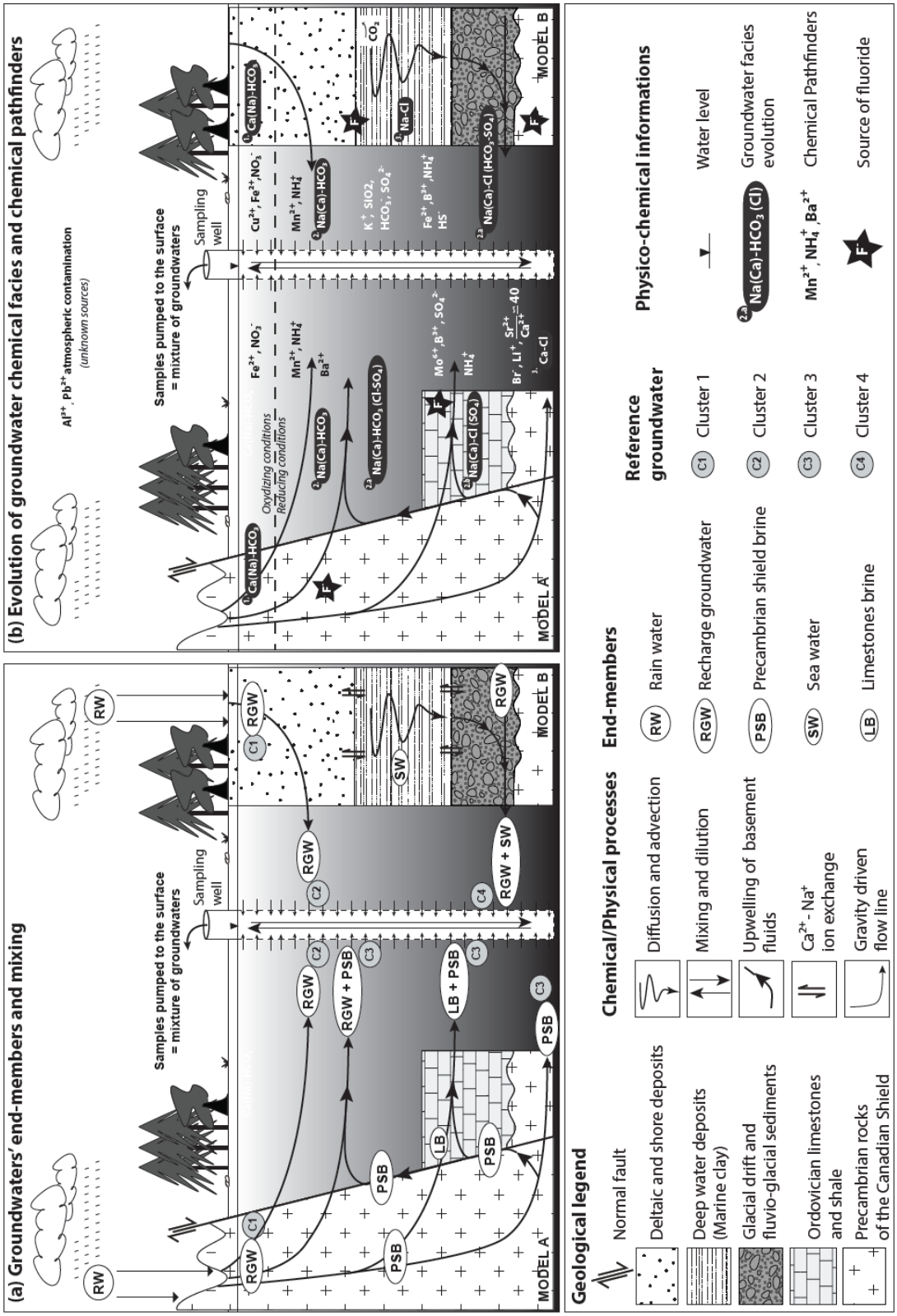

Figure 4.9 : Conceptual model of the groundwater chemical evolution in the study area (continued on next page).

Figure 4.9 (continued): In Figure (a) and (b), Model A represents the regional rock formations: Precambrian rocks of the Canadian Shield, Ordovician limestone and shale. A schematic vertical fault marks the discordant contact between Ordovician rocks and Precambrian rocks and schematizes the limits between the highlands and lowlands (Saguenay Graben). In Figure (a) and (b), Model B represents the regional Pleistocene units: Pleistocene glacial drifts and fluvio-glacial sediments, deep Pleistocene seawater deposits, and Pleistocene deltaic and shore deposits. Parts of or the complete sequence of Pleistocene units presented in Model B may also be present at the surface of the bedrock in Model A. Based on the principles of the gravity-driven flow model, flow lines in Figure 4.9 conceptualize the evolution of groundwater. The chemical content of groundwater will tend to increase as the length of the flow line increases. Mixing of the flow lines is potentially enhanced by pumping groundwater in either bedrock wells or granular deposit wells. Figure 4.9(a): groundwater end-members of the process of evolution from Rainwater (RW) toward Cluster 1 and Cluster 2 (recharge type *of* groundwater (RGW) in the bedrock and granular aquifers toward Cluster 3 (Precambrian Shield Brines (PSB) type of groundwater which can locally mix with Limestones Brines (LB)) and/or Cluster 4 (diluted seawater (SW) type of groundwater originating from the mixing of RGW with fossil SW). Dilution is also believed to occur in the bedrock as upwelling of basement fluids toward the surface along the graben fault system encounters RGW. Figure 4.9(b): Evolution of groundwater chemical facies and chemical pathfinders of groundwater chemical speciation along the proposed process of evolution (Step 1 to Step 3; Figure 10) illustrated in Figure 4.9(a).

4.8.2.1 STEP 1 AND 2: RAINWATER INFILTRATION AND GROUNDWATER EVOLUTION TOWARDS CLUSTER 2 CHEMISTRY

The chemistry of rainwater corresponds to the starting point of the geochemical evolution for groundwater. Groundwater evolution occurs as the chemistry of rainwater begins its alteration to become the water of cluster 1. Maturation indices for the first step are calculated as:

$$Step\ 1\ MI = \frac{[X]_{Cluster\ 1}}{[X]_{Rainwater}}$$ (Equation 4).

where $[X]_{Cluster\ 1}$ represents the average concentration of the chemical species X in cluster 1 (Table 2) and $[X]_{Rainwater}$ represents the average concentration of the chemical species X in rainwater (Table 4.1).

Chemical species presenting MI >1 for step 1 are enriched in comparison to rainwater. The chemical content for major elements Ca^{2+}, HCO_3^- and Mg^{2+}, as well as minor elements Sr^{2+}, Ba^{2+}, and SiO_2 are 100× higher in recharge groundwater (cluster 1) than in rainwater. Among chemical elements belonging to Factors 1 and 3, SO_4^{2-} is less enriched in cluster 1 (MI ~3) than the other chemical elements (MI ~100). A general enrichment is observed for Factor 2 (F^-, B^{3+}, Mo^{6+}, and Na^+). In Factor 4, the MI for Fe^{2+} (MI ~50) dominates for the MI of Mn^{2+} (MI ~10) leading to a standardized Fe^{2+}/Mn^{2+} ratio ~5.

The second step of groundwater evolution represents the modification of the hydrochemical facies from Ca(Na)-HCO_3 (cluster 1) to Na(Ca)-HCO_3 (cluster 2). The maturation index are calculated as:

$$Step\ 2\ MI = \frac{[X]_{Cluster\ 2}}{[X]_{Cluster\ 1}}$$ (Equation 5).

where $[X]_{Cluster\ 2}$ represents the mean concentration for the chemical species X in cluster 2 and $[X]_{Cluster\ 1}$ represents the mean concentration for chemical species X in cluster 1.

Some chemical elements (e.g., Ca^{2+} and HCO_3^-) remain unchanged during the chemical modification from cluster 1 to cluster 2 (MI = 1; Figure 4.10(b)). Among metallic ions, Ni^{2+}, Ag^+, Mn^{2+}, and Al^{3+} are enriched in cluster 2 relative to cluster 1 likely due to the natural process of recharge. The maximum concentration for Cu^{2+} is reached during step 1 and the depletion of Cu^{2+} and Fe^{2+}, during step 2 (Figures 4.10(b)) suggests that these chemical elements are apparently buffered by the environment early in groundwater evolution. In Step 2 groundwater interaction with its environment produces Mn^{2+} in solution while Fe^{2+} is mobilized by the physicochemical conditions of groundwater (i.e., the aquifer matrix and its environment).

Cluster 1 is enriched in NO_3^- (MI ~5) and depleted in NH_4^+ (MI ~0.1). The inversion of the standardized ratio NO_3^-/NH_4^+ between the step 1 and step 2 ($NO_3^-/NH_4^+ >1$ in Figure 10(a); and $NO_3^-/NH_4^+ <1$ in Figure 4.10(b)) suggests that free nitrogen has been released into solution by denitrification of NO_3^- during the chemical modification from rainwater to cluster 1 and then has been mobilized by ammonification to form NH_4^+ during the ongoing processes of "recharge" chemical evolution. The standardized ratios Fe^{2+}/Mn^{2+} and NO_3^-/NH_4^+ are both <1 although they had respective values of ~5 and ~40 in Step 1. These inversions of the standardized ratios for chemical elements sensitive to redox conditions suggests that redox conditions likely control chemical speciation during recharge, especially for metallic ions. Chemical modification from cluster 1 to cluster 2 may correspond to the transition from oxidizing toward more reducing conditions presented on Figure 4.9(b).

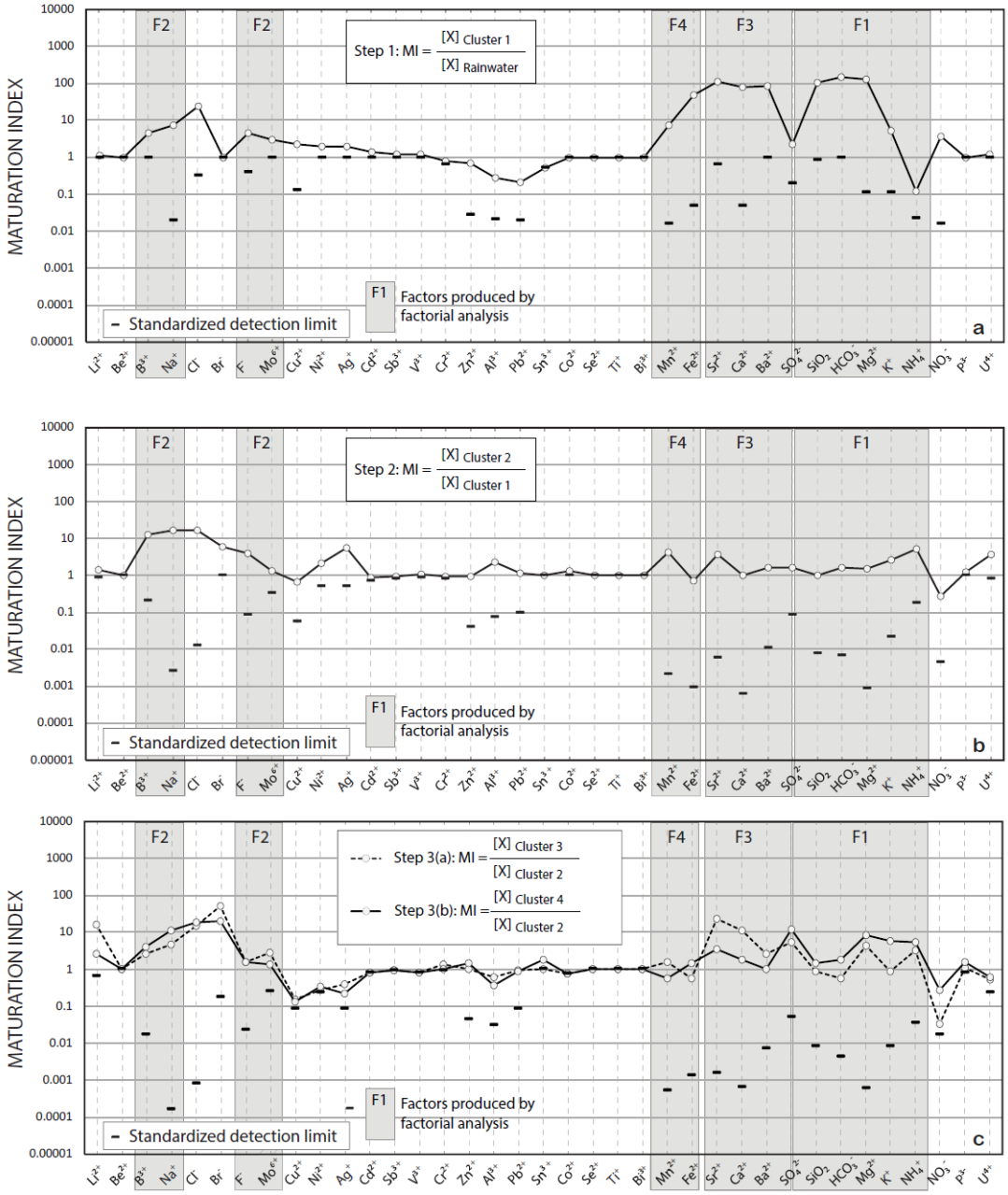

Figure 4.10 : Maturation Indexes (MI) calculated to quantify the chemical contribution of the natural environment to the chemistry of groundwater for three steps of the natural groundwater evolution (<u>Step 1</u>-Rainwater infiltration and evolution toward Cluster 1 chemistry: Fig. 4.10a; <u>Step 2</u>- Early stage of evolution for recharge groundwater toward Cluster 2 chemistry: Fig. 10b; <u>Step 3</u>- Groundwater maturation toward brackish endmembers: Fig. 10c). MI with a value of unity denotes no enrichment or depletion during the process of evolution. In respect to the water of reference, a value of *MI* greater than 1 indicates an enrichment during the process of evolution and a value of *MI* lower than 1 suggests a depletion during the process of evolution.

Copper, iron and nitrate are likely to be chemical pathfinders for early processes of the recharge event (Figure 4.9(b)). To support this observation, Figure 4.3 shows that in recharge groundwater, a higher number of values for those chemical elements were above DL (bicarbonate groundwater from granular aquifers; Group 1) and Appendix 3 (Supplementary material) shows that higher median and maximum values for copper, iron and nitrate were recorded in recharge groundwater.

The general enrichment in Cl^- for cluster 1 (Figure 4.10(a)) raises the question of the origin for Cl^-. Chloride is known to be very soluble and geochemically inert. Its concentrations and variations are considered to be entirely source-related [61]. A first explanation is the anthropogenic contribution of de-icing salt spread along the road during the winter. Investigation on the local scale should be performed. Otherwise, the primary dissolution of silicates in recharge areas might be at the origin of the dissolved Cl^-. Cluster 1 is highly enriched in Ca^{2+}, HCO_3^-, and Mg^{2+}, as well as the minor elements Sr^{2+}, Ba^{2+}, and SiO_2 (Figure 4.10(a)). In the study region, these elements are available in large amounts in groundwater recharge areas in the form of carbonate and silicate minerals. These minerals, particularly carbonates, are easily dissolved under acidic conditions [37]. Otherwise, if the source of Cl^- is rainwater, the Cl^- enrichment might be the result of an evaporative process in the vadose zone. Nothing supporting this assumption is found in the literature. A more plausible explanation is the mixing of recharge groundwater depleted in Cl^- with “Cl-rich” groundwater. In the region, “Cl-rich” groundwater is generated by water/rock interactions or water/marine-clay interactions. The term

water/clay interactions was introduced by Walter et al. [11] to account for a combination of processes: ion exchange and/or leaching of salt water trapped in the regional aquitard, as well as mixing with fossil seawater.

4.8.2.2 STEP 3: GROUNDWATER MATURATION TOWARDS CLUSTER 3 AND 4 BRACKISH END-MEMBERS

Evolutionary paths responsible for the chemistry of brackish groundwater follow two paths: 1) evolution towards a CaCl end-member (cluster 3) in bedrock aquifers and possibility of mixing with recharge groundwater (RGW) and Limestones Brines (LB) (Figure 4.9(a)); and 2) evolution towards a seawater NaCl end-member (cluster 4) in confined aquifers and mixing with RGW. The two MI for brackish groundwater are calculated as:

$$Step\ 3(a)\ MI = \frac{[X]_{Cluster\ 3}}{[X]_{Cluster\ 2}} \text{ (Equation 6);}$$

$$Step\ 3(b) = \frac{[X]_{Cluster\ 4}}{[X]_{Cluster\ 2}} \text{ (Equation 7)}$$

where in Equation 4, $[X]_{Group\ 3}$ represents the mean concentration for the chemical species X in cluster 3 and, in Equation 5, $[X]_{Group\ 4}$ represents the mean concentration for chemical species X in cluster 4. In both equations, $[X]_{Group\ 2}$ represents the mean concentration for chemical species X in cluster 2.

Enrichment in Cl^- is similar for both clusters. When compared to recharge groundwater (cluster 2), cluster 4 is characterized by a general enrichment (MI >1) of

Factor 1 chemical elements (SiO_2, HCO_3^-, and K^+) while cluster 3 has a slight depletion (MI <1) for these elements. Sulfate enrichment is limited for recharge groundwater (Figure 4.10(a)) but is very high for clusters 3 and 4 (Figure 4.10(c)). Compared to the previous steps, SO_4^{2-} shows a marked enrichment for both groups. This enrichment brings MI ratios for Ba^{2+}/SO_4^{2-}, SiO_2/SO_4^{2-}, Mg^{2+}/SO_4^{2-}, HCO_3^-/SO_4^{2-}, and NH_4^+/SO_4^{2-} to <1 for cluster 3 and 4. All these standardized ratios were previously ~25 when normalizing recharge groundwater (cluster 1) by rainwater (Figure 4.10(a)). As previously discussed, sulfate may have a marine origin (i.e., seawater trapped in the marine aquitard) and/or sulfate may be derived from the oxidation of sulphide minerals in the granitic rocks as well as in the shale rocks of the Ordovician sequence. Mixing with recharge groundwater will lead to the evolution of groundwater chemical facies toward a Na(Ca)-HCO_3(Cl-SO_4) profile in the vicinity of Ordovician limestones and shale, and in confined aquifers (Figure 4.9(b)). Deeper in the rock, the chemical facies of groundwater is believed to evolve toward Na(Ca)-Cl(SO_4) as the contribution of Cl-rich basement fluids (PSB and LB) become more important Figure 4.9(b). In confined aquifers, reduction of sulfate leads to the production of HS^- gas and CO_2 gas (Figure 4.9(b)).

For clusters 3 and 4, similar patterns are observed, although with some differences. In line with factorial analysis results, cluster 4 is characterized by a general enrichment (MI >1) of Factor 1 chemical elements (SiO_2, HCO_3^-, and K^+), explained by the chemical breakdown of silicate minerals (Figure 4.9(b)). Relative to cluster 4, cluster 3 is enriched in $Br^-$and Li^+. The MI for Li^+ is more than 5× higher in cluster 3 (MI ~15) than in

cluster 4 (MI ~2.5). The MI for Br^- is more than 3× higher in cluster 3 (MI ~70) than in cluster 4 (MI ~20). Walter et al. [11] discussed the upwelling of basement fluids based on bromide enrichment of some bedrock groundwater (Cl^-/Br^- mass ratios of 88) in comparison to seawater (Cl^-/Br^- mass ratios of 266). Figure 4.3 showed that bromide and lithium are readily detected in groundwater collected in bedrock aquifers and Appendix 3 (supplementary material) showed that maximum values in this study for bromide and lithium were recorded in groundwater from bedrock aquifers. Bromide and lithium are associated with basement fluids (PSB; Figure 4.9(b)).

In Figure 4.10(c), Factor 3 (Ca^{2+}, Ba^{2+}, SO_4^{2-}, Sr^{2+}) characterizes much of the cluster 3 chemistry in which the enrichment of Ca^{2+} and Sr^{2+} is striking (MI >10). This observation is in line with factorial analysis results and the observations of Frape et al. [43]. The strong linear correlation between calcium, strontium and chloride in PSB groundwater suggest a mass ratio $Ca^{2+}/Sr^{2+} \approx 40$ (derived from Figures 4.8) for salinization related to basement fluids (Figure 4.9(b)). A Strontium progressive increase downgradient due to the incongruent reactions of carbonate minerals [55] would explain why in step 2 (Figure 4.10(b)), the MI for Sr^{2+} is the greater of Factor 3. Enrichment in Ca^{2+} for cluster 3 is accompanied by an enrichment in Sr^{2+} and to a lesser extent in Ba^{2+}. It suggests that carbonate dissolution is more effective in the recharge area than plagioclase dissolution, an expected result as rainwater is slightly acid. Compared to rainwater (Figure 4.10(a)), Ba^{2+} has a similar MI as opposed to Sr^{2+} and Ca^{2+}. Relative to recharge groundwater (Figure 4.10(b)), Ba^{2+} has the lowest MI, which suggests that during Step 2, less Ba^{2+} is dissolved

relative to Sr^{2+} and Ca^{2+}. As discussed earlier in this paper, maximal Ba^{2+} concentrations are attained in recharge groundwater (*5.3 Fingerprinting of the Precambrian Shield Brines*). Barium content of cluster 3 might then be inherited from the early stage of groundwater evolution in crystalline bedrock where Na(Ca)-HCO_3 facies dominates (Figure 4.9(b)). This hypothesis should be tested with experimental water-rock interaction studies.

Figures 4.10(a) – 4.10(c) show a general enrichment in the elements of Factor 2 for every step in the chemical evolution. For Factor 2, B^{3+} and Na^{+} show a greater enrichment in *seawater-like* groundwater from cluster 4 compared to recharge groundwater from cluster 2. A marine origin might be proposed for boron (Figure 4.9(b)). Boron isotopes would help to test this hypothesis. Conversely, Mo^{6+} from Factor 2 presents a higher MI in *PSB-like* groundwater from cluster 3. As proposed previously, the presence of gas and oil in shale and limestone in the study area [17] would explain the Mo^{6+} enrichment in groundwater from cluster 3 in Figure 4.10(c), and implies that cluster 3 includes samples for which the chemistry is influenced by sedimentary rock-dominated aquifers. Figure 4.10(c) also showed that ammonium presented an enrichment in *seawater-like* groundwater (cluster 4) and *PSB-like* groundwater (cluster 3) compared to recharge groundwater from cluster 2. Factorial analysis results have led to the identification of ammonium as being correlated to *seawater-like* groundwater (cluster 4) which can be explained by degradation of organic matter from the regional aquitard in anaerobic conditions [49]. The same process is believed to occur in shale rocks with high organic

matter content and ammonium would also be a tracer of the groundwater chemistry influenced by sedimentary rock-dominated aquifers (Figure 4.9(b)).

The greater MI is recorded for F^- in step 2 (Figure 4.10(b)) which means that fluoride is preferentially added to groundwater in a recharge type of groundwater, more specifically in Na(Ca)-HCO_3 type (cluster 2) after Ca^{2+}_{water}-$Na^{+}_{mineral}$ ion exchange processes have led to a decrease in the groundwater Ca^{2+} content [11]. This latter process is believed to occur in bedrock aquifers and in granular aquifers in contact with the regional aquitard [11] (Figure 4.9(b)). Finally, the Factor 2 combination of F^- with B^{3+} and Mo^{6+}, two proposed chemical pathfinders of the groundwater evolution toward Limestone Brines (LB), would indicate that F^- originates from the groundwater interaction with sedimentary rocks present in the region (Figure 4.9(b)). Preliminary results obtained in column experiments performed with limestone rocks interacting with deionized water reveal fluoride enrichment of water after 7 days (unpublished results). Further water-rock experiments would confirm this hypothesis.

4.9 CONCLUSION

In this paper, origin of groundwater from the Saguenay-Lac-Saint-Jean area, Québec (Canada) is discussed according to an evolution due to (1) water/rock interactions and (2) due to water/clay interactions and groundwater mixing [11]. Particular attention was given to concentrations of certain elements which exceeded levels established in groundwater quality policies. In preparation for multivariate processing, the database of

321 samples was reduced to 51 samples. The newly formed dataset was called the subset. The reduction of the number of samples enabled the use of fluoride and iron for the multivariate processing, two parameters frequently found in excessive concentrations in the study area, based on groundwater quality policies. Factorial analysis (FA) was applied to the subset. Four factors account for 78.8% of the total variance. Factor 1, with high loadings for K^+, HCO_3^-, Mg^{2+}, SiO_2, NH_4^+ and SO_4^{2-}, characterizes groundwater that is in contact with the regional clay aquitard. The chemical transformation of microcline into illite and CO_2 production process (organic matter degradation and sulfide reduction with production of HS^-) are believed to control the chemistry of seawater-like groundwater. Loadings for F^-, B^{3+}, Mo^{6+} and Na^+ compose the second factor. The study showed that dissolved F^- can be generated either from the interaction of groundwater with marine clay or from the interaction of groundwater with bedrock aquifers (crystalline or sedimentary aquifers). Fluoride is preferentially added to groundwater in a recharge type of groundwater, more specifically in Na(Ca)-HCO_3 type after Ca^{2+}_{water}-$Na^+_{mineral}$ ion exchange processes have led to a decrease in the groundwater Ca^{2+} content. The third factor is dominated by Ca^{2+}, Ba^{2+}, Sr^{2+} and, in a lesser extent, SO_4^{2-}. The third factor characterizes samples from cluster 3. The use of log-log plots of [Ca^{2+}, Ba^{2+}, SO_4^{2-}, Sr^{2+}] *vs.* Cl^- concentrations showed that samples from cluster 3 correspond to a diluted endmember of the geochemical process leading to a composition like that of the Canadian Shield brines (*PSB-like*) compiled in this study. Finally, the fourth factor is strongly influenced by

Fe^{2+} and Mn^{2+}. The fourth factor characterizes preferentially the *Recharge-like* type of groundwater (cluster 1 and 2).

From the recharge area, the evolution of rainwater (RW) toward a brackish end-member follows two possible paths in the region. First, groundwater tends to evolve through water/rock interactions toward a CaCl end-member similar to the Precambrian Shield brines (PSB) described elsewhere in Canada. Secondly, groundwater mixing with the Pleistocene Laflamme Sea end-member within confined aquifers that are in contact with the regional aquitard (water/clay interactions) causes the evolution of recharge groundwater (RGW) toward an end-member having a NaCl composition similar to seawater (SW). In both cases, the recharge Ca(Na)-HCO_3 groundwater type first evolves toward a Na(Ca)-HCO_3 groundwater type. Mixing is believed to occur at different sites in the study area as confined and unconfined aquifers may exist in the fractured rock and the Pleistocene deposits and combine locally to form multilayered, interconnected aquifers. In the bedrock, Precambrian Shield Brines can locally mix with Limestone Brines (LB) by upwelling toward the surface along the graben fault system, giving rise to Na(Ca)-Cl(SO_4) groundwater type. When fossil seawater or Precambrian Shield Brines and Limestone Brines encounter recharge groundwater, groundwater chemistry is believed to evolve toward a Na(Ca)-HCO_3(Cl-SO_4) groundwater type. Mixing is potentially enhanced by pumping groundwater in either bedrock wells or granular deposit wells, which causes mixing of groundwaters of differing ages and chemistries.

Maturation indexes (MI) were introduced to describe the enrichment and/or the depletion of the chemical content of the rainwater and the *recharge-like* groundwater along its evolution toward a brackish end-member (*seawater-like* or *PSB-like*). Results obtained with the proposed normative method demonstrated the general ongoing enrichment for Factors 1, 2 and 3. This general trend suggests that Factors 1 and 3 correspond to indicators of groundwater ageing. Moreover, the standardized method helped to identify chemical pathfinders of groundwater's endmembers (RW, RGW, SW, PSB, LB). Compared to groundwater, the high content of (RW) in Al^{3+} and Pb^{2+} in rainwater suggests an atmospheric contamination by these metals. Sources of contamination should be investigated at a local scale. Copper, iron and nitrate are likely to be chemical pathfinders for early processes of the recharge event, that is to say, the modification of rainwater (RW) to Ca(Na)-HCO_3 groundwater type (RGW) (Step 1). Later in the recharge event, the transformation of Ca(Na)-HCO_3 groundwater type toward Na(Ca)-HCO_3 groundwater type (Step 2), is marked by a transition of the redox conditions from oxidising to more reducing conditions. This transition leads to the precipitation of hydroxides and the retreat of the metallic ions from the solution, as well as the transformation of NO_3^- by ammonification to form NH_4^+. At this stage, manganese is still present in dissolved form. Binary plot investigations combined with the MI approach results suggest that barium content is inherited from the early stage of groundwater evolution (RGW) in crystalline bedrock, where Na(Ca)-HCO_3 groundwater type dominates. Organic matter degradation is believed to be responsible for NH_4^+ groundwater content in

confined granular aquifers and sedimentary rock aquifers where shale units are present. Bromide and lithium particularly characterize PSB end-members, and a mass ratio $Ca^{2+}/Sr^{2+} \approx 40$ is proposed to identify *PSB-like* groundwater. The ratio was derived from binary plot investigations of chemical data for brines found at depth in the Canadian Shield compiled from the existing literature.

Based on the gravity-driven-flow principle, a conceptual model was created for specific chemical pathfinders and groundwater chemical facies modification according to the different stages of evolution; however, further work is needed to verify the exact process at the origin of the observed enrichment and/or depletion. As a next step in this research project, chemical analysis of the solid matrix of the aquifer and experimental tests where water and the solid matrix are interacting (batch experiments) are being performed with the objective of gaining very useful insights into the origin of some specific chemical elements. In addition, regional rainwater chemistry should be thoroughly investigated using more samples collected at different periods of time over the region, and isotope analysis should be performed on groundwater samples to decipher the possible origin of certain chemical elements highlighted in this study (boron and sulfide).

This proposed chemical pathfinder approach opens new avenues for improving the characterization of the chemistry of groundwater as for refining the understanding of the processes involved in the observed signatures of groundwater contents of major, minor and trace chemical elements. The proposed methodology leads to characterize the degree

of maturation for groundwater in a given area where the geology and the groundwater evolution path are known. This maturation could be ultimately translated in term of residence time and ageing for groundwater. The natural spatial variations in the geochemistry of groundwater can be interpreted to provide the geochemical background for groundwater evolution. Furthermore, considering the chemical characteristics of the salinization processes highlighted in this study, selected major, minor and trace elements in groundwater become some relevant chemical pathfinders for investigating groundwater dynamics, such as the interconnectivity of aquifer systems or groundwater flow dynamic, hydrogeological contexts and mixing. Finally, this approach has a real potential to decipher the anthropogenic component over natural signature of groundwater.

4.10 ACKNOWLEDGEMENTS

This project was funded by the Natural Sciences and Engineering Research Council of Canada (NSERC), the Fonds de recherche du Québec – Nature et technologies (FRQNT), the Fondation de l'Université du Québec à Chicoutimi and Rio Tinto Alcan (RTA), and the Programme d'acquisition de connaissances sur les eaux souterraines of Quebec (PACES), with contributions from the Quebec Ministère du Développement durable, de l'Environnement, de la Faune et des Parcs (MDDEFP), and the five county municipalities of the SLSJ region (Domaine-du-Roy, Du-Fjord-Du-Saguenay, Lac-Saint-Jean-Est; Maria-Chapdelaine and the City of Saguenay). The authors wish to acknowledge Professor

Philippe Pagé from the University of Quebec at Chicoutimi (UQAC) for the very constructive general conversations about geochemistry of rocks and minerals.

4.11 REFERENCES

[1] R. M. Garrels, R.M., and F. T. Mackenzie, "Origin of the chemical compositions of some springs and lakes," *Equilibrium concepts in natural water systems*, vol. 67, pp. 222-242, 1967.

[2] H. C. Helgeson, "Evaluation of irreversible reactions in geochemical processes involving minerals and aqueous solutions - I. Thermodynamic relations," *Geochimica et Cosmochimica Acta*, Vol. 32, No. 8, pp. 853–877, 1968.

[3] S. E. Ingebritsen, and W. E. Sanford, *Groundwater in geologic processes*. Cambridge University Press, 1999.

[4] N.Gassama, H. U. Kasper, A. Dia, C. Cocirta, and M. Bouhnik-Lecoz, "Discrimination between different water bodies from a multilayered aquifer (Kaluvelly watershed, India): Trace element signature," *Applied Geochemistry*, Vol. 27, No. 3, pp. 715–728, 2012.

[5] J. Tóth, 'Groundwater as a geologic agent: An overview of the causes, processes, and manifestations," *Hydrogeology Journal*, Vol. 7, No. 1, pp. 1–14, 1999.

[6] K. Bucher, and I. Stober, "Fluids in the upper continental crust," *Geofluids*, Vol. 10, No. 1–2, pp. 241–253, 2010.

[7] A. E. Kehew, *Applied chemical hydrogeology*. Prentice Hall, Upper Saddle River, NJ, 2001.

[8] I. I. Chebotarev, "Metamorphism of natural waters in the crust of weathering 1-2-3," *Geochimica et Cosmochimica Acta*, Vol. 8, No. 1–2, pp. 22–48, 1955.

[9] J. Tóth, "A conceptual model of the groundwater regime and the hydrogeologic environment," *Journal of Hydrology*, Vol. 10, No. 2, pp. 164–176, 1970.

[10] Z. Yu, L. Zhang, P. Jiang, C. Papelis, and Y. Li, “Study on water-rock interactions of trace elements in groundwater with leaching experiments,” *Ground Water*, Vol. 53, No. S1, Supplement 1, pp. 95–102, 2015.

[11] Walter, J., R. Chesnaux, V. Cloutier, and D. Gaboury. 2017. The influence of water/rock − water/clay interactions and mixing in the salinization processes of groundwater. *Journal of Hydrology: Regional Studies* 13 (2017) 168–188.

[12] World Health Organization. 2004. *Guidelines for drinking-water quality: recommendations, (Vol. 1)*. World Health Organization.
http://www.who.int/water_sanitation_health/publications/gdwq3rev/en/
(accessed October 2017).

[13] R. Dessureault, *Hydrogéologie du Lac Saint-Jean, partie nord-est.* Québec: Ministère des richesses naturelles, Direction générale des eaux, Service des eaux souterraines, Québec, 1975.

[14] G. Simard, and R. Des Rosiers, *Qualité des eaux souterraines du Québec*. H.G.-13, Ministère des richesses naturelles, Direction générale des eaux, Service des eaux souterraines, Québec, 1979.

[15] Walter, J., A. Rouleau, R. Chesnaux, M. Lambert, R. Daigneault. *Accepted*. Characterization of general and singular features of major aquifer systems in the Saguenay-Lac-Saint-Jean region. *Canadian Water Ressources Journal*.

[16] J. Walter, A. Rouleau, I. D. Clark, and J. Guha, “A first investigation of groundwater geochemistry in the crystalline bedrock around lake Saint-Jean, Québec,” *IAH - Canadian Chapter*, Vancouver, pp. 1553-1560, 2006.

[17] J. Walter, *Les eaux souterraines à salinité élevée autour du lac Saint-Jean, Québec : origines et incidences*, Université du Québec à Chicoutimi, Chicoutimi, M.Sc. Thesis, pp. 177, 2010.

[18] J. Walter, A. Rouleau, D. W. Roy, and R. Daigneault, “Hydrogéochimie des eaux souterraines de la région du Saguenay-Lac-Saint-Jean: résultats préliminaires,” *Proceedings of GeoHydro 2011*, Joint Meeting of the Canadian Quaternary Association and IAH Canada Chapter. 6 p., 2011.

[19] R. Du Berger, D. W. Roy, M. Lamontagne, G. Woussen, R. G. North, and R. J. Wetmiller. “The Saguenay (Quebec) earthquake of November 25, 1988: Seismologic data and geologic setting,” *Tectonophysics*, Vol. 186, No. 1-2, pp. 59–74, 1991.

[20] A. F. Laurin, and K. N. M. Sharma, *Région des rivières Mistassini, Péribonca, Saguenay: Mistassini, Péribonca, Saguenay Rivers area: Grenville 1965-1967*, Ministère des richesses naturelles, Direction générale des mines, Service de l'exploration géologique, 1975.

[21] S. Desbiens, and P. J. Lespérance, “Stratigraphy of the Ordovician of the Lac Saint-Jean and Chicoutimi outliers, Quebec,” *Canadian Journal of Earth Sciences*, Vol. 26, No. 6, pp. 1185–1202, 1989.

[22] R.A. Daigneault, P. A. Cousineau, É. Leduc, G. Beaudoin, S. Milette, N. Horth, D. W. Roy, M. Lamothe, and G. Allard, “Rapport final sur les travaux de cartographie des formations superficielles réalisés dans le territoire municipalisé du Saguenay-Lac-Saint-Jean (Québec) entre 2009 et 2011,” *Governemental Report for the Ministère des Ressources Naturelles et de la Faune (Québec)*, 2011.

[23] P. LaSalle, G. Tremblay, *Dépôts meubles: Saguenay Lac Saint-Jean*. Ministère des richesses naturelles, Ministère des richesses naturelles, Direction générale de la recherche géologique et minérale, 1978.

[24] J. Dionne, and C. Laverdière, “Sites fossilifères du golfe de Laflamme,” *La Revue de Géographie de Montréal*, Vol. 23, pp. 259–270, 1969.

[25] G. Tremblay, “Glaciation et déglaciation dans la région Saguenay-Lac-Saint-Jean, Québec, Canada,” *Cahiers de géographie du Québec*, Vol. 15, No. 36, pp. 467-494, 1971.

[26] R. Bouchard, D. J. Dion, and F. Tavenas, “Origine de la préconsolidation des argiles du Saguenay, Québec. *Canadian Geotechnical Journal*, Vol. 20, No. 2, pp. 315–328, 1983.

[27] R. Chesnaux, S. Rafini, and A.-P. Elliott, “A numerical investigation to illustrate the consequences of hydraulic connections between granular and fractured-rock aquifers,” *Hydrogeology Journal*, Vol. 20, No. 8, pp. 1669–1680, 2012.

[28] S. K. Richard, R. Chesnaux, A. Rouleau, R. Morin, J. Walter, and S. Rafini, “Field evidence of hydraulic connections between bedrock aquifers and overlying granular

aquifers: Examples from the Grenville Province of the Canadian Shield," *Hydrogeology Journal*, Vol. 22, No. 8, pp. 1889–1904, 2014.

[29] A. Hounslow, *Water quality data: Analysis and interpretation*. CRC Press, Boca Raton, 1995.

[30] C. A. J. Appelo, and D. Postma, *Geochemistry, Groundwater, Pollution*. AA Balkema Publishers, Amsterdam, 2005.

[31] Durov, S., 1948. Natural waters and graphic representation of their composition, Dokl Akad Nauk SSSR, pp. 87-90.

[32] I. M. Farnham, K. H. Johannesson, A. K. Singh, V. F. Hodge, and K. J. Stetzenbach, "Factor analytical approaches for evaluating groundwater trace element chemistry data," *Analytica Chimica Acta*, Vol. 490, No. 1-2, pp. 123–138. 2003.

[33] G. E. Box, and D. R. Cox, "An analysis of transformations," *Journal of the Royal Statistical Society. Series B. Methodological*, Vol. 26, No. 2, pp. 211-252, 1964.

[34] J. Davis, *Statistics and data analysis in geology. John Wiley & Sons, New York. Statistics and data analysis in geology*. John Wiley & Sons, New York, 2002.

[35] Statsoft, Inc., STATISTICA (Data Analysis Software System), Version 12, 2013.

[36] Alvin, C.R., *Methods of multivariate analysis*. Wiley Interscience, New York, 2002.

[37] C. E. Brown, *Applied multivariate statistics in geohydrology and related sciences*. Springer Berlin, 1998.

[38] V. Cloutier, R. Lefebvre, R. Therrien, and M. M. Savard, "Multivariate statistical analysis of geochemical data as indicative of the hydrogeochemical evolution of groundwater in a sedimentary rock aquifer system," *Journal of Hydrology*, Vol. 353, No. 3, pp. 294–313, 2008.

[39] Environment Canada, "The Canadian National Atmospheric Chemistry (NAtChem) Database and Analysis System," February 2016.

[40] S. Frape, and P. Fritz, “The chemistry and isotopic composition of saline groundwaters from the Sudbury Basin, Ontario,” *Canadian Journal of Earth Sciences*, Vol. 19, No. 4, pp. 645–661, 1982.

[41] D. J. Bottomley, A. Katz, L. H. Chan, A. Starinsky, M. Douglas, I. D. Clark, and K. G. Raven, “The origin and evolution of Canadian Shield brines: Evaporation or freezing of seawater? New lithium isotope and geochemical evidence from the Slave craton,” *Chemical Geology*, Vol. 155, No. 3–4, pp. 295–320, 1999.

[42] S. K. Frape, and P. Fritz, “Geochemical trends for groundwaters from the Canadian Shield. Saline water and gases in crystalline rocks,” *Geological Association of Canada Special Paper*, Vol. 33, pp. 19-38, 1987.

[43] S. K. Frape, P. Fritz, and R. H. McNutt, “Water-rock interaction and chemistry of groundwaters from the Canadian Shield,” *Geochimica et Cosmochimica Acta*, Vol. 48, No. 8, pp. 1617–1627, 1984.

[44] M. Gascoyne, and D. C. Kamineni, “The hydrogeochemistry of fractured plutonic rocks in the Canadian Shield,” *Applied Hydrogeology.*, Vol. 2, No. 2, pp. 43–49, 1994.

[45] C. Güler, G. D. Thyne, J. E. McCray, and K. A. Turner, “Evaluation of graphical and multivariate statistical methods for classification of water chemistry data,” *Hydrogeology Journal*, Vol. 10, No. 4, pp. 455–474, 2002.

[46] M. Gascoyne, “Evolution of redox conditions and groundwater composition in recharge-discharge environments on the Canadian Shield,” *Hydrogeology Journal*, Vol. 5, No. 3, pp. 4–18, 1997.

[47] W. Edmunds, A. H. Guendouz, A. Mamou, A. Moulla, P. Shand, and K. Zouari, “Groundwater evolution in the Continental Intercalaire aquifer of southern Algeria and Tunisia: Trace element and isotopic indicators,” *Applied Geochemistry*, Vol. 18, No. 6, pp. 805–822, 2003.

[48] T. Hatva, *Iron and manganese in groundwater in Finland: Occurrence in glacifluvial aquifers and removal by biofiltration*. Publications of the Water and Environment Research Institute. Vol. 4, 1989.

[49] Y. Wang, J. J. Jiao, J. A. Cherry, and C. M. Lee, “Contribution of the aquitard to the regional groundwater hydrochemistry of the underlying confined aquifer in the Pearl River Delta, China,” *Science of the Total Environment*, Vol. 461–462, pp. 663–671, 2013.

[50] Z. Miao, M. Brusseau, K.C. Carroll, C. Carreón-Diazconti, and B. Johnson, “Sulfate reduction in groundwater: characterization and applications for remediation,” Environmental Geochemistry and Health, Vol. 34, No. 4, pp. 539–550, 2012.

[51] CERM-PACES, *Résultats du programme d'acquisition de connaissances sur les eaux souterraines du Saguenay-Lac-Saint-Jean*, Centre d'études sur les ressources minérales, Université du Québec à Chicoutimi, Québec, 2013.

[52] J.-Y. Gravel, *Minéralogie de l’argile Champlain de St-Jean-Vianney*. MSc. Thesis, Université Laval, 1974.

[53] C. Beaucaire, and G. Michard, “Origin of dissolved minor elements (Li, Rb, Sr, Ba) in superificial waters in a granitic area,” *Geochemical Journal*, Vol. 16, No. 5, pp. 247–258, 1982.

[54] J. D. Hem, “Study and interpretation of the chemical characteristics of natural water,” *United States Geological Survey Water Supply Paper*, 2254, 1985.

[55] W. Edmunds, and P. Smedley, “Residence time indicators in groundwater: The East Midlands Triassic sandstone aquifer,” *Applied Geochemistry*, Vol. 15, No. 6, pp. 737–752, 2000.

[56] M. Gascoyne, J. D. Ross, R.L. Watson, and D. C. Kamineni, “Soluble salts in a Canadian Shield granite as contributors to groundwater salinity,” *Proceedings of the 6th International Symposium on Water-Rock Interactions*, Malvern, U.K., August 3-12, 1989, pp.247-249, 1989.

[57] D. C. Kamineni, “Halogen-bearing minerals in plutonic rocks: A possible source of chlorine in saline groundwater in the Canadian Shield. Saline water and gases in crystalline rocks,” *Geological Association of Canada Special Paper*, Vol. 33, pp. 69-79, 1987.

[58] Health Canada, *Guidelines for Canadian Drinking Water Quality—Summary Table.* Water and Air Quality Bureau, Healthy Environments and Consumer Safety Branch, Health Canada, Ottawa, Ontario, 2014.

[59] Carignan, J., Gariépy, C., 1992. Pb isotope geochemistry of molybdenite ores from the Grenville and Superior Provinces, Canadian Shield: geochronological potential. Mise en garde/Advice: 42.

[60] D. Wen, F. Zhang, E. Zhang, C. Wang, S. Han, and Y. Zheng, “Arsenic, fluoride and iodine in groundwater of China,” *Journal of Geochemical Exploration*, Vol. 135, pp. 1–21, 2013.

[61] S. Battaleb-Looie, F. Moore, H. Jafari, G. Jacks, and D. Ozsvath, “Hydrogeochemical evolution of groundwaters with excess fluoride concentrations from Dashtestan, South of Iran,” *Environmental Earth Sciences*, Vol. 67, No. 4, pp. 1173–1182, 2012.

[62] G.-T. Chae, S.-T. Yun, M.-J. Kwon, Y.-S. Kim, and B. Mayer, “Batch dissolution of granite and biotite in water: Implication for fluorine geochemistry in groundwater,” *Geochemical Journal*, Vol. 40, No. 1, pp. 95–102, 2006.

CHAPITRE 5

DISCUSSION ET RECOMMANDATIONS

5.1 CONNAISSANCES HYDROGÉOLOGIQUES RÉGIONALES

Le présent projet de thèse n'aurait pu être réalisé si préalablement un projet d'envergure régional orienté vers l'acquisition des connaissances hydrogéologiques n'avait pas été réalisé. Nous parlons ici du projet de cartographie réalisé entre les années 2009 et 2013 au Saguenay-Lac-Saint-Jean, dans le cadre du Programme d'acquisition des connaissances sur les eaux souterraines (PACES; MDDELCC, 2018). Ce projet a permis le développement de plusieurs cartes thématiques, d'importantes bases de données sur le sous-sol, de nombreux projets de recherche, ainsi que la formation de nombreuses personnes qualifiées dans divers aspects des eaux souterraines (Walter et al., 2018). La cartographie hydrogéologique est une prémisse indispensable à l'approfondissement des connaissances du fonctionnement hydrogéochimique à l'échelle d'un territoire, dans notre cas d'une superficie de 13 200 Km^2. Les connaissances acquises permettent de poser les bases physiques du modèle conceptuel hydrostratigraphique régional et donnent un aperçu du comportement hydraulique des principaux aquifères.

5.1.1 UNE PHYSIOGRAPHIE PARTICULIÈRE : LE GRABEN DU SAGUENAY

Comme le montre notre étude, la physiographie régionale en forme de graben a un impact majeur sur l'évolution naturelle de la chimie de l'eau souterraine de la région. La délimitation franche entre les basses-terres et les hautes-terres contrôle, d'une part l'accumulation de dépôts meubles quaternaires (sable, gravier, argile, etc.) et d'autre part, une partie de l'écoulement de l'eau souterraine en milieu fracturé. Cette physiographie

particulière a notamment pour effet la résurgence d'eau souterraine profonde salée, âgée de plusieurs milliers d'années et impropre à la consommation, au cœur des basses-terres qui concentre la majeure partie du territoire municipalisé et agricole. Cette observation additionnée au contexte géologique relativement simple de la région en fait un laboratoire unique pour l'étude de la dynamique géochimique des eaux souterraines.

5.1.2 LE ROC FRACTURÉ PRÉCAMBRIEN ET ORDOVICIEN

Dans le cadre de cette thèse, par manque d'information, les deux types d'aquifères rocheux fracturés ont été combinés dans nos interprétations hydrogéochimiques. Il ressort cependant de la répartition gééographique des résultats d'analyse statistique multivariée menée sur les 321 échantillons (figure 3.6; Walter et al., 2017) que tous les échantillons d'un groupe en particulier (*Cluster 1*) sont localisés à proximité des étendues de roches sédimentaires connues. Cette nouvelle piste mériterait d'être investiguée. De plus, les résultats discutés au chapitre 4 suggèrent que la présence de différents ions en solution dans l'eau souterraine puisse être caractéristique des roches sédimentaires d'une part (Mo^{6+}, B^{3+}, NH_4^+), et des roches cristallines d'autre part (Br^-, Li^+, $Sr^{2+}/Ca^{2+}\approx40$).

Aussi, la distinction entre les calcaires de Trenton et les shales d'Utica n'est pas faite. Par définition, ces deux types de roches sédimentaires ordoviciennes peuvent être distinguées sur la base de leur comportement hydraulique ainsi que d'après leur contenu minéralogique. Ces deux réservoirs sont ainsi capables d'imprimer une signature distincte à l'eau souterraine. Cette hypothèse n'a pas été testée dans le cadre de notre étude.

Les réservoirs constitués des roches cristallines pourraient aussi être mieux détaillés, notamment sur la base de leur minéralogie (roches felsiques à mafiques). La répartition géographique des résultats du traitement statistique réalisé sur les 321 échantillons de cette étude n'a pas permis de faire de telles distinctions. Toutefois, il est permis de croire que notre modèle du fonctionnement hydrogéochimique régional pourrait être affiné en détaillant mieux les réservoirs géologiques de l'eau souterraine des points de vue de leur minéralogie et de la chimie de l'eau souterraine qu'ils contiennent. Pour ce faire, la première étape serait la planification d'une campagne d'échantillonnage de l'eau souterraine en fonction du type de réservoir, menée parallèlement à la caractérisation quantitative du contenu minéralogique de la matrice des réservoirs considérés (*voir section 5.6. Travaux de recherche complémentaires*).

5.1.3 LES DÉPÔTS MEUBLES QUATERNAIRES

Comme pour les réservoirs de roc fracturé, l'assemblage des unités sédimentaires de sédiments meubles mériterait d'être mieux détaillé pour permettre une meilleure compréhension des écoulements et des divers mécanismes d'acquisition de la signature hydrogéochimique de l'eau souterraine. C'est le cas, entre autres, des édifices deltaïques. Ces derniers font partie des accumulations de sable de surface les plus répandues sur le territoire d'étude et qui sont parmi les plus épaisses. Ces dépôts deltaïques sont caractérisés par un assemblage stratifié d'alternances rythmées de sédiments fins à grossiers hérité de leur nature progradante. Il ne serait alors pas surprenant d'observer

plus d'une nappe (libre, semi-confinée à confinée) avant d'atteindre l'aquitard régional constitué des argiles marines. À la lumière de nos travaux, nous pensons que ces différentes nappes pourraient être distinguées sur la base de leur signature hydrogéochimique, considérant que l'aquitard peut localement contribuer à la dégradation de la qualité naturelle de l'eau souterraine, notamment en fluorures. Aussi, un contenu élevé en ions bicarbonatés et sulfatés combiné à la présence d'ammonium, le tout attribuable à la dégradation de la matière organique, pourraient nous mettre sur la piste de l'interaction de l'eau souterraine avec l'aquitard régional.

5.1.4 CADRE HYDROSTRATIGRAPHIQUE RÉGIONAL

Par endroit, le roc est confiné par l'unité d'argile de la mer Laflamme ou présente une connexion hydraulique avec des dépôts granulaires superficiels (Chesnaux et Elliott, 2011; Richard et al., 2014). À l'aide d'une analyse géochimique de routine (*i.e.* paramètres inorganiques), le phénomène de connexion hydraulique peut maintenant être investigué en considérant le modèle hydrogéochimique régional proposé dans notre étude, en cherchant notamment à identifier une signature hydrogéochimique propre au roc dans les dépôts granulaires, ou inversement.

5.1.5 CONTRIBUTION AU CYCLE DES CONNAISSANCES HYDROGÉOLOGIQUES RÉGIONALES

La cartographie hydrogéologique à l'échelle régionale réalisée dans le cadre du PACES constitue une image, à un temps donné, des connaissances hydrogéologiques d'un

territoire. Ces informations doivent maintenant être mises à jour régulièrement afin d'en assurer la pérennité et d'en maintenir la pertinence (Walter et al., 2018). Le présent projet de recherche doctoral est né de la cartographie hydrogéologique régionale, et contribue à son tour à la connaissance hydrogéologique régionale. L'approfondissement des connaissances lors de travaux tels que ceux présentés dans cette thèse permet ainsi l'amélioration générale des connaissances hydrogéologiques et rend l'état des connaissances hydrogéologiques régionales dynamique, à l'image du cycle présenté à la figure 5.1.

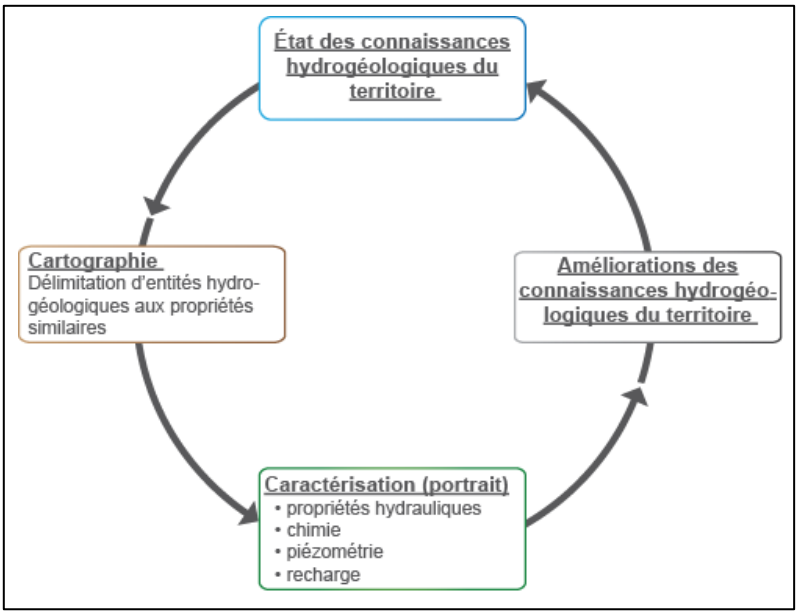

Figure 5.1: Cycle d'optimisation continue des connaissances hydrogéologiques régionales (tirée de CERM-PACES, 2015).

Le cycle d'amélioration des connaissances permet de faire la distinction entre la cartographie hydrogéologique (phase de délimitation spatiale d'entités

hydrogéologiques), la caractérisation hydrogéologique (inventaire des éléments hydrogéologiques descriptifs des entités), et finalement, l'amélioration générale des connaissances (c.-à-d. les contribution originales et significative à la science) qui inclut tout projet visant le regroupement et l'interprétation de l'ensemble des données existantes préalablement au projet. Le Québec a récemment acquis une expertise enviable sur l'acquisition de connaissances hydrogéologiques. Il faut poursuivre les efforts vers l'utilisation efficiente de ces connaissances et le développement de projets de recherche pertinents et innovants sur les eaux souterraines. Surtout, il faut que ces connaissances soient transférées efficacement vers les gestionnaires du territoire et autres utilisateurs des données hydrogéologiques (MRC, municipalités, OBV, firmes d'experts-conseil et les directions régionales de divers ministères), ce afin d'assurer une gestion durable de la ressource.

5.2 PÔLES DE L'ÉVOLUTION GÉOCHIMIQUE NATURELLE DE L'EAU SOUTERRAINE

Les interprétations qui découlent du traitement des données sont intimement liées à la qualité des données de même qu'à une méthode originale ayant pour but de rehausser le signal hydrogéochimique des données d'échantillonnage.

5.2.1 QUALITÉ DES DONNÉES HYDROGÉOCHIMIQUES ET LIMITES DE DÉTECTION

Les données ayant servi dans ce projet ont été produites dans le cadre d'un projet de cartographie régionale, et non aux fins du projet de recherche. Il en résulte des valeurs

de limites de détection analytiques élevées pour certains éléments chimiques, notamment ceux présents en traces. De ce fait avéré découle une conséquence majeure que sont les limites d'applicabilité des techniques d'analyses multivariées. En effet, il est de plus en plus commun de voir appliquer ces techniques sur des jeux de données sans que ne soit réellement prise en considération la quantité de données sous la limite de détection. Or, lorsque le principe de traitement multivarié repose sur la corrélation des paramètres (*i.e.* matrice de corrélation), comme dans la majorité des études, un nombre trop élevé de données sous la limite de détection induit un bruit de fond qui parasite les résultats et nuit à leur interprétation (Farnham et al., 2003). Ceci nous a donc conduit à tester une méthode de sous-échantillonnage de la banque d'échantillons originale, dans le but de considérer un maximum d'éléments chimiques dans le traitement statistique multivarié (Chapitre 4).

Ce sous-échantillonnage a pour effet la réduction du jeu de données disponible pour le traitement statistique. Nous pensons que cette étape permet d'améliorer la qualité des interprétations, et d'ouvrir de nouvelles pistes d'investigations des mécanismes d'interaction eau-roche à partir des techniques statistiques multivariées. D'une part, après réduction, ces interprétations sont basées sur un nouveau jeu de données au contenu géochimique plus homogène qu'avant la réduction, et d'autre part, la réduction du nombre d'échantillons nous permet de tenir compte dans l'analyse statistique multivariée d'un plus grand nombre paramètres chimiques, généralement retrouvés en trace dans l'eau souterraine.

5.2.2 REGROUPEMENT DES ÉCHANTILLONS ET RÉDUCTION DU JEU DE DONNÉES

La réduction du jeu de données repose sur l'identification de certains paramètres chimiques clés des mécanismes d'interactions eau-roche investigués, ou des paramètres qui présentent une bonne corrélation statistique avec ces paramètres clés. Alors que communément, les techniques multivariées servent à formuler des hypothèses a posteriori des résultats (Alvin, 2002), notre méthode de sélection d'échantillon repose sur des hypothèses formulées en amont du traitement statistique multivarié. Ces hypothèses sont ensuite vérifiées à partir des résultats obtenus. Parmi les hypothèses posées, la plus importante postule que l'eau souterraine des milieux rocheux fracturés est statistiquement distincte de celle des eaux souterraines des milieux granulaires poreux. La seconde, plus communément acceptée dans la littérature, veut que le faciès chloruré de l'eau souterraine corresponde à un stade avancé de l'évolution naturelle hydrogéochimique (Chebotarev, 1955 ; Ingebritsen et Sanford, 1999). Appuyée par ces hypothèses, la première étape de la réduction du jeu de données consiste alors à regrouper les échantillons d'après le type d'eau (Cl^- ou HCO_3^-) et le milieu aquifère d'où provient l'échantillon (Roc fracturé ou granulaire poreux). C'est dans chacun de ces groupes que les échantillons sont sélectionnés manuellement en fonction de leur contenu en divers paramètres chimiques (figure 5.2).

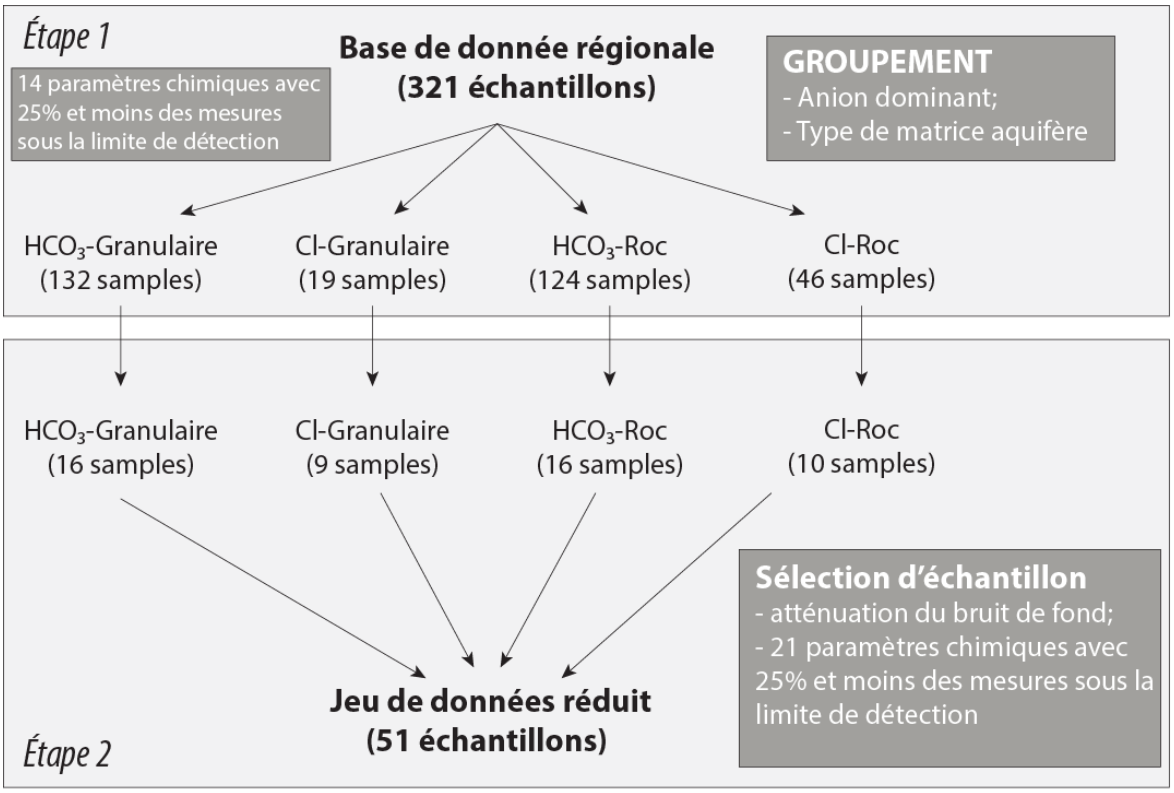

Figure 5.2 : Étapes de la méthode de réduction du jeu de données

Les paramètres considérés lors de la sélection correspondent à des ions pour lesquels un nombre important de données est supérieur à la limite de détection analytique de cet ion (>25% des enregistrements). En appliquant ce critère de sélection, des échantillons peuvent être ajoutés ; dans ce cas la teneur d'un ion en particulier ou d'une combinaison d'ions est au-dessus de la limite de détection, ou retiré ; dans ce cas la teneur d'un ion en particulier ou d'une combinaison d'ions est en-dessous de la limite de détection. Dans les deux cas, la proportion de mesures au-dessus de la limite de détection augmente pour certains ions, et diminue pour d'autres. Cette étape a été réalisée manuellement, et de manière semi-subjective, l'objectif étant d'atteindre plus de 75% de

données au-dessus de la limite de détection pour un maximum de paramètres chimiques, en plus du fluor et du fer, et ce, de manière indépendante dans chacun des quatre groupes d'échantillons. Plusieurs itérations ont parfois été nécessaires. Le nombre d'itérations, ainsi que le type d'ions ou les combinaisons d'ions considérés lors de la sélection des échantillons varient d'un groupe d'échantillons à un autre. A titre d'exemple, les figures 5.3 à 5.5 illustrent graphiquement la méthode de sélection réalisée pour le groupe d'échantillons constitué des échantillons d'eau bicarbonatée prélevée dans les aquifères granulaires poreux (Groupe 1 ; *HCO_3-Granulaire* ; N = 132). Sur chaque figure, l'axe vertical correspond au nombre de valeurs enregistrées au-dessus la limite de détection pour chaque élément chimique présenté sur l'axe horizontal. La Figure 5.3 présente le pourcentage de détection calculé à partir de l'ensemble des échantillons contenus dans la base de données régionale ($\%_{Detectés} = [N_{detecté}/N_{321}]* 100$). Cette figure s'apparente à la figure 4.3 présentée au chapitre 4.

La figure 5.3 montre que divers éléments critique pour l'identification de pôles d'eau souterraine se situe sous la barre de 75% requise pour considérés leur utilisation comme valides dans les traitements statistiques subséquents. Or, parmi ces éléments, le fer (~ 40% des données au-dessus de la limite de détection) et le fluor (~ 50% des données au-dessus de la limite de détection) sont considérés comme géologiquement et chimiquement importants pour le traitement statistique subséquent. Il n'est pas possible d'identifier sur des bases objectives une partie des échantillons qui se situent sous la

limite de détection qui pourraient être éliminé de la base de données afin de rehausser le pourcentage des données au-dessus de la barre de 75%.

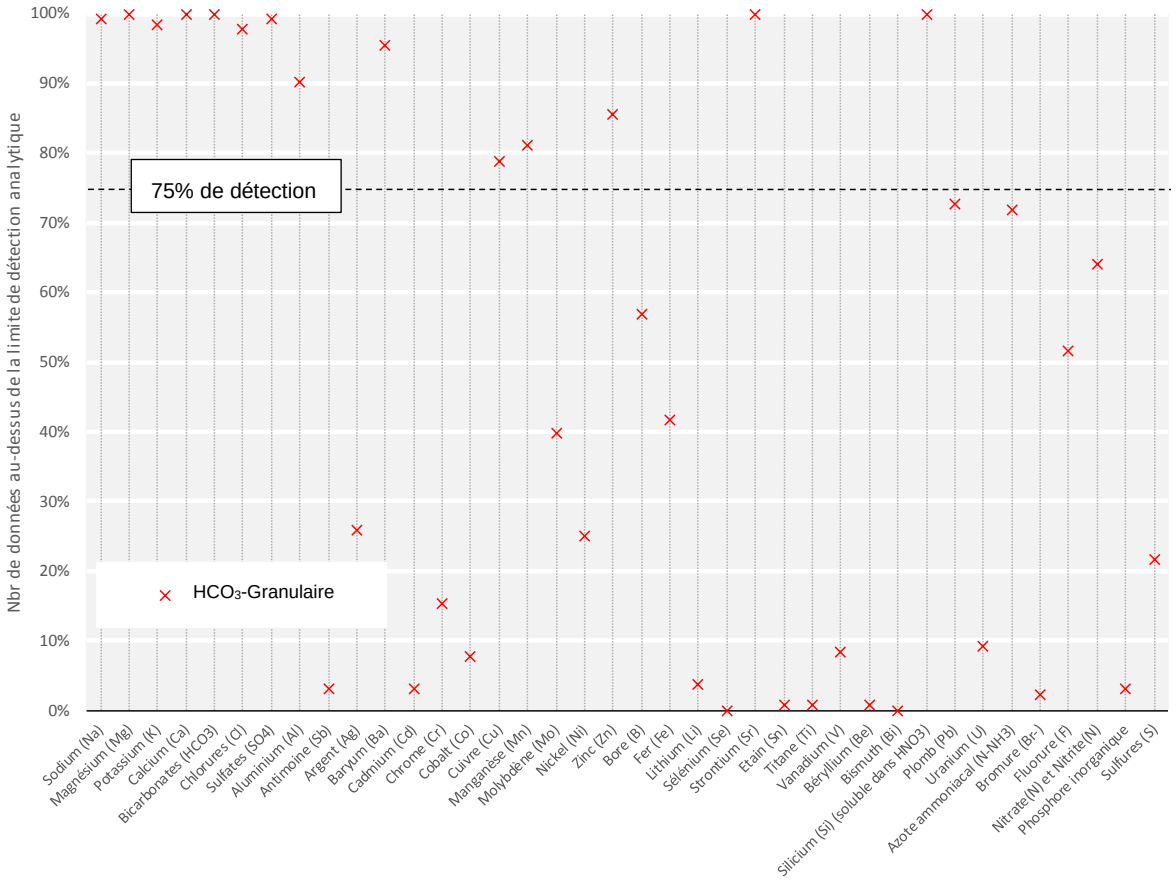

Figure 5.3 : Nombre total de détection (en %) pour chaque élément chimique analysé dans cette étude calculé à partir du nombre total d'échantillons contenus dans le groupe 1 : eaux souterraines bicarbonatées prélevées dans des aquifères granulaires poreux (HCO_3-Granulaire; N = 132).

Une première série d'échantillons est sélectionnée parmi les 132 échantillons qui composent le groupe 1, considérant 100% de détection pour le fer. , les nitrites-nitrates et le molybdène. L'effet de cette sélection sur le nombre de détection de chaque ion analysé dans cette étude est présenté à la Figure 5.4. En conséquence, l'ensemble des données

originalement avec une valeur sous la limite de détection a été retranché de la base de données. Toutefois, ce faisant, il y a eu un effet d'entrainement sur le positionnement dans le tableau du nombre de données au-dessus de la limite de détection. En effet, les matrices de corrélation montrent clairement que le fer est corrélé positivement (en général) ou négativement (parfois) avec d'autres éléments chimique (annexe 2).

L'établissement final de la base de données opère par itérations. Dans un premier temps, le fer est l'élément principal considéré. Sur des bases géologiques, le molybdène et les nitrates sont ajoutés. Conséquemment, ceci qui a permis d'identifié 7 échantillons significatifs pour le traitement statistique. Le nouveau tableau du pourcentage d'échantillons se situant au-dessus de la limite de sélection a été produit. Les éléments corrélés avec le fer, comme le manganèse, voient aussi leur pourcentage de données au-dessus de la limite de sélection augmenter.

Une nouvelle série d'échantillon est alors sélectionnée à partir des échantillons résiduels du groupe 1 ($N_{résiduel}$ = 132 – 7 = 125). Pour cette seconde sélection, nous cherchons à identifier les échantillons pour lesquels 100% de détection sont enregistrés pour les fluorures, mais aussi pour les éléments l'aluminium, le cuivre, le zinc, le bore, le plomb et l'ammonium.

Au total, 9 échantillons répondent à ce critère. Cette nouvelle sélection est additionnée à la précédente ($N_{Groupe\ réduit}$ = 7 + 9 = 16). Le pourcentage de valeurs au-

dessus de la limite de détection est à nouveau calculé pour chaque ion analysé dans le cadre de cette étude ($N_{detecté}/N_{Groupe\ réduit}$) (Figure 5.5).

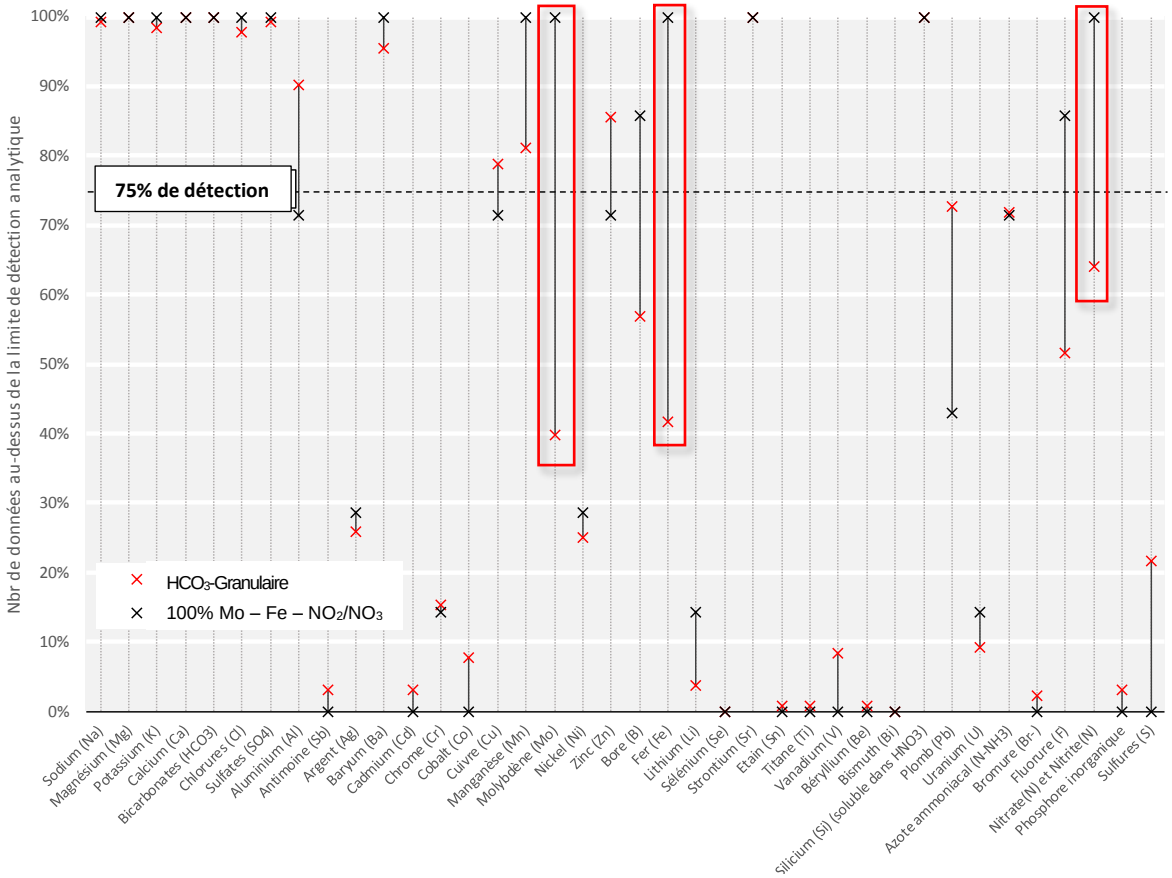

Figure 5.4 : Nombre total de détection (en %) calculé à partir d'une première sélection d'échantillons prélevés dans le groupe 1 (HCO_3-Granulaire; N = 132) pour lesquels le molybdène, le fer et les nitrites-nitrates (encadrés rouges) enregistrent 100% de leur valeur au-dessus de la limite de détection (N=7).

Si l'analyse statistique multivariée avait dû être réalisée avec le groupe 1 dans son ensemble (Groupe 1 ; *HCO_3-Granulaire* ; N = 132), 14 paramètres chimiques parmi les 38 de cette étude auraient pu être rigoureusement utilisés. Ces paramètres chimiques sont:

sodium, magnésium, calcium, potassium, bicarbonates, chlorures, sulfates, aluminium, baryum, cuivre, manganèse, zinc, strontium et silice (Figure 5.3). Pour le sous-groupe constitué des 16 échantillons sélectionnés parmi ceux du groupe 1, l'analyse statistique multivariée peut être rigoureusement appliquée en incluant 7 nouveaux paramètres chimiques, que sont : le molybdène, le plomb, les fluorures, le fer, le bore, l'ammonium, et les nitrites-nitrates, pour un total de 21 paramètres chimiques présentant un nombre de détection supérieur à la limite inférieure de 75% (Figure 5.5.).

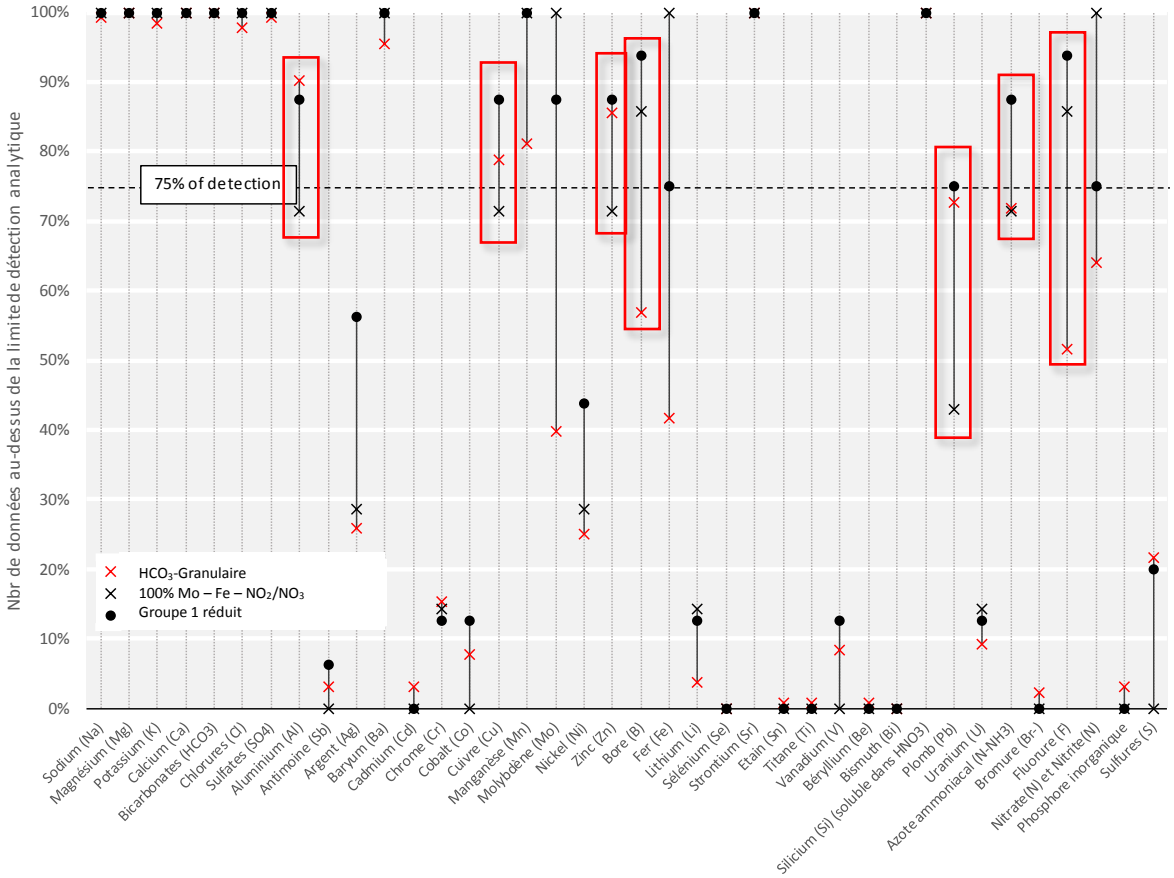

Figure 5.5: Nombre total de détection (en %) calculé à partir d'une seconde sélection d'échantillons prélevés dans le groupe 1: eaux souterraines bicarbonatées prélevées dans des aquifères granulaires poreux (HCO_3-Granulaire; N = 132) pour lesquels l'aluminium, le cuivre, le zinc, le bore, le plomb, l'ammonium et les fluorures (encadrés

rouges) enregistrent 100% de leur valeur au-dessus de la limite de détection (N=9). À ces échantillons s'ajoutent ceux identifiés à l'étape précédente (+ 7). Le sous-groupe du groupe 1 contient donc 16 échantillons.

Le jeu de données réduit présenté dans cette étude correspond à un assemblage original non reproductible et semi-aléatoire d'échantillons sélectionnés dans quatre groupes d'échantillons distingués sur la base du type d'eau et du type de matrice aquifère. En éliminant du jeu de données initial des échantillons pour lesquels certains paramètres ne sont pas détectés, cette méthode va à l'encontre d'un principe bien accepté en géochimie qui veut que « plus on a d'information, meilleures sont les interprétations ». En appliquant la réduction du jeu de données telle que nous l'avons présentée, nous introduisons un biais évident dans les interprétations qui en découlent. Ce biais est très difficilement qualifiable et quantifiable car il tire son origine de nombreuses manipulations uniques à chaque groupe. Ce biais peut être comparé au biais d'échantillonnage sur le terrain. Nous savons que seuls les échantillons prélevés sur le terrain contribuent aux interprétations, alors qu'il existe peut-être des « échantillons non-échantillonnés » susceptibles de contribuer à de nouvelles interprétations, qui infirmeraient ou confirmeraient celles formulées sans ces nouveaux échantillons.

Un des avantages de la réduction du jeu de données réside notamment dans le fait d'avoir pu inclure dans l'analyse statistique multivariée présentée au chapitre 4, un paramètre de santé important dans notre étude, que sont les ions fluorures. Ces derniers

n'avaient pas été inclus dans l'analyse réalisée avec les 321 échantillons. Les caractéristiques statistiques des deux jeux de données, et les résultats obtenus sont discutés et comparés entre eux. L'ensemble des résultats est aussi comparé avec des eaux de références de saumures continentales ayant évolué en milieu rocheux fracturé cristallin, compilées à partir de la littérature scientifique dans le cadre de cette étude. De manière générale, la convergence des observations et des résultats obtenus conforte nos interprétations. L'étude de l'évolution géochimique des eaux souterraines basée sur le traitement statistique du jeu de données réduit va même plus loin en suggérant entre autre une corrélation inverse du fer et du manganèse pour des eaux de type bicarbonaté, et une origine mixte du fluor dont la source peut être les argiles de la mer de Laflamme et/ou le socle rocheux précambrien.

Nous demeurons convaincus que le principe de réduction du jeu de donnée présente un intérêt pour la compréhension plus fine de phénomènes impliquant des éléments traces à ultra-traces caractéristiques de certains phénomènes d'interaction eau-roche. C'est pourquoi nous pensons que des recherches supplémentaires visant la réduction d'un jeu de données contenant plus d'une centaine d'échantillons et impliquant plusieurs dizaines de paramètres chimiques. La méthode de réduction du jeu de données pourrait s'avérer une nouvelle avenue pour l'étude des traceurs hydrogéochimiques des mécanismes d'interaction eau-roche dont les limites de détection sont encore trop élevées pour garantir une utilisation optimale des techniques d'analyses statistiques multivariées, et permettrait certainement de valoriser les nombreuses données

hydrogéochimiques acquises au fil du temps et dans le cadre d'étude diverses pour lesquelles les limites de détection sont parfois élevées.

5.3 MÉTHODE NORMATIVE ET EMPREINTE GÉOCHIMIQUE DES PÔLES RÉGIONAUX

La méthode normative proposée au chapitre 4 vise à discuter les différences et les similitudes entre les pôles identifiés à partir du jeu de données réduit, dans le but de déterminer de manière semi-quantitative certains paramètres chimiques caractéristiques d'un ou de plusieurs stades d'évolution de l'eau souterraine. Nous avons appelé les variations de chimie d'un pôle à l'autre des « indices de maturité » (*maturation index*).

On comprend que l'étude de ces indices de maturité est directement liée à la composition chimique respective des différentes grappes. L'ensemble des limites méthodologiques qui s'applique à la sélection des échantillons (section précédente), limite donc aussi la portée des interprétations qui peuvent être faites à partir des indices de maturité. Ainsi, les caractéristiques chimiques des différents stades d'évolution de l'eau souterraine, et les traceurs intrinsèques proposés sont intimement liées à la composition chimique des échantillons qui composent les grappes. Pour approfondir la connaissance de la spéciation chimique des éléments en fonction de l'évolution temporelle de l'eau, et pour doter ces derniers d'un caractère plus universel, d'autres travaux seraient à prévoir, notamment des études expérimentales d'interaction eau-roche en laboratoire, ou encore des études basées sur des résultats d'analyses chimiques obtenus suite à une campagne

d'échantillonnage d'eau souterraine planifiée en fonction de la composition minéralogique des réservoirs. Ces points sont discutés dans une section subséquente.

De la même manière, plusieurs interprétations concernant la chimie de l'eau de recharge (grappes 1 et 2) découlent directement de la signature chimique de l'eau de pluie. Dans le but de proposer la signature chimique la plus complète possible, la composition chimique que nous proposons correspond à une moyenne incluant des données compilées de la littérature, et des données obtenues après analyse en laboratoire de 4 échantillons prélevés sur le territoire d'étude. Des teneurs anomales en plomb et en aluminium ont été identifiées dans au moins deux des quatre échantillons prélevés, sans que leur source n'ait été identifiée (Walter et al., soumis). Ce point mériterait notamment d'être adressé dans une étude qui viserait la connaissance de la qualité de l'eau de recharge, incluant l'ensemble des paramètres géochimiques considérés dans cette étude, de même que les isotopes stables de la molécule d'eau (deutérium et oxygène 18). Les échantillons de pluie et de neige seraient prélevés à divers endroits sur le territoire et selon une fréquence mensuelle. Cette recommandation imposerait de mettre en place un réseau de suivi de la qualité de l'eau météoritique, en utilisant éventuellement les stations météorologiques avec pluviomètre collecteurs déjà existantes sur le territoire. La nouvelle signature chimique obtenue, ainsi que les variations saisonnières propres à la région, trouveraient certainement plusieurs applications pratiques dans le cadre d'autres projets hydrogéologiques et hydrologiques.

D'autres méthodes de normalisation pourraient aussi être testées, certaines ayant déjà fait leur preuve. En effet, nous savons que pour une même lithologie, en fonction du temps de transit qui conditionne le temps d'interaction eau-roche et du volume d'eau au contact des roches, un effet dilution-concentration peut donner des concentrations chimiques très différentes en différents points de l'aquifère. Afin de s'affranchir de cet effet lors de l'interprétation des données, une méthode consiste à normaliser les différents éléments chimiques par rapport à l'un d'entre eux (Négrel et al. 1993; Gaillardet et al., 1997, 1999; Négrel et al., 2008). Par exemple, Malcuit (2012) utilise le sodium pour normaliser les analyses chimiques de son étude, ce dernier étant produit essentiellement par la dissolution des aluminosilicates sodiques et à un degré moindre par la dissolution des évaporites. Il en résulte que les eaux drainant des roches carbonatées contiendront des quantités moindres de sodium, ce qui permet de différencier les eaux sous influence des roches silicatées de celles contrôlées par des roches carbonatées (Négrel et al., 1993). D'autres préfèreront utiliser l'aluminium pour s'affranchir de l'effet du pH sur les éléments métalliques dissous (Rafini, *communication personnelle*). La normalisation par un élément chimique en particulier implique de « sacrifier » cet élément au détriment des autres. En effet, les variations du paramètre servant à la normalisation ne pourront pas être discutées, étant égales à 1. Dans le cadre de notre étude, nous préconisons une technique de normalisation qui se rapproche de la normalisation au manteau primitif des *Mid Oceanic Ridge Basalt* (MORB) communément utilisée en pétrologie ignée pour discuter l'enrichissement ou l'appauvrissement en certains éléments chimiques d'une

roche « évoluée » comparée à une roche « parent » dont le contenu géochimique est réputé caractéristique (MORB) d'un environnement originel (le manteau terrestre). Cette technique permet une représentation sous forme de diagramme multiéléments de la totalité des paramètres chimiques considérés. Plusieurs compositions géochimiques normalisées peuvent être superposées. L'ordonnancement des paramètres chimiques conditionne la forme du spectre normalisé, ce qui facilite l'interprétation du spectre normalisé. Les différences et les similitudes entre les spectres renseignent sur certains mécanismes.

Donc, dans notre cas, si l'eau « parent » s'avère intrinsèquement liée à un environnement singulier, les formes du spectre normalisé à cette eau peuvent être comparées et discutées en référence à cet environnement singulier. À titre d'exemple, la figure 5.6 montre deux spectres multiéléments normalisés au pôle compositionnel régional de l'évolution de l'eau souterraine en milieu granulaire poreux confiné par l'argile marine (grappe 4). Mentionnons que pour cet exemple, la normalisation n'est pas effectuée avec une eau « parent » mais avec un des deux pôles régionaux présentés dans cette étude. Sur la figure 5.6, un spectre correspond à la normalisation de la composition moyenne du pôle régional de l'évolution de l'eau souterraine en milieu rocheux fracturé (grappe 3). Le second spectre correspond à la normalisation de la composition chimique de l'échantillon UQAC1105 (les données brutes pour cet échantillon sont données à l'annexe 1). Cet échantillon a été prélevé sur le territoire, dans le secteur de la municipalité de Rivière-Éternité. Ce village est situé en plein cœur des hautes-terres, à

l'extérieur de la limite de l'extension maximale de la mer Laflamme. À cet endroit, l'environnement géologique est dominé par des affleurements de roches cristallines du Bouclier Précambrien, et la couverture des dépôts meubles quaternaires est dominée par des dépôts discontinus de till peu épais (<1m). Le puits tubulaire d'où provient l'échantillon a une profondeur d'environ 130 m. Il a été abandonné par ses propriétaires car il présente une eau saumâtre (TSD = 5 227 mg/L) impropre à la consommation humaine. Toutefois, il n'a pas été colmaté et nous avons pu l'échantillonner. Il est important de préciser que l'échantillon UQAC1105 ne fait pas partie de la grappe 3.

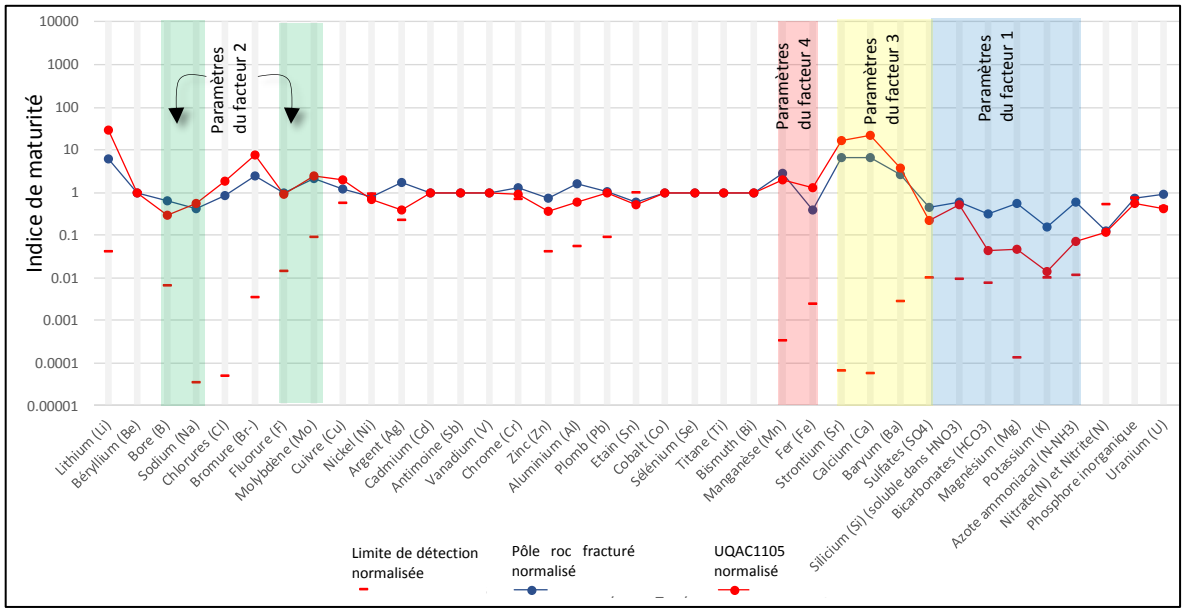

Figure 5.6: Spectres multiéléments du pôle compositionnel régional de l'évolution de l'eau souterraine en milieu rocheux fracturé et de l'échantillon UQAC1105 tous deux normalisés au pôle compositionnel régional de l'évolution de l'eau souterraine en milieu granulaire poreux confiné par l'argile marine. Les paramètres chimiques constituant les facteurs obtenus de l'analyse factorielle réalisée sur le jeu de données réduit sont aussi identifiés sur la figure.

La correspondance de la forme des spectres est frappante. Les indices de maturité suivent généralement la même tendance pour l'échantillon et pour le pôle régional de l'évolution de l'eau souterraine en milieu rocheux fracturé. La similitude des spectres multiéléments (Figure 5.6) suggère ainsi que la composition chimique de l'échantillon UQAC1105 s'apparente à celle du pôle régional de l'évolution de l'eau souterraine en milieu rocheux fracturé, et aussi, que la chimie de l'échantillon UQAC1105 est a priori plus mature et/ou moins diluée que le pôle hydrogéochimique régional des milieux rocheux fracturés dont la composition a été déterminée dans cette étude. Rappelons que, d'après le modèle proposé pour décrire l'évolution géochimique de l'eau souterraine (Figure 4.9), les bromures, les chlorures et le lithium constituent des traceurs intrinsèques de l'évolution naturelle de l'eau souterraine en milieu cristallin fracturé précambrien. Dans notre exemple (figure 5.6), les indices de maturité des bromures, des chlorures et du lithium sont plus grands pour l'échantillon UQAC1105 que pour le pôle hydrogéochimique régional des milieux rocheux fracturés. Cette observation renforce l'idée que la chimie de l'échantillon UQAC1105 est a priori plus mature et/ou moins diluée que notre pôle compositionnel hydrogéochimique régional des milieux rocheux fracturés.

5.4 PORTÉE DES RÉSULTATS

5.4.1 VARIABILITÉ SPATIALE ET TEMPORELLE

Les résultats présentés dans cette thèse permettent d'abord de définir un état de la situation en ce qui concerne les mécanismes d'acquisition de la qualité de l'eau

souterraine du territoire d'étude, et permet ensuite de discuter la variabilité spatiale et temporelle de la qualité naturelle de l'eau souterraine. Nous savons que cette qualité tend généralement à évoluer dans l'espace et dans le temps. À l'image de l'exemple présenté plus haut avec l'échantillon UQAC1105, la connaissance du détail de l'évolution géochimique de l'eau souterraine, rend possible la détermination d'un contexte hydrogéologique particulier à partir d'une analyse chimique inorganique de l'eau souterraine prélevée aléatoirement sur le territoire à l'occasion de tous projets impliquant une analyse chimique de l'eau souterraine (recherche en eau, projets de recherche universitaires aux objectifs et aux finalités diverses, …). La chimie de l'eau souterraine renseigne alors, non seulement sur la potabilité, mais aussi, de manière qualitative, sur la dynamique du milieu aquifère. Cette dynamique comprend les caractéristiques physiques et son écoulement (temps de transit), et les éventuels courts-circuits hydrauliques anthropiques ou naturels décrits localement entre les différentes nappes (Chesnaux et Elliott, 2011; Richard et al., 2014). Ces informations ne pourront évidemment être connues quantitativement qu'à la faveur d'essais hydrauliques réalisés sur le terrain. Nous pensons que les interprétations de ces tests seront bonifiées en les combinant avec des interprétations des variations de la qualité de l'eau souterraine prélevée à différents pas de temps au cours de ces essais hydrauliques.

Finalement, en ajoutant une dimension cinétique aux mécanismes que nous proposons dans notre étude pour expliquer l'évolution géochimique de l'eau souterraine dans la région, nous pensons qu'il serait alors possible, connaissant le mécanisme

dominant qui s'applique, de prédire la dégradation éventuelle de la qualité d'une eau souterraine prélevée sur le territoire. Ce point est abordé plus spécifiquement à la section 5.6.2 portant sur la modélisation hydrogéochimique.

5.4.2 NOUVEAUX CHAMPS D'INTERPRÉTATION GRAPHIQUE

En déterminant des pôles hydrogéochimiques régionaux, nous donnons une nouvelle dimension à l'ensemble des diagrammes communément utilisés en hydrogéochimie. Un bon exemple est donné à la figure 5.7. Cette figure se rapproche de celle présentée au chapitre 3 (Figure 3.9), à la différence que les grappes présentées sur cette figure (Cluster 1 à 4) correspondent à ceux qui ont été identifiés à l'aide du jeu de données réduit (pôles hydrogéochimiques régionaux), présentés au chapitre 4 de cette thèse. Les autres échantillons de cette étude sont aussi représentés. L'axe vertical correspond à la teneur en calcium et l'axe horizontal correspond à la teneur en sodium, exprimées en mmol/L. Ces deux éléments chimiques sont les plus communément analysés dans l'eau souterraine, ce qui en fait des éléments « usuels » pour l'étude de la qualité de l'eau souterraine. Ils constituent les deux cations majeurs dominants permettant de définir le faciès chimique de l'eau. La ligne pointillée d'équation $y = x$, permet de départager les échantillons dont la composition molaire est dominée par le calcium ($y > x$), et les échantillons dont la composition molaire est dominée par le sodium ($x > y$). Sur la figure 5.7, nous avons aussi placé le pôle compositionnel de l'eau de mer, ce qui nous permet de tracer une droite de dilution théorique de l'eau de mer. Les trajets d'évolution

vers les pôles chlorurés (trajet d'évolution 1 et 2; Figure 5.7) sont déterminés en reliant les grappes 1 et 2 (eaux de recharge) et les pôles hydrogéochimiques régionaux évolués (Grappe 3 et 4).

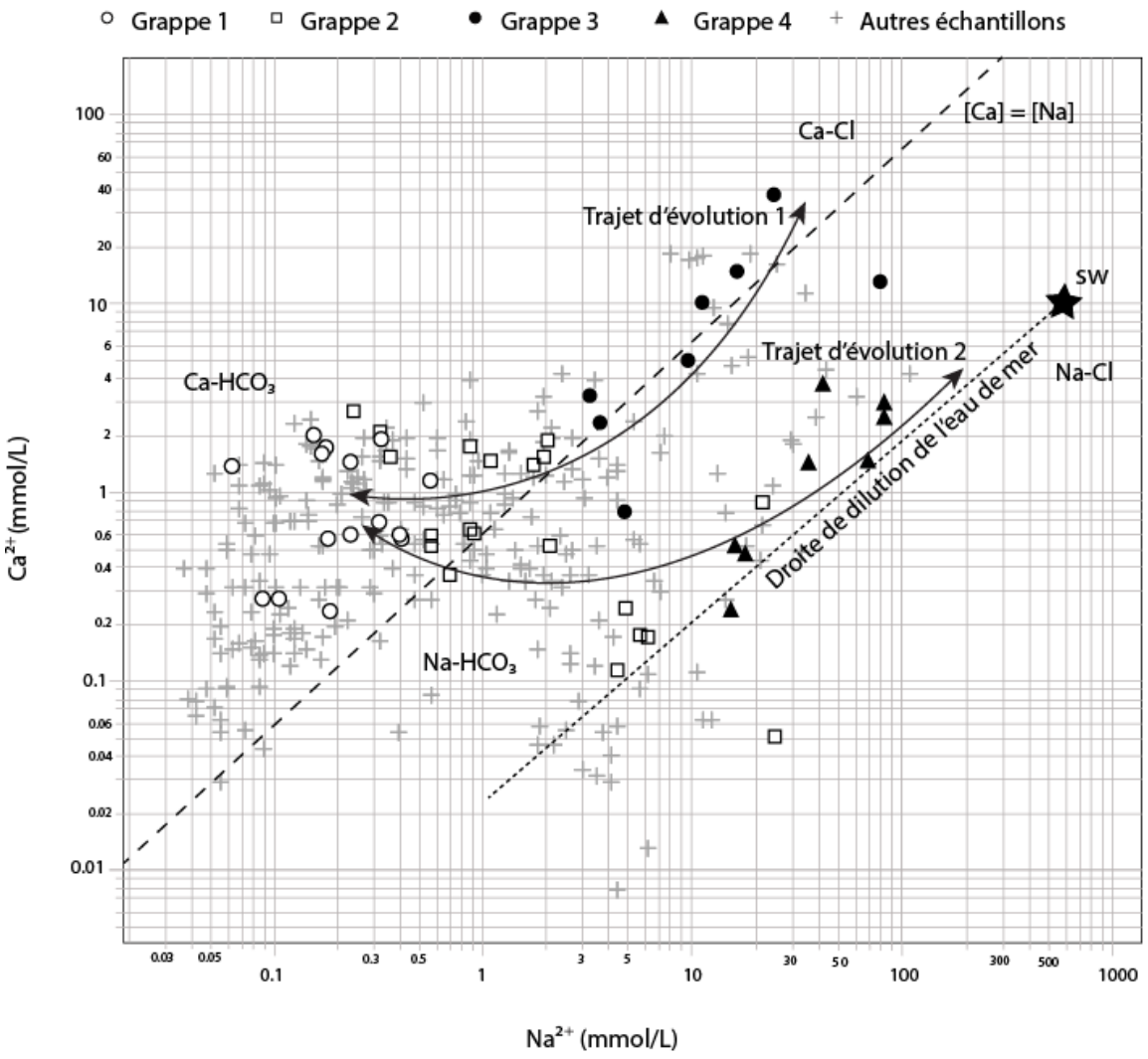

Figure 5.7 : Interprétation de la dynamique des eaux souterraines à partir de nouveaux champs graphiques définis par la connaissance des mécanismes d'interaction eau-roche des pôles hydrogéochimiques régionaux.

Les trajets d'évolution du contenu en calcium et en sodium définissent de nouveaux champs à l'intérieur de ce graphique qui peuvent être comparés à celui de la droite de dilution de l'eau de mer. Ces champs serviront à poser très rapidement une première série d'hypothèses quant à l'origine probable de la chimie des autres échantillons considérés. En effet, parmi les échantillons de cette étude qui ne sont pas inclus dans les groupes d'échantillons constituant les pôles, certains suivent le trajet d'évolution de l'eau en interaction avec les milieux rocheux fracturés (trajet d'évolution 1), et d'autres suivent la droite de dilution de l'eau de mer, marquée notamment par les échantillons de la grappe 4, correspondant au pôle de l'eau souterraine tirant en partie sa chimie des milieux granulaires poreux confinés par l'argile marine. Finalement, d'autres échantillons occupent des positions intermédiaires entre les pôles et les nouveaux champs définis par les trajets d'évolution, suggérant des phénomènes de mélange entre ces pôles.

Ainsi, un graphique « usuel » devient un outil pratique en appui à l'élaboration d'une série d'hypothèses visant la connaissance de la dynamique des milieux aquifères du territoire à l'étude. Un autre exemple du même type aurait pu être donné avec le diagramme de Piper, des diagrammes ternaires, ainsi que d'autres graphiques binaires. L'ensemble de ces hypothèses du fonctionnement hydrogéochimique, et dans une certaine mesure hydraulique, constituent les prémices d'études spécifiques d'échelle locale. Nous comprenons aussi qu'en augmentant la connaissance des pôles hydrogéochimiques régionaux, en termes de chimie et de leur correspondance avec un

type de réservoir en particulier, le nombre de champs disponibles pour l'interprétation graphique est augmenté.

5.4.3 CONTEXTES NATURELS FAVORABLES AU FLUOR

Bien que nous n'ayons pu identifier clairement la source des fluorures dans l'eau souterraine de la région, notre étude a permis de montrer que certains contextes hydrogéologiques naturels sont favorables à leur présence. En premier lieu, l'étude statistique univariée réalisée sur les quatre groupes d'eau souterraine formés d'après le type d'eau (Cl^- ou HCO_3^-) et le milieu aquifère d'où provient l'échantillon (Roc fracturé ou granulaire poreux) (Figure 5.4; étape 1; Annexe 4) montre que les concentrations médianes en fluor sont les plus élevées dans les eaux souterraines au faciès chloruré (Groupe 2 et 4). Ces groupes présentent aussi les valeurs les plus élevées pour le 75^e centile. Ces populations statistiques sont les moins populeuses ($N_{granulaire\text{-}Cl}$ = 19; $N_{roc\text{-}Cl}$ = 46), et il est possible que cette observation atteste d'un biais statistique plutôt que du lien entre le faciès de l'eau et la présence de fluor. Toutefois, le groupe d'échantillons d'eau souterraine bicarbonatée prélevée dans le socle rocheux fracturé (Groupe 3) présente une valeur de 75^e centile qui se rapproche de celle des groupes d'eau au faciès chloruré. Dans ce cas, la population statistique est considérée significative (N = 124). Ces observations suggèrent que les eaux salées de la région présentent généralement des teneurs en fluor supérieures aux eaux fraîches et de plus, qu'une source potentielle du fluor serait constituée de certains minéraux présents dans le socle rocheux fracturé. Ces observations

sont corroborées par l'observation de la figure 4.3, dans laquelle sont présentées les fréquences de détection des ions analysés. En effet, le plus grand nombre de détection des ions fluorures est enregistré dans le groupe d'eau chlorurée prélevée dans le socle rocheux fracturé (Groupe 4; $\%N_{detecté}$ = 96%), suivi du groupe d'eau bicarbonatée prélevée dans le socle rocheux fracturé (Groupe 3; $\%N_{detecté}$ = 90%). Pour l'eau souterraine des dépôts granulaires poreux, de type bicarbonaté et chloruré, la fréquence de détection du fluor se situe autour de 50%. Nous savons que la fréquence de détection est directement liée à la limite de détection du paramètre considéré, et donc, ne représente pas une grandeur physique. Elle est plutôt prise comme une probabilité d'occurrence d'un paramètre donné en fonction d'une valeur seuil, dans ce cas, la limite de détection. Dans notre étude, cette limite est fixée à 0.1 mg/L pour le fluor. Ainsi, de manière générale, nous pouvons dire que, dans notre étude, l'eau souterraine contenue dans le socle rocheux fracturé, de type chlorurée ou bicarbonatée, présente une probabilité d'occurrence du fluor largement supérieure à celle de l'eau souterraine prélevée dans les dépôts granulaires poreux, de type salée ou bicarbonatée.

Les résultats de l'analyse statistique multivariée (analyse factorielle) réalisée sur le jeu de données réduit montrent que les fluorures sont généralement corrélés au sodium, au bore et au molybdène (Facteur 4.2). Un survol de la littérature nous a permis d'investiguer en partie les sources potentielles de cette combinaison de paramètres chimiques. Premièrement, les résultats de tests expérimentaux de type « *batch* » réalisés avec des roches cristallines apparentées à celles présentes sur le territoire d'étude

suggèrent que le fluor est libéré dans l'eau lors de l'altération des micas (biotite) (Chae et al., 2006). Deuxièmement, la corrélation du sodium et du bore suggère que le fluor peut avoir une origine marine, et troisièmement, la combinaison du bore et du molybdène suggère l'influence d'hydrocarbures (Walter et al., soumis). La présence d'hydrocarbure est un fait avéré dans la région et pourrait donc expliquer en partie la présence de fluor dans l'eau souterraine. C'est pourquoi nous avons réalisé des tests expérimentaux dont les résultats préliminaires sont présentés sommairement ici, mais qui, nous l'espérons, avec quelques tests additionnels, feront l'objet d'une publication scientifique dans un avenir rapproché.

Les tests qui ont été réalisés à l'UQAC consistent en la percolation d'une eau déionisée à travers une colonne composée de fragments millimétriques (*cutting* de forage lavés et tamisés) de roches sédimentaires paléozoïques (mélange de shale et de calcaire). Le montage expérimental est présenté à la figure 5.8. Le système fonctionne en boucle ouverte, l'eau ne circule donc qu'une seule fois à travers la colonne de roche. Une charge constante est appliquée à l'aide d'un syphon de Marriotte d'une capacité de 5L. Le débit est contrôlé par une valve mécanique et mesuré par une balance à grande précision, sur laquelle est posée un erlenmeyer permettant de récupérer l'eau après circulation. Connaissant la masse volumique moyenne du fluide, la différence de poids en fonction du temps est convertie en débit. Le débit le plus faible que nous avons pu atteindre aura été d'environ 3 mL/heure. Les expériences ont été réalisées à température ambiante, soit en moyenne 22°C. Les essais ont débuté le 23 novembre 2015. Au total, 5 échantillons ont

été prélevés et ont été analysés par le même laboratoire, et selon les mêmes méthodes analytiques, que les échantillons qui font l'objet de ce projet de doctorat. Les résultats obtenus sont présentés au tableau 5.1 pour les quatre paramètres chimiques qui composent le facteur 2 (sodium, bore, molybdène et fluor).

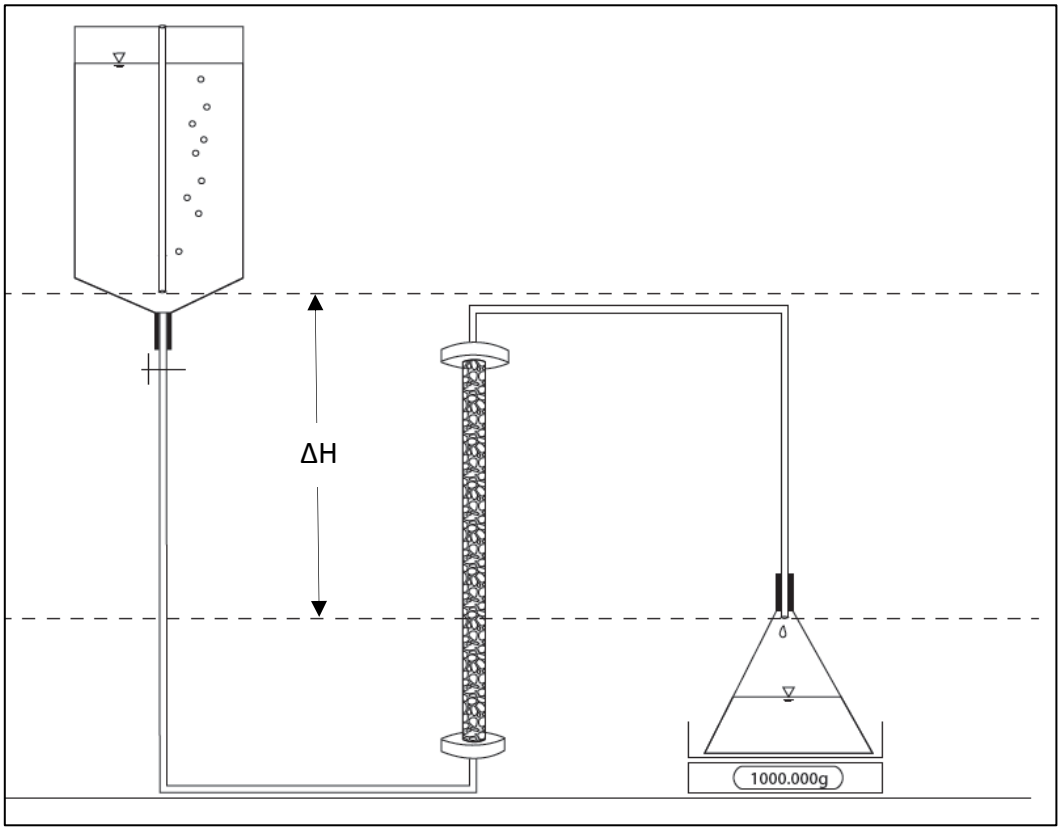

Figure 5.8 : Schéma du montage expérimental d'essais préliminaires d'interaction eau-roche sédimentaire paléozoïque en colonne

Tableau 5.1 : Résultats en mg/L des essais préliminaires d'interaction eau-roche sédimentaire paléozoïque en colonne pour les 4 paramètres du facteur 2 obtenus par analyse factorielle (Walter et al., soumis)

	Sodium (Na)	Bore (B)	Fluorure (F)	Molybdène (Mo)
COL001-30NOV2015	45.00	0.93	0.70	0.25
COL002-17DEC2015	15.00	0.84	1.20	0.26
COL003-5JAN2016	11.00	0.97	1.10	0.29
COL004-7JANV2016	7.00	0.67	1.30	0.20
COL005-8JANV2016	2.90	0.34	1.60	0.04

Les résultats obtenus montrent un enrichissement général en fluor au fur et à mesure de l'expérimentation. Après 7 jours d'expérimentation, soit le 30 novembre 2015, le taux de fluor dans l'eau déionisée est de l'ordre de 1 mg/L et finit légèrement au-dessus de la limite de potabilité fixée à 1,5 mg/L après 39 jours d'expérimentation (Échantillon Col005-8JAN2016 : 1.6 mg/L de fluor). Cette tendance à l'augmentation semble être suivie par le molybdène, dont la teneur passe de 0.25 mg/L après 7 jours d'expérimentation à 0.29 mg/L après 36 jours. Considérant la limite de détection du molybdène fixée à 0.001 mg/L, cette variation de 0.04 mg/L est peut-être à l'intérieur des limites analytiques, néanmoins, nous pouvons affirmer que l'eau s'est enrichie en molybdène et que sa concentration est restée relativement stable jusqu'au 38^{e} jour de l'essai expérimental, soit le 7 janvier 2016. À l'inverse, les teneurs en sodium et en bore tendent à diminuer avec le temps. Entre le 7^{e} jour et le 39^{e} jour d'expérimentation, la teneur en sodium passe de 45 mg/L à 2.9 mg/L, et celle du bore passe de 0.93 mg/L à 0.34 mg/L. Ces résultats, bien que préliminaires, ne contredisent pas certaines hypothèses tirées de l'étude statistique

présentée dans cette thèse, à savoir que les roches fracturées paléozoïques peuvent constituer localement une source de fluor.

À la lumière de l'ensemble des résultats obtenus dans le cadre de cette thèse, nous pensons qu'une « combinaison gagnante » pour trouver du fluor en solution dans l'eau souterraine est constituée, d'une part, d'un assemblage stratigraphique comprenant le socle cristallin granitique précambrien recouvert d'une épaisse couche d'argile d'origine marine, et d'autre part, des dépôts calcaires paléozoïques confinés par l'argile marine. Dans les deux cas, l'argile joue le rôle d'échangeur cationique grâce auquel le sodium est libéré dans l'eau en échange du calcium, qui se trouve alors fixé sur l'échangeur. Ce mécanisme permet d'appauvrir l'eau en calcium et d'abaisser ainsi le taux de solubilité de la fluorite (Ca_2F), ce qui aura pour effet la libération du fluor, si ce dernier est présent dans l'environnement considéré (roches cristallines ou sédimentaires). Ce phénomène d'échange cationique est décrit dans les basses terres du Saint-Laurent (Cloutier et al., 2010) ou encore dans la région de l'Outaouais (Montcoudiol et al., 2015) pour expliquer la présence du fluor dans l'eau dans des environnements similaires aux nôtres

Finalement, nous savons aussi que les argiles sensibles de la région contiennent une importante quantité d'eau interstitielle salée (Bouchard et al., 1993), datant de l'invasion de la mer Laflamme dans les basses terres de la région, il y a 10 000 ans. Considérant une teneur moyenne en fluor de 1.3 mg/L de l'eau de mer (Goldberg, 1971), les eaux interstitielles des argiles marines pourraient constituer une autre source

expliquant la présence du fluor dans les eaux souterraines de la région. Aucune analyse du fluor dans les eaux interstitielles des argiles n'a été réalisée à ce jour. L'ensemble de ces hypothèses (mécanismes d'interaction eau-roche cristalline; interaction eau-roche sédimentaire; lessivage de l'eau interstitielle des argiles) mériterait certainement d'être investigué dans le cadre d'une ou plusieurs études spécifiques visant à mieux contraindre la source du fluor dans l'eau souterraine de la région.

5.5 TRAVAUX DE RECHERCHE COMPLÉMENTAIRES

5.5.1 ÉTUDES MINÉRALOGIQUES

Pour Blum et al (2003), afin d'identifier des processus et/ou définir l'origine d'un élément, des analyses complémentaires au traitement statistique des données géochimiques peuvent s'avérer utiles, notamment sur la matrice rocheuse (encaissant). Dans le cadre de ce projet doctoral, la connaissance de la composition chimique des milieux réservoirs manque cruellement. Nous pensons cependant qu'elle est indispensable pour valider certaines de nos observations. Dans une étude récente, Adiaffi et al. (2012) ont utilisé la géochimie des roches et des eaux pour estimer l'apport en concentration molaire des minéraux constitutifs des aquifères schisteux à la nappe d'eau souterraine en zone équatoriale. Ils obtiennent la chimie des schistes par analyses sur roche totale. Par la suite, les auteurs réalisent l'étude des minéraux en débutant par une observation au Microscope Électronique à Balayage (MEB) et poursuivent par une analyse des minéraux par Diffraction aux Rayons X (DRX), permettant, dans leur cas, une

estimation semi-quantitative de l'assemblage minéralogique. Pour les auteurs, la conjugaison des trois méthodes d'analyse des schistes permet d'obtenir des résultats semi-quantitatifs très fiables. Dans le même ordre d'idée, le modèle géochimique d'acquisition de la minéralisation de l'eau souterraine contenue dans un aquifère du sud-ouest français, proposé par Malcuit (2012), a été construit en se basant sur la géochimie des eaux et la minéralogie des formations géologiques. Ses résultats reposent sur des analyses géochimiques et isotopiques, l'observation d'échantillons solides notamment sous forme de fragments de rejets de forage (*cuttings*), et des analyses minéralogiques (DRX – MEB). Dans le cadre du PACES-SLSJ, 3 forages ont permis la récupération de fragments de rejets de forage de roches cristallines, de même que de roches sédimentaires. De nouvelles études devraient donc porter sur l'identification d'assemblages minéralogiques propres à la région à partir de lames minces et d'un microscope à lumière transmise. Ces études bénéficieraient certainement de l'utilisation de techniques plus sophistiquées, telle que le MEB, sachant qu'un fournisseur de ce service est disponible en région.

5.5.2 MODÉLISATION HYDROGÉOCHIMIQUE

En connaissant la composition de l'eau d'infiltration et considérant une composition chimique et une minéralogie connues des milieux réservoirs régionaux, l'interaction entre la roche et l'eau pourrait être modélisée. La comparaison des résultats obtenus à l'aide de la modélisation et des résultats d'analyses chimiques d'eaux

souterraines contenues dans des granites a déjà montré une bonne correspondance lors d'études précédentes (Zuddas et al., 1995 ; Bruno et al., 2002). Ce type de modélisation se base sur les principes introduits par Helgeson (1968) qui interprète à l'aide des principes thermodynamiques l'approche par bilan de masse introduite initialement par Garrels et MacKenzy (1967). Helgeson (1968) montre que des états d'équilibres partiels successifs sont obtenus préalablement à l'état d'équilibre général. Ainsi, il est théoriquement possible de prévoir la composition chimique d'une eau souterraine à l'équilibre si l'assemblage minéral, le produit de solubilité (K_s) de chaque minéral et enfin la température et la pression sont connus (Zhu et Anderson, 2002 ; Federico et al., 2008; Sung et al., 2012). L'approche novatrice d'Helgeson et ses collègues a aussi permis de définir un cadre cinétique aux études subséquentes. Ainsi, Lasaga (1981, 1984) et Aagaard et Helgeson (1982) intègrent le facteur temps pour contraindre l'évolution et le devenir des systèmes géochimiques. En ajoutant la notion de cinétique chimique aux résultats de spéciation chimique et aux calculs d'indices de saturation pour une température et une pression données, les processus naturels peuvent être modélisés sous la forme de trajets de réaction (Zhu, 2009). Ce point est particulièrement intéressant pour prédire l'évolution temporelle d'un système géochimique, dès lors que les mécanismes d'interactions dominants sont connus. Ces modèles sont connus pour représenter une image simplifiée de la réalité des contextes hydrogéologiques présentant un écoulement lent et un temps de résidence long de l'eau souterraine (Sung et al., 2012). C'est pourquoi nous pensons que pour tenter de représenter plus fidèlement la réalité, l'utilisation de modèles couplés

de transport de masses réactives devrait être considérée. Les principaux processus impliqués dans le transport en milieux poreux et/ou fracturé sont l'advection, la dispersion mécanique, la diffusion moléculaire, et les réactions fluides-solides (dissolution et cristallisation) (Freeze et Cherry, 1979; Schott et al. 2009). Toutefois, l'application de tels modèles requiert une multitude de données de terrain et beaucoup de temps pour distiller l'information pertinente obtenue par modélisation numérique à l'aide d'algorithmes spécialisés (Zhu, 2009). À titre d'exemple, mentionnons les travaux significatifs de modélisation régionale réalisés par Montcoudiol et al. (2017) dans la région de l'Outaouais au Québec. Les auteurs proposent un modèle numérique d'écoulement et de transport vertical en deux dimensions afin de valider un modèle conceptuel d'évolution géochimique d'échelle régionale. Ce modèle a été réalisé à l'aide du logiciel de simulation numérique par éléments finis FLONET-TR2 (Molson and Frind, 2010). La calibration du modèle d'écoulement régional est basée sur les données de piézométrie et complétée par des teneurs en tritium, ainsi qu'en chlorures. Cette étude a permis de calibrer la zone active d'écoulement du modèle à une profondeur d'environ 100–150 m, au-delà de laquelle les auteurs n'identifient plus d'écoulement. Le modèle conceptuel d'écoulement préliminaire est dans ce cas bien supporté par les simulations numériques.

5.5.3 MONTAGES EXPÉRIMENTAUX

Durant les deux dernières décennies, des efforts importants ont été réalisés pour d'une part mesurer les constantes de dissolution/cristallisation en laboratoire, et d'autre

part pour développer des équations décrivant les constantes de réaction en vue de les intégrer aux algorithmes numériques utilisés par les géochimistes (Schott et al., 2009). Des essais expérimentaux de mise en solution à partir d'échantillons des matériaux géologiques de la région devraient donc permettre de tester les hypothèses de l'origine de certains traceurs géochimiques présentés dans cette étude de doctorat, et de déterminer les paramètres quantitatifs de leur mise en solution dans l'eau souterraine. Les constantes de dissolution mesurées expérimentalement en laboratoire n'impliquent généralement qu'un minéral et les réactions à la base de leur détermination sont relativement simples (Taylor et al., 2000). Dans le cadre de ce projet doctoral, un dispositif expérimental d'autoclave présentant une cellule d'écoulement à pression, température et débit variables (*Système d'hydrothermalisme expérimental; SHE)* a été testé sur des fragments de roches anorthositiques et de roches sédimentaires paléozoïques. Cette technique implique la collecte régulière, à des fins d'analyse chimique, des fluides ayant réagi avec l'échantillon solide, ainsi qu'un suivi continu, pendant l'expérimentation, des paramètres physico-chimiques de l'eau (Eh, pH, température, conductivité électrique-matière dissoute totale, oxygène dissous, pression partielle de CO_2) (Gobeil, 2013). La durée des expérimentations a varié d'une semaine à plusieurs dizaines de jours. Les tests ont été réalisés à des températures variant de 100°C à 130°C, et à une pression variant de 1000 à 2000 psi. Malheureusement, les expérimentations sont restées au stade de test étant donné le manque de temps du personnel hautement qualifié indispensable pour réaliser les manipulations techniques du *SHE*, et le trop grand degré d'incertitude quant aux

résultats préliminaires obtenus (Gobeil, 2013). Par contre, des expériences préliminaires en colonne à des conditions de pression et de température ambiantes ont été menées avec des échantillons de roches sédimentaires paléozoïques et montrent un enrichissement en fluor après 7 jours d'interaction. Une partie des résultats préliminaires a été présentée à la section 5.5.3).

5.5.4 ANALYSES ISOTOPIQUES

Les rapports isotopiques n'ont pas été utilisés dans le cadre de ce projet doctoral, et pourtant, il en aurait certainement bénéficié. L'étude de Clark et *al.* (2000) a notamment permis de définir 3 pôles hydrogéochimiques d'après leurs teneurs en chlorures et en ^{18}O. De plus, Walter (2010) a montré à l'aide des isotopes stables de l'eau (^{18}O et ^{2}H) que certains échantillons d'eau souterraine salée, collectés au SLSJ, présentent une signature se rapprochant de celles de saumures du Bouclier Canadien. Avec l'accessibilité toujours croissante aux techniques d'analyses isotopiques, des études complémentaires à ce projet doctoral devraient considérer leur utilisation. En plus des isotopes stables de l'eau, l'étude des isotopes du bore pourrait permettre de trancher sur l'origine marine, ou autre, de cet élément chimique (Chapitre 4). De la même manière, nous proposons dans notre étude qu'une partie des sulfates mesurés dans l'eau souterraine possède une origine marine, ce qui pourrait être investigué à l'aide des isotopes du soufre. De plus, les analyses isotopiques d'eau pourraient être réalisées sur les

fluides des montages expérimentaux d'interaction eau-roche, de manière à pouvoir alimenter les discussions des résultats obtenus sur des échantillons prélevés sur le terrain.

5.5.5 PROJET D'ENVERGURE

Grâce aux connaissances acquises dans le cadre de ce projet de doctorat, nous sommes aujourd'hui en mesure de proposer un projet d'envergure qui intègre la globalité des étapes visant la connaissance de la dynamique hydrogéochimique d'un territoire. Nous comprenons aussi que les résultats présentés dans cette thèse, et les moyens employés pour les obtenir, ne constituent que les premières étapes d'un tel projet d'envergure. Nous sommes pleinement conscients que cette thèse ne permet pas de déterminer de manière quantitative les interactions eau-roche proposées, et pourtant, si nous voulons connaître l'évolution spatiale et temporelle de la qualité de l'eau souterraine, c'est justement en quantifiant les divers aspects de cette évolution que nous y arriverons. Pour ce faire, nous avons besoin d'atteindre trois objectifs:

1. ***Résumer et compléter la connaissance de la composition chimique des roches régionales;***
2. ***Réaliser des expériences d'interaction eau-roche en laboratoire, en colonne et à l'aide du système d'hydrothermalisme expérimental (SHE);***
3. ***Simuler numériquement (avec la thermodynamique et la cinétique) cette évolution considérant les données acquises et leur interprétation sous la forme de modèles conceptuels.***

La figure 5.9 présente les principales étapes méthodologiques d'un tel projet d'envergure. L'étape 1 consiste en l'analyse statistique multivariée des données disponibles à l'échelle régionale, dans le but de définir des pôles hydrogéochimiques tirés des données disponibles (Étape 2; Figure 5.9). Les résultats sont discutés et présentés sous forme de différents graphiques afin de discuter des phénomènes de mélanges ou autres mécanismes de dilution/concentration ayant court sur le territoire (Étape 3; Figure 5.9). Ces trois premières étapes ont donc été réalisées dans le cadre de ce projet de doctorat et font l'objet de cette thèse. L'étape 4 se rapporte aux essais expérimentaux réalisés à l'aide du système d'hydrothermalisme expérimental (SHE) disponible à l'UQAC, ainsi que des essais en colonne gravitaires à l'image de ceux réalisés de manière préliminaire dans le cadre de ce projet (Section 5.5.3). Ces essais impliquent la collecte d'échantillons de roche, l'examen de lame mince, l'analyse chimique de roches et de minéraux, et des analyses d'eaux extraites des montages expérimentaux (Figure 5.9). En plus de l'étude des ratio isotopiques (section 5.6.4), les résultats des montages expérimentaux permettront d'identifier des traceurs géochimiques d'interaction eau – roche pouvant servir de paramètres normatifs, ou de pôles théoriques de l'interaction eau-roche venant en appui au traitement graphique, à l'image de la méthodologie présentée au chapitre 4 de cette thèse. De plus, les résultats et le paramétrage des essais avec le SHE pourront servir de paramètres d'entrée et de calage des modèles géochimiques (étape 5 – Figure 5.9). En faisant évoluer la chimie de l'eau d'infiltration (eau de pluie, eau de mer et eau sous-glaciaire) au contact des divers assemblages minéralogiques constituant les principaux

réservoirs régionaux, la modélisation géochimique a pour but d'établir une composition chimique théorique de pôles hydrogéochimiques régionaux évolués pour certains paramètres chimiques, principalement les éléments majeurs. Ainsi, les groupes d'échantillons obtenus lors de l'analyse statistique (étape 1 – figure 5.9) peuvent être décrits en termes de degré d'avancement des réactions chimiques du modèle, ou de mélanges entre les pôles compositionnels théoriques. Comme le montre la figure 5.9, les résultats des travaux de modélisation complètent les résultats des autres étapes. La cinquième étape intègre les notions fondamentales d'écoulement aux réactions cinétiques pour expliquer la chimie des eaux souterraines (étape 6 – figure 5.9). Pour ce faire, les modèles géochimiques intégrant le transport de masses réactives devront être alimentés par des essais hydrauliques, des levés piézométriques, et l'échantillonnage multi-niveaux de l'eau souterraine. De tels modèles ne sont envisageables que sur de petites portions du territoire à l'étude, là où les informations présenteront une quantité suffisante et une répartition relativement homogène. Finalement, toutes ces étapes convergent vers la spatialisation des résultats qui permettra d'interpréter localement la dynamique des contextes hydrogéochimiques.

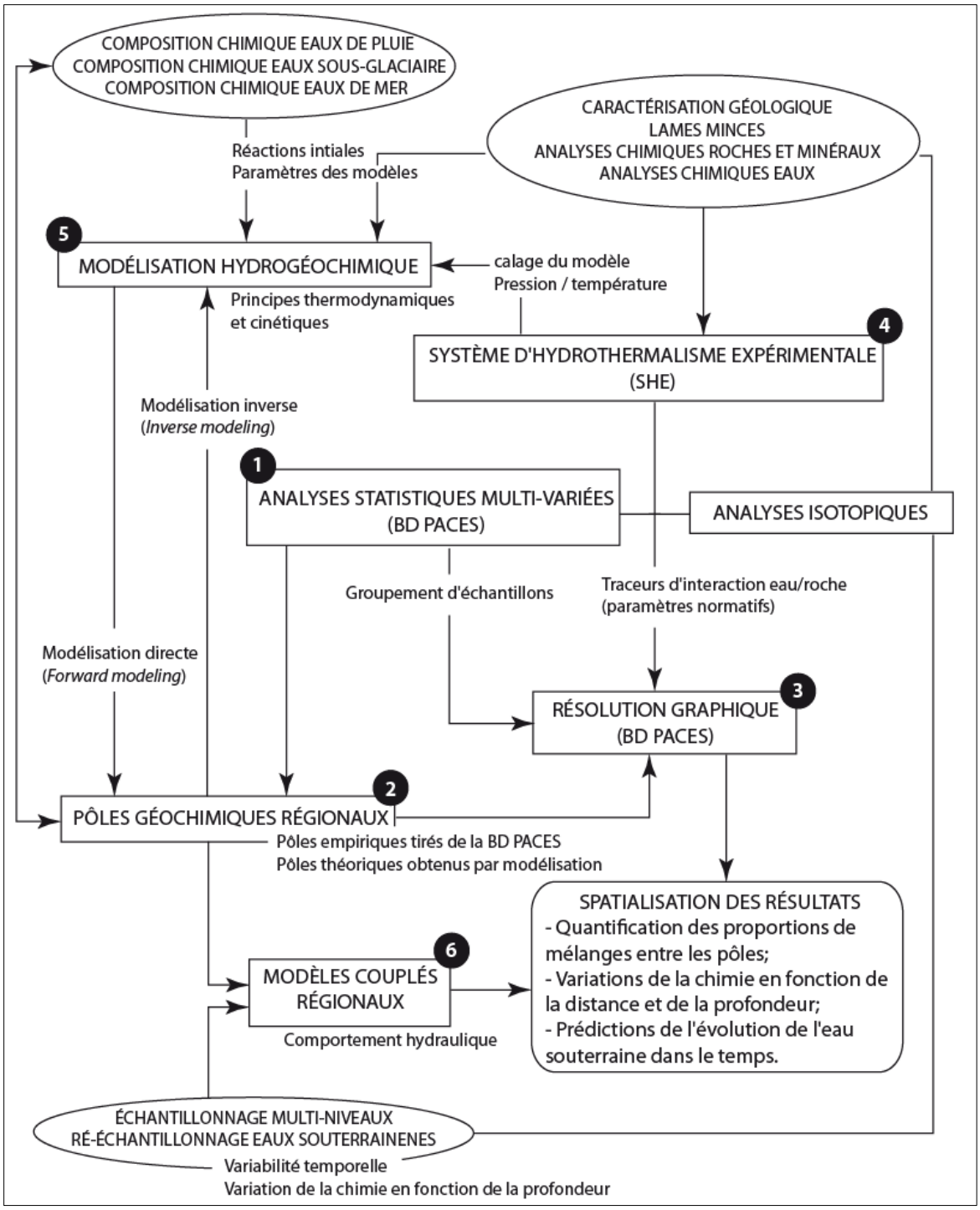

Figure 5.9 : Principales étapes méthodologiques d'un projet d'envergure visant la connaissance de la dynamique hydrogéochimique d'un territoire. Les numéros réfèrent à une proposition de la séquence chronologique de réalisation des étapes. À noter que les étapes 1 à 3 ont été réalisées dans le cadre de cette thèse de doctorat et que l'étape 4 a fait l'objet de tests préliminaires.

5.6 RÉFÉRENCES

Alvin, C.R., 2002. Methods of multivariate analysis. Wiley Interscience.

Aagaard, P., and Helgeson, H. C.; 1982. *Thermodynamic and kinetic constraints on reaction rates among minerals and aqueous solutions I, Theoretical considerations*: American journal of Science, v. 282, no. 3, p. 237-285.

Adiaffi, B., Marlin, C., Oga, Y. M. S., Pichon, R., and Biemi, J.; 2012. *Approche semi-quantitative de la minéralisation des aquifères schisteux en zone Équatoriale de transition: Cas de la région Sikensi-Agboville (Côte d'Ivoire)*: International Journal of Biological and Chemical Sciences, v. 6, no. 5, p. 2228-2240.

Blum, A., Chery, L., Barbier, J., Baudry, D., and Petelet-giraud, E.; 2003. *Le fonds géochimique naturel des eaux souterraines. État des connaissances et méthodologie*: La Houille Blanche, no. 2, p. 120-124.

Bouchard, R., Dion, D. J., and Tavenas, F.; 1983. *Origine de la préconsolidation des argiles du Saguenay, Québec*: Canadian Geotechnical Journal, v. 20, no. 2, p. 315-328.

Bruno, J., Duro, L., and Grivé, M.; 2002. *The applicability and limitations of thermodynamic geochemical models to simulate trace element behaviour in natural waters. Lessons learned from natural analogue studies*: Chemical Geology, v. 190, no. 1, p. 371-393.

Chae, G.-T., Yun, S.-T., Kwon, M.-J., Kim, Y.-S. and Mayer, B. 2006. "Batch dissolution of granite and biotite in water: Implication for fluorine geochemistry in groundwater," *Geochemical Journal*, Vol. 40, No. 1, pp. 95–102.

Chebotarev; 1955. Metamorphism of natural waters in the crust of weathering 1-2-3: Geochimica et Cosmochimica Acta, v. 8, no. 1, p. 22-48.

Chesnaux, R., and A.-P. Elliott. 2011. Demonstrating evidence of hydraulic connections between granular aquifers and fractured rock aquifers. (In Proceedings of GeoHydro 2011, Joint Meeting of the Canadian Quaternary Association and the Canadian Chapter of the International Association of Hydrogeologists, August 28–31, 2011, Quebec City, 8 pp).

Chesnaux, R., M. Lambert, J. Walter, V. Dugrain, A. Rouleau, and R. Daigneault. 2017. A simplified geographical information system (GIS)-based methodology for modeling the topography of bedrock: Illustration using the Canadian Shield. Journal of Applied Geomatics, DOI 10.1007/s12518-017-0183-1.

Clark, I. D., Douglas, M., Raven, K., and Bottomley, D.; 2000. Recharge and preservation of Laurentide glacial melt water in the Canadian Shield: Groundwater, v. 38, no. 5, p. 735-742.

Cloutier, V., Lefebvre, R., Savard, M.M., Therrien, R., 2010. Desalination of a sedimentary rock aquifer system invaded by Pleistocene Champlain Sea water and processes controlling groundwater geochemistry. Environmental Earth Sciences, 59(5): 977-994.

Farnham, I. M., Johannesson, K. H., Singh, A. K., Hodge, V. F. and Stetzenbach, K. J.; "Factor analytical approaches for evaluating groundwater trace element chemistry data," Analytica Chimica Acta, Vol. 490, No. 1-2, pp. 123–138. 2003.

Federico, C., Pizzino, L., Cinti, D., De Gregorio, S., Favara, R., Galli, G., Giudice, G., Gurrieri, S., Quattrocchi, F., and Voltattorni, N.; 2008. *Inverse and forward modelling of groundwater circulation in a seismically active area (Monferrato, Piedmont, NW Italy): Insights into stress-induced variations in water chemistry*: Chemical Geology, v. 248, no. 1, p. 14-39.

Freeze, R. A., and Cherry, J. A.; 1979. *Groundwater, 1979*, Printice-Hall, New Jersey.

Gaillardet, J., Dupré, B., Allègre, C. J., and Négrel, P.; 1997. *Chemical and physical denudation in the Amazon River Basin*: Chemical Geology, v. 142, no. 3, p. 141-173.

Garrels, R. M., and Mackenzie, F. T.; 1967. *Origin of the chemical compositions of some springs and lakes*: Equilibrium concepts in natural water systems, v. 67, p. 222-242.

Gobeil, P.-Y.; 2013. *Utilisation du système d'hydrothermalisme expérimental selon une approche hydrogéochimique: mode opératoire et résultats préliminaires*: Université du Québec à Chicoutimi, 40 p.

Goldberg, E., Broecker, W., Gross, M., Turekian, K., 1971. Radioactivity in the marine environment. National Academy of Science, Washington, DC: 137.

Helgeson, H. C.; 1968. *Evaluation of irreversible reactions in geochemical processes involving minerals and aqueous solutions - I. Thermodynamic relations*: Geochimica et Cosmochimica Acta, v. 32, no. 8, p. 853-877.

Ingebritsen, S. E., and Sanford, W. E.; 1999. *Groundwater in geologic processes*. Cambridge University Press.

Lasaga, A. C., Soler, J. M., Ganor, J., Burch, T. E., and Nagy, K. L.; 1994. *Chemical weathering rate laws and global geochemical cycles*: Geochimica et Cosmochimica Acta, v. 58, no. 10, p. 2361-2386.

Malcuit, E.; 2012. *Origine de la minéralisation des eaux dans un aquifère multicouche profond: Exemple de la « zone minéralisée de l'Entre-Deux-Mers » (Bassin Aquitain, France)*: Université Michel de Montaigne-Bordeaux III.

MDDEFP, Programme d'acquisition des connaissances sur les eaux souterraines http://www.mddelcc.gouv.qc.ca/eau/souterraines/programmes/acquisition-connaissance.htm , Consulté le 28 janvier 2018.

Molson, J., Frind, E., 2010. FLONET/TR2. Two-dimensional simulator for groundwater flownets, contaminant transport and residence time. User guide version 3.0, April 2010. Univ. Laval, Québec City, and Univ. of Waterloo.

Montcoudiol, N., Molson, J., Lemieux, J.-M., 2017. Numerical modelling in support of a conceptual model for groundwater flow and geochemical evolution in the southern Outaouais Region, Quebec, Canada. Canadian Water Resources Journal/Revue canadienne des ressources hydriques: 1-22.

Negrel, P., Allègre, C. J., Dupré, B., and Lewin, E.; 1993. *Erosion sources determined by inversion of major and trace element ratios and strontium isotopic ratios in river water: the Congo Basin case*: Earth and Planetary Science Letters, v. 120, no. 1, p. 59-76.

Négrel, P., Petelet-giraud, E., Brenot, A., Millot, R., and Innocent, C.; 2008. *caractérisation isotopique et géochimique des masses d'eau dans le bassin Adour-Garonne: interconnexions et hétérogénéités - CARISMEAU. Rapport Final. Tome 1: les outils isotopiques appliqués à la gestion des ressources en eau. Exemple de la masse d'eau des sables Infra-molassiques.*: BRGM, BRGM/RP-56291-FR. 192p. 45 ill.

Richard, S. K., R. Chesnaux, A. Rouleau, R. Morin, J. Walter, and S. Rafini. 2014. Field evidence of hydraulic connections between bedrock aquifers and overlying granular aquifers: examples from the Grenville Province of the Canadian Shield. *Hydrogeology Journal* 22(8): 1889–1904.

Schott, J., Pokrovsky, O. S., and Oelkers, E. H.; 2009. *The link between mineral dissolution/precipitation kinetics and solution chemistry*: Reviews in mineralogy and geochemistry, v. 70, no. 1, p. 207-258.

Sung, K.-Y., Yun, S.-T., Park, M.-E., Koh, Y.-K., Choi, B.-Y., Hutcheon, I., and Kim, K.-H.; 2012. *Reaction path modeling of hydrogeochemical evolution of groundwater in granitic bedrocks, South Korea*: Journal of Geochemical Exploration, v. 118, p. 90-97.

Taylor, A. S., Blum, J. D., Lasaga, A. C., and MacInnis, I. N.; 2000. *Kinetics of dissolution and Sr release during biotite and phlogopite weathering*: Geochimica et Cosmochimica Acta, v. 64, no. 7, p. 1191-1208.

Walter, J.; 2010. *Les eaux souterraines à salinité élevée autour du lac Saint-Jean, Québec : origines et incidences*: Msc. Université du Québec à Chicoutimi, ix, 177 f. p.

Walter, J., R. Chesnaux, V. Cloutier, and D. Gaboury. 2017. The influence of water/rock − water/clay interactions and mixing in the salinization processes of groundwater. *Journal of Hydrology: Regional Studies* 13 (2017) 168–188.

Walter, J., A. Rouleau, R. Chesnaux, M. Lambert, R. Daigneault. *In press.* Characterization of general and singular features of major aquifer systems in the Saguenay-Lac-Saint-Jean region. *Canadian Water Ressources Journal*.

Walter, J., R. Chesnaux, V. Cloutier, and D. Gaboury. *Submitted.* Chemical pathfinders for the natural evolution of groundwater toward brackish end-members in Precambrian bedrock aquifers and Pleistocene granular aquifers. *Geofluids.*.

Zhu, C.; 2009. *Geochemical modeling of reaction paths and geochemical reaction networks*: Reviews in Mineralogy and Geochemistry, v. 70, no. 1, p. 533-569.

Zhu, C., and Anderson, G.; 2002. *Environmental applications of geochemical modeling*, Cambridge: Cambridge University Press.

Zuddas, P., Seimbille, F., and Michard, G.; 1995. *Granite-fluid interaction at near-equilibrium conditions: Experimental and theoretical constraints from Sr contents and isotopic ratios*: Chemical geology, v. 121, no. 1, p. 145-154.

CHAPITRE 6

CONCLUSION

Le présent projet de recherche visait la détermination d'un modèle conceptuel du fonctionnement hydrogéochimique régional et l'identification de traceurs inorganiques de l'évolution temporelle de la signature géochimique de l'eau souterraine. Pour ce faire, cinq objectifs avaient été fixés :

1. Conceptualiser stratigraphiquement les principaux réservoirs d'eau souterraine présents sur le territoire d'étude;
2. Appliquer des méthodes statistiques multivariées sur une base de données hydrogéochimiques pour définir des pôles hydrogéochimiques régionaux de l'interaction eau-roche;
3. Comparer les pôles hydrogéochimiques régionaux identifiés avec des eaux de références dont l'origine est connue;
4. Décrire l'enrichissement ou l'appauvrissement de l'eau souterraine en certaines espèces chimiques dissoutes, notamment en éléments indésirables tels que les fluorures, le fer et le manganèse, au cours de l'évolution chimique naturelle de l'eau souterraine vers l'un ou l'autre des pôles identifiés;
5. Proposer des ions ou des groupements d'ions dissous caractéristiques de l'évolution naturelle de l'eau souterraine vers l'un ou l'autre des pôles hydrogéochimiques régionaux identifiés.

Les résultats de cette étude répondent aux objectifs fixés. Nous avons pu réaliser un modèle de fonctionnement hydrogéochimique régional en déterminant des pôles compositionnels régionaux de l'interaction entre l'eau souterraine et deux principaux réservoirs que sont les roches précambriennes fracturées et les aquifères confinés par l'argile marine; ces derniers étant principalement de type poreux, constitués des sables et des graviers quaternaires. Les conclusions permettent d'expliquer la présence en solution de certains éléments chimiques hérités de divers stades d'évolution de l'eau souterraine. Ces traceurs géochimiques aident à la compréhension de la variabilité spatiale de la qualité de l'eau souterraine retrouvée sur le territoire d'étude et pourront permettre d'émettre des hypothèses quant au fonctionnement hydraulique des aquifères locaux. Les principales contributions de ce projet de recherche sont présentées et discutées ci-dessous.

Dans le cadre de cette thèse, nous avions comme objectif de mieux comprendre l'évolution hydrogéochimique naturelle de l'eau souterraine dans la région du Saguenay-Lac-Saint-Jean (Québec, Canada). Cette nouvelle connaissance définit l'état des lieux de la qualité naturelle de l'eau souterraine dans la région et permet de proposer des mécanismes à l'origine de la dégradation locale de cette qualité, notamment en fluor, un paramètre chimique dont la concentration a été fréquemment retrouvée au-dessus de la limite de potabilité dans la région. Pour arriver à nos fins, et considérant une base de données hydrogéochimiques régionale disponible contenant plus de 300 échantillons et près de 40 paramètres physico-chimiques analysés, nous avons préconisé une approche

statistique dans laquelle sont combinées les techniques conventionnelles (statistiques standards) et des techniques plus sophistiquées telles que l'analyse hiérarchique en grappe, l'analyse en composante principale et l'analyse factorielle (statistiques multivariées). Les résultats obtenus permettent une mise en graphique des observations (diagrammes binaires, diagramme de Piper, diagrammes multiéléments) et la détermination de pôles hydrogéochimiques compositionnels régionaux de l'évolution naturelle de l'eau souterraine. C'est à partir des compositions moyennes de ces pôles que le modèle conceptuel de l'évolution naturelle de l'eau souterraine est élaboré.

Les principales contributions du projet sont sous la forme de trois articles scientifiques publiés (2) et soumis (1). Les principaux résultats et implications sont présentés ci-dessous :

1. Le programme d'acquisition des connaissances sur les eaux souterraines du MDDELCC a été réalisé dans plusieurs régions du Québec (Outaouais, Mauricie, Montérégie, Bas-Saint-Laurent, Abitibi-Témiscamingue, Charlevoix-Haute-Côte-Nord, Saguenay-Lac-Saint-Jean, …). L'ensemble de ces connaissances constitue une avancée majeure de la Province pour une « appropriation » efficiente de la ressource en eau, et c'est par des projets de la nature de ce doctorat que les données produites au fil du temps sont valorisées. Nous pensons que la synthèse géologique et hydrogéologique des connaissances régionales acquises dans les dernières années dans la

région, et qui est présentée dans cette thèse, constitue un bon outil de diffusion auprès de gestionnaires du territoire dont le mandat est d'assurer la pérennité de la ressource en eau souterraine, mais devient aussi un bon outil pour partager la connaissance avec d'autres universitaires travaillant sur des problématiques similaires ailleurs au Québec. (implication sociale).

2. Les statistiques multivariées sont de plus en plus utilisées dans le cadre de projets hydrogéochimiques, et l'avènement de logiciels intégrant ce type d'analyses statistiques n'est pas étranger à ce phénomène. Ce projet s'interroge entre autre sur les limites d'application de ces méthodes et tente, par des tests réalisés sur un jeu de données réduit plutôt que sur l'ensemble des données, de vérifier si dans certains cas « moins » de données ne vaut pas mieux que « plus » de données. Il ressort de notre projet qu'il existe un effet d'échelle qui, dans certains cas, peut nuire à l'interprétation de bases de données dont le contenu est très variable, c'est-à-dire dont les données présentent de larges gammes de valeurs pour certains paramètres. De plus, les limites de détection des paramètres considérés jouent un rôle prépondérant dans l'application de ces techniques d'analyses statistiques multivariées, car trop de données sous ces limites biaisent l'éventuelle corrélation de certains paramètres avec les autres. Ainsi, nous pensons que l'utilisation des statistiques multivariées pourrait être optimisée en considérant la possibilité de les appliquer sur un

ou plusieurs sous-ensembles de données extraits d'une base de données d'échelle régionale. La représentativité du sous-ensemble doit évidemment être bien investiguée. (Implication méthodologique).

3. La compréhension de certains mécanismes d'évolution naturelle de l'eau souterraine, et de certains mécanismes d'acquisition sous forme dissoute de certains éléments chimiques parfois indésirables, devrait être considérée dans le cadre des recherches en eau potable. En effet, certaines municipalités connaissent des problèmes parfois criant d'alimentation en eau potable, notamment à cause d'une qualité médiocre. En testant localement les processus d'évolution proposés dans cette thèse, nous devrions être en mesure de développer des outils pratiques permettant entre autres de mieux cibler géographiquement les aquifères à potentiel qualitatif acceptable, ou l'inverse, les limites des environnements qui sont susceptibles de contenir une eau impropre à la consommation. À titre d'exemple, mentionnons le cas du fluor, pour lequel nous proposons un environnement spécifique favorable à sa présence dans l'eau souterraine. Il existe au Québec, des municipalités aux prises avec cette problématique particulière. Il s'agirait donc de comparer notre modèle avec la réalité terrain, d'une part pour le valider de manière empirique, et si tel est le cas, pour tenter d'en définir les limites en termes d'extension latérale et verticale. (Implication pratique)

4. Au niveau du fonctionnement hydrogéochimique mis en évidence dans ce projet (implication pratique), les principales conclusions sont à l'effet que :
    a. Il existe une distinction géochimique entre l'eau souterraine qui évolue dans les milieux rocheux fracturés et celle qui évolue dans les milieux granulaires poreux confinés par l'argile marine;
    b. La délimitation franche entre les basses-terres et les hautes-terres, résultat de la physiographie de la région en graben, contrôlant, d'une part l'accumulation de dépôts meubles quaternaires et d'autre part, une partie de l'écoulement de l'eau souterraine en milieu fracturé, a notamment pour effet la remontée d'eau souterraine profonde salée, âgée de plusieurs milliers d'années et impropre à la consommation, le long des failles normales bordant le graben.
    c. Le fluor tire son origine de sources variées mais limitées. Les environnements de mise en solution les plus favorables impliquent les roches cristallines précambriennes ou les roches sédimentaires paléozoïques confinées par l'argile marine;
    d. Le molybdène, le bore et le fluor combinés peuvent signifier la présence de milieux contenant des hydrocarbures;

e. Le lithium, les bromures et un rapport $Ca^{2+}/Sr^{2+} \approx 40$ sont des caractéristiques de l'eau souterraine ayant eu un contact prolongé avec les roches cristallines précambriennes;

f. L'eau de recharge est « rapidement » appauvrie en métaux ce qui suggère une modification des conditions d'oxydo-réduction dans les premiers moments de la recharge;

g. L'altération des minéraux de feldspaths potassiques (microcline), présents dans l'argile marine, en illite, explique en partie la présence de potassium et de silice dissous dans les aquifères confinés;

h. La dégradation de la matière organique joue un rôle prépondérant dans la production de CO_2 et donc d'ions bicarbonates. De plus, cette dégradation sous des conditions anaérobies semble aussi jouer un rôle sur la présence sous forme dissoute de l'ammonium, ce qui fait de ce paramètre chimique un bon traceur de l'interaction de l'eau souterraine avec les argiles marines, ou avec les unités de shale d'Utica, deux réservoirs suspectés riches en matière organique.

5. Finalement, nous avons compris en réalisant ce projet de doctorat que de nombreuses données demeuraient encore manquantes pour bien connaître l'évolution naturelle de la qualité de l'eau souterraine dans la région, mais surtout,

nous avons réalisé à quel point le contexte géologique et hydrogéolgique (physiographie en graben, roches cristallines du Bouclier Canadien, lambeaux épars de roches sédimentaires paléozoïques, épais dépôts stratifiés de sédiments pulvérulents et cohésifs pléistocènes) font de la région du Saguenay-Lac-Saint-Jean un formidable laboratoire pour l'étude de la dynamique des milieux aquifères. Nous pensons qu'une approche globale qui combinerait des essais expérimentaux, des analyses chimiques et isotopiques, un échantillonnage multi-niveaux à l'aide d'obturateurs gonflables, l'étude fine de la géochimie des roches de la région et la modélisation numérique hydrogéochimique, est indispensable à la pleine compréhension des mécanismes d'évolution naturelle hydrogéochimique régionale (implication scientifique fondamentale).

ANNEXES

ANNEXE 1 (Annexe 3; Chapitre 3.): Chimie détaillée, types d'eau, groupes d'eau (résultats de l'analyse en grappe), type d'aquifères et autres paramètres physiques de tous les échantillons et des puits d'échantillonnage.

Sample	Cluster	Depth	Hydrogeological Context	X	Y	Aquifer type	Water type	TDS (Mg/L)	Temperature (Deg. Celcius)	Eh (mV)
UQAC1011	1	15.24	UNK	278347	5335240	Rock	Ca-Cl	630.0	6.6	-27.1
UQAC1019	1	94.5	Semiconfined	209074	5357458	Rock	Ca-Cl	725.4	7.4	8.2
UQAC1048	1	18.29	Confined	157475	5420350	Granular	Na-Cl	1359.6	9.5	-21.2
UQAC1071	1	36.576	Water table	164793	5399922	Granular	Na-Cl	3576.0	7.83	-132.4
UQAC1098	1	91.44	Semiconfined	231564	5372099	Rock	Na-Cl	1163.3	10.01	UNK
UQAC2047	1	UNK	UNK	192785	5410166	Granular	Na-Cl	1352.8	7.75	104.9
UQAC2048	1	2.43	UNK	193851	5405421	Granular	Na-Cl	1167.9	8.31	108.2
UQAC2091	1	3.35	UNK	267964	5370748	Granular	Na-Cl	1387.7	7.49	107.5
UQAC2128	1	62.9	Confined	197459	5393959	Rock	Na-Cl	1794.8	7.3	102.5
UQAC3024	1	73.152	Confined	160458	5406356	Rock	Na-Cl	1697.2	7.8	UNK
UQAC3036	1	76.19	Confined	164583	5399819	Rock	Na-Cl	3546.0	7.34	-177.5
UQAC3052	1	68.58	Confined	268168	5372366	Rock	Ca-HCO3	1325.1	7.21	-298.6
UQAC6007	1	52.1	Confined	179977	5406833	Granular	Na-Cl	1679.6	7.58	-147
1JW01	1	127	Confined	231034	5367634	Rock	Na-HCO3	574.9	8.00	-375.60
1JW02	1	40	Confined	226750	5387893	Rock	Na-Cl	2102.4	5.80	-326.00
1JW07	1	50.292	Semiconfined	256166	5368280	Rock	Na-Cl	2795.8	7.70	100.60
1JW15	1	32.918	Confined	192580	5411744	Granular	Na-Cl	2709.1	9.40	-8.30
1JW26	1	0	Semiconfined	187977	5370073	Rock	Ca-HCO3	2255.8	13.30	44.70
1JW28	1	73.152	Confined	169248	5394039	Rock	Na-Cl	2216.2	7.40	-46.20
1JW38	1	0	Confined	191557	5407193	Rock	Na-Cl	2328.8	7.20	53.60
2JW02	1	91.44	Semiconfined	255864	5368317	Rock	Na-Cl	4196.9	6.70	-23.00
2JW04	1	56.998	Confined	191533	5409524	Rock	Ca-Cl	1929.1	11.30	-12.00
2JW08	1	91.44	Water table	209470	5378176	Rock	Na-Cl	1706.5	7.10	-13.00
2JW12	1	38.1	Semiconfined	188355	5369647	Rock	Na-Cl	949.6	7.50	39.90
2JW19	1	93.269	Confined	214920	5384625	Rock	Na-HCO3	917.9	8.10	-40.00
2JW20	1	0	Confined	214920	5384625	Rock	Ca-Cl	763.3	7.30	-12.80
3JW05	1	22.86	Confined	192820	5411584	Granular	Na-Cl	1283.2	9.40	-75.30
3JW08	1	60.96	Confined	192578	5411888	Rock	Na-Cl	1660.5	10.30	-65.70
3JW10	1	0	Confined	191557	5407193	Rock	Na-Cl	2479.2	9.20	-47.10
3JW12	1	93.269	Confined	214920	5384625	Rock	Na-HCO3	1014.9	10.90	-94.40
UQAC1001	2	44.28	UNK	256114	5358221	Rock	Na-HCO3	286.6	8.66	-164.7
UQAC1002	2	83.82	UNK	263118	5358381	Rock	Na-Cl	538.4	8.66	195.4
UQAC1003	2	45.72	Water table	281899	5349326	Rock	Ca-HCO3	628.2	9.2	-1.4
UQAC1004	2	42.672	Confined	244759	5369455	Rock	Na-HCO3	307.0	6.9	-45.4
UQAC1005	2	119.87	Water table	228440	5361358	Rock	Na-Cl	499.0	7.3	-29.9
UQAC1006	2	47.244	Water table	252582	5352085	Rock	Ca-HCO3	106.4	7.2	8.2
UQAC1008	2	64	Confined	266043	5380632	Rock	Na-HCO3	209.9	7.4	-44
UQAC1012	2	91.44	UNK	279311	5343770	Rock	Ca-HCO3	125.5	10.7	133.5

Sample	Cluster	Depth	Hydrogeological Context	X	Y	Aquifer type	Water type	TDS (Mg/L)	Temperature (Deg. Celcius)	Eh (mV)
UQAC1013	2	91.44	UNK	243354	5370400	Granular	Na-HCO3	370.1	13.2	-69.5
UQAC1014	2	83.82	Confined	235966	5372842	Rock	Ca-HCO3	282.0	8.4	56.7
UQAC1015	2	106.7	Confined	224119	5375025	Rock	Na-HCO3	363.9	7.6	-24.5
UQAC1016	2	51.82	Water table	211129	5380527	Rock	Ca-HCO3	372.2	7.9	95.2
UQAC1017	2	UNK	UNK	210978	5360498	Granular	Ca-HCO3	326.5	6.3	55.7
UQAC1020	2	45.72	Water table	291645	5365727	Rock	Ca-HCO3	171.9	9.5	23.8
UQAC1021	2	85.36	UNK	300777	5360803	Rock	Na-HCO3	260.6	6.9	-89
UQAC1022	2	74.676	Water table	255332	5352148	Rock	Ca-Cl	425.8	6.9	10.3
UQAC1023	2	60.96	Water table	174208	5374867	Rock	Ca-HCO3	329.4	8.3	57.7
UQAC1024	2	100.5	Confined	173104	5373609	Rock	Ca-HCO3	324.1	7.1	-27.6
UQAC1025	2	109.73	Water table	263581	5369058	Rock	Na-HCO3	291.7	8.3	-39.3
UQAC1026	2	92.964	Water table	282343	5367913	Rock	Na-HCO3	205.5	6.9	0.1
UQAC1028	2	4.27	Confined	186297	5436995	Granular	Ca-HCO3	105.8	10.1	59.8
UQAC1029	2	9.14	Semiconfined	178659	5430424	Rock	Ca-HCO3	242.9	6.9	74.3
UQAC1030	2	UNK	UNK	168230	5438043	Granular	Ca-HCO3	322.9	9.9	92
UQAC1032	2	UNK	Water table	185779	5402479	Granular	Ca-HCO3	111.2	10.4	77
UQAC1033	2	11.58	Confined	196680	5410702	Granular	Na-HCO3	294.2	7.2	2.7
UQAC1035	2	21.34	Confined	212317	5403045	Granular	Na-HCO3	117.6	7.4	137.7
UQAC1036	2	32	Water table	281216	5351537	Rock	Ca-HCO3	469.0	7.8	103.9
UQAC1038	2	91.44	Semiconfined	242175	5356099	Rock	Ca-HCO3	643.8	6.8	26.9
UQAC1040	2	UNK	UNK	235854	5382983	Granular	Ca-HCO3	35.1	10.3	71.8
UQAC1041	2	48.768	UNK	243590	5386258	Rock	Na-HCO3	332.1	6.8	-99
UQAC1042	2	33.528	Water table	151724	5438683	Rock	Ca-HCO3	72.0	7.9	100.5
UQAC1043	2	106.68	UNK	156622	5426407	Rock	Ca-HCO3	304.0	7.2	7.8
UQAC1044	2	12.19	UNK	154799	5429102	Granular	Ca-HCO3	229.6	11.3	5.63
UQAC1045	2	12.19	Water table	157786	5424897	Granular	Na-HCO3	403.8	13.1	43.1
UQAC1046	2	2.5	Water table	168824	5391126	Granular	Ca-HCO3	170.9	10.8	41.2
UQAC1049	2	6.09	Confined	142586	5401887	Granular	Ca-HCO3	92.6	10.2	66.2
UQAC1050	2	44.196	Confined	142148	5404884	Rock	Ca-HCO3	229.1	6.6	42.5
UQAC1051	2	15	UNK	150187	5395475	Granular	Ca-HCO3	84.7	7	64.5
UQAC1052	2	54.864	Water table	240498	5406201	Rock	Na-HCO3	111.4	6.2	3
UQAC1053	2	80.467	Water table	232718	5393566	Rock	Ca-HCO3	228.2	7	9.7
UQAC1055	2	47.244	Confined	267867	5370703	Rock	Ca-HCO3	321.9	8.16	UNK
UQAC1058	2	27.432	Water table	164175	5381504	Granular	Ca-HCO3	211.5	6.87	-58.6
UQAC1059	2	9.75	Water table	188833	5362749	Granular	Ca-HCO3	384.8	7.86	-37.5
UQAC1063	2	75.286	Water table	209514	5358343	Rock	Ca-HCO3	383.0	7.48	153
UQAC1064	2	6.68	Water table	264621	5373255	Granular	Ca-HCO3	49.7	7.36	67
UQAC1065	2	19.4	Water table	238250	5372681	Granular	Ca-HCO3	280.9	8.29	71.4

Sample	Cluster	Depth	Hydrogeological Context	X	Y	Aquifer type	Water type	TDS (Mg/L)	Temperature (Deg. Celcius)	Eh (mV)
UQAC1066	2	67.36	Confined	335917	5341290	Rock	Ca-HCO3	198.7	6.07	-10.4
UQAC1067	2	60.96	Water table	293399	5350108	Rock	Ca-HCO3	279.4	7.17	-192.3
UQAC1069	2	64.008	Confined	173765	5383858	Granular	Ca-HCO3	459.4	7.64	79.4
UQAC1073	2	18.4	Water table	158467	5384872	Granular	Ca-HCO3	198.2	6.53	76.2
UQAC1074	2	UNK	Confined	162853	5389148	Rock	Ca-HCO3	393.0	6.31	-182.1
UQAC1075	2	60.96	Semiconfined	196008	5365124	Rock	Ca-HCO3	291.1	8.73	UNK
UQAC1076	2	76.2	UNK	241638	5394281	Rock	Na-HCO3	198.0	6.88	UNK
UQAC1077	2	5.5	Water table	239831	5397414	Granular	Ca-HCO3	107.6	7.4	158.1
UQAC1078	2	5.5	Confined	237932	5391615	Granular	Ca-HCO3	83.6	6.75	145.6
UQAC1079	2	UNK	UNK	278892	5338219	Rock	Ca-HCO3	153.6	5.97	524.9
UQAC1080	2	UNK	UNK	280437	5328305	Rock	Ca-HCO3	388.2	6	-153.3
UQAC1081	2	UNK	UNK	257353	5350717	Granular	Ca-HCO3	238.5	6.69	155.8
UQAC1082	2	64	Semiconfined	190793	5364655	Rock	Ca-HCO3	293.1	7.42	-263.2
UQAC1083	2	8.95	Water table	203378	5361246	Granular	Ca-HCO3	354.6	8.28	37.9
UQAC1084	2	38.32	Confined	241270	5395372	Granular	Ca-HCO3	70.2	7.37	73.1
UQAC1086	2	8.5	Confined	241430	5381792	Granular	Ca-HCO3	332.9	9.22	55.3
UQAC1087	2	UNK	Confined	185242	5352894	Rock	Ca-HCO3	153.2	6.75	680
UQAC1088	2	68.68	Semiconfined	180675	5354492	Rock	Ca-HCO3	233.0	7.63	194.7
UQAC1089	2	22.86	Semiconfined	179874	5350801	Rock	Ca-HCO3	188.8	6.92	-98.7
UQAC1090	2	86.868	Water table	211212	5383976	Rock	Ca-HCO3	391.2	7.23	59.7
UQAC1092	2	106.68	Confined	226563	5374583	Rock	Na-Cl	458.3	8	-314.1
UQAC1094	2	102.11	Semiconfined	227624	5362092	Rock	Na-HCO3	329.7	7.98	-201.5
UQAC1095	2	76.2	Water table	233691	5367279	Rock	Ca-HCO3	439.6	7.72	115.4
UQAC1096	2	UNK	Confined	240893	5365656	Rock	Na-HCO3	270.9	6.9	-271.6
UQAC1097	2	76.2	Water table	237885	5366329	Rock	Na-HCO3	201.0	7.28	UNK
UQAC1099	2	60.96	Confined	219998	5364695	Rock	Na-HCO3	621.9	7.07	-220.2
UQAC1101	2	94.488	UNK	175323	5375931	Rock	Ca-Cl	408.1	7.12	UNK
UQAC1103	2	70.12	Semiconfined	298787	5363546	Rock	Na-Cl	1018.7	7.44	110.1
UQAC1108	2	99.06	Semiconfined	217997	5384949	Rock	Ca-HCO3	306.4	7.58	UNK
UQAC1109	2	15.38	Confined	261940	5381748	Rock	Ca-HCO3	244.1	7.61	UNK
UQAC1110	2	33.528	Semiconfined	254049	5391063	Rock	Ca-HCO3	153.4	6.95	UNK
UQAC1111	2	8.23	UNK	227413	5393944	Granular	Ca-HCO3	58.9	7.33	UNK
UQAC1112	2	73.15	Confined	232622	5390459	Rock	Ca-HCO3	333.0	7.02	UNK
UQAC1113	2	3.04	Water table	266562	5376357	Granular	Ca-HCO3	44.3	10.83	UNK
UQAC1114	2	1.2	Water table	228790	5380279	Granular	Ca-HCO3	287.1	10.37	UNK
UQAC1115	2	79.85	UNK	218034	5385006	Rock	Na-HCO3	334.9	6.7	UNK
UQAC1116	2	76.2	Water table	230751	5359679	Rock	Ca-HCO3	353.6	7.99	UNK
UQAC1117	2	53.34	Semiconfined	241487	5364335	Rock	Ca-HCO3	322.8	8.82	UNK

Sample	Cluster	Depth	Hydrogeological Context	X	Y	Aquifer type	Water type	TDS (Mg/L)	Temperature (Deg. Celcius)	Eh (mV)
UQAC1118	2	7.62	Water table	266838	5380141	Granular	Ca-HCO3	67.1	9.38	UNK
UQAC1119	2	85.36	Confined	252701	5359220	Rock	Na-HCO3	488.4	6.73	UNK
UQAC1120	2	58.12	Semiconfined	273917	5372487	Rock	Ca-HCO3	227.5	7.94	UNK
UQAC1121	2	85.344	Semiconfined	279226	5366840	Rock	Na-HCO3	228.0	6.63	UNK
UQAC1123	2	18	UNK	226024	5396580	Granular	Ca-HCO3	46.1	UNK	UNK
UQAC2001	2	2.74	Water table	227519	5362015	Granular	Ca-HCO3	223.3	10.19	139.6
UQAC2002	2	19.8	Water table	253081	5394483	Granular	Ca-HCO3	42.9	6.14	142.26
UQAC2003	2	5.18	Water table	261981	5381855	Granular	Ca-HCO3	198.3	8.34	142.7
UQAC2004	2	0	Confined	249695	5368716	Granular	Ca-HCO3	59.9	6.43	142.8
UQAC2005	2	2.43	Water table	248353	5388192	Granular	Ca-HCO3	107.3	6.04	135.7
UQAC2008	2	6.09	Water table	314296	5336700	Granular	Ca-HCO3	86.9	9.93	137.6
UQAC2009	2	1.37	Water table	311390	5345994	Granular	Ca-HCO3	74.1	9.66	137.9
UQAC2010	2	1.52	Water table	311336	5346463	Granular	Ca-HCO3	109.2	9.49	140.4
UQAC2011	2	3.65	Water table	234382	5404765	Granular	Ca-HCO3	59.5	8.9	101.4
UQAC2012	2	9.14	Water table	235199	5396736	Granular	Ca-HCO3	58.2	7.11	136.6
UQAC2013	2	7.31	Water table	251109	5375045	Granular	Ca-HCO3	25.5	6.87	128.6
UQAC2014	2	3.96	Water table	248450	5374794	Granular	Ca-HCO3	22.5	6.12	131
UQAC2015	2	121.9	Semiconfined	294231	5351191	Rock	Ca-HCO3	152.8	6.77	107.8
UQAC2016	2	74.69	Confined	303965	5348264	Rock	Ca-HCO3	162.8	7.07	128.2
UQAC2017	2	56.4	Semiconfined	209680	5357670	Rock	Ca-HCO3	284.0	8.13	128.6
UQAC2018	2	4.87	Water table	208116	5371803	Granular	Ca-HCO3	467.2	8.02	131.1
UQAC2019	2	4.57	Water table	186491	5361733	Granular	Ca-HCO3	484.6	8.23	124.6
UQAC2020	2	6.09	Water table	187368	5370638	Granular	Ca-HCO3	435.8	8.83	131.1
UQAC2021	2	UNK	UNK	261048	5352326	Rock	Na-HCO3	316.3	8.86	139
UQAC2022	2	106.7	Confined	257141	5355663	Rock	Ca-HCO3	260.7	8.01	126.3
UQAC2023	2	11.5	Water table	224969	5402159	Granular	Ca-HCO3	22.1	7.9.	129.7
UQAC2025	2	21.34	UNK	228740	5386783	Granular	Ca-HCO3	55.8	7.48	133.36
UQAC2026	2	27.43	UNK	227597	5385472	Granular	Na-HCO3	222.9	10.63	138.8
UQAC2029	2	3.96	Water table	213070	5384506	Granular	Ca-HCO3	272.3	7.94	109.5
UQAC2030	2	4.87	Water table	227256	5363132	Granular	Ca-HCO3	468.6	10.09	193.8
UQAC2031	2	7.62	Water table	255892	5351991	Granular	Ca-HCO3	406.5	8.27	110.3
UQAC2033	2	74.6	Semiconfined	212528	5386165	Rock	Na-HCO3	364.8	8.16	103.9
UQAC2035	2	UNK	Confined	339463	5335381	Rock	Ca-HCO3	170.6	7.03	119.3
UQAC2036	2	42.68	Confined	287485	5353119	Rock	Ca-HCO3	220.0	7.58	112.5
UQAC2038	2	67.07	Confined	169149	5416981	Rock	Na-HCO3	236.8	6.78	9.54
UQAC2039	2	76.2	UNK	172041	5418057	Rock	Na-HCO3	474.5	7.74	93
UQAC2042	2	44.2	Confined	179239	5419672	Rock	Ca-HCO3	110.2	13.09	101.8
UQAC2044	2	UNK	UNK	175982	5423126	Rock	Na-HCO3	512.4	7.26	111.5

Sample	Cluster	Depth	Hydrogeological Context	X	Y	Aquifer type	Water type	TDS (Mg/L)	Temperature (Deg. Celcius)	Eh (mV)
UQAC2045	2	9.14	Semiconfined	189241	5419767	Granular	Na-HCO3	261.0	7.02	101.2
UQAC2046	2	6.09	Confined	199344	5426357	Granular	Ca-HCO3	218.7	8.51	109.3
UQAC2050	2	60.97	UNK	245817	5355712	Rock	Ca-HCO3	162.6	7.75	101.5
UQAC2051	2	4.26	Water table	174962	5332927	Granular	Ca-HCO3	74.9	8.78	109.5
UQAC2052	2	27.13	Water table	176401	5338415	Granular	Ca-HCO3	112.8	7.62	106.4
UQAC2053	2	2.43	Water table	175693	5337161	Granular	Ca-HCO3	57.5	7.66	102.3
UQAC2054	2	45.73	UNK	276734	5360224	Rock	Ca-HCO3	223.3	8.19	96.8
UQAC2055	2	76.2	UNK	276971	5349526	Rock	Na-Cl	453.6	8.41	100.6
UQAC2059	2	5.79	Water table	166859	5403043	Granular	Ca-Cl	211.4	10.07	93.7
UQAC2060	2	10.6	Confined	165372	5391060	Granular	Ca-HCO3	459.7	8.74	94.5
UQAC2062	2	3.04	UNK	167877	5396093	Granular	Ca-HCO3	154.3	10.87	92.3
UQAC2063	2	91.4	Confined	152495	5414870	Rock	Na-HCO3	599.4	8.61	91.6
UQAC2064	2	82.3	Confined	152351	5412252	Rock	Na-HCO3	252.4	7	89.5
UQAC2069	2	27.43	Confined	158959	5412836	Granular	Na-HCO3	607.9	15.05	91.1
UQAC2071	2	57	Semiconfined	342238	5339331	Rock	Na-HCO3	173.6	7.3	92
UQAC2073	2	74.69	Confined	320343	5337511	Rock	Ca-HCO3	160.6	6.91	82.2
UQAC2074	2	4.57	Water table	233221	5375335	Granular	Ca-HCO3	86.8	12.29	91
UQAC2075	2	7.62	UNK	232524	5376542	Granular	Ca-HCO3	662.2	7.57	91.4
UQAC2076	2	125	Semiconfined	140373	5428643	Rock	Ca-Cl	590.7	7.36	91.1
UQAC2077	2	4.57	Water table	140414	5428564	Granular	Ca-HCO3	90.0	9.87	89.2
UQAC2078	2	137.19	Semiconfined	144188	5418088	Rock	Na-HCO3	323.8	6.84	88.7
UQAC2079	2	6.09	Water table	141096	5426955	Granular	Ca-HCO3	44.0	7.75	87.6
UQAC2081	2	6.4	Water table	145138	5422643	Granular	Ca-HCO3	48.7	8.36	88.8
UQAC2082	2	7.62	Water table	142026	5418285	Granular	Na-HCO3	217.4	9.75	88.7
UQAC2086	2	4.57	UNK	170505	5389329	Granular	Ca-HCO3	91.4	8.63	88.9
UQAC2088	2	UNK	Water table	271027	5352847	Granular	Ca-HCO3	427.2	6.89	90.6
UQAC2089	2	UNK	Water table	271228	5352575	Granular	Ca-HCO3	335.4	6.63	90.2
UQAC2090	2	115	Confined	298350	5363827	Rock	Ca-Cl	391.3	6.71	129.6
UQAC2092	2	UNK	UNK	322408	5338532	Granular	Ca-HCO3	129.5	6.36	94.5
UQAC2093	2	UNK	UNK	319770	5336222	Granular	Ca-HCO3	114.6	6.11	89.9
UQAC2094	2	UNK	Confined	277435	5351746	Rock	Ca-HCO3	427.9	9.47	94.9
UQAC2096	2	50	Semiconfined	141189	5423291	Granular	Ca-HCO3	174.9	7.29	97.7
UQAC2097	2	UNK	UNK	156752	5418463	Granular	Ca-HCO3	247.9	6.77	98.9
UQAC2098	2	UNK	UNK	172776	5432604	Granular	Ca-HCO3	228.6	6.04	91.6
UQAC2099	2	UNK	Confined	183196	5429954	Granular	Ca-HCO3	58.1	11.43	90.6
UQAC2100	2	UNK	Confined	295508	5348632	Granular	Ca-HCO3	507.5	7.48	89.1
UQAC2101	2	22	UNK	207137	5419073	Granular	Ca-HCO3	140.5	8.43	111.4
UQAC2103	2	37.19	UNK	206780	5419251	Rock	Ca-HCO3	93.0	7.08	101

Sample	Cluster	Depth	Hydrogeological Context	X	Y	Aquifer type	Water type	TDS (Mg/L)	Temperature (Deg. Celcius)	Eh (mV)
UQAC2104	2	UNK	UNK	207280	5415967	Granular	Ca-HCO3	28.7	8.42	98.8
UQAC2106	2	UNK	UNK	214083	5359561	Granular	Ca-HCO3	180.1	7.74	109.8
UQAC2107	2	76.21	Confined	224842	5360015	Rock	Ca-HCO3	230.5	8.12	11.7
UQAC2108	2	24.39	UNK	214008	5359782	Rock	Ca-HCO3	134.7	8.86	107.1
UQAC2112	2	12.1	Water table	219627	5397040	Granular	Ca-HCO3	44.1	8.02	99.1
UQAC2114	2	24.39	Confined	195694	5354626	Granular	Ca-HCO3	200.5	5.63	93.9
UQAC2116	2	4.57	UNK	206925	5361167	Granular	Ca-HCO3	295.0	14.14	106.9
UQAC2117	2	48.78	UNK	197416	5364935	Granular	Ca-HCO3	396.7	7.13	120.4
UQAC2118	2	UNK	UNK	197588	5364765	Granular	Ca-HCO3	405.9	6.37	101.1
UQAC2119	2	UNK	Water table	241455	5362601	Granular	Ca-HCO3	169.4	14.12	109.6
UQAC2120	2	27.43	Water table	156145	5427133	Granular	Ca-HCO3	200.1	7.68	116.4
UQAC2121	2	UNK	Confined	145716	5397702	Granular	Na-HCO3	201.1	6.93	93.7
UQAC2122	2	7.31	Water table	141407	5407026	Granular	Ca-HCO3	209.0	9.49	96.6
UQAC2123	2	16.76	Confined	169223	5439016	Granular	Na-HCO3	313.7	8.57	104
UQAC2124	2	19.81	UNK	149745	5420935	Granular	Ca-HCO3	124.9	6.05	93
UQAC2125	2	UNK	UNK	149558	5422557	Granular	Ca-HCO3	267.6	6.28	91.9
UQAC2126	2	UNK	UNK	209984	5404557	Granular	Ca-HCO3	158.4	5.81	107.5
UQAC2129	2	UNK	UNK	230393	5394595	Granular	Ca-HCO3	54.5	6.18	101.1
UQAC2130	2	UNK	UNK	230595	5394404	Granular	Ca-HCO3	52.7	6.31	94.5
UQAC2131	2	UNK	UNK	246184	5370597	Granular	Ca-HCO3	311.6	8.1	97.8
UQAC2132	2	70.73	Water table	211089	5386749	Rock	Na-Cl	485.9	6.73	78.4
UQAC2133	2	22.25	Confined	184770	5367721	Rock	Ca-HCO3	342.2	6.68	85.1
UQAC2135	2	112.8	Confined	218796	5363857	Rock	Ca-HCO3	524.9	7.09	77.2
UQAC3000	2	3.04	Confined	234884	5373252	Granular	Ca-HCO3	23.5	4.01	92.7
UQAC3002	2	20.12	Water table	238815	5382014	Granular	Na-Cl	476.7	7.69	26.4
UQAC3004	2	85.34	Semiconfined	239300	5387389	Rock	Na-HCO3	182.2	6.61	-79.3
UQAC3009	2	76.8	Water table	229716	5370637	Rock	Na-HCO3	431.6	7.35	-89.5
UQAC3011	2	22.86	Water table	225708	5359041	Granular	Ca-HCO3	238.3	9.09	UNK
UQAC3013	2	9.144	Confined	242714	5386501	Granular	Na-HCO3	234.3	7.84	-58.7
UQAC3014	2	100.6	Water table	259769	5351811	Rock	Na-HCO3	381.3	9.34	-137.4
UQAC3015	2	7.62	UNK	266869	5358307	Granular	Ca-HCO3	751.4	6.08	162.2
UQAC3018	2	4.57	Water table	169648	5421643	Granular	Na-HCO3	12.1	7.95	291.9
UQAC3019	2	89.9	Confined	152373	5412114	Rock	Na-HCO3	260.4	7.02	79.3
UQAC3021	2	95.5	Confined	155641	5416213	Rock	Na-HCO3	310.4	6.73	40.1
UQAC3022	2	UNK	Water table	179979	5423336	Granular	Na-HCO3	51.8	6.34	204.6
UQAC3023	2	16.76	Confined	151856	5424314	Granular	Ca-HCO3	204.4	7.17	80.9
UQAC3025	2	100.5	Confined	173104	5373609	Rock	Ca-HCO3	304.9	7.18	307.2
UQAC3027	2	76.21	Water table	163431	5376869	Granular	Ca-HCO3	243.3	6.95	298.7

Sample	Cluster	Depth	Hydrogeological Context	X	Y	Aquifer type	Water type	TDS (Mg/L)	Temperature (Deg. Celcius)	Eh (mV)
UQAC3028	2	50.292	Water table	171536	5373205	Rock	Ca-HCO3	281.6	7.18	UNK
UQAC3032	2	6.09	Water table	172693	5433417	Granular	Ca-HCO3	22.6	5.49	3.7
UQAC3035	2	3.96	Water table	173707	5408692	Granular	Ca-Cl	37.3	6.47	128
UQAC3037	2	UNK	Water table	198025	5400661	Granular	Na-Cl	39.4	10.99	UNK
UQAC3038	2	54.87	Confined	169530	5416214	Rock	Na-HCO3	292.1	7.79	-30.3
UQAC3039	2	1.52	Water table	154974	5408391	Granular	Ca-HCO3	15.0	7.67	200.4
UQAC3040	2	30.48	Confined	160254	5387053	Rock	Ca-HCO3	218.2	6.72	UNK
UQAC3041	2	91.4	Confined	169184	5368461	Rock	Ca-HCO3	139.9	7.78	UNK
UQAC3042	2	99.06	Water table	241964	5395217	Rock	Na-HCO3	162.5	6.59	-12.3
UQAC3045	2	69.24	Water table	265724	5367518	Rock	Ca-HCO3	343.4	7.88	53.9
UQAC3047	2	8.53	Water table	178298	5409045	Granular	Ca-Cl	79.8	8.64	161.1
UQAC3049	2	6.09	Water table	169233	5397978	Granular	Ca-HCO3	197.2	10.91	90.5
UQAC3050	2	1.52	UNK	245065	5357875	Granular	Na-Cl	816.4	9.34	68.9
UQAC4000	2	28.96	Semiconfined	225797	5351865	Rock	Ca-HCO3	261.7	6.26	327.3
UQAC4001	2	UNK	UNK	258480	5394530	Granular	Ca-HCO3	49.1	5.3	UNK
UQAC4002	2	UNK	UNK	156622	5426407	Granular	Ca-HCO3	41.0	7.91	743.9
UQAC4003	2	UNK	UNK	166326	5373105	Granular	Ca-HCO3	236.6	6.53	UNK
UQAC4004	2	15.24	Water table	209973	5378685	Rock	Na-HCO3	491.7	9.43	-198
UQAC4006	2	149.3	Water table	245377	5355654	Rock	Ca-HCO3	260.0	10.6	91.8
UQAC4007	2	4.87	Water table	208113	5371090	Granular	Ca-HCO3	328.5	9.44	37.5
UQAC4008	2	7.01	Water table	208952	5371466	Granular	Ca-HCO3	292.2	7.56	-22.7
UQAC4009	2	76.21	UNK	245937	5356010	Rock	Ca-HCO3	393.3	7.95	-105.2
UQAC4010	2	198.17	UNK	208242	5362090	Rock	Ca-HCO3	508.6	UNK	UNK
UQAC4011	2	4.57	Water table	207084	5370344	Granular	Ca-HCO3	280.4	8.91	89.2
UQAC4012	2	68.59	Water table	241852	5366027	Rock	Na-HCO3	170.6	7.17	-158.1
UQAC4013	2	38.1	Water table	242040	5366098	Rock	Ca-HCO3	207.7	7.26	-98.9
UQAC4015	2	106.7	UNK	224475	5375517	Rock	Na-HCO3	397.7	6.86	-277.3
UQAC4016	2	UNK	Water table	175750	5369860	Granular	Ca-HCO3	283.5	8.63	86.3
UQAC4018	2	68.59	UNK	162214	5384229	Rock	Ca-HCO3	280.2	7.62	UNK
UQAC4019	2	7.62	Confined	167073	5383042	Granular	Ca-HCO3	194.3	9.48	190
UQAC4021	2	56.09	UNK	174997	5384033	Rock	Ca-HCO3	374.8	7.86	505.4
UQAC4022	2	53.35	Confined	175105	5384029	Rock	Ca-HCO3	419.3	8.74	505.1
UQAC4023	2	UNK	Water table	224031	5377258	Granular	Ca-HCO3	454.7	9.12	-75
UQAC4024	2	92.98	Semiconfined	217548	5385342	Rock	Ca-HCO3	232.4	7.56	218.1
UQAC4029	2	4.87	Water table	150878	5404897	Granular	Ca-HCO3	99.8	10.04	113.3
UQAC4030	2	35.06	UNK	152814	5393558	Rock	Ca-HCO3	87.5	9.04	-53
UQAC4031	2	48.78	Confined	157001	5388711	Granular	Ca-HCO3	233.4	7.35	-255.7
UQAC4033	2	25.91	Confined	156560	5397823	Granular	Na-HCO3	200.0	10.03	-194.6

Sample	Cluster	Depth	Hydrogeological Context	X	Y	Aquifer type	Water type	TDS (Mg/L)	Temperature (Deg. Celcius)	Eh (mV)
UQAC4034	2	53.35	Confined	181250	5420048	Rock	Ca-HCO3	487.2	7.83	-210.6
UQAC4036	2	6.09	UNK	186808	5424099	Granular	Ca-HCO3	106.3	11.81	-123.7
UQAC4037	2	76.2	UNK	193418	5418738	Rock	Na-HCO3	497.4	8.56	UNK
UQAC4038	2	3.04	Water table	188966	5406099	Granular	Ca-HCO3	79.6	10.57	UNK
UQAC4041	2	4.57	Water table	178548	5401075	Granular	Ca-HCO3	209.0	8.79	UNK
UQAC4042	2	12.192	Water table	161440	5422474	Granular	Ca-HCO3	102.8	8.69	166.9
UQAC4044	2	50.3	Confined	181250	5420048	Rock	Na-HCO3	351.3	7.98	UNK
UQAC4045	2	7.62	Water table	180694	5413524	Granular	Na-Cl	62.0	7.33	148.9
UQAC4047	2	5.48	Water table	185940	5413296	Granular	Na-HCO3	25.5	7.12	187.1
UQAC4048	2	82.29	UNK	205378	5392014	Rock	Na-HCO3	401.0	7.69	58.1
UQAC4049	2	3.04	Water table	224349	5392459	Granular	Ca-HCO3	137.2	11.19	144.3
UQAC4051	2	UNK	Confined	204515	5400535	Granular	Na-Cl	174.4	7.78	UNK
UQAC4052	2	85.36	Confined	204486	5401711	Rock	Na-Cl	817.0	8.05	720.1
UQAC4053	2	0	Confined	205387	5399715	Granular	Ca-HCO3	28.6	9.42	278
UQAC4054	2	91.4	Confined	206253	5391069	Rock	Na-HCO3	378.9	11.82	-104.7
UQAC4057	2	UNK	UNK	256547	5357715	Rock	Na-HCO3	443.0	7.36	-225.4
UQAC4060	2	45.73	UNK	299304	5352057	Rock	Na-HCO3	179.6	8.77	-276.7
UQAC4064	2	3.65	Water table	213761	5401268	Granular	Na-Cl	183.6	12.18	78
UQAC4065	2	76.21	UNK	244469	5362091	Rock	Ca-HCO3	171.6	7.23	-38.6
UQAC4067	2	9.14	UNK	256248	5392384	Granular	Ca-HCO3	65.8	10.01	110.3
UQAC4068	2	0	Confined	255108	5390654	Granular	Ca-HCO3	59.7	UNK	UNK
UQAC4069	2	3.04	Water table	237039	5369923	Granular	Ca-HCO3	463.9	15.6	6.4
UQAC4071	2	6.09	Water table	213780	5401351	Granular	Ca-HCO3	49.5	14.31	124.5
UQAC4072	2	6.7	Water table	214920	5400032	Granular	Ca-HCO3	108.3	10.48	107.2
UQAC6002	2	17.7	Water table	166210	5403924	Granular	Ca-HCO3	43.7	7.85	UNK
UQAC6006	2	140.2	Confined	179981	5406834	Rock	Na-Cl	1092.6	7.39	-152.8
UQAC6010	2	9.1	Water table	255031	5390453	Granular	Ca-HCO3	80.8	7.64	80
1JW04	2	82.296	Water table	231788	5366922	Rock	Ca-HCO3	62.4	6.60	-134.20
1JW05	2	131.06	Water table	230983	5367699	Rock	Na-HCO3	228.3	10.70	-99.40
1JW08	2	91.44	Semiconfined	255864	5368317	Rock	Na-Cl	1236.5	8.00	57.90
1JW31	2	76.2	Confined	233735	5367073	Rock	Na-HCO3	306.5	6.80	100.90
1JW37	2	106.68	Confined	233558	5367172	Rock	Ca-HCO3	181.3	10.60	8.30
2JW15	2	25.908	Confined	192529	5411685	Granular	Na-HCO3	836.7	7.30	8.00
2JW17	2	36.576	Semiconfined	255810	5368354	Rock	Na-Cl	577.0	7.30	-65.40
3JW01	2	50.292	Confined	243535	5386048	Rock	Na-HCO3	331.2	8.90	-131.80
3JW21	2	115.82	Confined	224981	5386608	Rock	Ca-HCO3	285.0	6.70	28.30
3JW29	2	85.344	Semiconfined	168657	5394899	Rock	Na-HCO3	627.3	7.10	-24.00
3JW34	2	30.48	Semiconfined	228893	5363586	Rock	Ca-HCO3	988.9	7.80	7.10

Sample	Cluster	Depth	Hydrogeological Context	X	Y	Aquifer type	Water type	TDS (Mg/L)	Temperature (Deg. Celcius)	Eh (mV)
UQAC1105	3	131.06	Semiconfined	311371	5345987	Rock	Ca-Cl	5227.9	8.48	-245.7
UQAC2034	3	UNK	UNK	210671	5381047	Rock	Ca-Cl	2113.4	9.23	82.9
UQAC3046	3	106.68	Semiconfined	210795	5384669	Rock	Ca-Cl	2857.2	8.42	-101.9
UQAC4066	3	153.9	Semiconfined	255033	5390451	Rock	Na-Cl	2182.8	6.92	-110.9
1JW03	3	106.68	Water table	231034	5367634	Rock	Na-Cl	3658.4	6.50	-258.50
1JW35	3	0	Confined	159455	5387750	Rock	Ca-Cl	2739.9	6.10	108.40
2JW09	3	0	Water table	210633	5380830	Rock	Ca-Cl	2185.5	7.40	-1.30
2JW10	3	106.68	Semiconfined	172254	5376840	Rock	Ca-Cl	2873.8	6.80	-13.10
2JW11	3	64.008	Semiconfined	172373	5376792	Rock	Ca-Cl	2762.6	6.90	3.20
2JW16	3	0	Water table	222812	5377818	Rock	Ca-Cl	2863.4	7.30	29.30
2JW18	3	91.44	Water table	210559	5380888	Rock	Ca-Cl	3904.0	7.60	-20.90
3JW04	3	118.87	Confined	225396	5386060	Rock	Ca-Cl	3157.3	8.30	-32.50
UQAC1034	4	8	Confined	201983	5404056	Granular	Na-Cl	5573.4	7.5	27.9
UQAC4059	4	UNK	Water table	249534	5379654	Rock	Na-Cl	7291.4	7.79	-21.8
UQAC6012	4	105.2	Confined	166207	5403920	Rock	Na-Cl	6301.0	7.22	-100
UQAC6013	4	69.3	Confined	166210	5403924	Granular	Na-Cl	6107.6	7.55	-97.9
2JW14	4	0	Confined	193695	5406277	Rock	Na-Cl	8266.6	4.90	3.90

Sample	pH	Dissolved Oxygen	Sodium	Magnesium	Potassium	Calcium	Bicarbonates	Chlorides	Sulfates
UQAC1011	7.72	UNK	75	3.3	0.54	130	104.92	280	9.5
UQAC1019	7.44	UNK	20	6.9	3.7	160	86.62	64	360
UQAC1048	7.31	UNK	350	13	13	9.8	536.8	340	79
UQAC1071	7.61	0.73	980	52	21	150	317.2	1900	120
UQAC1098	8.24	0	240	12	1.9	170	92.72	590	29
UQAC2047	8.1	0	220	15	11	200	183	630	63
UQAC2048	7.22	0	330	13	14	11	439.2	310	26
UQAC2091	8.71	0	410	18	14	19	207.4	570	130
UQAC2128	10.06	0	560	12	20	2.1	683.2	510	1
UQAC3024	7.55	0.02	480	20	20	18	500.2	590	69
UQAC3036	7.57	0	990	79	33	180	244	1900	120
UQAC3052	5.53	0	450	0.007	1.3	0.06	353.8	390	130
UQAC6007	7.41	0	490	20	34	36	341.6	690	68
1JW01	8.37	0.00	100	7	2	57	113	29	250
1JW02	8.48	2.24	550	34	18	44	268	770	400
1JW07	7.99	0.00	880	19	11	100	195	1500	60
1JW15	8.09	0.00	830	33	31	58	381	1100	250
1JW26	6.93	0.00	840	0	7	0	288	1100	5
1JW28	8.10	0.00	760	33	23	20	287	870	200
1JW38	6.37	0.00	700	30	27	72	484	890	100
2JW02	7.68	0.70	1400	20	15	130	122	2400	70
2JW04	7.66	9.90	340	16	3	310	156	920	150
2JW08	7.62	0.12	350	51	8	190	144	930	5
2JW12	6.47	0.05	160	42	23	66	303	330	1
2JW19	8.23	0.22	260	3	9	3	510	110	5
2JW20	7.60	0.16	79	10	3	160	118	360	15
3JW05	8.47	0.11	370	13	15	21	354	390	100
3JW08	8.30	0.19	500	16	19	27	486	530	60
3JW10	7.99	0.17	680	31	29	77	576	860	200
3JW12	8.79	0.24	280	4	10	3	554	100	45
UQAC1001	6.18	0	42	5.4	4.4	21	183	1.7	16
UQAC1002	7.88	0	120	8.3	4.5	23	219.6	130	21
UQAC1003	7.1	UNK	42	16	3.5	110	292.8	130	20
UQAC1004	7.92	UNK	60	3.3	1.9	15	158.6	37	18
UQAC1005	7.62	UNK	110	7.8	3.2	32	134.2	170	25
UQAC1006	6.89	UNK	2.2	1.8	0.89	19	61	0.66	9.3
UQAC1008	7.89	UNK	24	4.3	1.6	19	134.2	2	8.6
UQAC1012	4.7	UNK	4.3	2.1	2.5	23	70.76	3	4.8

Sample	pH	Dissolved Oxygen	Sodium	Magnesium	Potassium	Calcium	Bicarbonates	Chlorides	Sulfates
UQAC1013	8.47	UNK	97	1.7	2	7	183	45	21
UQAC1014	6.23	UNK	25	5.6	4.3	32	183	7.6	11
UQAC1015	7.74	UNK	54	9.7	5.2	24	207.4	30	20
UQAC1016	5.58	UNK	25	7.2	2.8	60	231.8	10	26
UQAC1017	6.29	UNK	4.2	3.5	2.7	70	207.4	8.6	11
UQAC1020	6.67	UNK	9.4	4.3	0.88	26	84.18	21	14
UQAC1021	8.77	UNK	60	1.1	1.1	5.7	146.4	18	15
UQAC1022	6.96	UNK	31	13	2	67	158.6	120	20
UQAC1023	6.14	UNK	3.7	4.4	1.6	69	170.8	34	35
UQAC1024	7.66	UNK	10	6.2	1.3	54	219.6	1.7	15
UQAC1025	7.85	UNK	65	1.4	3.2	3.2	195.2	1.9	12
UQAC1026	7.11	UNK	41	1.2	0.52	11	92.72	30	16
UQAC1028	6.02	UNK	4.1	3.5	1.9	13	59.78	4.1	7.3
UQAC1029	5.73	UNK	6.1	15	3.8	30	146.4	12	9.3
UQAC1030	5.41	UNK	14	19	5.1	33	219.6	7.1	5.6
UQAC1032	5.55	UNK	2.7	6.8	1.8	10	65.88	2.2	7.8
UQAC1033	6.96	UNK	38	9.4	6.4	16	195.2	3.3	4.7
UQAC1035	4.38	UNK	11	2.4	2.2	11	67.1	0.6	0.7
UQAC1036	5.12	UNK	14	8.4	14	79	292.8	34	11
UQAC1038	6.59	UNK	49	17	7.8	89	341.6	110	5.5
UQAC1040	5.7	UNK	1.4	0.5	0.53	3.9	14.64	0.8	3.4
UQAC1041	8.96	UNK	80	0.56	3.1	1.3	219.6	4.5	8.6
UQAC1042	4.49	UNK	2.1	1.5	0.92	11	40.26	0.07	4
UQAC1043	6.27	UNK	85	0.007	0.19	0.06	134.2	48	24
UQAC1044	4.2	UNK	9.3	11	3.3	24	146.4	5.4	9.4
UQAC1045	5.64	UNK	48	15	5.9	21	256.2	24	18
UQAC1046	5.66	UNK	1.6	1.4	0.4	33	114.68	0.4	3.4
UQAC1049	5.61	UNK	4	3.2	1.3	7.1	45.14	3.6	3.9
UQAC1050	6.02	UNK	21	6.3	2.4	25	102.48	45	12
UQAC1051	5.56	UNK	4.4	2.1	1.3	9.6	51.24	0.4	3.3
UQAC1052	6.78	UNK	13	1	1.8	11	58.56	1.1	16
UQAC1053	6.7	UNK	18	3.3	2.4	32	106.14	6.4	49
UQAC1055	7.62	25.1	7.4	4.9	2	63	207.4	7.9	16
UQAC1058	7.81	0	2.1	1.4	0.51	45	146.4	6.7	2.9
UQAC1059	7.43	0	7.9	5.3	0.9	90	256.2	12	0.2
UQAC1063	7.34	0	6.2	7.2	3.3	79	244	7.4	24
UQAC1064	9.26	5.92	1.5	0.7	0.69	6.1	28.06	0.3	1.4
UQAC1065	7.83	4.41	6.3	7	4.2	48	183	4.2	11

Sample	pH	Dissolved Oxygen	Sodium	Magnesium	Potassium	Calcium	Bicarbonates	Chlorides	Sulfates
UQAC1066	8.14	0.94	7.8	6.5	1.6	36	122	2.7	11
UQAC1067	8.6	0	29	5.6	0.55	35	134.2	49	7.6
UQAC1069	8.04	0	40	11	3.1	56	292.8	35	2.1
UQAC1073	7.78	4.08	1.6	1.3	0.99	44	134.2	1.1	6.3
UQAC1074	7.55	0	20	6.7	2.8	71	207.4	45	25
UQAC1075	7.94	0	11	12	4.5	36	207.4	5.2	0.1
UQAC1076	9.74	0	50	0.29	1.4	1.9	122	2	12
UQAC1077	6.48	3.59	4.8	3	1.2	13	57.34	3.9	3
UQAC1078	6.26	3.56	3.1	2	0.71	13	42.7	6.7	3.2
UQAC1079	8.06	0.22	5.4	4.3	1	24	104.92	0.5	1.1
UQAC1080	7.85	0	7.9	7.5	2.2	68	207.4	31	13
UQAC1081	7.91	2.54	5.6	3.8	1.7	45	146.4	19	5.7
UQAC1082	8.11	0	5.8	7.7	2.3	49	207.4	0.9	4.7
UQAC1083	7.51	2.27	3.3	6.9	1.6	73	219.6	8.1	28
UQAC1084	6.51	3.09	2.3	1.7	0.45	7.8	39.04	0.5	3.6
UQAC1086	7.57	3.83	7.5	8.1	2.2	60	219.6	6.8	7
UQAC1087	7.01	3.75	2.8	2.4	0.54	29	98.82	1.1	5.8
UQAC1088	7.68	0	4.9	6.5	1.5	40	158.6	4.8	5
UQAC1089	8.07	0	2.4	3.3	1.4	38	122	0.5	10
UQAC1090	6.51	0	20	4.4	3.3	77	207.4	61	8.7
UQAC1092	9.12	0	130	3.9	1.3	22	120.78	160	7.8
UQAC1094	8.4	0	61	6.6	1.6	20	146.4	61	17
UQAC1095	7.61	0	40	11	7	49	280.6	16	23
UQAC1096	8.93	0	60	1.4	1.1	5.1	170.8	8.9	2.6
UQAC1097	8.94	0	31	3.8	2.4	14	118.34	12	7.5
UQAC1099	8.85	0	150	3.9	1.8	14	353.8	35	35
UQAC1101	8.08	0	45	5.3	4.5	74	134.2	110	17
UQAC1103	7	1.69	300	3.9	2.8	51	231.8	380	38
UQAC1108	8.2	0.97	17	9.2	4.9	37	183	17	20
UQAC1109	7.99	6.04	8.2	7.1	2	36	158.6	1.4	18
UQAC1110	8.73	0	11	4.8	1.8	15	92.72	11	2.1
UQAC1111	6.13	43.7	2.1	0.75	0.84	5.8	26.84	0.3	3.7
UQAC1112	7.62	0	14	8.2	2.7	48	219.6	8.2	16
UQAC1113	5.93	3.77	2	0.27	0.6	5.3	19.52	0.5	5.7
UQAC1114	6.16	4.54	15	9.4	5.3	47	122	47	12
UQAC1115	9.05	0	82	1.6	0.7	8.6	183	27	15
UQAC1116	7.95	0.24	29	9.7	1.9	51	183	53	15
UQAC1117	7.44	5.59	5.5	7.5	2.9	58	219.6	5.1	13

Sample	pH	Dissolved Oxygen	Sodium	Magnesium	Potassium	Calcium	Bicarbonates	Chlorides	Sulfates
UQAC1118	5.59	6.32	1.1	0.59	0.4	12	41.48	0.07	3.6
UQAC1119	8.39	0.69	69	10	5.6	47	219.6	36	84
UQAC1120	7.92	5.2	4	4.9	1.8	46	134.2	9.1	17
UQAC1121	9.32	1.03	58	0.42	1.4	2.3	122	9.1	22
UQAC1123	UNK	UNK	2	0.56	0.99	5.6	21.96	0.18	1
UQAC2001	8.06	0	1.2	1.2	0.56	51	158.6	0.32	3.2
UQAC2002	6.59	10	1.6	0.77	0.52	6.5	18.3	1.9	3.1
UQAC2003	6.93	1.25	2.2	2.4	0.86	42	134.2	3.1	5.8
UQAC2004	7.04	11.75	1.8	0.95	0.6	9.5	32.94	0.63	5.3
UQAC2005	5.9	3.5	6.6	1.1	2.5	20	41.48	12	13
UQAC2008	6.62	8.14	1.1	0.95	0.33	16	54.9	0.34	4.6
UQAC2009	7.6	8.85	1.5	0.99	0.38	13	45.14	0.33	3.5
UQAC2010	8.26	9.22	1.8	1.3	0.73	19	68.32	0.63	4.5
UQAC2011	6.44	0	1.8	0.58	0.52	6.2	30.5	0.59	1.2
UQAC2012	6.41	7.72	2.9	1.2	0.81	5.8	28.06	0.58	3.3
UQAC2013	5.68	10.6	0.9	0.15	0.19	3.3	8.54	0.31	2.5
UQAC2014	6.29	11.17	0.98	0.19	0.19	2.7	8.54	0.38	2.4
UQAC2015	8.73	0	7.7	4.3	1.7	22	95.16	0.49	9.9
UQAC2016	8.43	0	7.5	4.4	1.4	24	106.14	0.9	6.6
UQAC2017	8.09	0	7.4	4.9	2.3	63	134.2	8.9	48
UQAC2018	7.84	3.62	62	2.8	2.1	78	195.2	98	18
UQAC2019	7.12	0	19	7.2	1.2	95	317.2	26	10
UQAC2020	6.99	6.67	2.9	6.7	1.1	93	305	1.6	11
UQAC2021	8.94	0.13	86	0.39	0.13	2.2	183	19	13
UQAC2022	8.51	0	32	5	1.8	38	119.56	34	17
UQAC2023	5.71	6.77	1.3	0.16	0.23	2.2	7.32	0.69	2.4
UQAC2025	10.8	8.5	1.9	1.1	2	6.7	24.4	2.8	6.8
UQAC2026	9.24	0	20	6.9	4.5	18	146.4	1.5	11
UQAC2029	7.45	1.38	4	5	1.4	48	183	2.6	8.7
UQAC2030	7.09	90	3.5	4.6	0.96	99	329.4	10	7.1
UQAC2031	7.84	8.95	31	8.6	2.3	66	195.2	70	17
UQAC2033	8	0	74	2.8	1.5	15	195.2	47	16
UQAC2035	8.47	2.4	13	2.4	0.64	22	109.8	1.2	9.7
UQAC2036	7.77	0	14	5	0.87	33	108.58	33	12
UQAC2038	8.53	0	33	3.5	0.79	20	158.6	1	5.1
UQAC2039	8.64	0	110	3	3	10	292.8	22	18
UQAC2042	6.48	0	2.8	4.1	1.5	7.4	54.9	0.62	3
UQAC2044	8.01	0	140	2.6	3.3	7.1	256.2	65	24

Sample	pH	Dissolved Oxygen	Sodium	Magnesium	Potassium	Calcium	Bicarbonates	Chlorides	Sulfates
UQAC2045	8.43	0	35	5.7	5.9	16	170.8	2.3	5.2
UQAC2046	6.37	4.24	4.7	5.1	3.7	35	111.02	29	1.6
UQAC2050	6.19	6.46	7.5	3.9	1.5	28	69.54	19	13
UQAC2051	6.15	6.76	1.7	1	0.72	13	43.92	0.07	4.1
UQAC2052	8.51	8.12	1.4	1.3	1.1	20	71.98	0.9	3.6
UQAC2053	6.69	9.03	1.3	0.42	1.3	8	31.72	0.5	2.7
UQAC2054	7.87	0	57	0.021	1	0.12	134.2	2	16
UQAC2055	7.7	3.14	62	3.9	2.1	54	183	120	15
UQAC2059	5.66	3.24	3.8	1.2	1.4	59	37.82	100	3.8
UQAC2060	7.46	0	35	10	4.6	51	305	12	23
UQAC2062	8.07	3.17	1.7	1.7	0.69	28	107.36	0.3	3.6
UQAC2063	8.01	0	83	13	5.5	61	244	96	81
UQAC2064	8.65	0	48	2.4	4.5	9.9	158.6	6.1	12
UQAC2069	8.57	0	140	3.5	6.7	4.5	414.8	14	6
UQAC2071	8.2	0	27	3.4	3.6	9.2	107.36	4.4	8.4
UQAC2073	8.46	0	2.9	3.5	1	29	101.26	1.5	11
UQAC2074	6.81	9.07	2	1.6	0.48	14	48.8	0.3	6.7
UQAC2075	7.12	0	12	19	3.8	120	427	33	23
UQAC2076	8.53	0	84	17	1.6	94	104.92	230	45
UQAC2077	6.32	6.99	4.7	1.8	1.1	13	45.14	2.8	4.9
UQAC2078	8.79	0	79	1.6	6.2	4.9	158.6	39	24
UQAC2079	6.09	8.79	2	1.7	0.66	3.9	17.08	1.3	3.6
UQAC2081	6.21	7.64	2.8	1.6	0.54	5	18.3	3.4	3.3
UQAC2082	8.22	0	16	8.7	7.1	15	146.4	4.3	3.5
UQAC2086	5.61	0	3.3	2.6	0.68	6.1	26.84	12	3.5
UQAC2088	7.73	1.7	3.6	11	3.9	81	268.4	6.4	41
UQAC2089	8.01	8.63	4	6.1	2.5	64	219.6	4.8	25
UQAC2090	7.54	7.55	45	3.9	0.65	62	117.12	110	40
UQAC2092	8.1	6.85	1.9	2.2	0.69	24	82.96	1.6	8.3
UQAC2093	8.51	9.42	1.4	0.9	0.35	22	75.64	0.3	3.4
UQAC2094	7.35	0	22	13	4.2	59	280.6	13	20
UQAC2096	7.84	10.29	6.9	9.3	2.3	20	107.36	2.9	11
UQAC2097	7.57	8.48	13	14	4.8	21	170.8	1.1	5
UQAC2098	8.33	0	13	11	5.6	24	134.2	14	9.2
UQAC2099	5.85	0.99	1.2	0.54	1.1	9.5	32.94	0.07	2.4
UQAC2100	7.21	4.48	49	8.2	2.7	79	231.8	110	10
UQAC2101	8.56	0	4	3.5	2.8	21	86.62	1.7	4.7
UQAC2103	7.83	0.9	2.5	2.8	2.1	11	50.02	0.5	6.3

Sample	pH	Dissolved Oxygen	Sodium	Magnesium	Potassium	Calcium	Bicarbonates	Chlorides	Sulfates
UQAC2104	5.67	0	1.2	0.34	0.33	3	7.32	0.4	3.1
UQAC2106	7.81	2.78	3.3	1.5	0.98	37	113.46	11	5.1
UQAC2107	8.01	0	2	5.4	1.8	44	146.4	1.6	15
UQAC2108	8.31	0	2.4	0.8	0.54	28	92.72	3	2.1
UQAC2112	6.57	5.77	2.1	0.68	0.8	5.8	19.52	1.4	2.9
UQAC2114	8.03	0	2.5	3.7	1.1	39	134.2	1.8	5.7
UQAC2116	7.31	7.49	5.2	8.9	2.2	52	195.2	1.3	14
UQAC2117	7.39	3.33	7.6	10	2.4	76	256.2	9.1	23
UQAC2118	7.68	0	3.7	13	2	76	256.2	7	37
UQAC2119	6.89	1.98	3.4	3.9	2.6	29	111.02	4.4	4.8
UQAC2120	7.63	2.85	9.5	9.7	3.6	23	118.34	8.3	10
UQAC2121	8.32	0	21	4.6	4	20	117.12	12	5.2
UQAC2122	7.52	4.13	15	3.6	1	31	122	13	7.2
UQAC2123	7.79	0	26	16	7	26	195.2	16	9
UQAC2124	6.87	7.3	6.7	5.7	1.7	13	64.66	11	5.7
UQAC2125	7.89	0	12	13	3.2	34	158.6	9.7	23
UQAC2126	8.48	7.73	11	3.4	2.9	22	89.06	12	7.1
UQAC2129	6.52	7.85	2.3	0.45	0.69	7.2	25.62	1	1.9
UQAC2130	6.02	1.5	3.2	0.57	0.87	7.4	20.74	3.5	3.3
UQAC2131	7.49	0.77	13	8.2	3.5	46	207.4	9.6	7
UQAC2132	7.21	0	100	16	3.2	37	146.4	130	13
UQAC2133	7.8	1.54	3.5	8	1.1	71	219.6	10	21
UQAC2135	7.64	0	8.5	26	5.3	76	341.6	17	28
UQAC3000	5.51	9.24	1.1	0.81	0.44	3.8	12.2	0.58	4.6
UQAC3002	6.74	2.14	89	14	2.7	49	122	190	10
UQAC3004	8.81	4.4	42	2.1	1.7	6.1	104.92	8.4	17
UQAC3009	9	4.13	130	1.7	0.36	3.8	219.6	72	4.1
UQAC3011	7.67	2.45	1.5	3	0.77	55	170.8	1.4	5.8
UQAC3013	8.39	3.95	45	5.2	4.1	15	122	31	12
UQAC3014	7.25	0.25	56	6.5	1.8	46	183	70	18
UQAC3015	7.22	5.43	45	26	6.4	130	366	150	28
UQAC3018	4.91	8.14	1.3	0.25	0.31	1.2	7.32	0.9	0.8
UQAC3019	8.36	0	49	4.4	4.4	14	158.6	14	16
UQAC3021	8.24	0.4	39	11	4.6	30	170.8	33	22
UQAC3022	5.07	5.34	7.4	0.31	0.86	6.7	25.62	7	3.9
UQAC3023	6.53	0.76	9.1	12	3.9	24	146.4	2.3	6.7
UQAC3025	7.53	4.73	8.4	6.8	1.8	63	207.4	3.5	14
UQAC3027	7.44	7.81	2.1	1.4	0.9	58	170.8	4.1	6

Sample	pH	Dissolved Oxygen	Sodium	Magnesium	Potassium	Calcium	Bicarbonates	Chlorides	Sulfates
UQAC3028	6.76	2.67	4	3.6	2.2	64	183	6.8	18
UQAC3032	5.61	7.54	1	0.58	1.1	3.2	10.98	0.7	5
UQAC3035	5.05	2.76	3.9	1.6	0.74	5.4	14.64	11	0.1
UQAC3037	4.93	1.74	9.2	0.31	0.4	2.2	14.64	9.5	3.1
UQAC3038	8.72	0.04	57	2.5	1.6	19	183	13	16
UQAC3039	5.34	6.16	1.7	0.42	0.14	2.3	7.32	1.1	2
UQAC3040	7.15	0.98	6.4	4.6	1.8	42	146.4	3	14
UQAC3041	6.63	0.92	12	2.9	1.1	23	76.86	12	12
UQAC3042	9.43	0	43	0.19	0.75	2.4	102.48	5.4	8.3
UQAC3045	7.77	1.2	29	15	3.6	40	231.8	10	14
UQAC3047	5	6.22	3.8	0.89	1.2	21	6.1	41	5.8
UQAC3049	7.31	4.36	5.5	1.6	1.1	46	117.12	19	6.9
UQAC3050	7.27	4.44	120	25	15	96	268.4	270	22
UQAC4000	7.76	7.15	1.6	5.1	1.9	56	170.8	2.1	12
UQAC4001	5.79	13.3	2.3	1.1	0.89	5.7	21.96	1.7	4
UQAC4002	5.49	4.39	1.3	0.93	1.3	5.7	20.74	0.16	2.8
UQAC4003	7.58	5.78	4	2.6	1.4	49	158.6	3.6	4.3
UQAC4004	7.45	3.6	140	0.007	0.6	0.54	268.4	54	16
UQAC4006	7.77	3.37	20	6	1.8	36	158.6	9.6	15
UQAC4007	7.03	0.59	14	2	2.2	67	207.4	14	12
UQAC4008	7.58	0.21	10	2.6	1.3	61	183	15	8.6
UQAC4009	6.83	1.01	100	0.007	0.12	0.33	256.2	8.7	5
UQAC4010	UNK	UNK	47	12	3.7	77	195.2	110	45
UQAC4011	7.45	1.48	20	1.4	1.4	50	170.8	12	15
UQAC4012	8.21	0.39	24	2.6	1.8	16	95.16	8	12
UQAC4013	8.21	1.18	20	5.7	1.4	26	111.02	16	15
UQAC4015	8.44	0.42	81	8.9	3.7	21	170.8	65	33
UQAC4016	7.41	2.32	2.4	7.2	1.7	56	195.2	0.9	10
UQAC4018	7.7	1.58	6.1	2.7	1	63	146.4	18	26
UQAC4019	6.39	2.49	9.3	8.3	2.2	25	109.8	3.8	11
UQAC4021	7.25	0.91	21	13	4.3	50	256.2	11	3.7
UQAC4022	7.21	0.86	10	9.4	3.1	79	292.8	9.1	2.7
UQAC4023	6.93	0.72	7.5	15	5.6	84	280.6	16	30
UQAC4024	6.44	3.85	5.5	2.7	0.92	43	146.4	8.3	11
UQAC4029	5.41	3.92	5.2	4.1	1.5	8.7	47.58	0.57	4.6
UQAC4030	6.41	0	2.9	1.9	0.62	6.9	41.48	1.5	0.7
UQAC4031	7.92	0	17	3.3	2.1	40	122	9.8	22
UQAC4033	8.25	0	23	6	6.1	15	119.56	9.6	2.3

Sample	pH	Dissolved Oxygen	Sodium	Magnesium	Potassium	Calcium	Bicarbonates	Chlorides	Sulfates
UQAC4034	7.37	0	46	22	5.6	50	256.2	67	18
UQAC4036	5.45	0	7	3.2	2.2	12	46.36	11	2.7
UQAC4037	8.06	0	130	3	5.3	7.3	256.2	64	16
UQAC4038	6.03	3.51	2.4	0.91	0.8	13	41.48	1.6	4.9
UQAC4041	6.29	0	0.15	5.3	3	35	134.2	3.5	3.1
UQAC4042	6.08	5.76	3.8	4.4	1.9	11	57.34	3.7	5.8
UQAC4044	8.37	0	55	11	10	13	244	0.8	0.1
UQAC4045	4.96	5.07	13	0.62	0.78	3.5	7.32	26	2.4
UQAC4047	4.51	3.44	2.1	0.19	0.52	1.8	7.32	3.1	2.2
UQAC4048	8.54	0.87	100	1.9	4.4	4.7	231.8	39	3.3
UQAC4049	5.75	3.33	2.3	3.3	2.1	28	73.2	2.3	12
UQAC4051	5.59	2.02	35	3.3	2.1	17	26.84	67	8.6
UQAC4052	7.62	0.33	170	14	3.1	81	256.2	260	12
UQAC4053	5.06	6.71	1.3	0.27	0.6	2.6	9.76	1	3
UQAC4054	8.68	1	100	0.73	1.3	2.4	244	19	0.9
UQAC4057	8.01	0	71	6.8	8.2	38	244	44	17
UQAC4060	8.78	0	42	0.32	0.51	1.9	98.82	6.3	14
UQAC4064	5.5	0.44	37	1.7	4	14	40.26	55	12
UQAC4065	7.75	1.22	3.4	3.5	2.1	31	111.02	0.6	7.6
UQAC4067	5.8	7.1	2.5	0.79	0.57	9.2	26.84	4.1	10
UQAC4068	UNK	UNK	4.6	0.44	0.57	8	30.5	3.4	2.7
UQAC4069	6.84	1.57	5.6	4	7.5	110	305	2.6	12
UQAC4071	5.51	2.45	1.2	0.44	1	6.9	26.84	0.33	2.9
UQAC4072	6.39	5.36	8.5	2	2.4	16	46.36	8.7	10
UQAC6002	8.07	0	1.4	0.9	0.73	3.8	14.64	0.6	4.6
UQAC6006	6.89	0	330	13	20	32	219.6	440	38
UQAC6010	6.27	1.46	0.87	0.44	0.26	16	53.68	0.5	0.1
1JW04	5.90	7.50	2.9	2.7	1.0	7.8	21.5	4.0	6.5
1JW05	9.19	0.00	69.0	0.3	0.3	1.4	129.5	4.7	10.0
1JW08	9.11	0.00	410.0	4.6	5.6	21.0	199.1	560.0	20.0
1JW31	5.48	0.00	94.0	0.3	0.4	1.7	163.5	16.0	16.0
1JW37	7.22	2.73	18.6	4.6	3.0	22.0	103.7	5.6	10.0
2JW15	7.10	0.08	240.0	4.1	8.5	4.6	377.0	170.0	11.0
2JW17	8.66	0.79	160.0	3.1	2.7	12.3	217.2	130.0	40.0
3JW01	9.42	0.16	94.0	0.6	3.3	1.2	205.0	7.2	6.5
3JW21	6.41	0.13	15.9	7.5	4.8	34.0	153.7	32.0	16.0
3JW29	7.53	0.08	100.0	16.8	5.2	53.0	296.5	110.0	29.0
3JW34	6.90	0.16	55.0	14.0	4.3	170.0	438.0	170.0	110.0

Sample	pH	Dissolved Oxygen	Sodium	Magnesium	Potassium	Calcium	Bicarbonates	Chlorides	Sulfates
UQAC1105	8.6	0	570.0	3.0	1.6	1500.0	6.1	3000.0	53.0
UQAC2034	7.78	0	260.0	60.0	4.5	400.0	231.8	1000.0	110.0
UQAC3046	7.82	0	380.0	54.0	3.6	580.0	158.6	1600.0	81.0
UQAC4066	7.09	0.35	420.0	80.0	14.0	210.0	207.4	1200.0	1.2
1JW03	7.92	0.00	790.0	45.0	3.2	460.0	100.2	2200.0	7.5
1JW35	5.18	0.00	180.0	12.3	7.6	730.0	40.3	1700.0	7.0
2JW09	7.33	0.13	290.0	60.0	5.0	380.0	176.9	1100.0	130.0
2JW10	7.59	0.23	260.0	12.6	3.1	720.0	75.6	1500.0	250.0
2JW11	7.26	0.08	240.0	7.8	3.5	690.0	134.2	1400.0	240.0
2JW16	6.71	0.39	220.0	49.0	13.5	680.0	83.0	1700.0	70.0
2JW18	7.70	0.08	580.0	96.0	7.3	650.0	112.2	2100.0	300.0
3JW04	7.74	0.14	430.0	42.0	3.6	740.0	93.9	1800.0	5.5
UQAC1034	6.47	UNK	1600.0	100.0	55.0	60.0	695.4	2700.0	330.0
UQAC4059	7.59	1.82	1800.0	140.0	16.0	520.0	134.2	4200.0	420.0
UQAC6012	7.23	0	1900.0	160.0	64.0	120.0	427.0	3200.0	430.0
UQAC6013	7.2	0	1900.0	160.0	64.0	100.0	463.6	3000.0	420.0
2JW14	7.19	UNK	2500.0000	220.0000	82.0000	170.0	522.2	4200.0	530.0

Sample	Aluminium	Antimoine	Silver	Barium	Cadmium	Chromium	Cobalt	Copper	Manganese	Molybdene	Nickel
UQAC1011	0.0028	0.0005	0.00005	0.22	0.0001	0.0005	0.0005	0.0005	0.19	0.0078	0.0005
UQAC1019	0.018	0.0005	0.00012	0.017	0.0001	0.0005	0.0005	0.0005	0.062	0.0038	0.0005
UQAC1048	0.012	0.0005	0.00028	0.029	0.0001	0.00098	0.0005	0.0011	0.031	0.0044	0.0005
UQAC1071	0.0021	0.0005	0.00033	0.25	0.0001	0.0005	0.0005	0.0005	0.055	0.0016	0.0011
UQAC1098	0.0044	0.0005	0.00005	0.089	0.0001	0.0005	0.0005	0.0027	0.024	0.0009	0.0005
UQAC2047	0.02	0.0005	0.00005	0.07	0.0001	0.0005	0.0005	0.0005	0.061	0.0028	0.0005
UQAC2048	0.0085	0.0005	0.00005	0.037	0.0001	0.0005	0.0005	0.0005	0.0071	0.0017	0.0005
UQAC2091	0.013	0.0005	0.00005	0.053	0.0001	0.0005	0.0005	0.0005	0.011	0.0055	0.0005
UQAC2128	0.0048	0.0005	0.009	0.012	0.0001	0.0005	0.0005	0.0012	0.0092	0.006	0.001
UQAC3024	0.002	0.0005	0.00005	0.053	0.0001	0.0005	0.0005	0.0018	0.057	0.0028	0.0005
UQAC3036	0.0058	0.0005	0.00005	0.32	0.0001	0.0005	0.0005	0.0011	0.038	0.0005	0.0098
UQAC3052	0.0064	0.0005	0.00005	0.0005	0.0001	0.00054	0.0005	0.00078	0.0011	0.024	0.0005
UQAC6007	0.087	0.0005	0.00005	0.094	0.0001	0.0005	0.0005	0.0005	0.15	0.00056	0.0005
1JW01	0.0120	0.0005	0.00005	0.0800	0.0001	0.0005	0.0005	0.0005	0.0310	0.0026	0.0030
1JW02	0.0070	0.0005	0.00005	0.0500	0.0001	0.0005	0.0005	0.0005	0.0340	0.0026	0.0020
1JW07	0.0070	0.0005	0.00005	0.1700	0.0001	0.0005	0.0005	0.0070	0.0690	0.0026	0.0005
1JW15	0.0070	0.0005	0.00005	0.0600	0.0001	0.0005	0.0005	0.0020	0.0670	0.0026	0.0005
1JW26	0.0070	0.0005	0.00005	0.0005	0.0001	0.0005	0.0005	0.0005	0.0003	0.0026	0.0005
1JW28	0.0070	0.0005	0.00005	0.0200	0.0001	0.0005	0.0005	0.0005	0.0150	0.0026	0.0005
1JW38	0.0070	0.0005	0.00005	0.0700	0.0001	0.0005	0.0005	0.0005	0.0370	0.0026	0.0005
2JW02	0.0070	0.0005	0.00005	0.1600	0.0001	0.0005	0.0005	0.0005	0.1300	0.0026	0.0009
2JW04	0.0070	0.0005	0.00005	0.0200	0.0001	0.0005	0.0005	0.0005	0.1100	0.0026	0.0005
2JW08	0.0100	0.0005	0.00005	0.4700	0.0001	0.0005	0.0005	0.0005	0.1300	0.0026	0.0010
2JW12	0.0070	0.0005	0.00005	0.7600	0.0001	0.0005	0.0005	0.0005	0.0140	0.0026	0.0005
2JW19	0.0070	0.0005	0.00005	0.0100	0.0001	0.0005	0.0005	0.0005	0.0040	0.0026	0.0005
2JW20	0.0200	0.0005	0.00005	0.3100	0.0001	0.0005	0.0005	0.0030	0.0680	0.0026	0.0020
3JW05	0.0070	0.0005	0.00005	0.0430	0.0001	0.0005	0.0005	0.0005	0.0180	0.0026	0.0005
3JW08	0.0070	0.0005	0.00005	0.0390	0.0001	0.0005	0.0005	0.0005	0.0230	0.0026	0.0030
3JW10	0.0070	0.0005	0.00005	0.0800	0.0001	0.0005	0.0005	0.0005	0.0400	0.0026	0.0005
3JW12	0.0070	0.0005	0.00005	0.0110	0.0001	0.0005	0.0005	0.0005	0.0030	0.0026	0.0005
UQAC1001	0.0066	0.0005	0.00013	0.41	0.0001	0.0005	0.0005	0.0013	0.027	0.0011	0.0005
UQAC1002	0.013	0.0005	0.00014	0.33	0.0001	0.0005	0.0005	0.013	0.062	0.001	0.0005
UQAC1003	0.0028	0.0005	0.0004	0.26	0.0001	0.0005	0.0005	0.0013	0.57	0.0039	0.0005
UQAC1004	0.0042	0.0005	0.00023	0.59	0.0001	0.00052	0.0005	0.0005	0.006	0.00093	0.0005
UQAC1005	0.0029	0.0005	0.0012	0.32	0.0001	0.0005	0.0005	0.0005	0.025	0.0016	0.0005
UQAC1006	0.0028	0.0005	0.00005	0.1	0.0001	0.0005	0.0005	0.0011	0.0001	0.0027	0.0005
UQAC1008	0.0019	0.0005	0.0004	0.15	0.0001	0.0005	0.0005	0.0005	0.014	0.0015	0.0005
UQAC1012	0.0076	0.0005	0.00005	0.022	0.0001	0.0005	0.0005	0.026	0.0025	0.0005	0.0005

Sample	Aluminium	Antimoine	Silver	Barium	Cadmium	Chromium	Cobalt	Copper	Manganese	Molybdene	Nickel
UQAC1013	0.004	0.0005	0.00048	0.057	0.00067	0.0005	0.0005	0.0005	0.0052	0.0011	0.0005
UQAC1014	0.0088	0.0005	0.00034	0.061	0.0001	0.0005	0.0005	0.0005	0.00044	0.00085	0.0005
UQAC1015	0.0033	0.0005	0.00032	0.011	0.0001	0.0005	0.0005	0.016	0.023	0.0013	0.0005
UQAC1016	0.0096	0.0005	0.00029	0.16	0.0001	0.0005	0.0005	0.029	0.0087	0.00099	0.0012
UQAC1017	0.0075	0.0005	0.00015	0.026	0.0001	0.0005	0.0005	0.0007	0.062	0.0006	0.0005
UQAC1020	0.018	0.0005	0.00005	0.13	0.0001	0.0005	0.0005	0.012	0.00091	0.0005	0.0005
UQAC1021	0.0071	0.0005	0.00005	0.0099	0.0001	0.011	0.0005	0.0005	0.045	0.0023	0.02
UQAC1022	0.009	0.0005	0.00005	0.33	0.0001	0.0005	0.0005	0.054	0.079	0.00069	0.0012
UQAC1023	0.0075	0.0005	0.00014	0.03	0.0001	0.0005	0.0005	0.0063	0.072	0.0032	0.0014
UQAC1024	0.0071	0.0005	0.00026	0.1	0.0001	0.0005	0.0005	0.0005	0.011	0.004	0.0005
UQAC1025	0.008	0.0005	0.00005	0.047	0.0001	0.0005	0.0005	0.0005	0.01	0.0014	0.0005
UQAC1026	0.004	0.0005	0.00005	0.09	0.0001	0.0005	0.0005	0.0005	0.022	0.0026	0.0005
UQAC1028	0.018	0.0005	0.00005	0.028	0.0001	0.0005	0.00089	0.0005	0.075	0.0005	0.0005
UQAC1029	0.003	0.0005	0.00023	0.029	0.0001	0.0005	0.0005	0.038	0.0001	0.0005	0.0005
UQAC1030	0.002	0.0005	0.00015	0.015	0.0001	0.0005	0.0005	0.0005	0.0001	0.0038	0.0005
UQAC1032	0.0039	0.0005	0.00005	0.018	0.0001	0.0005	0.0005	0.0005	0.069	0.0026	0.0005
UQAC1033	0.026	0.0005	0.00005	0.011	0.0001	0.0005	0.0005	0.0005	0.053	0.002	0.0005
UQAC1035	0.011	0.0005	0.00005	0.014	0.0001	0.0005	0.0005	0.0005	0.0037	0.00073	0.0005
UQAC1036	0.007	0.0005	0.00015	0.11	0.0001	0.0005	0.0005	0.0005	1	0.001	0.0035
UQAC1038	0.0049	0.0005	0.00014	1.2	0.0001	0.0005	0.0005	0.0005	0.26	0.00055	0.0005
UQAC1040	0.0043	0.0005	0.00005	0.0069	0.0001	0.0005	0.0005	0.027	0.00099	0.0005	0.0005
UQAC1041	0.23	0.0005	0.00025	0.025	0.0001	0.0005	0.0005	0.0099	0.0058	0.0044	0.0005
UQAC1042	0.0095	0.0005	0.00041	0.018	0.0001	0.0005	0.0005	0.035	0.0094	0.0005	0.0005
UQAC1043	0.0031	0.0005	0.00031	0.0005	0.0001	0.0005	0.0005	0.0026	0.0013	0.0018	0.0005
UQAC1044	0.0005	0.0005	0.00018	0.02	0.0001	0.0005	0.0005	0.012	0.014	0.0006	0.0005
UQAC1045	0.0097	0.0005	0.00016	0.043	0.0001	0.0005	0.0005	0.011	0.00081	0.0031	0.0005
UQAC1046	0.0028	0.0005	0.00005	0.017	0.0001	0.0005	0.0005	0.0005	0.057	0.0005	0.0005
UQAC1049	0.0063	0.0005	0.00021	0.021	0.0001	0.0014	0.0005	0.019	0.0034	0.0005	0.0018
UQAC1050	0.023	0.0005	0.00021	0.087	0.0001	0.0017	0.0005	0.0049	0.038	0.002	0.0011
UQAC1051	0.0095	0.0005	0.00018	0.0055	0.0001	0.0018	0.0005	0.0092	0.00089	0.00087	0.0005
UQAC1052	0.01	0.0005	0.00005	0.024	0.0001	0.00082	0.0005	0.0017	0.0043	0.018	0.001
UQAC1053	0.0071	0.0005	0.00013	0.015	0.0001	0.0013	0.0005	0.0052	0.00081	0.0041	0.0005
UQAC1055	0.0058	0.0012	0.00037	0.04	0.0001	0.00073	0.0005	0.012	0.00096	0.0007	0.0005
UQAC1058	0.0028	0.0005	0.00005	0.018	0.0001	0.0005	0.0005	0.0005	0.0037	0.0005	0.0005
UQAC1059	0.0085	0.0005	0.00005	0.029	0.00028	0.0005	0.0021	0.0005	1.1	0.00078	0.0039
UQAC1063	0.0034	0.0005	0.00005	0.19	0.0001	0.0005	0.0005	0.002	0.17	0.00071	0.0005
UQAC1064	0.021	0.0005	0.00005	0.0038	0.0001	0.0005	0.0005	0.00062	0.00047	0.0005	0.0005
UQAC1065	0.0066	0.0005	0.00005	0.01	0.0001	0.001	0.0005	0.0005	0.00055	0.0005	0.0005

Sample	Aluminium	Antimoine	Silver	Barium	Cadmium	Chromium	Cobalt	Copper	Manganese	Molybdene	Nickel
UQAC1066	0.0025	0.0005	0.00005	0.016	0.0001	0.0005	0.0005	0.0045	0.028	0.001	0.0005
UQAC1067	0.0034	0.0005	0.00005	0.065	0.0001	0.0005	0.0005	0.00098	0.074	0.0019	0.0005
UQAC1069	0.036	0.0014	0.00069	0.055	0.0001	0.0005	0.0005	0.0009	0.042	0.0005	0.0005
UQAC1073	0.0079	0.0005	0.00005	0.046	0.0001	0.00094	0.0005	0.001	0.0012	0.00056	0.0014
UQAC1074	0.0072	0.0005	0.00018	0.11	0.00061	0.0005	0.0005	0.028	0.015	0.0011	0.0039
UQAC1075	0.0033	0.0005	0.00015	0.096	0.0001	0.0005	0.0005	0.00053	0.0053	0.0005	0.0005
UQAC1076	0.013	0.0005	0.00012	0.016	0.0001	0.0005	0.0005	0.0012	0.0015	0.0019	0.0005
UQAC1077	0.0033	0.0005	0.00013	0.0025	0.0001	0.0005	0.0005	0.01	0.0001	0.0005	0.0005
UQAC1078	0.023	0.0005	0.00011	0.039	0.0001	0.0005	0.0005	0.013	0.0014	0.0005	0.0005
UQAC1079	0.007	0.0005	0.00005	0.015	0.0001	0.0005	0.0005	0.0034	0.048	0.008	0.0012
UQAC1080	0.0049	0.0005	0.00005	0.086	0.0001	0.0005	0.0005	0.00096	0.048	0.0011	0.0005
UQAC1081	0.0054	0.0005	0.00005	0.077	0.00033	0.0005	0.0005	0.045	0.0001	0.00074	0.0005
UQAC1082	0.0043	0.0005	0.00005	0.38	0.0001	0.0005	0.0005	0.0011	0.05	0.00093	0.0005
UQAC1083	0.0015	0.0011	0.00033	0.037	0.0001	0.0005	0.0005	0.0005	0.0001	0.0012	0.0005
UQAC1084	0.0051	0.0005	0.00005	0.007	0.0001	0.0005	0.0005	0.0005	0.0001	0.0005	0.0005
UQAC1086	0.004	0.0005	0.00005	0.064	0.0001	0.00051	0.0005	0.00096	0.0001	0.00098	0.0005
UQAC1087	0.0035	0.0005	0.00005	0.24	0.0001	0.0005	0.0005	0.017	0.0001	0.0022	0.0005
UQAC1088	0.0005	0.0005	0.00005	0.064	0.0001	0.0005	0.0005	0.0005	0.18	0.0036	0.0005
UQAC1089	0.0043	0.0005	0.00005	0.038	0.0001	0.0005	0.0005	0.0005	0.026	0.0013	0.0005
UQAC1090	0.07	0.0005	0.00005	0.033	0.0001	0.0005	0.0005	0.018	0.21	0.0005	0.0025
UQAC1092	0.0016	0.0005	0.00005	0.15	0.0001	0.0005	0.0005	0.0005	0.011	0.0011	0.0005
UQAC1094	0.009	0.0005	0.00005	0.72	0.0001	0.0005	0.0005	0.0035	0.021	0.00089	0.0005
UQAC1095	0.0066	0.0005	0.00005	0.37	0.0001	0.0005	0.0005	0.07	0.018	0.0032	0.0011
UQAC1096	0.0071	0.0005	0.00005	0.046	0.0001	0.0028	0.0005	0.0055	0.021	0.00085	0.0011
UQAC1097	0.0053	0.0005	0.00005	0.28	0.0001	0.0005	0.0005	0.00098	0.013	0.0005	0.0005
UQAC1099	0.016	0.0005	0.0019	0.093	0.0001	0.0016	0.0005	0.0098	0.032	0.00094	0.0005
UQAC1101	0.01	0.0005	0.0014	0.078	0.0001	0.0005	0.0005	0.0005	0.032	0.0043	0.0005
UQAC1103	0.013	0.0005	0.00005	0.083	0.0001	0.00087	0.0005	0.0005	0.0011	0.0017	0.0005
UQAC1108	0.011	0.0005	0.0013	0.036	0.0001	0.0005	0.0005	0.0022	0.021	0.0034	0.0005
UQAC1109	0.0056	0.0005	0.00038	0.18	0.0001	0.0005	0.0005	0.0012	0.041	0.002	0.0005
UQAC1110	0.032	0.0005	0.00005	0.038	0.00066	0.0016	0.0013	0.0028	0.0066	0.0005	0.0005
UQAC1111	0.0085	0.0031	0.00005	0.0005	0.0001	0.0005	0.0005	0.0055	0.0001	0.0025	0.0014
UQAC1112	0.0005	0.0016	0.00005	0.4	0.0001	0.0005	0.0005	0.012	0.006	0.0031	0.0005
UQAC1113	0.0029	0.0005	0.00005	0.0094	0.0001	0.0005	0.0005	0.0052	0.0099	0.0005	0.0005
UQAC1114	0.0074	0.0005	0.00005	0.057	0.0001	0.0005	0.0005	0.0043	0.14	0.0005	0.0015
UQAC1115	0.0026	0.0005	0.00005	0.0005	0.0001	0.0005	0.0005	0.0005	0.0056	0.0015	0.0005
UQAC1116	0.0031	0.0005	0.00005	0.41	0.0001	0.0005	0.0005	0.00068	0.045	0.0008	0.0005
UQAC1117	0.0048	0.002	0.00005	0.12	0.0001	0.0005	0.0005	0.0098	0.0019	0.0005	0.0005

#

Sample	Aluminium	Antimoine	Silver	Barium	Cadmium	Chromium	Cobalt	Copper	Manganese	Molybdene	Nickel
UQAC1118	0.0064	0.0052	0.00005	0.038	0.0001	0.0005	0.0005	0.0076	0.0015	0.0005	0.0005
UQAC1119	0.0039	0.0005	0.00005	0.24	0.00027	0.0005	0.0005	0.0005	0.066	0.0068	0.0005
UQAC1120	0.027	0.0005	0.00005	0.051	0.0001	0.0005	0.0005	0.0042	0.0001	0.0011	0.0005
UQAC1121	0.016	0.0005	0.00005	0.011	0.0001	0.0005	0.0005	0.0013	0.0001	0.0033	0.0005
UQAC1123	0.16	0.0005	0.0003	0.0038	0.0001	0.0005	0.0005	0.00097	0.004	0.0005	0.0005
UQAC2001	0.032	0.0005	0.00028	0.024	0.0001	0.0005	0.0005	0.0017	0.0071	0.0005	0.0005
UQAC2002	0.0005	0.0005	0.00005	0.0005	0.0001	0.0005	0.0005	0.0068	0.0018	0.0005	0.0005
UQAC2003	0.0061	0.0005	0.00005	0.3	0.0001	0.0005	0.0005	0.015	0.0001	0.00064	0.0005
UQAC2004	0.011	0.0005	0.00005	0.015	0.0001	0.0005	0.0005	0.0005	0.0001	0.0005	0.0005
UQAC2005	0.065	0.0005	0.00005	0.08	0.0001	0.0005	0.0005	0.0056	0.0026	0.0005	0.0005
UQAC2008	0.027	0.0005	0.00033	0.0086	0.0001	0.0005	0.0005	0.011	0.0001	0.0005	0.0005
UQAC2009	0.034	0.0005	0.00033	0.0062	0.0001	0.0005	0.0005	0.0055	0.0015	0.0005	0.0005
UQAC2010	0.0051	0.0005	0.00028	0.0048	0.0001	0.0005	0.0005	0.0028	0.00066	0.0005	0.0005
UQAC2011	0.015	0.0005	0.00005	0.0033	0.0001	0.0005	0.0005	0.00089	0.095	0.0005	0.0005
UQAC2012	0.0023	0.0005	0.00005	0.0005	0.0001	0.0005	0.0005	0.013	0.0001	0.00066	0.0005
UQAC2013	0.0042	0.0005	0.00005	0.0058	0.0001	0.0005	0.0005	0.0005	0.0013	0.0005	0.0005
UQAC2014	0.0053	0.0005	0.00005	0.0005	0.0001	0.0005	0.0005	0.0005	0.00086	0.0005	0.0005
UQAC2015	0.0067	0.0005	0.00005	0.021	0.0001	0.0005	0.0005	0.0005	0.051	0.0039	0.0005
UQAC2016	0.0005	0.0005	0.00005	0.075	0.0001	0.0005	0.0005	0.0005	0.25	0.0039	0.0005
UQAC2017	0.0042	0.0005	0.00011	0.063	0.0001	0.0005	0.0005	0.0005	0.052	0.0016	0.0005
UQAC2018	0.0044	0.0005	0.00005	0.053	0.0001	0.0005	0.0005	0.0038	0.00058	0.0005	0.0005
UQAC2019	0.0057	0.0005	0.00005	0.037	0.0001	0.0005	0.0005	0.0036	0.0014	0.0005	0.0005
UQAC2020	0.0027	0.0005	0.00005	0.038	0.0001	0.0005	0.0005	0.057	0.00074	0.00054	0.0005
UQAC2021	0.0024	0.0005	0.00005	0.011	0.0001	0.0005	0.0005	0.00091	0.0001	0.0025	0.0005
UQAC2022	0.0019	0.0005	0.00005	0.085	0.0001	0.0005	0.0005	0.0005	0.085	0.0031	0.0005
UQAC2023	0.016	0.0005	0.00005	0.008	0.0001	0.0005	0.0005	0.0068	0.0057	0.0005	0.0005
UQAC2025	0.019	0.0005	0.00013	0.069	0.0001	0.0005	0.0005	0.35	0.0044	0.0005	0.0005
UQAC2026	0.034	0.0005	0.00011	0.024	0.0001	0.0005	0.0005	0.0005	0.0063	0.002	0.0005
UQAC2029	0.014	0.0005	0.00005	0.016	0.0001	0.0005	0.0005	0.00085	0.016	0.0005	0.0028
UQAC2030	0.021	0.0005	0.00005	0.038	0.0001	0.0005	0.0005	0.011	0.00099	0.0005	0.0005
UQAC2031	0.0005	0.0005	0.00005	0.1	0.0001	0.0005	0.0005	0.0056	0.00051	0.0005	0.0005
UQAC2033	0.017	0.0005	0.00005	0.0092	0.0001	0.0005	0.0005	0.0005	0.016	0.0019	0.0005
UQAC2035	0.0033	0.0005	0.00005	0.0088	0.0001	0.0005	0.0005	0.0005	0.034	0.0073	0.0005
UQAC2036	0.0048	0.0005	0.00005	0.0086	0.0001	0.0005	0.0005	0.0005	0.032	0.0017	0.0005
UQAC2038	0.0005	0.0005	0.00005	0.2	0.0001	0.0005	0.0005	0.0005	0.011	0.0017	0.0005
UQAC2039	0.017	0.0005	0.00005	0.037	0.0001	0.0005	0.0005	0.0005	0.013	0.0015	0.0005
UQAC2042	0.0005	0.0005	0.00005	0.012	0.0001	0.0005	0.0005	0.0005	0.11	0.0005	0.0005
UQAC2044	0.0078	0.0005	0.00005	0.03	0.0001	0.0005	0.0005	0.0005	0.0035	0.0027	0.0005

Sample	Aluminium	Antimoine	Silver	Barium	Cadmium	Chromium	Cobalt	Copper	Manganese	Molybdene	Nickel
UQAC2045	0.015	0.0005	0.00005	0.026	0.0001	0.0005	0.0005	0.0005	0.018	0.0006	0.0073
UQAC2046	0.01	0.0005	0.00005	0.031	0.0001	0.0005	0.0027	0.0039	0.24	0.0005	0.001
UQAC2050	0.0092	0.0005	0.00005	0.047	0.00073	0.0005	0.0005	0.01	0.0043	0.0005	0.0011
UQAC2051	0.01	0.0005	0.00025	0.013	0.0001	0.0005	0.0005	0.041	0.0049	0.0005	0.0005
UQAC2052	0.0021	0.0005	0.0003	0.01	0.0001	0.0005	0.0005	0.0005	0.0001	0.00069	0.0005
UQAC2053	0.0024	0.0005	0.00049	0.0095	0.0001	0.0014	0.0005	0.0017	0.0007	0.0005	0.0005
UQAC2054	0.0092	0.0005	0.00015	0.0005	0.0001	0.00096	0.0005	0.0014	0.0001	0.0071	0.0005
UQAC2055	0.0022	0.0005	0.00015	0.026	0.0001	0.0005	0.0005	0.029	0.0001	0.0023	0.0005
UQAC2059	0.064	0.0005	0.0001	0.041	0.0001	0.00051	0.0005	0.039	0.0099	0.0005	0.0005
UQAC2060	0.0095	0.0005	0.00011	0.039	0.0001	0.0005	0.0005	0.011	0.011	0.0018	0.0005
UQAC2062	0.024	0.0005	0.00005	0.0065	0.0001	0.00077	0.0005	0.0013	0.00085	0.0005	0.0005
UQAC2063	0.0005	0.0005	0.00005	0.08	0.0001	0.0005	0.0005	0.005	0.079	0.004	0.0005
UQAC2064	0.0048	0.0005	0.00011	0.053	0.0001	0.0005	0.0005	0.00071	0.014	0.0024	0.0005
UQAC2069	0.16	0.0005	0.00005	0.0078	0.0001	0.00054	0.0005	0.0012	0.0081	0.0028	0.0005
UQAC2071	0.0017	0.001	0.00014	0.0005	0.0001	0.00056	0.0005	0.00098	0.028	0.014	0.0005
UQAC2073	0.02	0.0022	0.00055	0.0092	0.0001	0.00054	0.0005	0.26	0.021	0.0016	0.0031
UQAC2074	0.022	0.0005	0.00025	0.004	0.0001	0.00056	0.0005	0.076	0.0001	0.0005	0.0005
UQAC2075	0.0045	0.0005	0.00005	0.065	0.0001	0.0005	0.0005	0.043	0.2	0.0005	0.0046
UQAC2076	0.0037	0.0005	0.00005	0.054	0.0001	0.0005	0.0005	0.0005	0.081	0.0036	0.0005
UQAC2077	0.018	0.0005	0.00005	0.054	0.0001	0.0017	0.0005	0.0063	0.0063	0.0005	0.0005
UQAC2078	0.0005	0.0005	0.00005	0.043	0.0001	0.0005	0.0005	0.0005	0.0071	0.0043	0.0005
UQAC2079	0.0005	0.0005	0.00005	0.028	0.0001	0.0005	0.0005	0.019	0.0001	0.0005	0.0005
UQAC2081	0.0005	0.0005	0.00031	0.0035	0.0001	0.0005	0.0005	0.002	0.00083	0.0005	0.0005
UQAC2082	0.0022	0.0005	0.00005	0.05	0.0001	0.0005	0.0005	0.0005	0.021	0.003	0.0005
UQAC2086	0.0054	0.0005	0.00005	0.026	0.0001	0.00053	0.0025	0.003	0.5	0.0005	0.0082
UQAC2088	0.003	0.0005	0.00005	0.14	0.0001	0.0005	0.0005	0.0027	0.039	0.0018	0.0029
UQAC2089	0.0005	0.0005	0.00005	0.08	0.0001	0.0005	0.0005	0.0005	0.015	0.0013	0.0021
UQAC2090	0.0005	0.0005	0.00005	0.018	0.0001	0.0005	0.0005	0.0005	0.0001	0.0015	0.0005
UQAC2092	0.012	0.0005	0.00005	0.0083	0.00021	0.0005	0.0005	0.0012	0.00055	0.00057	0.0005
UQAC2093	0.0069	0.0005	0.00005	0.0035	0.0001	0.0005	0.0005	0.0048	0.0013	0.0005	0.0005
UQAC2094	0.0013	0.0005	0.00005	0.078	0.0003	0.0005	0.0005	0.0005	0.11	0.0028	0.0005
UQAC2096	0.0051	0.0005	0.00012	0.035	0.0001	0.0005	0.0005	0.0023	0.0015	0.0025	0.0013
UQAC2097	0.0039	0.0005	0.0001	0.031	0.0001	0.0005	0.0005	0.016	0.011	0.0017	0.011
UQAC2098	0.0044	0.0005	0.00012	0.078	0.0001	0.0005	0.0005	0.00088	0.033	0.0029	0.0005
UQAC2099	0.025	0.0005	0.00011	0.019	0.0001	0.0005	0.0005	0.013	0.021	0.0005	0.0005
UQAC2100	0.0032	0.0005	0.00013	0.048	0.0001	0.0005	0.0005	0.0031	0.097	0.0005	0.0005
UQAC2101	0.008	0.0005	0.00005	0.042	0.0001	0.0005	0.0005	0.00053	0.011	0.00061	0.0005
UQAC2103	0.0067	0.0005	0.00005	0.018	0.0001	0.0005	0.0005	0.002	0.0041	0.002	0.0005

Sample	Aluminium	Antimoine	Silver	Barium	Cadmium	Chromium	Cobalt	Copper	Manganese	Molybdene	Nickel
UQAC2104	0.014	0.0005	0.00005	0.0026	0.0001	0.0005	0.0005	0.0064	0.025	0.0005	0.0005
UQAC2106	0.0078	0.0005	0.00005	0.07	0.0001	0.0005	0.0005	0.0042	0.081	0.00064	0.0005
UQAC2107	0.0083	0.0005	0.00005	0.064	0.0001	0.0005	0.0005	0.002	0.028	0.0032	0.0005
UQAC2108	0.015	0.0005	0.00005	0.048	0.0001	0.0005	0.0005	0.00082	0.028	0.0005	0.0005
UQAC2112	0.0042	0.0005	0.00005	0.0005	0.0001	0.0005	0.0005	0.031	0.003	0.0005	0.0015
UQAC2114	0.004	0.0005	0.00005	0.12	0.0001	0.0005	0.0005	0.0005	0.15	0.0041	0.0005
UQAC2116	0.0078	0.0005	0.00005	0.12	0.0001	0.0005	0.0005	0.0055	0.31	0.0062	0.0005
UQAC2117	0.022	0.0005	0.0001	0.027	0.0001	0.0005	0.0005	0.0059	0.03	0.0015	0.0019
UQAC2118	0.0035	0.0005	0.00005	0.069	0.0001	0.0005	0.0005	0.0015	0.027	0.0015	0.0013
UQAC2119	0.0061	0.0005	0.00005	0.034	0.0001	0.0005	0.0005	0.014	0.013	0.0005	0.0005
UQAC2120	0.0088	0.0005	0.00005	0.017	0.0001	0.0005	0.0005	0.0019	0.0024	0.00075	0.0005
UQAC2121	0.0038	0.0005	0.00005	0.042	0.0001	0.0005	0.00063	0.25	0.026	0.0015	0.0005
UQAC2122	0.0019	0.0005	0.00005	0.1	0.0001	0.0005	0.0005	0.0092	0.001	0.0005	0.0005
UQAC2123	0.0034	0.0005	0.00005	0.022	0.0001	0.0005	0.0005	0.0079	0.032	0.0057	0.0005
UQAC2124	0.0045	0.0005	0.00005	0.019	0.0001	0.0005	0.0005	0.0032	0.0048	0.0005	0.0012
UQAC2125	0.0039	0.0005	0.00005	0.064	0.0001	0.0005	0.0005	0.0034	0.14	0.0018	0.0005
UQAC2126	0.0062	0.0005	0.00005	0.0078	0.0001	0.0005	0.0005	0.0005	0.0001	0.0018	0.0005
UQAC2129	0.0043	0.0005	0.00005	0.0005	0.0001	0.0005	0.0005	0.0013	0.0001	0.0005	0.0005
UQAC2130	0.029	0.0005	0.00005	0.013	0.0001	0.0005	0.0005	0.0087	0.022	0.0005	0.0005
UQAC2131	0.0053	0.0005	0.00005	0.055	0.0001	0.0005	0.0005	0.015	0.032	0.0021	0.0016
UQAC2132	0.0065	0.0005	0.00005	0.02	0.0001	0.0005	0.0014	0.0005	1.1	0.00099	0.015
UQAC2133	0.0068	0.0005	0.00005	0.018	0.0001	0.0005	0.0005	0.0005	0.019	0.0018	0.0013
UQAC2135	0.0005	0.0005	0.00005	0.3	0.0001	0.0005	0.0005	0.0005	0.35	0.0019	0.0033
UQAC3000	0.022	0.0005	0.00005	0.0047	0.0001	0.0005	0.0005	0.018	0.0001	0.0005	0.0005
UQAC3002	0.0063	0.0005	0.00005	0.058	0.0001	0.0005	0.00096	0.00089	0.28	0.00058	0.0015
UQAC3004	0.0054	0.0005	0.00005	0.12	0.0001	0.0005	0.0005	0.0005	0.0052	0.00069	0.0005
UQAC3009	0.016	0.0005	0.00011	0.0005	0.0001	0.0014	0.0005	0.0038	0.0011	0.0005	0.0011
UQAC3011	0.002	0.0005	0.00005	0.058	0.0001	0.00071	0.0005	0.0012	0.094	0.00083	0.0005
UQAC3013	0.0039	0.0005	0.00005	0.089	0.0001	0.0011	0.0005	0.0005	0.0001	0.0086	0.0005
UQAC3014	0.0017	0.0005	0.00005	0.54	0.0001	0.0005	0.0005	0.0005	0.28	0.002	0.0005
UQAC3015	0.0005	0.0005	0.00005	0.05	0.0001	0.0005	0.0005	0.0098	0.0016	0.0014	0.0015
UQAC3018	0.0047	0.0005	0.00005	0.015	0.0001	0.0005	0.0005	0.044	0.0069	0.0005	0.0005
UQAC3019	0.0036	0.0005	0.00005	0.085	0.0001	0.0005	0.0005	0.00081	0.014	0.0023	0.0005
UQAC3021	0.0013	0.0005	0.00005	0.1	0.0001	0.0005	0.0005	0.00059	0.035	0.0027	0.0005
UQAC3022	0.015	0.0005	0.00005	0.0066	0.0001	0.0005	0.0005	0.0074	0.0044	0.0005	0.0005
UQAC3023	0.0005	0.0005	0.00005	0.26	0.0001	0.0005	0.0005	0.0019	0.00078	0.0031	0.0005
UQAC3025	0.0005	0.0005	0.00016	0.13	0.0001	0.0005	0.0005	0.0025	0.013	0.0029	0.0005
UQAC3027	0.0005	0.0005	0.00016	0.014	0.0001	0.0005	0.0005	0.002	0.00042	0.0005	0.0005

Sample	Aluminium	Antimoine	Silver	Barium	Cadmium	Chromium	Cobalt	Copper	Manganese	Molybdene	Nickel
UQAC3028	0.026	0.0005	0.00005	0.12	0.0001	0.0005	0.0005	0.025	0.00081	0.0005	0.0005
UQAC3032	0.01	0.0005	0.00005	0.016	0.0001	0.0005	0.0005	0.017	0.001	0.0005	0.0005
UQAC3035	0.032	0.0005	0.00005	0.054	0.0001	0.0005	0.0005	0.053	0.036	0.0005	0.0016
UQAC3037	0.029	0.0005	0.00005	0.035	0.0001	0.0005	0.0005	0.0064	0.04	0.0005	0.0005
UQAC3038	0.0042	0.0005	0.00005	0.31	0.0001	0.0005	0.0005	0.0005	0.006	0.0022	0.0005
UQAC3039	0.024	0.0005	0.00005	0.01	0.0001	0.00063	0.0005	0.0065	0.0027	0.0005	0.0005
UQAC3040	0.039	0.0005	0.00005	0.024	0.0001	0.00051	0.0005	0.0005	0.0024	0.00075	0.0021
UQAC3041	0.0038	0.0005	0.00005	0.13	0.0001	0.0005	0.0005	0.0021	0.0012	0.0087	0.0005
UQAC3042	0.025	0.0005	0.00016	0.0005	0.0001	0.0005	0.0005	0.0005	0.001	0.00057	0.0011
UQAC3045	0.0064	0.0005	0.00026	0.077	0.0001	0.0005	0.0005	0.002	0.0023	0.0015	0.0019
UQAC3047	0.17	0.0005	0.00005	0.096	0.0001	0.0005	0.0005	0.0024	0.025	0.0005	0.0005
UQAC3049	0.0058	0.0005	0.00005	0.029	0.0001	0.0005	0.0005	0.003	0.0001	0.0005	0.0005
UQAC3050	0.0051	0.0005	0.00005	0.65	0.0001	0.0005	0.0005	0.0058	0.011	0.0005	0.0005
UQAC4000	0.0051	0.0005	0.00005	0.069	0.0001	0.0012	0.0005	0.0023	0.0099	0.0005	0.0005
UQAC4001	0.011	0.0005	0.00017	0.01	0.0001	0.0005	0.0005	0.0005	0.0001	0.0005	0.0005
UQAC4002	0.05	0.0005	0.00005	0.026	0.0001	0.00054	0.0005	0.052	0.0024	0.0005	0.0015
UQAC4003	0.011	0.0005	0.00005	0.03	0.0001	0.00089	0.0005	0.0016	0.00074	0.0005	0.001
UQAC4004	0.008	0.0005	0.00022	0.0005	0.0001	0.0005	0.0005	0.0029	0.0001	0.0017	0.0024
UQAC4006	0.0079	0.0005	0.00061	0.11	0.0001	0.0005	0.0005	0.027	0.004	0.00087	0.0005
UQAC4007	0.0029	0.0005	0.00029	0.031	0.0001	0.0005	0.0005	0.0035	0.99	0.0005	0.0005
UQAC4008	0.0053	0.0005	0.00005	0.032	0.0001	0.0005	0.0005	0.0028	0.37	0.00064	0.0015
UQAC4009	0.015	0.0005	0.00011	0.0005	0.0001	0.0005	0.0005	0.0041	0.0061	0.0005	0.0011
UQAC4010	0.058	0.0005	0.00005	0.065	0.0001	0.0005	0.0005	0.002	0.065	0.0018	0.0021
UQAC4011	0.0053	0.0005	0.00005	0.019	0.0001	0.0005	0.0005	0.0047	0.073	0.00054	0.0013
UQAC4012	0.0097	0.0005	0.00005	0.12	0.0001	0.0005	0.0005	0.0047	0.0069	0.00057	0.0005
UQAC4013	0.0054	0.0005	0.00005	0.24	0.0001	0.0005	0.0005	0.014	0.009	0.0012	0.0058
UQAC4015	0.0029	0.0005	0.00005	0.055	0.0001	0.0013	0.0005	0.0005	0.018	0.0014	0.0019
UQAC4016	0.0029	0.0005	0.00005	0.035	0.0001	0.0005	0.0005	0.0068	0.0001	0.0015	0.0005
UQAC4018	0.0024	0.0005	0.00012	0.094	0.0001	0.0005	0.0005	0.0077	0.017	0.0022	0.0005
UQAC4019	0.0018	0.0005	0.00005	0.0092	0.0001	0.0005	0.0005	0.011	0.0001	0.0005	0.0005
UQAC4021	0.011	0.0005	0.00005	0.38	0.0001	0.0005	0.0005	0.067	0.017	0.0005	0.0005
UQAC4022	0.0034	0.0005	0.00005	0.18	0.0001	0.0005	0.0005	0.038	0.054	0.0005	0.0005
UQAC4023	0.0063	0.0005	0.00014	0.06	0.0001	0.0005	0.0026	0.00058	0.9	0.0022	0.0031
UQAC4024	0.011	0.0005	0.00005	0.008	0.0001	0.0005	0.0005	0.01	0.0014	0.0013	0.0005
UQAC4029	0.046	0.0005	0.00005	0.0062	0.0001	0.0005	0.0005	0.017	0.076	0.0005	0.003
UQAC4030	0.0032	0.0005	0.00005	0.033	0.0001	0.0005	0.0005	0.026	0.12	0.0005	0.0019
UQAC4031	0.004	0.0005	0.00005	0.19	0.0001	0.0005	0.0005	0.0005	0.0095	0.0005	0.0005
UQAC4033	0.011	0.0005	0.00005	0.072	0.0001	0.0005	0.0005	0.00099	0.2	0.00078	0.0017

Sample	Aluminium	Antimoine	Silver	Barium	Cadmium	Chromium	Cobalt	Copper	Manganese	Molybdene	Nickel
UQAC4034	0.0061	0.0005	0.00005	0.038	0.0001	0.0005	0.0005	0.0005	0.072	0.0037	0.0013
UQAC4036	0.052	0.0005	0.00005	0.018	0.0001	0.0005	0.0026	0.0046	0.1	0.0005	0.0054
UQAC4037	0.02	0.0005	0.00005	0.015	0.0001	0.0005	0.0005	0.0014	0.013	0.0029	0.0039
UQAC4038	0.0005	0.0005	0.00005	0.015	0.0001	0.0005	0.0005	0.027	0.0039	0.0005	0.0005
UQAC4041	0.016	0.0005	0.00005	0.067	0.0001	0.002	0.0066	0.0015	2.4	0.0016	0.0044
UQAC4042	0.0005	0.0005	0.00005	0.011	0.0001	0.0005	0.0005	0.0005	0.0001	0.0005	0.0005
UQAC4044	0.0005	0.0005	0.00005	0.013	0.0001	0.0005	0.0005	0.0005	0.011	0.0005	0.0005
UQAC4045	0.0005	0.0005	0.00005	0.027	0.0001	0.0005	0.0005	0.0005	0.0094	0.0005	0.0005
UQAC4047	0.0005	0.0005	0.00005	0.013	0.0001	0.0011	0.0005	0.004	0.01	0.0005	0.0005
UQAC4048	0.0005	0.0005	0.00005	0.0005	0.0001	0.0005	0.0005	0.0005	0.015	0.00065	0.0005
UQAC4049	0.0005	0.0005	0.00005	0.055	0.0001	0.0021	0.0005	0.048	0.0047	0.0005	0.0005
UQAC4051	0.0051	0.0005	0.00005	0.013	0.0001	0.0005	0.0005	0.08	0.0001	0.0005	0.0005
UQAC4052	0.0057	0.0005	0.00005	0.025	0.0001	0.0005	0.0005	0.02	0.011	0.0005	0.0005
UQAC4053	0.0082	0.0005	0.00005	0.0039	0.0001	0.0005	0.0005	0.014	0.0001	0.0005	0.0005
UQAC4054	0.0034	0.0005	0.00005	0.0005	0.0001	0.0005	0.0005	0.012	0.0029	0.0005	0.0005
UQAC4057	0.011	0.0005	0.00005	0.62	0.0001	0.0005	0.0005	0.00063	0.055	0.0005	0.0005
UQAC4060	0.0018	0.0005	0.00017	0.006	0.0001	0.0018	0.0005	0.0005	0.0021	0.0084	0.0005
UQAC4064	0.029	0.0005	0.00005	0.08	0.0001	0.0005	0.00076	0.0073	0.2	0.0005	0.0005
UQAC4065	0.0066	0.0005	0.00005	0.02	0.0001	0.00083	0.0005	0.0034	0.0011	0.0005	0.0005
UQAC4067	0.0084	0.0005	0.00005	0.0041	0.0001	0.0013	0.0005	0.0066	0.0011	0.0005	0.0005
UQAC4068	0.024	0.0005	0.00005	0.0068	0.0001	0.0005	0.0005	0.002	0.0012	0.0005	0.0005
UQAC4069	0.022	0.0005	0.00005	0.094	0.0001	0.0005	0.0019	0.0035	0.66	0.0005	0.0042
UQAC4071	0.014	0.0005	0.00005	0.03	0.0001	0.0005	0.001	0.028	0.019	0.0005	0.011
UQAC4072	0.0041	0.0005	0.00005	0.011	0.0001	0.0005	0.0005	0.02	0.00069	0.0005	0.0036
UQAC6002	0.023	0.0005	0.00005	0.016	0.0001	0.0005	0.0005	0.00067	0.13	0.0005	0.0005
UQAC6006	0.0005	0.0005	0.00010	0.074	0.0001	0.0011	0.0011	0.0005	0.49	0.0005	0.0005
UQAC6010	0.079	0.0005	0.00005	0.0067	0.0001	0.0005	0.0005	0.0005	0.0001	0.0005	0.0005
1JW04	0.0090	0.0005	0.00005	0.0200	0.0001	0.0005	0.0005	0.0040	0.0170	0.0026	0.0030
1JW05	0.0070	0.0005	0.00005	0.0200	0.0001	0.0005	0.0005	0.0005	0.0006	0.0026	0.0005
1JW08	0.0070	0.0005	0.00005	0.0900	0.0001	0.0005	0.0005	0.0009	0.0160	0.0026	0.0005
1JW31	0.0110	0.0005	0.00005	0.0300	0.0001	0.0005	0.0005	0.0005	0.0020	0.0026	0.0005
1JW37	0.0080	0.0005	0.00005	0.0500	0.0001	0.0005	0.0005	0.0450	0.0030	0.0026	0.0005
2JW15	0.1500	0.0005	0.00005	0.0080	0.0001	0.0005	0.0005	0.0005	0.0090	0.0026	0.0010
2JW17	0.0090	0.0005	0.00005	0.0600	0.0001	0.0005	0.0005	0.0005	0.0050	0.0026	0.0005
3JW01	0.1900	0.0005	0.00005	0.0230	0.0001	0.0005	0.0005	0.0005	0.0040	0.0026	0.0005
3JW21	0.0070	0.0005	0.00005	0.0390	0.0001	0.0005	0.0005	0.0380	0.0010	0.0026	0.0005
3JW29	0.0070	0.0005	0.00005	0.0550	0.0001	0.0005	0.0005	0.0040	0.0420	0.0026	0.0005
3JW34	0.0090	0.0005	0.00005	0.2300	0.0001	0.0005	0.0005	0.0020	0.3100	0.0026	0.0005

Sample	Aluminium	Antimoine	Silver	Barium	Cadmium	Chromium	Cobalt	Copper	Manganese	Molybdene	Nickel
UQAC1105	0.0035	0.0005	0.00005	0.26	0.0001	0.0005	0.0005	0.0015	0.11	0.0065	0.0005
UQAC2034	0.026	0.0005	0.0002	0.16	0.0001	0.0005	0.0005	0.00056	0.046	0.0017	0.001
UQAC3046	0.0072	0.0005	0.00005	0.18	0.0001	0.0005	0.0005	0.0026	0.077	0.0059	0.0005
UQAC4066	0.005	0.0005	0.00005	2.8	0.0001	0.001	0.0005	0.0005	0.018	0.0005	0.0005
1JW03	0.0070	0.0005	0.00005	2.1000	0.0001	0.0005	0.0005	0.0005	0.0930	0.0026	0.0005
1JW35	0.0070	0.0005	0.00005	0.1000	0.0001	0.0005	0.0005	0.0005	0.7100	0.0026	0.0009
2JW09	0.0120	0.0005	0.00005	0.1800	0.0001	0.0005	0.0005	0.0005	0.0410	0.0026	0.0005
2JW10	0.0200	0.0005	0.00005	0.0500	0.0001	0.0005	0.0005	0.0030	0.0800	0.0026	0.0020
2JW11	0.0200	0.0005	0.00005	0.0400	0.0001	0.0005	0.0005	0.0030	0.0910	0.0026	0.0020
2JW16	0.0200	0.0005	0.00005	0.2200	0.0001	0.0005	0.0005	0.0220	0.1500	0.0026	0.0020
2JW18	0.0200	0.0005	0.00005	0.0600	0.0001	0.0005	0.0005	0.0030	0.0650	0.0026	0.0020
3JW04	0.0070	0.0005	0.00005	0.0400	0.0001	0.0005	0.0005	0.0010	0.2200	0.0026	0.0005
UQAC1034	0.0046	0.0005	0.00016	0.039	0.0001	0.0005	0.0005	0.0005	0.071	0.0015	0.0016
UQAC4059	0.0091	0.0005	0.00015	0.2	0.0001	0.0024	0.0005	0.0005	0.61	0.0150	0.0005
UQAC6012	0.0005	0.0005	0.00005	0.024	0.0001	0.0005	0.0005	0.0005	0.089	0.0014	0.0005
UQAC6013	0.0005	0.0005	0.00005	0.064	0.0001	0.00052	0.0005	0.0005	0.098	0.0015	0.0005
2JW14	0.0200	0.0005	0.00005	0.0300	0.0001	0.0005	0.0005	0.0030	0.0430	0.0026	0.0020

Sample	Zinc	Boron	Iron	Lithium	Selenium	Strontium	Tin	Titane	Vanadium	Beryllium	Bismuth	Silicium
UQAC1011	0.0041	0.22	0.15	0.07	0.005	4.1	0.0005	0.0005	0.001	0.0005	0.0005	8.2
UQAC1019	0.012	0.028	0.032	0.005	0.005	1.6	0.0005	0.0005	0.001	0.0005	0.0005	9.9
UQAC1048	0.026	0.36	0.13	0.005	0.005	0.19	0.0034	0.0005	0.001	0.0005	0.0005	6.9
UQAC1071	0.015	0.38	1	0.031	0.005	5.8	0.0005	0.0005	0.001	0.0005	0.0005	9.1
UQAC1098	0.019	0.26	0.0005	0.005	0.005	5.9	0.0005	0.0005	0.001	0.0005	0.0005	6.3
UQAC2047	0.0066	0.17	0.29	0.012	0.005	7.8	0.0005	0.0005	0.001	0.0005	0.0005	6.5
UQAC2048	0.023	0.38	0.041	0.005	0.005	0.37	0.0005	0.0005	0.001	0.0005	0.0005	10
UQAC2091	0.15	0.19	0.19	0.005	0.005	0.71	0.0005	0.0005	0.001	0.0005	0.0005	6.7
UQAC2128	0.0067	0.35	0.15	0.01	0.005	0.22	0.0005	0.0005	0.001	0.0005	0.0005	0.22
UQAC3024	0.014	0.3	0.59	0.005	0.005	0.6	0.0005	0.0005	0.001	0.0005	0.0005	6.4
UQAC3036	0.0053	0.42	0.3	0.039	0.005	6.4	0.0005	0.0005	0.001	0.0005	0.0005	11
UQAC3052	0.032	0.47	0.0005	0.005	0.005	0.0033	0.0005	0.0005	0.001	0.0005	0.0005	4.4
UQAC6007	0.0092	0.29	3.1	0.017	0.005	0.49	0.0005	0.0005	0.001	0.0005	0.0005	9.2
1JW01	0.0080	0.2000	0.0500	0.0100	0.0005	1.50	0.0005	0.0005	0.0005	0.0005	0.0005	6.80
1JW02	0.0020	0.2800	0.0530	0.0060	0.0005	1.10	0.0005	0.0005	0.0005	0.0005	0.0005	6.40
1JW07	0.0060	0.1800	0.0050	0.0300	0.0005	6.60	0.0005	0.0005	0.0005	0.0005	0.0005	5.10
1JW15	0.0140	0.6000	0.1900	0.0200	0.0005	1.90	0.0005	0.0005	0.0005	0.0005	0.0005	9.10
1JW26	0.0020	3.4000	0.0080	0.1400	0.0005	0.01	0.0005	0.0005	0.0005	0.0005	0.0005	3.30
1JW28	0.0020	0.5200	0.2700	0.0200	0.0005	1.00	0.0005	0.0005	0.0005	0.0005	0.0005	9.10
1JW38	0.0070	0.4400	0.4100	0.0200	0.0005	2.10	0.0005	0.0005	0.0005	0.0005	0.0005	9.20
2JW02	0.0060	0.2500	0.0990	0.0400	0.0005	9.10	0.0005	0.0005	0.0005	0.0005	0.0005	3.90
2JW04	0.0020	0.5600	0.1600	0.0400	0.0005	9.00	0.0005	0.0005	0.0005	0.0005	0.0005	6.00
2JW08	0.0020	0.3400	0.0005	0.0300	0.0005	5.90	0.0005	0.0005	0.0005	0.0005	0.0005	4.80
2JW12	0.0020	1.9000	0.9100	0.1800	0.0005	6.40	0.0005	0.0005	0.0005	0.0005	0.0005	3.70
2JW19	0.0020	0.5800	0.0590	0.0030	0.0005	0.13	0.0005	0.0005	0.0005	0.0005	0.0005	6.80
2JW20	0.0100	0.1000	0.0970	0.0050	0.0005	3.80	0.0005	0.0005	0.0005	0.0005	0.0005	5.50
3JW05	0.0110	0.3600	0.0470	0.0090	0.0005	0.98	0.0005	0.0005	0.0005	0.0005	0.0005	7.70
3JW08	0.0210	0.5000	0.0650	0.0100	0.0005	0.89	0.0005	0.0005	0.0005	0.0005	0.0005	9.10
3JW10	0.0100	0.4500	0.4100	0.0200	0.0005	2.10	0.0005	0.0005	0.0005	0.0005	0.0005	9.30
3JW12	0.0020	0.5900	0.0390	0.0030	0.0005	0.11	0.0005	0.0005	0.0005	0.0005	0.0005	7.20
UQAC1001	0.0051	0.026	0.0005	0.005	0.005	1.2	0.0005	0.0005	0.001	0.0005	0.0005	4.8
UQAC1002	0.0034	0.054	0.04	0.005	0.005	0.48	0.0005	0.0005	0.001	0.0005	0.0005	4.9
UQAC1003	0.006	0.035	0.13	0.005	0.005	1.1	0.0005	0.0005	0.001	0.0005	0.0005	5.6
UQAC1004	0.0051	0.11	0.0005	0.005	0.005	0.6	0.0005	0.0005	0.001	0.0005	0.0005	5.3
UQAC1005	0.001	0.25	0.066	0.013	0.005	1.4	0.0005	0.0005	0.001	0.0005	0.0005	5.6
UQAC1006	0.001	0.002	0.0005	0.005	0.005	0.16	0.0005	0.0005	0.001	0.0005	0.0005	5.2
UQAC1008	0.001	0.058	0.0005	0.005	0.005	0.9	0.0005	0.0005	0.001	0.0005	0.0005	6.6
UQAC1012	0.052	0.002	0.046	0.005	0.005	0.068	0.0005	0.0005	0.001	0.0005	0.0005	5.6

Sample	Zinc	Boron	Iron	Lithium	Selenium	Strontium	Tin	Titane	Vanadium	Beryllium	Bismuth	Silicium
UQAC1013	0.028	0.13	0.046	0.005	0.005	0.34	0.0005	0.0005	0.001	0.0005	0.0005	4.9
UQAC1014	0.0071	0.016	0.0005	0.005	0.005	0.17	0.0005	0.0005	0.001	0.0005	0.0005	6.2
UQAC1015	0.0031	0.12	0.0005	0.005	0.005	0.56	0.0005	0.0005	0.001	0.0005	0.0005	6
UQAC1016	0.0086	0.12	0.0005	0.005	0.005	1.2	0.0005	0.0005	0.001	0.0005	0.0005	3.4
UQAC1017	0.0073	0.002	0.062	0.005	0.005	0.19	0.0005	0.0005	0.001	0.0005	0.0005	6.2
UQAC1020	0.011	0.002	0.0005	0.005	0.005	0.1	0.0005	0.0005	0.001	0.0005	0.0005	5.6
UQAC1021	0.021	0.063	0.074	0.005	0.005	0.1	0.0005	0.0005	0.001	0.0005	0.0005	6.1
UQAC1022	0.026	0.012	0.11	0.005	0.005	0.8	0.0005	0.0005	0.001	0.0005	0.0005	6.2
UQAC1023	0.0055	0.096	0.0005	0.005	0.005	0.27	0.0005	0.0005	0.001	0.0005	0.0005	4.6
UQAC1024	0.001	0.033	0.0005	0.005	0.005	2.8	0.0005	0.0005	0.001	0.0005	0.0005	5.4
UQAC1025	0.001	0.072	0.38	0.005	0.005	0.09	0.0005	0.0005	0.001	0.0005	0.0005	3.9
UQAC1026	0.0055	0.048	0.15	0.015	0.005	0.38	0.0005	0.0005	0.001	0.0005	0.0005	5.3
UQAC1028	0.026	0.002	0.31	0.005	0.005	0.13	0.0005	0.0005	0.001	0.0005	0.0005	5.6
UQAC1029	0.029	0.0078	0.0005	0.005	0.005	0.12	0.0005	0.0005	0.001	0.0005	0.0005	7.8
UQAC1030	0.0091	0.023	0.0005	0.005	0.005	0.33	0.0005	0.0005	0.0033	0.0005	0.0005	9.1
UQAC1032	0.011	0.0056	0.25	0.005	0.005	0.019	0.0005	0.0005	0.001	0.0005	0.0005	6.8
UQAC1033	0.001	0.059	0.07	0.005	0.005	0.14	0.0005	0.0005	0.001	0.0005	0.0005	10
UQAC1035	0.001	0.02	0.0005	0.005	0.005	0.056	0.0005	0.0005	0.001	0.0005	0.0005	11
UQAC1036	0.013	0.032	0.24	0.005	0.005	0.59	0.0005	0.0005	0.001	0.0005	0.0005	6.7
UQAC1038	0.0052	0.051	0.13	0.005	0.005	3.1	0.0005	0.0005	0.0026	0.0005	0.0005	9.1
UQAC1040	0.017	0.011	0.04	0.005	0.005	0.025	0.0005	0.0005	0.001	0.0005	0.0005	4.9
UQAC1041	0.004	0.16	0.085	0.005	0.005	0.027	0.0005	0.0005	0.0031	0.0005	0.0005	5.9
UQAC1042	0.038	0.0086	0.12	0.005	0.005	0.18	0.0005	0.0005	0.001	0.0005	0.0005	5.6
UQAC1043	0.002	0.22	0.0005	0.011	0.005	0.0015	0.0005	0.0005	0.001	0.0005	0.0005	5.3
UQAC1044	0.058	0.01	0.14	0.013	0.005	0.21	0.0005	0.0005	0.001	0.0005	0.0005	9.6
UQAC1045	0.012	0.068	0.0005	0.005	0.005	0.27	0.0005	0.0005	0.001	0.0005	0.0005	7.1
UQAC1046	0.001	0.002	0.42	0.005	0.005	0.063	0.0005	0.0005	0.001	0.0005	0.0005	7.7
UQAC1049	0.11	0.0095	0.092	0.005	0.005	0.058	0.0005	0.0005	0.001	0.0005	0.0005	12
UQAC1050	0.014	0.024	0.09	0.005	0.005	0.33	0.0005	0.0005	0.001	0.0005	0.0005	6.8
UQAC1051	0.055	0.011	0.0005	0.005	0.005	0.033	0.0005	0.0005	0.0023	0.0005	0.0005	5.7
UQAC1052	0.019	0.028	0.0005	0.005	0.005	0.18	0.0005	0.0005	0.001	0.0005	0.0005	4
UQAC1053	0.023	0.034	0.032	0.005	0.005	0.49	0.0005	0.0005	0.001	0.0005	0.0005	5
UQAC1055	0.031	0.0068	0.0005	0.005	0.005	0.21	0.0005	0.0005	0.001	0.0005	0.0005	6.5
UQAC1058	0.0052	0.002	0.0005	0.005	0.005	0.18	0.0005	0.0005	0.001	0.0005	0.0005	3.1
UQAC1059	0.013	0.002	0.0005	0.005	0.005	0.22	0.0005	0.0005	0.001	0.0005	0.0005	5.3
UQAC1063	0.011	0.0079	0.0005	0.005	0.005	0.79	0.0005	0.0005	0.001	0.0005	0.0005	5.2
UQAC1064	0.011	0.002	0.049	0.005	0.005	0.021	0.0005	0.0005	0.001	0.0005	0.0005	5.4
UQAC1065	0.013	0.002	0.0005	0.005	0.005	0.13	0.0005	0.0005	0.0039	0.0005	0.0005	8

Sample	Zinc	Boron	Iron	Lithium	Selenium	Strontium	Tin	Titane	Vanadium	Beryllium	Bismuth	Silicium
UQAC1066	0.0054	0.008	0.0005	0.005	0.005	0.15	0.0005	0.0005	0.001	0.0005	0.0005	5.4
UQAC1067	0.024	0.081	0.0005	0.011	0.005	0.84	0.0005	0.0005	0.001	0.0005	0.0005	8.2
UQAC1069	0.004	0.13	0.78	0.018	0.005	0.96	0.0005	0.0005	0.001	0.0005	0.0005	8.1
UQAC1073	0.018	0.002	0.0005	0.005	0.005	0.086	0.0005	0.0005	0.001	0.0005	0.0005	4.1
UQAC1074	0.028	0.03	0.32	0.005	0.005	0.72	0.0005	0.0005	0.001	0.0005	0.0005	6.7
UQAC1075	0.017	0.14	0.22	0.015	0.005	1.1	0.0005	0.0005	0.001	0.0005	0.0005	6.2
UQAC1076	0.0056	0.059	0.0005	0.005	0.005	0.036	0.0005	0.0005	0.001	0.0005	0.0005	3.7
UQAC1077	0.081	0.0061	0.0005	0.005	0.005	0.077	0.0005	0.0005	0.001	0.0005	0.0005	10
UQAC1078	0.14	0.002	0.0005	0.005	0.005	0.087	0.0005	0.0005	0.001	0.0005	0.0005	5.2
UQAC1079	0.036	0.021	0.032	0.005	0.005	0.23	0.0005	0.0005	0.001	0.0005	0.0005	5.5
UQAC1080	0.0046	0.018	0.34	0.005	0.005	0.58	0.0005	0.0005	0.001	0.0005	0.0005	8.5
UQAC1081	0.058	0.0062	0.0005	0.005	0.005	0.33	0.0005	0.0005	0.001	0.0005	0.0005	5.1
UQAC1082	0.0068	0.05	0.052	0.005	0.005	0.93	0.0005	0.0005	0.001	0.0005	0.0005	6
UQAC1083	0.001	0.0082	0.0005	0.005	0.005	0.21	0.0005	0.0005	0.001	0.0005	0.0005	5.2
UQAC1084	0.003	0.002	0.0005	0.005	0.005	0.044	0.0005	0.0005	0.001	0.0005	0.0005	7.3
UQAC1086	0.018	0.0075	0.0005	0.005	0.005	0.17	0.0005	0.0005	0.001	0.0005	0.0005	9.9
UQAC1087	0.021	0.0057	0.0005	0.005	0.005	0.067	0.0005	0.0005	0.001	0.0005	0.0005	5.9
UQAC1088	0.0033	0.0095	0.0005	0.005	0.005	0.17	0.0005	0.0005	0.001	0.0005	0.0005	5.4
UQAC1089	0.0037	0.002	0.12	0.005	0.005	0.09	0.0005	0.0005	0.001	0.0005	0.0005	5.4
UQAC1090	0.069	0.0055	0.0005	0.005	0.005	0.2	0.0005	0.0005	0.001	0.0005	0.0005	4.1
UQAC1092	0.001	0.18	0.097	0.005	0.005	0.73	0.0005	0.0005	0.001	0.0005	0.0005	5.2
UQAC1094	0.001	0.17	0.0005	0.012	0.005	0.95	0.0005	0.0005	0.001	0.0005	0.0005	6.5
UQAC1095	0.01	0.04	0.0005	0.005	0.005	0.99	0.0005	0.0005	0.001	0.0005	0.0005	4.9
UQAC1096	0.023	0.2	5	0.005	0.005	0.19	0.0005	0.0005	0.001	0.0005	0.0005	6.9
UQAC1097	0.0097	0.049	0.0005	0.005	0.005	0.43	0.0005	0.0005	0.001	0.0005	0.0005	5.2
UQAC1099	0.001	0.64	0.049	0.017	0.005	0.4	0.0005	0.0005	0.001	0.0005	0.0005	13
UQAC1101	0.012	0.093	0.34	0.005	0.005	1.6	0.0005	0.0005	0.001	0.0005	0.0005	6.2
UQAC1103	0.0096	0.0061	0.039	0.005	0.005	0.35	0.0005	0.0005	0.001	0.0005	0.0005	5.3
UQAC1108	0.036	0.048	0.44	0.005	0.005	0.21	0.0005	0.0005	0.001	0.0005	0.0005	8.3
UQAC1109	0.024	0.043	0.047	0.005	0.005	2.4	0.0005	0.0005	0.001	0.0005	0.0005	4.2
UQAC1110	0.013	0.082	0.12	0.005	0.005	0.38	0.0005	0.0005	0.001	0.0008	0.00072	6.9
UQAC1111	0.017	0.016	0.0005	0.005	0.005	0.023	0.0021	0.0005	0.001	0.0005	0.0005	9.1
UQAC1112	0.0055	0.029	0.0005	0.005	0.005	0.22	0.0005	0.0005	0.001	0.0005	0.0005	7.6
UQAC1113	0.023	0.002	1.1	0.005	0.005	0.038	0.0005	0.0005	0.001	0.0005	0.0005	4.9
UQAC1114	0.006	0.014	0.096	0.005	0.005	0.4	0.0005	0.0005	0.001	0.0005	0.0005	10
UQAC1115	0.001	0.18	2	0.005	0.042	0.21	0.0005	0.0005	0.001	0.0005	0.0005	6.4
UQAC1116	0.001	0.094	0.058	0.005	0.005	0.99	0.0005	0.0005	0.001	0.0005	0.0005	4.3
UQAC1117	0.0081	0.002	0.071	0.005	0.005	0.43	0.0005	0.0005	0.001	0.0005	0.0005	4.9

Sample	Zinc	Boron	Iron	Lithium	Selenium	Strontium	Tin	Titane	Vanadium	Beryllium	Bismuth	Silicium
UQAC1118	0.26	0.002	0.056	0.005	0.005	0.054	0.0005	0.0005	0.001	0.0005	0.0005	3.6
UQAC1119	0.008	0.064	0.0005	0.005	0.005	3.5	0.0005	0.0005	0.001	0.0005	0.0005	5.7
UQAC1120	0.014	0.0059	0.0005	0.005	0.005	0.17	0.0005	0.0005	0.001	0.0005	0.0005	4.5
UQAC1121	0.0095	0.068	0.0005	0.005	0.005	0.053	0.0005	0.0005	0.001	0.0005	0.0005	5.5
UQAC1123	0.0065	0.002	0.064	0.005	0.005	0.016	0.0005	0.0005	0.001	0.0005	0.0005	6.7
UQAC2001	0.0044	0.002	0.0005	0.005	0.005	0.094	0.0005	0.0005	0.001	0.0005	0.0005	3.4
UQAC2002	0.001	0.0079	0.0005	0.005	0.005	0.035	0.0005	0.0005	0.001	0.0005	0.0005	4.8
UQAC2003	0.014	0.0067	0.0005	0.005	0.005	0.22	0.0005	0.0005	0.001	0.0005	0.0005	3.1
UQAC2004	0.001	0.002	0.0005	0.005	0.005	0.041	0.0005	0.0005	0.001	0.0005	0.0005	3.9
UQAC2005	0.19	0.0053	0.035	0.005	0.005	0.084	0.0005	0.0005	0.001	0.0005	0.0005	3.2
UQAC2008	0.001	0.002	0.0005	0.005	0.005	0.036	0.0005	0.0005	0.001	0.0005	0.0005	4.2
UQAC2009	0.001	0.002	0.083	0.005	0.005	0.041	0.0005	0.0005	0.001	0.0005	0.0005	4.5
UQAC2010	0.001	0.002	0.0005	0.005	0.005	0.057	0.0005	0.0005	0.001	0.0005	0.0005	6.4
UQAC2011	0.0055	0.002	2.9	0.005	0.005	0.046	0.0005	0.0005	0.001	0.0005	0.0005	7.1
UQAC2012	0.006	0.002	0.0005	0.005	0.005	0.03	0.0005	0.0005	0.001	0.0005	0.0005	7.6
UQAC2013	0.4	0.002	0.047	0.005	0.005	0.023	0.0005	0.0005	0.001	0.0005	0.0005	4.5
UQAC2014	0.11	0.002	0.0005	0.005	0.005	0.019	0.0005	0.0005	0.001	0.0005	0.0005	3.5
UQAC2015	0.018	0.018	0.2	0.005	0.005	0.31	0.0005	0.0005	0.001	0.0005	0.0005	5.2
UQAC2016	0.0019	0.008	0.047	0.005	0.005	0.097	0.0005	0.0005	0.001	0.0005	0.0005	5.4
UQAC2017	0.001	0.012	0.036	0.005	0.005	0.51	0.0005	0.0005	0.001	0.0005	0.0005	6.5
UQAC2018	0.07	0.0064	0.0005	0.005	0.005	0.2	0.0005	0.0005	0.001	0.0005	0.0005	4.5
UQAC2019	0.012	0.0072	0.0005	0.005	0.005	0.26	0.0005	0.0005	0.001	0.0005	0.0005	3.5
UQAC2020	0.034	0.013	0.0005	0.005	0.005	0.24	0.0005	0.0005	0.001	0.0005	0.0005	4.6
UQAC2021	0.001	0.1	0.0005	0.005	0.005	0.036	0.0005	0.0005	0.001	0.0005	0.0005	4.9
UQAC2022	0.001	0.041	0.08	0.005	0.005	1	0.0005	0.0005	0.001	0.0005	0.0005	4.6
UQAC2023	0.0026	0.002	0.073	0.005	0.005	0.014	0.0005	0.0005	0.001	0.0005	0.0005	3.8
UQAC2025	0.013	0.002	0.06	0.005	0.005	0.047	0.0005	0.0005	0.001	0.0005	0.0005	4.3
UQAC2026	0.0039	0.033	0.0005	0.005	0.005	0.15	0.0005	0.0005	0.001	0.0005	0.0005	6.9
UQAC2029	0.033	0.002	0.041	0.005	0.005	0.15	0.0005	0.0005	0.001	0.0005	0.0005	9.6
UQAC2030	0.057	0.028	0.0005	0.005	0.005	0.25	0.0005	0.0005	0.001	0.0005	0.0005	6.8
UQAC2031	0.057	0.011	0.0005	0.005	0.005	0.25	0.0005	0.0005	0.001	0.0005	0.0005	6
UQAC2033	0.001	0.22	0.0005	0.005	0.005	0.43	0.0005	0.0005	0.001	0.0005	0.0005	5.2
UQAC2035	0.001	0.029	0.052	0.005	0.005	0.48	0.0005	0.0005	0.001	0.0005	0.0005	4.8
UQAC2036	0.0082	0.03	0.086	0.005	0.005	0.74	0.0005	0.0005	0.001	0.0005	0.0005	6.1
UQAC2038	0.001	0.11	0.0005	0.005	0.005	0.45	0.0005	0.001	0.001	0.0005	0.0005	6
UQAC2039	0.001	0.18	0.12	0.005	0.005	0.4	0.0005	0.0005	0.001	0.0005	0.0005	6.1
UQAC2042	0.16	0.002	3.5	0.005	0.005	0.037	0.0005	0.0005	0.001	0.0005	0.0005	16
UQAC2044	0.001	0.14	0.032	0.005	0.005	0.28	0.0005	0.0005	0.001	0.0005	0.0005	5.3

Sample	Zinc	Boron	Iron	Lithium	Selenium	Strontium	Tin	Titane	Vanadium	Beryllium	Bismuth	Silicium
UQAC2045	0.015	0.047	0.13	0.005	0.005	0.16	0.0005	0.0005	0.001	0.0005	0.0005	9.4
UQAC2046	0.074	0.002	0.063	0.005	0.005	0.13	0.0005	0.0005	0.001	0.0005	0.0005	14
UQAC2050	0.037	0.002	0.033	0.005	0.005	0.18	0.0005	0.0005	0.001	0.0005	0.0005	8.3
UQAC2051	0.071	0.012	0.0005	0.005	0.005	0.059	0.0005	0.0005	0.001	0.0005	0.0005	5.1
UQAC2052	0.0054	0.013	0.0005	0.005	0.005	0.054	0.0005	0.0005	0.002	0.0005	0.0005	6.2
UQAC2053	0.092	0.013	0.034	0.005	0.005	0.032	0.0005	0.0005	0.001	0.0005	0.0005	5.7
UQAC2054	0.0096	0.051	0.03	0.005	0.005	0.0015	0.0005	0.0005	0.001	0.0005	0.0005	5
UQAC2055	0.0085	0.012	0.0005	0.005	0.005	0.19	0.0005	0.0005	0.0021	0.0005	0.0005	6
UQAC2059	0.099	0.002	0.061	0.005	0.005	0.16	0.0005	0.0005	0.001	0.0005	0.0005	1.3
UQAC2060	0.038	0.1	0.0005	0.011	0.005	0.41	0.0005	0.0005	0.0022	0.0005	0.0005	8.7
UQAC2062	0.0087	0.002	0.0005	0.005	0.005	0.057	0.0005	0.0005	0.001	0.0005	0.0005	5.4
UQAC2063	0.029	0.11	0.1	0.012	0.005	2.2	0.0005	0.0005	0.001	0.0005	0.0005	5.4
UQAC2064	0.001	0.048	0.0005	0.005	0.005	0.28	0.0005	0.0005	0.001	0.0005	0.0005	4.2
UQAC2069	0.001	0.22	0.16	0.005	0.005	0.063	0.0005	0.0044	0.001	0.0005	0.0005	7.8
UQAC2071	0.022	0.073	0.0005	0.005	0.005	0.079	0.0005	0.0005	0.001	0.0005	0.0005	3.9
UQAC2073	0.029	0.0076	0.2	0.005	0.005	0.096	0.0005	0.0005	0.001	0.0005	0.0005	4.8
UQAC2074	0.023	0.002	0.0005	0.005	0.005	0.053	0.0005	0.0005	0.001	0.0005	0.0005	6.3
UQAC2075	0.054	0.017	0.0005	0.005	0.005	0.48	0.0005	0.0005	0.001	0.0005	0.0005	11
UQAC2076	0.0016	0.15	0.13	0.014	0.005	2.3	0.0005	0.0005	0.001	0.0005	0.0005	3.4
UQAC2077	0.031	0.002	0.047	0.005	0.005	0.11	0.0005	0.0005	0.001	0.0005	0.0005	6.7
UQAC2078	0.001	0.059	0.0005	0.005	0.005	0.12	0.0005	0.0005	0.0026	0.0005	0.0005	3.7
UQAC2079	0.13	0.002	0.0005	0.005	0.005	0.017	0.0005	0.0005	0.001	0.0005	0.0005	6.3
UQAC2081	0.29	0.002	0.03	0.005	0.005	0.033	0.0005	0.0005	0.001	0.0005	0.0005	6.5
UQAC2082	0.0021	0.011	0.13	0.005	0.005	0.14	0.0005	0.0005	0.001	0.0005	0.0005	7.7
UQAC2086	0.71	0.002	13	0.005	0.005	0.04	0.0005	0.0005	0.001	0.0005	0.0005	11
UQAC2088	0.0052	0.0055	1.1	0.005	0.005	0.2	0.0005	0.0005	0.001	0.0005	0.0005	5.1
UQAC2089	0.001	0.011	0.11	0.005	0.005	0.17	0.0005	0.0005	0.001	0.0005	0.0005	4.4
UQAC2090	0.0041	0.037	0.0005	0.021	0.005	0.69	0.0005	0.0005	0.001	0.0005	0.0005	5.4
UQAC2092	0.16	0.002	0.0005	0.005	0.005	0.059	0.0005	0.0005	0.001	0.0005	0.0005	3.7
UQAC2093	0.012	0.002	0.04	0.005	0.005	0.046	0.0005	0.0005	0.001	0.0005	0.0005	5.2
UQAC2094	0.021	0.013	0.46	0.005	0.005	0.29	0.0005	0.0005	0.001	0.0005	0.0005	7.4
UQAC2096	0.013	0.0058	0.0005	0.005	0.005	0.075	0.0005	0.0005	0.0027	0.0005	0.0005	7.4
UQAC2097	0.015	0.015	0.0005	0.005	0.005	0.16	0.0005	0.0005	0.001	0.0005	0.0005	8.6
UQAC2098	0.0023	0.016	0.081	0.005	0.005	0.35	0.0005	0.0005	0.001	0.0005	0.0005	8
UQAC2099	0.018	0.002	0.045	0.005	0.005	0.036	0.0005	0.0005	0.001	0.0005	0.0005	4.7
UQAC2100	0.0073	0.0077	0.031	0.005	0.005	0.31	0.0005	0.0005	0.001	0.0005	0.0005	7.9
UQAC2101	0.0057	0.016	0.0005	0.005	0.005	0.086	0.0005	0.0005	0.001	0.0005	0.0005	7.6
UQAC2103	0.012	0.011	0.043	0.005	0.005	0.041	0.0005	0.0005	0.0023	0.0005	0.0005	8.5

Sample	Zinc	Boron	Iron	Lithium	Selenium	Strontium	Tin	Titane	Vanadium	Beryllium	Bismuth	Silicium
UQAC2104	0.032	0.007	0.82	0.005	0.005	0.014	0.0005	0.0005	0.001	0.0005	0.0005	6
UQAC2106	0.0097	0.0074	0.0005	0.005	0.005	0.17	0.0005	0.0005	0.001	0.0005	0.0005	3.6
UQAC2107	0.0047	0.0095	0.096	0.005	0.005	0.15	0.0005	0.0005	0.001	0.0005	0.0005	6.8
UQAC2108	0.0056	0.0056	0.098	0.005	0.005	0.06	0.0005	0.0005	0.0026	0.0005	0.0005	2.4
UQAC2112	0.024	0.002	0.0005	0.005	0.005	0.024	0.0005	0.0005	0.001	0.0005	0.0005	5.3
UQAC2114	0.011	0.0056	0.28	0.005	0.005	0.17	0.0005	0.0005	0.001	0.0005	0.0005	5.6
UQAC2116	0.015	0.019	0.0005	0.005	0.005	0.45	0.0005	0.0005	0.001	0.0005	0.0005	6.8
UQAC2117	0.017	0.014	0.0005	0.005	0.005	0.21	0.0005	0.0005	0.001	0.0005	0.0005	5.7
UQAC2118	0.01	0.016	0.13	0.005	0.005	0.23	0.0005	0.0005	0.001	0.0005	0.0005	5.1
UQAC2119	0.015	0.0062	0.042	0.005	0.005	0.13	0.0005	0.0005	0.001	0.0005	0.0005	4.9
UQAC2120	0.024	0.0072	0.3	0.005	0.005	0.16	0.0005	0.0005	0.001	0.0005	0.0005	8.1
UQAC2121	0.014	0.022	1.1	0.005	0.005	0.31	0.0005	0.0005	0.001	0.0044	0.0005	7.3
UQAC2122	0.01	0.002	0.0005	0.005	0.005	0.34	0.0005	0.0005	0.001	0.0005	0.0005	7.5
UQAC2123	0.014	0.026	0.0005	0.005	0.005	0.3	0.0005	0.0005	0.001	0.0005	0.0005	8.6
UQAC2124	0.014	0.002	0.18	0.005	0.005	0.079	0.0005	0.0005	0.001	0.0005	0.0005	7.9
UQAC2125	0.013	0.013	0.086	0.005	0.005	0.25	0.0005	0.0005	0.001	0.0005	0.0005	6.7
UQAC2126	0.0052	0.009	0.0005	0.005	0.005	0.12	0.0005	0.0005	0.001	0.0005	0.0005	5.1
UQAC2129	0.0068	0.002	0.0005	0.005	0.005	0.018	0.0005	0.0005	0.001	0.0005	0.0005	7.5
UQAC2130	0.001	0.002	0.11	0.005	0.005	0.034	0.0005	0.0005	0.001	0.0005	0.0005	5.9
UQAC2131	0.026	0.015	3.4	0.005	0.005	0.14	0.0005	0.0005	0.001	0.0005	0.0005	6.3
UQAC2132	0.041	0.21	18	0.005	0.005	0.89	0.0005	0.0005	0.001	0.0005	0.0005	8.9
UQAC2133	0.012	0.0089	0.17	0.005	0.005	0.27	0.0005	0.0005	0.001	0.0005	0.0005	3.7
UQAC2135	0.0072	0.022	5.6	0.005	0.005	0.53	0.0005	0.0013	0.001	0.0005	0.0005	7.6
UQAC3000	0.001	0.002	0.0005	0.005	0.005	0.022	0.0005	0.0005	0.001	0.0005	0.0005	3.9
UQAC3002	0.0084	0.014	5.4	0.005	0.005	0.36	0.0005	0.0005	0.001	0.0005	0.0005	13
UQAC3004	0.0058	0.1	0.0005	0.005	0.005	0.2	0.0005	0.0005	0.001	0.0005	0.0005	4.8
UQAC3009	0.001	0.69	0.0005	0.01	0.005	0.13	0.0005	0.0005	0.001	0.0005	0.0005	4.7
UQAC3011	0.001	0.02	2.4	0.005	0.005	0.14	0.0005	0.0005	0.001	0.0005	0.0005	5.7
UQAC3013	0.001	0.058	0.0005	0.005	0.005	0.27	0.0005	0.0005	0.0042	0.0005	0.0005	6.1
UQAC3014	0.036	0.092	0.67	0.012	0.005	1	0.0005	0.0005	0.001	0.0005	0.0005	6.5
UQAC3015	0.036	0.027	0.0005	0.005	0.005	0.62	0.0005	0.0005	0.0025	0.0005	0.0005	7.5
UQAC3018	0.028	0.002	0.0005	0.005	0.005	0.016	0.0005	0.0005	0.001	0.0005	0.0005	4
UQAC3019	0.0081	0.043	0.0005	0.005	0.005	0.55	0.0005	0.0005	0.001	0.0005	0.0005	5.3
UQAC3021	0.0082	0.045	0.0005	0.005	0.005	1.3	0.0011	0.0005	0.001	0.0005	0.0005	5.7
UQAC3022	0.11	0.0051	0.0005	0.005	0.005	0.018	0.0005	0.0005	0.001	0.0005	0.0005	2.5
UQAC3023	0.26	0.011	0.0005	0.005	0.005	0.24	0.0005	0.0005	0.001	0.0005	0.0005	9.9
UQAC3025	0.011	0.022	0.0005	0.005	0.005	2	0.0005	0.0005	0.001	0.0005	0.0005	6.1
UQAC3027	0.018	0.002	0.0005	0.005	0.005	0.08	0.0005	0.0005	0.001	0.0005	0.0005	5.7

Sample	Zinc	Boron	Iron	Lithium	Selenium	Strontium	Tin	Titane	Vanadium	Beryllium	Bismuth	Silicium
UQAC3028	0.041	0.002	0.0005	0.005	0.005	0.12	0.0005	0.0005	0.001	0.0005	0.0005	5.8
UQAC3032	0.001	0.0074	0.0005	0.005	0.005	0.022	0.0005	0.0005	0.001	0.0005	0.0005	2.8
UQAC3035	0.19	0.002	1.3	0.005	0.005	0.042	0.0005	0.0005	0.001	0.0005	0.0005	6.5
UQAC3037	0.001	0.002	0.0005	0.005	0.005	0.016	0.0005	0.0005	0.001	0.0005	0.0005	4.5
UQAC3038	0.007	0.067	0.0005	0.005	0.005	0.42	0.0005	0.0005	0.001	0.0005	0.0005	4.6
UQAC3039	0.001	0.0051	0.0005	0.005	0.005	0.024	0.0005	0.0005	0.001	0.0005	0.0005	3.5
UQAC3040	0.0067	0.013	0.0005	0.005	0.005	0.56	0.0005	0.0005	0.001	0.0005	0.0005	8.8
UQAC3041	0.021	0.025	0.0005	0.005	0.005	0.78	0.0005	0.0005	0.001	0.0005	0.0005	4.3
UQAC3042	0.0094	0.097	0.0005	0.005	0.005	0.049	0.0005	0.0005	0.001	0.0005	0.0005	4.5
UQAC3045	0.018	0.03	0.0005	0.005	0.005	0.31	0.0005	0.0005	0.001	0.0005	0.0005	5.6
UQAC3047	0.027	0.013	0.0005	0.005	0.005	0.15	0.0005	0.0005	0.001	0.0005	0.0005	2.9
UQAC3049	0.0062	0.0055	0.0005	0.005	0.005	0.32	0.0005	0.0005	0.001	0.0005	0.0005	4.2
UQAC3050	0.014	0.013	0.0005	0.005	0.005	0.72	0.0005	0.0005	0.001	0.0005	0.0005	7.3
UQAC4000	0.025	0.0081	1	0.005	0.005	0.11	0.0005	0.0005	0.001	0.0005	0.0005	4.8
UQAC4001	0.001	0.002	0.0005	0.005	0.005	0.031	0.0005	0.0005	0.001	0.0005	0.0005	5.6
UQAC4002	0.013	0.002	0.0005	0.005	0.005	0.037	0.0005	0.0005	0.001	0.0005	0.0005	3.7
UQAC4003	0.014	0.002	0.0005	0.005	0.005	0.11	0.0005	0.0005	0.001	0.0005	0.0005	5.5
UQAC4004	0.021	0.21	0.0005	0.005	0.005	0.0015	0.0005	0.0005	0.001	0.0005	0.0005	5.5
UQAC4006	0.018	0.17	0.0005	0.005	0.005	1.4	0.0005	0.0005	0.001	0.0005	0.0005	5.2
UQAC4007	0.028	0.017	0.0005	0.005	0.005	0.22	0.0005	0.0005	0.001	0.0005	0.0005	3.3
UQAC4008	0.036	0.012	0.0005	0.005	0.005	0.18	0.0005	0.0005	0.001	0.0005	0.0005	4.9
UQAC4009	0.084	0.046	0.56	0.005	0.005	0.0015	0.0005	0.0005	0.001	0.0005	0.0005	11
UQAC4010	0.02	0.057	0.36	0.005	0.005	1.6	0.0005	0.0005	0.001	0.0005	0.0005	7.1
UQAC4011	0.019	0.021	0.0005	0.005	0.005	0.14	0.0005	0.0005	0.001	0.0005	0.0005	4.3
UQAC4012	0.02	0.065	0.0005	0.005	0.005	0.69	0.0005	0.0005	0.001	0.0005	0.0005	4.5
UQAC4013	0.032	0.042	0.0005	0.005	0.005	2.2	0.0005	0.0005	0.001	0.0005	0.0005	4.5
UQAC4015	0.032	0.2	0.0005	0.005	0.005	0.71	0.0005	0.0005	0.001	0.0005	0.0005	6
UQAC4016	0.017	0.002	0.0005	0.005	0.005	0.11	0.0005	0.0005	0.0022	0.0005	0.0005	4.8
UQAC4018	0.02	0.031	0.0005	0.005	0.005	4.3	0.0005	0.0005	0.001	0.0005	0.0005	5.5
UQAC4019	0.025	0.0066	0.0005	0.005	0.005	0.12	0.0005	0.0005	0.0054	0.0005	0.0005	11
UQAC4021	0.001	0.18	0.0005	0.017	0.005	2.8	0.0005	0.0005	0.0032	0.0005	0.0005	5.6
UQAC4022	0.037	0.075	0.35	0.005	0.005	0.77	0.0005	0.0005	0.001	0.0005	0.0005	5.7
UQAC4023	0.09	0.017	2	0.005	0.005	0.31	0.0005	0.0005	0.001	0.0005	0.0005	6.1
UQAC4024	0.067	0.002	0.0005	0.005	0.005	0.11	0.0005	0.0005	0.001	0.0005	0.0005	6.9
UQAC4029	0.035	0.002	1	0.005	0.005	0.06	0.0005	0.0005	0.001	0.0005	0.0005	13
UQAC4030	0.35	0.002	13	0.005	0.005	0.035	0.0005	0.0005	0.001	0.0005	0.0005	8.9
UQAC4031	0.0074	0.15	0.0005	0.012	0.005	2.4	0.0005	0.0005	0.001	0.0005	0.0005	5.9
UQAC4033	0.0063	0.028	0.0005	0.005	0.005	0.21	0.0005	0.0005	0.001	0.0005	0.0005	8.5

Sample	Zinc	Boron	Iron	Lithium	Selenium	Strontium	Tin	Titane	Vanadium	Beryllium	Bismuth	Silicium
UQAC4034	0.0084	0.11	0.16	0.011	0.005	1.5	0.0005	0.0005	0.001	0.0005	0.0005	9.6
UQAC4036	0.023	0.002	6.1	0.005	0.005	0.079	0.0005	0.0005	0.001	0.0005	0.0005	7.7
UQAC4037	0.011	0.3	0.0005	0.005	0.005	0.16	0.0005	0.0005	0.001	0.0005	0.0005	6.7
UQAC4038	0.0072	0.002	0.0005	0.005	0.005	0.06	0.0005	0.0005	0.001	0.0005	0.0005	7
UQAC4041	0.018	0.002	2.3	0.005	0.005	0.093	0.0005	0.0005	0.001	0.0005	0.0005	9.9
UQAC4042	0.091	0.002	0.0005	0.005	0.005	0.058	0.0005	0.0005	0.001	0.0005	0.0005	7.1
UQAC4044	0.038	0.046	0.13	0.005	0.005	0.13	0.0005	0.0005	0.001	0.0005	0.0005	8
UQAC4045	0.001	0.002	0.0005	0.005	0.005	0.033	0.0005	0.0005	0.001	0.0005	0.0005	4.1
UQAC4047	0.0093	0.002	0.14	0.005	0.005	0.018	0.0005	0.0005	0.001	0.0005	0.0005	4
UQAC4048	0.13	0.46	0.19	0.011	0.005	0.077	0.0005	0.0005	0.001	0.0005	0.0005	6.5
UQAC4049	0.001	0.002	0.0005	0.005	0.005	0.092	0.0005	0.0005	0.001	0.0005	0.0005	3.8
UQAC4051	0.056	0.016	0.0005	0.005	0.005	0.15	0.0005	0.0005	0.001	0.0005	0.0005	6
UQAC4052	0.0074	0.29	0.0005	0.005	0.005	2	0.0005	0.0005	0.001	0.0005	0.0005	7.7
UQAC4053	0.022	0.0073	0.0005	0.005	0.005	0.018	0.0005	0.0005	0.001	0.0005	0.0005	5.3
UQAC4054	0.016	0.75	0.0005	0.018	0.005	0.069	0.0005	0.0005	0.001	0.0005	0.0005	3.6
UQAC4057	0.01	0.049	0.0005	0.005	0.005	0.75	0.0005	0.0005	0.001	0.0005	0.0005	5.2
UQAC4060	0.013	0.095	0.0005	0.005	0.005	0.06	0.0005	0.0005	0.001	0.0005	0.0005	7.3
UQAC4064	0.015	0.1	0.15	0.005	0.005	0.087	0.0005	0.0005	0.001	0.0005	0.0005	7.1
UQAC4065	0.051	0.0083	0.0005	0.005	0.005	0.1	0.0005	0.0005	0.001	0.0005	0.0005	6.1
UQAC4067	0.045	0.0053	0.0005	0.005	0.005	0.05	0.0005	0.0005	0.001	0.0005	0.0005	5.6
UQAC4068	0.12	0.002	0.0005	0.005	0.005	0.035	0.0005	0.0005	0.001	0.0005	0.0005	4.5
UQAC4069	0.072	0.025	0.21	0.005	0.005	0.46	0.0005	0.0005	0.0069	0.0005	0.0005	6.5
UQAC4071	0.079	0.0086	0.0005	0.005	0.005	0.045	0.0005	0.0005	0.001	0.0005	0.0005	4.8
UQAC4072	0.0069	0.01	0.0005	0.005	0.005	0.13	0.0005	0.0005	0.001	0.0005	0.0005	6.1
UQAC6002	0.11	0.002	3.2	0.005	0.005	0.021	0.0005	0.0005	0.001	0.0005	0.0005	6.7
UQAC6006	0.001	0.20	35	0.014	0.005	0.40	0.0005	0.0005	0.001	0.0005	0.0005	15
UQAC6010	0.022	0.002	0.0005	0.005	0.005	0.036	0.0005	0.0005	0.001	0.0005	0.0005	4.4
1JW04	0.0100	0.0040	0.0130	0.0010	0.0005	0.0700	0.0005	0.0005	0.0005	0.0005	0.0005	4.9
1JW05	0.0020	0.4400	0.0005	0.0020	0.0005	0.1000	0.0005	0.0005	0.0005	0.0005	0.0005	5.4
1JW08	0.0020	0.1800	0.0870	0.0200	0.0005	1.3000	0.0005	0.0005	0.0005	0.0005	0.0005	3.9
1JW31	0.0020	0.5200	0.0040	0.0040	0.0005	0.1200	0.0005	0.0005	0.0005	0.0005	0.0005	6.0
1JW37	0.0070	0.0400	0.0050	0.0020	0.0005	0.4000	0.0005	0.0005	0.0005	0.0005	0.0005	5.3
2JW15	0.0020	0.3500	0.0250	0.0030	0.0005	0.0900	0.0005	0.0005	0.0005	0.0005	0.0005	8.9
2JW17	0.0020	0.1100	0.0050	0.0080	0.0005	0.5900	0.0005	0.0005	0.0005	0.0005	0.0005	4.0
3JW01	0.0020	0.1700	0.0170	0.0020	0.0005	0.0200	0.0005	0.0005	0.0005	0.0005	0.0005	5.8
3JW21	0.0140	0.0360	0.0020	0.0020	0.0005	0.1800	0.0005	0.0005	0.0005	0.0005	0.0005	9.3
3JW29	0.0090	0.2000	0.0030	0.0200	0.0005	0.5400	0.0005	0.0005	0.0005	0.0005	0.0005	6.1
3JW34	0.0170	0.0240	5.1000	0.0060	0.0005	0.4400	0.0005	0.0005	0.0005	0.0005	0.0005	10.0

Sample	Zinc	Boron	Iron	Lithium	Selenium	Strontium	Tin	Titane	Vanadium	Beryllium	Bismuth	Silicium
UQAC1105	0.012	0.14	0.7	0.57	0.005	37	0.0005	0.0005	0.001	0.0005	0.0005	4.5
UQAC2034	0.0029	0.32	0.1	0.084	0.005	18	0.0005	0.0005	0.001	0.0005	0.0005	5.2
UQAC3046	0.064	0.75	0.0005	0.082	0.005	22	0.0005	0.0005	0.001	0.0005	0.0005	5.0
UQAC4066	0.01	0.76	1.3	0.2	0.005	13	0.0005	0.0005	0.001	0.0005	0.0005	4.2
1JW03	0.0080	0.6800	0.0150	0.0080	0.0005	19.0000	0.0005	0.0005	0.0005	0.0005	0.0005	6.5
1JW35	0.0110	0.0600	17.0000	0.0400	0.0005	19.0000	0.0005	0.0005	0.0005	0.0005	0.0005	1.3
2JW09	0.0020	0.3800	0.0150	0.0800	0.0005	17.0000	0.0005	0.0005	0.0005	0.0005	0.0005	5.3
2JW10	0.0100	0.2800	0.0360	0.0600	0.0005	23.0000	0.0005	0.0005	0.0005	0.0005	0.0005	4.0
2JW11	0.0100	0.2700	0.2600	0.0500	0.0005	17.0000	0.0005	0.0005	0.0005	0.0005	0.0005	4.6
2JW16	0.0100	0.0500	0.0080	0.0030	0.0005	16.0000	0.0005	0.0005	0.0005	0.0005	0.0005	5.9
2JW18	0.0290	0.8100	0.0260	0.1600	0.0005	22.0000	0.0005	0.0005	0.0005	0.0005	0.0005	4.0
3JW04	0.0080	0.1800	0.0930	0.0100	0.0005	11.0000	0.0005	0.0005	0.0005	0.0005	0.0005	5.4
UQAC1034	0.044	0.57	0.19	0.018	0.005	1.4	0.0005	0.0005	0.001	0.0005	0.0005	8.8
UQAC4059	0.1	0.46	0.27	0.12	0.005	27	0.0005	0.0005	0.001	0.0005	0.0005	4.8
UQAC6012	0.001	0.68	1.3	0.037	0.005	3.7	0.0005	0.0005	0.001	0.0005	0.0005	11.0
UQAC6013	0.001	0.66	1.3	0.030	0.005	2.9	0.0005	0.0005	0.001	0.0005	0.0005	13.0
2JW14	0.0100	0.8200	1.0000	0.0500	0.0005	6.8000	0.0005	0.0005	0.0005	0.0005	0.0005	9.6

Sample	Lead	Uranium	Ammonium	Bromide	Fluoride	Nitrate	Phosphorus	Sulfide
UQAC1011	0.0005	0.0019	0.01	3.5	1.9	0.01	0.02	0.01
UQAC1019	0.00033	0.0024	0.05	1	1.6	0.01	0.02	0.01
UQAC1048	0.00021	0.0021	0.47	1.1	1.8	0.01	0.07	NA
UQAC1071	0.00019	0.0005	1.4	7	1.7	0.01	0.05	NA
UQAC1098	0.0005	0.0005	0.76	7.1	0.9	0.01	0.02	NA
UQAC2047	0.0005	0.0011	0.41	8	1	0.01	0.02	NA
UQAC2048	0.00028	0.0005	0.49	0.05	2.9	0.4	0.11	0.01
UQAC2091	0.0001	0.0005	0.81	1.6	1.7	0.46	0.02	NA
UQAC2128	0.0005	0.0005	1.8	1.9	1.6	0.01	0.02	NA
UQAC3024	0.0004	0.0005	0.69	2.4	2	0.01	0.02	0.01
UQAC3036	0.00017	0.0005	1.6	11	0.8	0.01	0.02	0.01
UQAC3052	0.0005	0.0014	0.01	1.6	4.9	0.01	0.02	0.01
UQAC6007	0.0005	0.0005	0.46	2.8	0.7	0.01	0.09	0.01
1JW01	0.0020	0.0011	1.16	0.20	1.10	0.07	0.04	0.01
1JW02	0.0020	0.0011	1.16	2.44	1.10	0.07	0.04	0.01
1JW07	0.0020	0.0011	1.16	12.10	1.40	0.07	0.04	0.01
1JW15	0.0001	0.0011	1.16	4.11	1.30	0.07	0.04	0.01
1JW26	0.0020	0.0011	1.16	4.00	1.70	0.07	0.04	0.01
1JW28	0.0020	0.0011	1.16	2.38	1.40	0.07	0.04	0.01
1JW38	0.0020	0.0011	1.16	3.05	1.20	0.07	0.04	0.04
2JW02	0.0020	0.0011	1.16	19.44	2.70	0.07	0.04	0.01
2JW04	0.0020	0.0011	1.16	9.63	2.40	0.07	0.04	0.01
2JW08	0.0020	0.0011	1.16	11.34	0.60	0.07	0.04	0.01
2JW12	0.0020	0.0011	1.16	4.97	3.00	0.07	0.04	0.01
2JW19	0.0020	0.0011	1.16	0.46	3.20	0.07	0.04	0.01
2JW20	0.0080	0.0011	1.16	0.43	2.30	0.07	0.04	0.01
3JW05	0.0020	0.0011	1.16	1.48	1.60	0.07	0.04	0.01
3JW08	0.0020	0.0011	1.16	1.78	1.60	0.07	0.04	0.01
3JW10	0.0020	0.0011	1.16	3.08	1.60	0.07	0.04	0.01
3JW12	0.0020	0.0011	1.16	2.78	1.80	0.07	0.04	0.01
UQAC1001	0.00026	0.0005	0.1	0.05	1.7	0.01	0.02	NA
UQAC1002	0.00026	0.0005	0.12	0.05	1.1	0.01	0.02	NA
UQAC1003	0.00021	0.0019	0.39	0.05	0.2	0.01	0.02	NA
UQAC1004	0.0005	0.0005	0.08	0.3	0.8	0.08	0.02	NA
UQAC1005	0.00019	0.0005	0.51	2	1	0.01	0.02	0.01
UQAC1006	0.0005	0.0005	0.01	0.05	0.8	0.04	0.02	NA
UQAC1008	0.0005	0.0005	0.15	0.05	1.7	0.01	0.02	0.01
UQAC1012	0.001	0.0005	0.03	0.05	0.1	3.5	0.02	NA

Sample	Lead	Uranium	Ammonium	Bromide	Fluoride	Nitrate	Phosphorus	Sulfide
UQAC1013	0.0005	0.0005	0.27	0.4	2.3	0.01	0.02	0.01
UQAC1014	0.00037	0.0005	0.07	0.05	0.4	0.41	0.02	NA
UQAC1015	0.0003	0.0005	0.29	0.05	0.6	0.01	0.02	0.01
UQAC1016	0.00067	0.0005	0.06	0.05	0.8	0.21	0.02	NA
UQAC1017	0.00031	0.0005	0.05	0.05	0.02	6.3	0.02	NA
UQAC1020	0.00067	0.0005	0.04	0.05	0.3	0.34	0.02	NA
UQAC1021	0.00015	0.0005	0.06	0.1	0.6	0.01	0.02	0.01
UQAC1022	0.00046	0.0021	0.04	0.05	0.3	0.01	0.02	NA
UQAC1023	0.00039	0.0053	0.06	0.2	0.8	0.16	0.02	NA
UQAC1024	0.00019	0.0078	0.11	0.05	1.8	0.6	0.02	NA
UQAC1025	0.0005	0.0005	0.13	0.05	1.3	0.01	0.02	NA
UQAC1026	0.00028	0.0005	0.08	0.2	1.5	0.01	0.02	NA
UQAC1028	0.0005	0.0005	0.06	0.05	0.02	0.3	0.02	NA
UQAC1029	0.00057	0.002	0.03	0.05	0.02	4.4	0.02	NA
UQAC1030	0.00012	0.0023	0.04	0.05	0.6	0.29	0.02	NA
UQAC1032	0.0005	0.0005	0.01	0.05	0.02	0.01	0.02	NA
UQAC1033	0.0005	0.0005	0.21	0.05	0.6	0.01	0.02	0.01
UQAC1035	0.0005	0.0005	0.12	0.05	0.4	0.01	0.02	0.01
UQAC1036	0.00019	0.0005	0.21	0.05	0.02	0.17	0.02	0.01
UQAC1038	0.00012	0.0005	0.52	0.05	0.4	0.01	0.02	0.01
UQAC1040	0.00086	0.0005	0.04	0.05	0.02	0.01	0.02	NA
UQAC1041	0.0019	0.001	0.15	0.05	1.9	0.01	0.35	0.01
UQAC1042	0.00042	0.0005	0.32	0.05	0.2	0.1	0.02	NA
UQAC1043	0.00026	0.0005	0.14	0.05	1.6	0.01	0.02	NA
UQAC1044	0.00022	0.0005	0.06	0.05	0.2	0.9	0.02	NA
UQAC1045	0.00041	0.001	0.08	0.05	0.7	0.3	0.02	NA
UQAC1046	0.00041	0.0005	0.04	0.05	0.02	0.01	0.02	NA
UQAC1049	0.00086	0.0005	0.02	0.05	0.02	0.01	0.02	NA
UQAC1050	0.00045	0.0005	0.09	0.05	0.6	0.01	0.02	NA
UQAC1051	0.0014	0.0005	0.04	0.05	0.6	0.2	0.02	NA
UQAC1052	0.00033	0.0005	0.11	0.05	0.6	0.01	0.02	NA
UQAC1053	0.0005	0.0041	0.05	0.05	0.3	0.01	0.02	NA
UQAC1055	0.00058	0.0005	0.01	0.05	0.02	0.01	0.02	NA
UQAC1058	0.0005	0.0005	0.01	0.05	0.1	0.03	0.02	NA
UQAC1059	0.00015	0.0005	0.11	0.05	0.2	0.01	0.02	NA
UQAC1063	0.00028	0.0037	0.08	0.05	0.2	0.05	0.02	NA
UQAC1064	0.0005	0.0005	0.01	0.05	0.02	0.01	0.02	NA
UQAC1065	0.001	0.0005	0.01	0.05	0.02	1	0.02	NA

Sample	Lead	Uranium	Ammonium	Bromide	Fluoride	Nitrate	Phosphorus	Sulfide
UQAC1066	0.00028	0.0005	0.03	0.05	0.1	0.01	0.02	NA
UQAC1067	0.00026	0.0005	0.05	0.05	0.9	0.01	0.02	0.01
UQAC1069	0.00016	0.0005	0.51	0.05	0.4	0.01	0.02	0.3
UQAC1073	0.0005	0.0005	0.05	0.05	0.1	0.2	0.02	NA
UQAC1074	0.00032	0.0005	0.08	0.05	0.4	0.01	0.02	NA
UQAC1075	0.0005	0.0005	0.6	0.05	0.4	0.01	0.02	NA
UQAC1076	0.00014	0.0005	0.21	0.05	0.7	0.01	0.02	NA
UQAC1077	0.00053	0.0005	0.06	0.05	0.02	1.1	0.02	NA
UQAC1078	0.00044	0.0005	0.04	0.05	0.2	1.2	0.02	NA
UQAC1079	0.00041	0.0013	0.05	0.05	0.9	0.01	0.02	NA
UQAC1080	0.0005	0.0005	0.08	0.05	0.3	0.01	0.02	0.01
UQAC1081	0.0013	0.0005	0.03	0.05	0.4	0.1	0.02	NA
UQAC1082	0.0005	0.002	0.21	0.05	1.6	0.01	0.02	NA
UQAC1083	0.00032	0.0011	0.08	0.05	0.1	3.3	0.02	NA
UQAC1084	0.0005	0.0005	0.15	0.05	0.02	0.01	0.02	NA
UQAC1086	0.00026	0.0005	0.05	0.05	0.02	1.6	0.02	NA
UQAC1087	0.00047	0.0021	0.03	0.05	0.6	0.01	0.02	NA
UQAC1088	0.0005	0.0032	0.07	0.05	0.4	0.01	0.02	NA
UQAC1089	0.00015	0.0005	0.06	0.05	0.1	0.01	0.02	NA
UQAC1090	0.00071	0.0005	0.02	0.05	0.02	0.6	0.02	NA
UQAC1092	0.0005	0.0005	0.32	0.05	0.6	0.01	0.02	0.01
UQAC1094	0.0005		0.49	0.05	0.6	0.1	0.02	0.01
UQAC1095	0.0005	0.0014	0.08	0.05	0.2	1.4	0.02	NA
UQAC1096	0.0005	0.0005	0.29	0.05	1.4	0.01	0.02	0.01
UQAC1097	0.0005	0.0005	0.27	0.05	0.3	0.01	0.02	0.16
UQAC1099	0.00038	0.0005	0.68	0.05	0.5	0.01	0.02	NA
UQAC1101	0.00013	0.0005	0.31	1.5	1.7	0.01	0.02	NA
UQAC1103	0.0005	0.0031	0.03	0.05	0.1	0.01	0.02	NA
UQAC1108	0.00016	0.001	0.25	0.05	0.6	0.01	0.02	NA
UQAC1109	0.00023	0.0005	0.05	0.05	1.6	0.01	0.02	0.01
UQAC1110	0.0015	0.0005	0.3	0.05	0.2	0.01	0.02	0.01
UQAC1111	0.0004	0.0005	0.04	0.05	0.02	0.3	0.02	NA
UQAC1112	0.0005	0.0029	0.07	0.05	0.4	0.1	0.5	NA
UQAC1113	0.0003	0.0005	0.06	0.05	0.02	0.01	0.02	NA
UQAC1114	0.00022	0.0005	0.06	0.05	0.02	8.6	0.02	NA
UQAC1115	0.0005	0.0005	0.29	0.05	1.4	0.01	0.02	0.11
UQAC1116	0.00024	0.0005	0.16	0.05	0.6	0.01	0.02	NA
UQAC1117	0.00047	0.0005	0.03	0.05	0.02	0.7	0.02	NA

Sample	Lead	Uranium	Ammonium	Bromide	Fluoride	Nitrate	Phosphorus	Sulfide
UQAC1118	0.00044	0.0005	0.01	0.05	0.02	0.3	0.02	NA
UQAC1119	0.0005	0.013	0.1	0.05	1.7	0.1	0.02	NA
UQAC1120	0.00017	0.0012	0.01	0.05	0.1	1.1	0.02	NA
UQAC1121	0.00062	0.0005	0.01	0.05	1.6	0.01	0.02	NA
UQAC1123	0.00034	0.0005	0.02	0.05	0.02	0.09	0.07	NA
UQAC2001	0.00028	0.0005	0.05	0.05	0.2	0.01	0.02	NA
UQAC2002	0.00011	0.0005	0.01	0.05	0.02	0.57	0.02	NA
UQAC2003	0.00023	0.0005	0.01	0.05	0.5	0.52	0.02	NA
UQAC2004	0.0005	0.0005	0.01	0.05	0.02	0.33	0.02	NA
UQAC2005	0.0011	0.0005	0.01	0.05	0.02	3.8	0.02	NA
UQAC2008	0.00045	0.0005	0.01	0.05	0.1	0.06	0.02	NA
UQAC2009	0.00016	0.0005	0.01	0.05	0.02	0.08	0.02	NA
UQAC2010	0.0005	0.0005	0.01	0.05	0.02	0.06	0.02	NA
UQAC2011	0.0005	0.0005	0.85	0.05	0.02	0.01	0.02	0.01
UQAC2012	0.0004	0.0005	0.01	0.05	0.1	0.19	0.02	NA
UQAC2013	0.00047	0.0005	0.01	0.05	0.02	0.14	0.02	NA
UQAC2014	0.0005	0.0005	0.01	0.05	0.02	0.01	0.02	NA
UQAC2015	0.0005	0.0005	0.04	0.05	0.5	0.01	0.02	0.01
UQAC2016	0.0005	0.01	0.04	0.05	0.5	0.01	0.02	0.01
UQAC2017	0.00019	0.0066	0.03	0.05	1.6	0.01	0.02	0.01
UQAC2018	0.00048	0.0005	0.06	0.05	0.3	1.4	0.02	NA
UQAC2019	0.0024	0.0005	0.01	0.05	0.3	1.4	0.02	NA
UQAC2020	0.00074	0.0005	0.01	0.05	0.4	4.5	0.02	NA
UQAC2021	0.00016	0.02	0.02	0.05	2.4	0.18	0.02	0.01
UQAC2022	0.0005	0.0005	0.03	0.5	2.3	0.01	0.02	0.01
UQAC2023	0.00092	0.0005	0.07	0.05	0.02	0.05	0.02	NA
UQAC2025	0.00081	0.0005	0.02	0.05	0.02	0.88	0.02	NA
UQAC2026	0.00021	0.0005	0.09	0.05	0.5	0.01	0.02	NA
UQAC2029	0.00024	0.0005	0.03	0.05	0.02	0.14	0.02	0.01
UQAC2030	0.00042	0.0005	0.05	0.05	0.02	0.01	0.02	NA
UQAC2031	0.00044	0.0005	0.03	0.05	0.02	3.9	0.02	NA
UQAC2033	0.00045	0.0024	0.16	0.5	1.5	0.03	0.02	NA
UQAC2035	0.00012	0.0041	0.04	0.05	1.6	0.01	0.02	0.01
UQAC2036	0.00022	0.0005	0.03	0.05	0.4	0.01	0.02	NA
UQAC2038	0.0005	0.0013	0.15	0.05	1.8	0.06	0.02	0.01
UQAC2039	0.0005	0.0054	0.29	0.1	2.3	0.02	0.05	0.01
UQAC2042	0.0005	0.0005	0.05	0.05	0.02	0.01	0.02	NA
UQAC2044	0.0024	0.0089	0.06	0.2	2.3	0.5	0.02	NA

Sample	Lead	Uranium	Ammonium	Bromide	Fluoride	Nitrate	Phosphorus	Sulfide
UQAC2045	0.0005	0.0005	0.29	0.05	0.6	0.01	0.02	0.01
UQAC2046	0.0007	0.0005	0.07	0.05	0.02	0.01	0.02	NA
UQAC2050	0.00055	0.0005	0.01	0.05	0.02	3.2	0.02	NA
UQAC2051	0.0036	0.0005	0.01	0.05	0.02	0.01	0.02	NA
UQAC2052	0.0005	0.0005	0.01	0.05	0.02	0.01	0.02	NA
UQAC2053	0.00027	0.0005	0.01	0.05	0.02	0.01	0.02	NA
UQAC2054	0.00027	0.0005	0.01	0.05	2.9	0.01	0.02	NA
UQAC2055	0.0003	0.0017	0.01	0.05	0.1	1.2	0.02	NA
UQAC2059	0.0021	0.0005	0.01	0.05	0.02	1.3	0.06	NA
UQAC2060	0.00013	0.0005	0.12	0.05	0.7	0.3	0.14	NA
UQAC2062	0.0005	0.0005	0.05	0.05	0.02	0.01	0.02	NA
UQAC2063	0.0005	0.0031	0.21	0.7	1.6	0.01	0.02	NA
UQAC2064	0.0005	0.0005	0.21	0.05	1.9	0.01	0.02	NA
UQAC2069	0.00015	0.0005	0.27	0.05	1.6	0.01	0.5	0.32
UQAC2071	0.0005	0.016	0.22	0.05	2	0.01	0.02	NA
UQAC2073	0.00033	0.0005	0.01	0.05	0.2	0.01	0.02	NA
UQAC2074	0.00059	0.0005	0.01	0.05	0.02	0.1	0.02	NA
UQAC2075	0.00073	0.0034	0.04	0.05	0.02	1.5	0.02	NA
UQAC2076	0.00011	0.0036	0.07	3	1.6	0.01	0.02	0.01
UQAC2077	0.00019	0.0005	0.03	0.05	0.02	2.9	0.02	NA
UQAC2078	0.0005	0.0014	0.15	0.1	2.6	0.03	0.02	0.01
UQAC2079	0.0015	0.0005	0.02	0.05	0.02	0.94	0.02	NA
UQAC2081	0.00014	0.0005	0.03	0.05	0.02	0.37	0.02	NA
UQAC2082	0.00014	0.0005	0.28	0.05	0.3	0.02	0.02	0.01
UQAC2086	0.00072	0.0005	0.08	0.05	0.02	0.01	0.02	NA
UQAC2088	0.00049	0.0005	0.02	0.05	0.2	0.01	0.02	NA
UQAC2089	0.0005	0.0005	0.01	0.05	0.1	0.1	0.02	NA
UQAC2090	0.0005	0.0096	0.01	0.2	0.7	0.11	0.02	NA
UQAC2092	0.00016	0.0005	0.01	0.05	0.1	0.08	0.02	NA
UQAC2093	0.0005	0.0005	0.01	0.05	0.02	0.08	0.02	NA
UQAC2094	0.0005	0.0005	0.03	0.05	0.3	0.01	0.02	0.01
UQAC2096	0.00024	0.0005	0.04	0.05	0.2	0.01	0.02	NA
UQAC2097	0.00051	0.0005	0.07	0.05	0.2	0.5	0.02	NA
UQAC2098	0.00022	0.0005	0.23	0.05	0.8	0.01	0.02	NA
UQAC2099	0.0041	0.0005	0.03	0.05	0.02	0.8	0.02	0.01
UQAC2100	0.0005	0.0005	0.05	0.05	0.02	0.4	0.02	NA
UQAC2101	0.0005	0.0005	0.05	0.05	0.8	0.01	0.02	NA
UQAC2103	0.00029	0.0005	0.04	0.05	0.4	0.2	0.02	NA

Sample	Lead	Uranium	Ammonium	Bromide	Fluoride	Nitrate	Phosphorus	Sulfide
UQAC2104	0.00047	0.0005	0.04	0.05	0.02	0.01	0.02	0.01
UQAC2106	0.00048	0.0005	0.04	0.05	0.2	0.01	0.02	NA
UQAC2107	0.0005	0.0005	0.07	0.05	0.3	0.01	0.02	NA
UQAC2108	0.0002	0.0005	0.04	0.05	0.02	0.01	0.02	NA
UQAC2112	0.0073	0.0005	0.09	0.05	0.02	0.1	0.02	NA
UQAC2114	0.0005	0.0005	0.16	0.05	0.4	0.01	0.02	0.01
UQAC2116	0.00031	0.003	0.1	0.05	1.6	0.01	0.02	NA
UQAC2117	0.00023	0.0005	0.05	0.05	0.1	0.51	0.02	NA
UQAC2118	0.0005	0.0005	0.14	0.05	0.2	0.01	0.02	0.01
UQAC2119	0.00024	0.0005	0.15	0.05	0.02	0.09	0.02	0.01
UQAC2120	0.0005	0.0005	0.07	0.05	0.1	0.8	0.02	NA
UQAC2121	0.0005	0.0005	0.16	0.05	0.7	0.01	0.04	0.01
UQAC2122	0.0005	0.0005	0.02	0.05	0.5	0.2	0.02	NA
UQAC2123	0.00014	0.0013	0.04	0.05	0.9	0.01	0.02	NA
UQAC2124	0.0005	0.0005	0.03	0.05	0.02	0.3	0.02	NA
UQAC2125	0.0005	0.0005	0.04	0.05	0.1	0.01	0.02	NA
UQAC2126	0.00013	0.0021	0.01	0.05	0.5	0.1	0.02	NA
UQAC2129	0.00013	0.0005	0.01	0.05	0.02	0.3	0.02	NA
UQAC2130	0.0022	0.0005	0.46	0.05	0.02	0.6	0.02	NA
UQAC2131	0.0005	0.0011	0.01	0.05	0.3	0.3	0.02	0.01
UQAC2132	0.0005	0.0005	0.6	1.2	0.4	0.01	0.02	0.01
UQAC2133	0.00016	0.0015	0.04	0.05	0.1	0.01	0.02	0.01
UQAC2135	0.0005	0.0005	0.22	0.05	0.3	0.01	0.02	0.01
UQAC3000	0.00043	0.0005	0.01	0.05	0.02	0.1	0.02	NA
UQAC3002	0.0011	0.0005	0.37	0.05	0.02	0.01	0.02	0.01
UQAC3004	0.0005	0.0005	0.19	0.05	0.5	0.01	0.02	0.01
UQAC3009	0.00012	0.0005	0.01	1.2	2	0.01	0.02	0.01
UQAC3011	0.0005	0.0005	0.05	0.05	0.2	0.02	0.02	0.01
UQAC3013	0.0005	0.0011	0.01	0.4	0.9	0.08	0.02	NA
UQAC3014	0.0005	0.0005	0.56	0.05	2	0.01	0.02	0.01
UQAC3015	0.0011	0.0018	0.07	0.05	0.2	5.3	0.02	NA
UQAC3018	0.0012	0.0005	0.06	0.05	0.1	0.01	0.02	NA
UQAC3019	0.00014	0.0005	0.24	0.05	1.8	0.01	0.02	0.01
UQAC3021	0.00066	0.0014	0.08	0.05	1.6	0.01	0.02	NA
UQAC3022	0.00028	0.0005	0.05	0.05	0.02	0.9	0.02	NA
UQAC3023	0.00014	0.0015	0.05	0.05	0.6	0.4	0.02	NA
UQAC3025	0.00088	0.0054	0.05	0.05	1.7	1.7	0.02	NA
UQAC3027	0.00022	0.0005	0.01	0.05	0.2	0.4	0.02	NA

Sample	Lead	Uranium	Ammonium	Bromide	Fluoride	Nitrate	Phosphorus	Sulfide
UQAC3028	0.001	0.0005	0.04	0.05	1.4	2.3	0.02	NA
UQAC3032	0.00022	0.0005	0.01	0.05	0.1	0.1	0.02	NA
UQAC3035	0.00063	0.0005	0.01	0.05	0.02	0.01	0.02	NA
UQAC3037	0.00099	0.0005	0.06	0.05	0.02	0.1	0.02	NA
UQAC3038	0.00018	0.0017	0.29	0.05	1.6	0.01	0.02	0.01
UQAC3039	0.00023	0.0005	0.06	0.05	0.02	0.5	0.02	NA
UQAC3040	0.00043	0.0005	0.06	0.05	0.2	1.9	0.02	0.01
UQAC3041	0.00011	0.0027	0.06	0.05	1.5	0.7	0.02	NA
UQAC3042	0.00023	0.0005	0.12	0.05	0.3	0.01	0.02	NA
UQAC3045	0.00031	0.0005	0.01	0.05	0.2	0.3	0.02	NA
UQAC3047	0.00023	0.0005	0.01	0.05	0.02	1.2	0.02	0.01
UQAC3049	0.00011	0.0005	0.01	0.05	0.02	0.7	0.02	0.01
UQAC3050	0.00019	0.0005	0.04	0.05	0.02	0.01	0.02	0.01
UQAC4000	0.00022	0.0005	0.01	0.05	0.1	1.3	0.02	0.01
UQAC4001	0.0005	0.0005	0.03	0.05	0.1	0.1	0.02	0.01
UQAC4002	0.00088	0.0005	0.05	0.05	0.2	0.28	0.02	0.01
UQAC4003	0.00012	0.0017	0.05	0.05	0.4	1.5	0.02	0.01
UQAC4004	0.00018	0.0005	0.06	0.05	1.4	0.01	0.02	0.06
UQAC4006	0.00035	0.0005	0.02	0.05	0.6	0.2	0.02	0.01
UQAC4007	0.0005	0.0005	0.03	0.05	0.1	1.9	0.02	0.01
UQAC4008	0.00019	0.0005	0.12	0.05	0.1	0.01	0.02	0.01
UQAC4009	0.00078	0.0005	0.01	0.05	0.2	0.01	0.02	0.01
UQAC4010	0.00043	0.0005	0.11	0.05	1	0.01	0.02	1.2
UQAC4011	0.00017	0.0005	0.01	0.05	0.2	0.7	0.02	0.01
UQAC4012	0.00054	0.0005	0.09	0.05	1	0.01	0.02	0.01
UQAC4013	0.002	0.0005	0.16	0.05	0.8	0.1	0.02	0.01
UQAC4015	0.0005	0.0005	0.54	0.05	0.7	0.01	0.02	0.01
UQAC4016	0.00073	0.0005	0.07	0.05	0.3	0.01	0.02	0.01
UQAC4018	0.0008	0.0005	0.12	0.05	1.3	0.1	0.02	0.01
UQAC4019	0.00021	0.0005	0.03	0.05	0.2	2.5	0.02	0.01
UQAC4021	0.00012	0.0005	0.5	0.05	0.4	0.01	0.02	0.01
UQAC4022	0.00043	0.0005	0.14	0.05	0.2	0.01	0.02	0.01
UQAC4023	0.0002	0.0005	0.34	0.05	0.1	0.01	0.02	0.01
UQAC4024	0.00041	0.0005	0.03	0.05	0.3	0.2	0.02	0.01
UQAC4029	0.00077	0.0005	0.06	0.05	0.1	0.19	0.02	0.01
UQAC4030	0.00093	0.0005	0.03	0.05	0.02	0.08	0.02	0.01
UQAC4031	0.0005	0.0005	0.35	0.05	1.5	0.01	0.02	0.78
UQAC4033	0.00018	0.0005	0.25	0.05	0.6	0.01	0.02	0.06

Sample	Lead	Uranium	Ammonium	Bromide	Fluoride	Nitrate	Phosphorus	Sulfide
UQAC4034	0.0005	0.0074	0.16	0.5	0.6	0.01	0.02	0.01
UQAC4036	0.00029	0.0005	0.1	0.05	0.02	0.01	0.02	0.01
UQAC4037	0.00058	0.0055	0.23	0.05	1.3	0.1	0.02	0.01
UQAC4038	0.00011	0.0005	0.01	0.05	0.02	0.4	0.02	0.01
UQAC4041	0.00012	0.0005	0.08	0.05	0.1	0.01	0.02	0.01
UQAC4042	0.00014	0.0005	0.06	0.05	0.1	0.3	0.02	NA
UQAC4044	0.0005	0.0005	0.28	0.05	0.7	0.14	0.02	0.01
UQAC4045	0.0005	0.0005	0.06	0.05	0.02	0.09	0.02	0.01
UQAC4047	0.0021	0.0005	0.06	0.05	0.02	0.02	0.02	0.01
UQAC4048	0.0005	0.0005	0.45	0.05	1.2	0.4	0.02	0.01
UQAC4049	0.00029	0.0005	0.07	0.05	0.02	6.1	0.02	0.01
UQAC4051	0.0019	0.0005	0.04	0.05	0.1	2.1	0.02	0.01
UQAC4052	0.00046	0.0005	0.04	2.5	0.3	0.1	0.02	0.01
UQAC4053	0.0011	0.0005	0.04	0.05	0.02	0.01	0.02	0.01
UQAC4054	0.00045	0.0005	0.79	0.05	1.5	0.01	0.02	0.21
UQAC4057	0.0005	0.0005	0.12	0.05	2	0.01	0.02	0.03
UQAC4060	0.0005	0.0005	0.01	0.05	1	0.01	0.02	0.01
UQAC4064	0.0002	0.0005	1.1	0.05	0.02	3.7	0.02	0.01
UQAC4065	0.0005	0.0005	0.01	0.05	0.02	0.01	0.3	0.01
UQAC4067	0.00028	0.0005	0.01	0.05	0.02	0.5	0.02	0.01
UQAC4068	0.00013	0.0005	0.01	0.05	0.02	0.3	0.02	0.01
UQAC4069	0.00015	0.0005	0.4	0.05	0.1	2.1	0.02	0.01
UQAC4071	0.00069	0.0005	0.01	0.05	0.02	0.04	0.02	0.01
UQAC4072	0.00027	0.0005	0.03	0.05	0.02	1.9	0.02	0.01
UQAC6002	0.0005	0.0005	0.13	0.05	0.02	0.01	0.02	0.01
UQAC6006	0.0005	0.0005	0.34	1.7	0.5	0.01	0.02	0.01
UQAC6010	0.0005	0.0005	0.05	0.05	0.02	0.1	0.02	NA
1JW04	0.0020	0.0011	1.16	5.96	0.02	0.1	0.0	NA
1JW05	0.0020	0.0011	1.16	0.40	1.30	0.1	0.0	0.01
1JW08	0.0020	0.0011	1.16	4.64	2.00	0.1	0.0	0.01
1JW31	0.0020	0.0011	1.16	0.40	1.50	0.1	0.0	0.05
1JW37	0.0020	0.0011	1.16	2.47	0.12	0.1	0.0	0.01
2JW15	0.0020	0.0011	1.16	0.52	2.00	0.1	0.0	0.59
2JW17	0.0020	0.0011	1.16	0.92	2.00	0.1	0.0	0.01
3JW01	0.0020	0.0011	1.16	0.20	1.00	0.1	0.0	0.01
3JW21	0.0020	0.0011	1.16	1.27	0.90	0.1	0.0	0.01
3JW29	0.0020	0.0011	1.16	3.76	0.02	0.1	0.0	0.01
3JW34	0.0020	0.0011	1.16	0.20	1.1	0.1	0.0	0.01

Sample	Lead	Uranium	Ammonium	Bromide	Fluoride	Nitrate	Phosphorus	Sulfide
UQAC1105	0.0005	0.0005	0.12	45	1.3	0.0	0.0	NA
UQAC2034	0.0015	0.0005	1.70	15	1.3	0.0	0.1	0.01
UQAC3046	0.00062	0.0005	1.30	24	2.4	0.0	0.0	0.01
UQAC4066	0.0005	0.0005	5.70	18	0.02	0.0	0.0	0.01
1JW03	0.0060	0.0011	1.16	16.19	0.02	0.1	0.0	1.40
1JW35	0.0100	0.0011	1.16	22.45	0.7200	0.1	0.0	0.01
2JW09	0.0020	0.0011	1.16	13.82	1.40	0.1	0.0	0.10
2JW10	0.0080	0.0011	1.16	19.39	1.50	0.1	0.0	0.01
2JW11	0.0080	0.0011	1.16	18.69	1.50	0.1	0.0	0.01
2JW16	0.0080	0.0011	1.16	19.07	0.60	0.1	0.0	0.01
2JW18	0.0080	0.0011	1.16	25.44	1.80	0.1	0.0	0.01
3JW04	0.0080	0.0011	1.16	19.79	0.06	0.1	0.0	0.01
UQAC1034	0.0005	0.0018	2.20	10	0.9	0.0	0.0	0.01
UQAC4059	0.0005	0.0005	3.00	19	0.8	0.0	0.0	0.01
UQAC6012	0.0005	0.0016	2.80	12	1.1	0.0	0.0	0.01
UQAC6013	0.0005	0.0012	2.40	11	1.1	0.0	0.0	0.01
2JW14	0.0080	0.0011	1.16	13.21	1.2000	0.1	0.0	0.01

ANNEXE 2 (Annexe 1; Chapitre 4): Matrice de correlation des 4 groupes d'eau souterraine identifies à partir de la base de données régionale (321 échantillons) (Groupe 1: Ca(Na)-HCO3_ GranAq; 132 samples; Groupe 2: Na(Ca)-Cl_GranAq; 19 samples; Groupe 3: (NaCa)-HCO3_RockAq; 124 samples; Groupe 4: (NaCa)-Cl_RockAq; 46 samples).

	Mg	K	Ca	HCO3	Cl	SO4	Al	Ag	Ba	Cu	Mn	Mo	Zn	B	Fe	Sr	Si	Pb	U	NH4	F	NO3
Na	-0.21		-0.39	0.49	0.79	0.58						0.45		0.67						0.20	0.65	
Mg		0.56	0.66	0.48					0.39		0.37					0.44	0.23			0.21	-0.29	
K			0.33	0.51					0.32		0.50					0.23				0.29		
Ca				0.38					0.37		0.47	-0.19		-0.35		0.46					-0.36	
Al				HCO3	0.45	0.33		0.19	0.31		0.31		-0.19	0.41		0.26				0.37	0.19	
Ag		Ag			Cl	0.69						0.47		0.39							0.45	
Ba			Ba			SO4						0.51				0.25			0.21		0.44	
Cu				Cu																		
Mn			0.24		Mn																	
Mo						Mo																
Zn							Zn															
B		0.28						Ba														
Fe							0.75		Fe													
Sr			0.48							Sr												
Si		0.30				-0.20	0.38		0.32		Si											
Pb	0.39											Pb										
U						0.29							U									
NH4		0.26	0.29					0.51		0.19				NH4								
F				-0.20		0.50	-0.21	0.37			-0.28		0.31		F							
NO3														-0.21	-0.19	NO3						

Correlations (NaCaHCO3-Roc)
Marked correlations are significant at p < .05000
N=124

Correlation matrix 1

	Mg	K	Ca	HCO3	Cl	SO4	Al	Ag	Ba	Co	Cu	Mn	Mo	Ni	Zn	B	F	Sr	Si	Pb	NH4	Fe	NO3	P
Na	0.20	0.56		0.50	0.72	0.20	0.53						0.17			0.90			0.19			0.70		0.42
Mg		0.69	0.55	0.68	0.37	0.59			0.30				0.46	0.18				0.38	0.44			0.23	0.22	
K			0.27	0.62	0.43	0.38	0.19		0.24				0.45	0.20		0.51		0.30	0.46		0.30	0.49		0.24
Ca				0.80	0.36	0.60	-0.20		0.36			0.25						0.41					0.37	
Al				HCO3	0.48	0.60			0.32			0.18	0.27		-0.18	0.48		0.41	0.21		0.18	0.42	0.20	0.29
Ag		Ag			Cl	0.34	0.20									0.51		0.25				0.33	0.28	
Ba			Ba			SO4			0.37				0.24			0.20		0.41				0.23	0.27	
Co				Co																				
Cu					Cu																			
Mn				0.85		Mn																		
Mo			0.29				Mo																	
Ni				0.39		0.30		Ni																
Zn				0.18				0.24	Zn															
B	0.54									Ba														
Fe				0.44		0.26		0.40	0.56		Fe													
Sr			0.50							0.38		Sr												
Si				0.25			0.17	0.25		0.18	0.22		Si											
Pb														Pb										
NH4										0.27		0.35	0.17		NH4									
F	0.27		0.32				0.46			0.76		0.43			0.25	Fe								
NO3																	NO3							
P	0.54									0.45						0.33		P						

Correlations (NaCaHCO3-Gran)
Marked correlations are significant at p < .05000
N=132

Correlation matrix 2

	Mg	K	Ca	HCO3	Cl	SO4	Al	Ba	Cu	Mn	Mo	Ni	Zn	B	Fe	Li	Sr	Si	Pb	NH4	Br	F
Na	0.90	0.80			0.90	0.74					0.42		0.41	0.60			0.41			0.58	0.43	
Mg		0.75			0.81	0.73							0.42	0.75						0.75		
K				0.58	0.55	0.57								0.56						0.51		
Ca					0.64						0.45					0.93	0.93				0.94	
Al				HCO3																		
Ba		Ba			Cl	0.67					0.56		0.52	0.58		0.57	0.76			0.54	0.76	
Cu			Cu			SO4					0.42											
Mn				Mn																		
Mo					Mo																	
Ni				0.65		Ni																
Zn				0.52	0.68		Zn															
B		0.47						B														
Fe				0.65					Fe													
Li										Li												
Sr					0.57		0.52	0.41		0.83	Sr											
Si									0.63			Si										
Pb	0.50												Pb									
NH4		0.74						0.82						NH4								
Br					0.41			0.48		0.90	0.95				Br							
F					0.43											F						

Correlations (NaCaCl-Roc)
Marked correlations are significant at p < .05000
N=46

Correlation matrix 3

	Mg	K	Ca	HCO3	Cl	SO4	Al	Ba	Cu	Mn	Mo	Zn	B	Fe	Li	Sr	Si	Pb	NH4	Br	F	NO3	P
Na	0.96	0.95		0.77	0.99	0.97							0.92		0.85		0.59		0.94	0.89			
Mg		0.93		0.67	0.95	0.97							0.83		0.80		0.60		0.89	0.85			
K				0.80	0.93	0.94							0.90		0.78		0.60		0.87	0.84			
Ca															0.60	0.93				0.68			
Al				HCO3	0.72	0.72							0.89		0.52		0.57		0.69	0.63	0.68		
Ba		Ba			Cl	0.95							0.88		0.88		0.56		0.93	0.92			
Cu			Cu			SO4							0.87		0.75		0.53		0.92	0.87			
Mn				Mn																			
Mo					Mo																		
Zn			0.53			Zn																	
B							B																
Fe				0.80				Fe															
Li							0.75		Li														
Sr									0.62	Sr													
Si				0.59			0.61	0.63	0.52		Si												
Pb			0.71									Pb											
NH4							0.87		0.77		0.60		NH4										
Br							0.79		0.85	0.71			0.83	Br									
F					0.67		0.69								Fe								
NO3																NO3							
P															0.65		P						

Correlations (NaCaCl-Gran)
Marked correlations are significant at p < .05000
N=19

Correlation matrix 4

ANNEXE 3 (Annexe 2; Chapitre 4): Compilation des données chimiques d'échantillons prélevés profondément dans le Bouclier Canadien. Ces données ont été compilées de la littérature. Au total, 137 analyses chimiques ont été extraites des cinq études suivantes: Frape and Fritz (1982), 33 échantillons; Bottomley et al. (1999), 24 échantillons; Frape and Fritz (1987), 36 échantillons; Frape et al. (1984), 35 échantillons; and Gascoyne and Kamineni (2002), 17 échantillons.

Table:

N	Sample	Samples sources	Aquifer Type	TDS (mg/L)	Sodium (mg/L)	Magnesium (mg/L)	Potassium (mg/L)	Calcium (mg/L)	Bicarbonate (mg/L)	Chloride (mg/L)	Sulfate (mg/L)	Lithium (mg/L)	Bromide (mg/L)
88	5	Frape et al. (1984)	Roc	325000	45000	5100	199	64000	19	207000	284	-	1760
104	11	Frape et al. (1984)	Roc	254000	22000	48	320	62000	2	168000	213	-	1530
102	9	Frape et al. (1984)	Roc	252000	18500	23.5	371	63800	43	166200	265	-	1200
106	12	Frape et al. (1984)	Roc	249121	18900	78	430	63800	58	162700	223	-	1250
108	13	Frape et al. (1984)	Roc	240632	16880	12	122	65000	2	156000	138	-	1090
103	10	Frape et al. (1984)	Roc	240000	21000	29	220	64000	2	153000	335	-	1370
84	1	Frape et al. (1984)	Roc	237107	32600	920	495	57300	2	1420000	0.8	-	1520
98	3	Frape et al. (1984)	Roc	193000	30000	890	430	44700	2	115000	57	-	1010
99	6	Frape et al. (1984)	Roc	182600	17000	1960	126	46300	9	115000	107	-	1110
97	4	Frape et al. (1984)	Roc	172900	21700	820	164	39300	2	109000	54	-	935
101	8	Frape et al. (1984)	Roc	117292	10100	2490	59.9	28600	19	74600	6	-	896
95	2	Frape et al. (1984)	Roc	108799	17500	563	236	22800	65	65900	231	-	633
100	7	Frape et al. (1984)	Roc	101433	8670	637	59.9	26800	15	63800	2	-	793
116	22	Frape et al. (1984)	Roc	95039	8350	105	36.6	27100	48	58300	123	-	579
113	20	Frape et al. (1984)	Roc	83373	7130	81	122	19300	25	55600	116	-	461
112	19	Frape et al. (1984)	Roc	65437	6800	549	45.7	15900	10	41400	2	-	405
108	15	Frape et al. (1984)	Roc	63136	10900	268	111	12900	28	37100	746	-	358
107	14	Frape et al. (1984)	Roc	58337	9420	250	110	15700	69	35900	198	-	324
111	18	Frape et al. (1984)	Roc	22495	2930	233	92.6	4840	28	13700	444	-	115
109	16	Frape et al. (1984)	Roc	20481	3200	68	230	3740	141	11500	391	-	767
110	17	Frape et al. (1984)	Roc	20338	2740	160	32.1	4540	55	12600	1	-	111
114	21	Frape et al. (1984)	Roc	18812	2300	2	23.1	4470	15	11300	533	-	78.7
118	25	Frape et al. (1984)	Roc	8831	1600	174	29.8	1400	280	5250	-	-	96.8
120	27	Frape et al. (1984)	Roc	5371	908	145	7.8	820	263	3120	28	-	34.4
121	28	Frape et al. (1984)	Roc	4278	180	330	23.5	480	213	97	2950	-	-
117	24	Frape et al. (1984)	Roc	4223	757	115	18.8	648	243	2360	45	-	36.3
119	26	Frape et al. (1984)	Roc	1798	281	65	11.7	212	349	783	76	-	7.02
116	23	Frape et al. (1984)	Roc	1770	290	55	3.2	264	190	542	602	-	4.9
122	29	Frape et al. (1984)	Roc	850	107	42	4.3	80	341	51	227	-	0.4
123	30	Frape et al. (1984)	Roc	740	26	46	5.7	103	350	4	197	-	0.18
126	32	Frape et al. (1984)	Roc	589	20	60	13.8	38	319	121	4	-	2.1
124	31	Frape et al. (1984)	Roc	580	119	22	6.2	24	264	123	9.2	-	1.4
128	35	Frape et al. (1984)	Roc	186	30	6	1.8	21	23	63	25	-	-
127	34	Frape et al. (1984)	Roc	127	12	3	2.2	16	32	7	43	-	-
126	33	Frape et al. (1984)	Roc	117	4	4	1.1	16	27	3	51	-	0.18
145	WB17	Gascoyne et Kamineni (1994)	Roc	50735	11000	51	24	8410	10	30200	1040	-	-
140	ATK19A	Gascoyne et Kamineni (1994)	Roc	39620	1830	4	10	11900	45	25400	430	-	-
144	URL1213	Gascoyne et Kamineni (1994)	Roc	4900	530	25	10	1070	32	2455	775	-	-
138	EBL42	Gascoyne et Kamineni (1994)	Roc	4350	1160	2.2	3.4	455	14	2580	108	-	-
139	ATK14	Gascoyne et Kamineni (1994)	Roc	4309	331	0.7	1.5	1180	6	1910	880	-	-
142	B342	Gascoyne et Kamineni (1994)	Roc	1493	410	15	4.4	85	83	595	300	-	-
131	CR138	Gascoyne et Kamineni (1994)	Roc	688	209	2.4	1	35	50	325	54	-	-
138	ATK56	Gascoyne et Kamineni (1994)	Roc	558	82	2.7	2.4	101	21	199	149	-	-
130	CR1310/9	Gascoyne et Kamineni (1994)	Roc	344	95	1.8	1	15	92	110	21	-	-
143	M8	Gascoyne et Kamineni (1994)	Roc	326	70	1.7	1	14	204	21	14	-	-
136	EBL41	Gascoyne et Kamineni (1994)	Roc	309	72	0.9	0.4	3.6	186	31	2	-	-
141	URL103	Gascoyne et Kamineni (1994)	Roc	272	22	10	2	35	185	1.5	16	-	-
134	EBL2	Gascoyne et Kamineni (1994)	Roc	258	65	0.6	0.2	0.4	157	11	10	-	-
129	CR1314	Gascoyne et Kamineni (1994)	Roc	228	36	2.8	0.4	17	158	1	8	-	-
133	P2	Gascoyne et Kamineni (1994)	Roc	207	55	0.2	0.4	1.7	131	0.8	9	-	-
132	P4	Gascoyne et Kamineni (1994)	Roc	153	8	4.7	1.6	25	103	0.8	4	-	-
137	ATK8A	Gascoyne et Kamineni (1994)	Roc	96	6	3.7	2.6	13.7	66	1.4	3	-	-

Table:

N	Sample	Samplec source	Aquifer Type	TDS (mg/L)	Sodium (mg/L)	Magnesium (mg/L)	Potassium (mg/L)	Calcium (mg/L)	Bicarbonate (mg/L)	Chloride (mg/L)	Sulfate (mg/L)	Lithium (mg/L)	Bomide (mg/L)
17	L261400	Frape and Fritz (1982)	Roc	-	213	0.05	47.1	150	-	431	259	-	-
20	L261750	Frape and Fritz (1982)	Roc	-	190	0.05	30	140	-	322	241	-	-
6	N3651	Frape and Fritz (1982)	Roc	240632	16880	12	122	65000	-	156000	138	-	1090
3	N3640	Frape and Fritz (1982)	Roc	225446	20750	18.3	250	58750	30.6	142000	155	-	1420
29	OCS3250	Frape and Fritz (1982)	Roc	94097	8000	96	44	24500	8.4	60400	81.1	-	632
28	OCS3200	Frape and Fritz (1982)	Roc	85789	7500	82	42	22000	14.3	55200	75.6	-	570
8	Fr33182	Frape and Fritz (1982)	Roc	29737	3500	13.95	87	6800	8.8	18500	566	-	125
12	L40140	Frape and Fritz (1982)	Roc	23170	2313	5.15	24.7	4988	42.1	15500	42.8	-	117
10	Fr33300	Frape and Fritz (1982)	Roc	22594	2625	4	32	4800	9.9	14400	530	-	91.5
7	Fr33170	Frape and Fritz (1982)	Roc	21689	2400	2.15	22.8	4650	10.5	13900	516	-	87.5
9	Fr33192	Frape and Fritz (1982)	Roc	17713	2200	1.9	20.8	3825	9.3	11000	498	-	74
14	L40143	Frape and Fritz (1982)	Roc	13128	1375	4.23	19.4	2938	68.1	8540	26.7	-	66
13	L40141	Frape and Fritz (1982)	Roc	6862	900	3.78	12.2	1560	95.2	4160	40	-	39
2	N3602	Frape and Fritz (1982)	Roc	6290	800	1.78	8.6	1380	7.6	3820	190	-	37.4
1	N3601	Frape and Fritz (1982)	Roc	5303	675	1.38	7.4	1050	8.7	3310	180	-	29.5
11	L40139	Frape and Fritz (1982)	Roc	4538	700	2.65	26	855	113	2710	46.2	-	22
30	G1600	Frape and Fritz (1982)	Roc	4279	180	330	23.5	480	213	97	2950	-	-
4	N3643	Frape and Fritz (1982)	Roc	4113	500	6.1	6.4	800	28.2	2250	160	-	24.8
26	OCS205002	Frape and Fritz (1982)	Roc	3989	425	42	9.2	580	107	1470	1320	-	-
25	OCS205001	Frape and Fritz (1982)	Roc	3544	440	44.5	8	590	111	985	1340	-	-
27	OCS205003	Frape and Fritz (1982)	Roc	3076	385	8.1	5.8	625	19.3	1280	738	-	-
18	L261450	Frape and Fritz (1982)	Roc	2596	370	0.05	300	208	864	620	223	-	-
16	L261350	Frape and Fritz (1982)	Roc	1964	250	15.45	7.6	380	127	870	282	-	7.4
22	OCS508421	Frape and Fritz (1982)	Roc	1888	70	103.5	17	217	152	38	1240	-	-
23	OCS508422	Frape and Fritz (1982)	Roc	1295	36	74	11.7	155	190	26	768	-	-
21	L22450	Frape and Fritz (1982)	Roc	1282	140	16.3	5.8	207	211	408	237	-	37.7
19	L261650	Frape and Fritz (1982)	Roc	1061	145	0.05	44	129	213	160	365	-	11.6
24	OCS508481	Frape and Fritz (1982)	Roc	791	26	29	4.4	118	129	11	460	-	-
5	N3644	Frape and Fritz (1982)	Roc	264	59	3.06	1.3	22	24	84	61.5	-	-
31	1	Frape and Fritz (1982)	Roc	220	31	7.88	2.4	28	18.8	92	24.3	-	-
32	2	Frape and Fritz (1982)	Roc	187	30	6.03	1.8	21	23.2	63	25.4	-	-
15	L26000	Frape and Fritz (1982)	Roc	128	12	2.85	2.2	16	32.5	7	43.1	-	-
33	3	Frape and Fritz (1982)	Roc	107	19	2.9	2	10	11.8	34	17.5	-	-
34	Y5	Bottomley et al. (1999)	Roc	-	995	75	7.8	728	256	2015	1168	0.099	14
35	B646	Bottomley et al. (1999)	Roc	-	195	68	5.1	268	256	309	514	0.049	2
36	Seep	Bottomley et al. (1999)	Roc	-	1585	324	12.5	2265	112	6471	880	0.23	54
37	B8906	Bottomley et al. (1999)	Roc	-	205	32	2.9	194	425	388	113	0.039	2
38	B9362	Bottomley et al. (1999)	Roc	-	2614	40	10.3	2095	20	7136	640	0.218	55
39	B9452	Bottomley et al. (1999)	Roc	-	1990	150	13	2405	98	7164	726	0.558	65
40	B?	Bottomley et al. (1999)	Roc	-	10650	136	61	20598	15	52084	290	1.353	450
41	Ditch	Bottomley et al. (1999)	Roc	-	5477	287	33.4	7938	44	22332	460	0.276	198
42	B33164	Bottomley et al. (1999)	Roc	-	22005	260	176	48997	-	123066	489	2.775	1103
43	B3362	Bottomley et al. (1999)	Roc	-	13887	233	108	28968	27	69798	408	1.763	645
44	B34571	Bottomley et al. (1999)	Roc	-	2858	57	13.8	3037	22	9266	300	0.265	76
45	B34572	Bottomley et al. (1999)	Roc	-	3339	63	17.1	3767	27	11235	628	0.328	88
46	B53161	Bottomley et al. (1999)	Roc	-	10341	301	74.8	18396	15	48104	210	0.837	436
47	B53162	Bottomley et al. (1999)	Roc	-	10564	306	75.2	18576	15	48429	440	0.95	445
48	B5318	Bottomley et al. (1999)	Roc	-	7404	145	55.9	14408	51	36510	476	0.805	323
49	B5310	Bottomley et al. (1999)	Roc	-	13970	241	81.9	23892	10	60633	701	1.644	515
50	ditch	Bottomley et al. (1999)	Roc	-	22169	217	177	48055	15	120548	57	2.844	1071
51	B55864	Bottomley et al. (1999)	Roc	-	30558	222	285	73010	26	174134	229	3.827	1544
52	B6419	Bottomley et al. (1999)	Roc	-	31453	290	265	74468	5	177954	83	3.652	1615
53	B67093	Bottomley et al. (1999)	Roc	-	32459	319	292	76136	11	178140	93	3.975	1474
54	B67094	Bottomley et al. (1999)	Roc	-	32838	278	304	79574	31	188440	130	3.718	1682
55	B71261	Bottomley et al. (1999)	Roc	-	30219	231	258	72755	5	172822	123	4.205	1615
56	B71263	Bottomley et al. (1999)	Roc	-	29997	223	259	69715	10	160122	122	4.349	1543
57	B71264	Bottomley et al. (1999)	Roc	-	30670	198	278	73789	28	174582	247	3.975	1567
58	40004	Frape and Fritz (1987)	Roc	324500	45000	5100	199	64000	19	207000	284	0.07	1760
59	N3644b	Frape and Fritz (1987)	Roc	255800	22000	48	320	62000	-	168000	213	0.7	1530
60	N3646A	Frape and Fritz (1987)	Roc	249100	18900	78	430	63800	58	162700	223	0.81	1250
61	N3651	Frape and Fritz (1987)	Roc	240700	16880	12	122	65000	-	156000	138	0.6	1090
62	45006C	Frape and Fritz (1987)	Roc	237100	32600	920	495	57300	2	142000	1	1.67	1520
63	R36	Frape and Fritz (1987)	Roc	227200	14800	3400	338	61300	101	143581	405	0.25	1785
64	YK2041	Frape and Fritz (1987)	Roc	193100	30000	890	430	44700	-	115000	57	0.74	1010
65	40005	Frape and Fritz (1987)	Roc	182600	17000	1960	126	46300	9	115000	107	0.09	1110
66	YK2042	Frape and Fritz (1987)	Roc	172900	21700	820	164	39300	-	109000	54	0.72	935
67	4.00E+85	Frape and Fritz (1987)	Roc	139100	13300	4200	335	29100	75.9	90000	5	0.28	1134
68	YK45006A	Frape and Fritz (1987)	Roc	119300	15000	550	118	28600	-	73600	219	0.58	667
69	40006	Frape and Fritz (1987)	Roc	101400	8670	637	59.9	26800	15	63800	2	0.12	793
70	OCS3250B	Frape and Fritz (1987)	Roc	95040	8350	105	36.6	27100	48	58300	123	0.2	579
71	N3645	Frape and Fritz (1987)	Roc	83370	7130	80.5	122	19300	25	55600	116	0.56	451
72	R46	Frape and Fritz (1987)	Roc	81090	4850	1500	62.5	22600	72	50828	5	0.13	628
73	40003	Frape and Fritz (1987)	Roc	65440	6800	549	45.7	15900	10	41400	2	0.1	405
74	45003	Frape and Fritz (1987)	Roc	63140	10900	268	111	12900	28	37100	746	0.78	358
75	45002	Frape and Fritz (1987)	Roc	58340	9420	250	110	15700	69	31900	198	0.4	324
76	UN242	Frape and Fritz (1987)	Roc	27300	2200	1000	35	5700	29	17905	5	0.13	234
77	22001	Frape and Fritz (1987)	Roc	22490	2930	233	92.6	4840	28	13700	444	0.05	115
78	49002	Frape and Fritz (1987)	Roc	20480	3200	67.5	230	3740	141	11520	391	0.3	767
79	T32000	Frape and Fritz (1987)	Roc	20340	2740	160	32.1	4540	55	12600	1	0.05	111
80	FR33192B	Frape and Fritz (1987)	Roc	18810	2300	2	23.1	4470	15	11300	533	0.14	78.7
81	UN249	Frape and Fritz (1987)	Roc	12090	1050	525	16.5	2640	38	7600	5	0.1	118
82	5	Frape and Fritz (1987)	Roc	8883	1600	174	29.8	1400	280	5250	-	0.06	96.8
83	10022	Frape and Fritz (1987)	Roc	5371	908	145	7.8	820	263	3120	28	0.07	34.4
84	G1600	Frape and Fritz (1987)	Roc	4277	180	330	23.5	480	213	97	2950	0.19	-
85	4	Frape and Fritz (1987)	Roc	4223	757	115	18.8	548	243	2360	45	-	36.3
86	R42	Frape and Fritz (1987)	Roc	2231	110	130	3.1	370	161	287	1160	0.05	3.6
87	YK2388	Frape and Fritz (1987)	Roc	1770	290	55	3.2	264	-	542	602	0.04	4.9
88	14	Frape and Fritz (1987)	Roc	853	107	42.3	4.3	80	341	51	227	-	0.41
89	6	Frape and Fritz (1987)	Roc	739	26	45.9	5.7	103	350	4	197	-	0.1
90	4001	Frape and Fritz (1987)	Roc	579	119	21.6	6.2	23.6	264	123	9	0.08	1.4
91	DOW0002	Frape and Fritz (1987)	Roc	185	30	6	1.8	21	23	63	25	-	-
92	L26000	Frape and Fritz (1987)	Roc	126	12	2.9	2.2	16	32	7	43	-	-
93	40007	Frape and Fritz (1987)	Roc	117	3.5	4.1	1.1	16.5	27	3	51	0.01	0.18

ANNEXE 4 (Annexe 3; Chapitre 4): Statistiques descriptives (nombre de données au-dessus de la limite de détection (*N*), la médiane, le premier (*25*) et le troisième (*75*) quartiles, le maximum (*Max)* et le minimum (*Min*)) des 4 groupes d'eaux souterraines formés à partir de la base de données régionales (321 échantillons) (Groupe 1: Ca(Na)-HCO3_ GranAq; 132 échantillons; Groupe 2: Na(Ca)-Cl_GranAq; 19 échantillons; Groupe 3: (NaCa)-HCO3_RockAq; 124 échantillons; Groupe 4: (NaCa)-Cl_RockAq; 46 échantillons). Les statistiques descriptives pour des 321 échantillons combines sont présentées au chapitre 3.

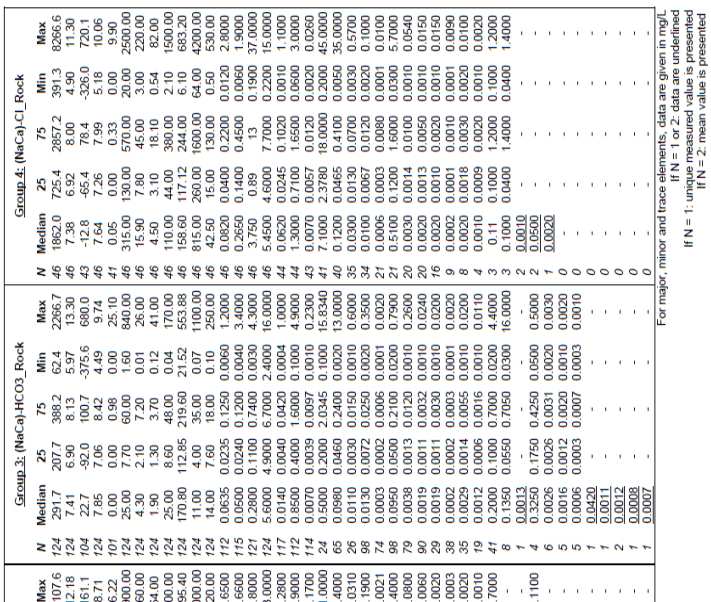

PARAMETER	Group 1: Ca(Na)-HCO3_Q. Sediment						Group 2: Na(Ca)-Cl_Q. Sediment						Group 3: (NaCa)-HCO3_Rock						Group 4: (NaCa)-Cl_Rock					
	N	Median	25	75	Min	Max	*N*	Median	25	75	Min	Max	*N*	Median	25	75	Min	Max	*N*	Median	25	75	Min	Max
TDS (mg/L)	*132*	170.2	62.9	282.2	12.1	836.7	*19*	1167.9	174.4	1679.6	37.3	6107.6	*124*	291.7	207.7	388.2	62.4	2266.7	*46*	1862.0	725.4	2857.2	391.3	8266.6
Temperature (Celcius)*	*129*	8.02	7.02	9.75	4.01	15.60	*19*	7.83	7.55	9.40	6.47	12.18	*124*	7.41	6.90	8.13	5.97	13.30	*46*	7.38	6.92	8.00	4.90	11.30
Redox potential (mV)*	*120*	97.2	79.7	130.4	-255.7	743.9	*17*	68.9	-21.2	107.5	-147.0	161.1	*104*	22.7	-92.0	100.7	-375.6	680.0	*43*	-12.8	-65.4	78.4	-326.0	720.1
pH*	*130*	6.98	6.03	7.81	4.38	108.80	*19*	7.20	5.50	7.61	4.93	8.71	*124*	7.85	7.06	8.42	4.49	9.74	*46*	7.64	7.26	7.99	5.18	10.06
Dissolved oxygen (mg/L)*	*117*	3.62	7.30	0.00	90.00	*17*	0.73	0.00	2.76	0.00	6.22	*101*	0.00	0.00	0.98	0.00	25.10	*41*	0.05	0.00	0.33	0.00	9.90	
Sodium**	*131*	3.80	1.90	10.00	0.87	240.00	*19*	220.00	13.00	490.00	3.80	1900.00	*124*	25.00	7.70	60.00	1.60	840.00	*46*	315.00	130.00	570.00	20.00	2500.00
Magnesium**	*132*	2.60	0.95	6.75	0.15	26.00	*19*	13.40	1.60	25.00	0.31	160.00	*124*	4.30	2.10	7.20	0.01	26.00	*46*	15.90	7.80	45.00	3.00	220.00
Potassium**	*130*	1.30	0.72	2.70	0.14	8.50	*19*	13.00	1.40	21.00	0.40	64.00	*124*	1.90	1.30	3.70	0.12	41.00	*46*	4.50	3.10	18.10	0.54	82.00
Calcium**	*132*	19.50	7.30	46.00	1.20	130.00	*19*	21.00	11.00	60.00	2.20	200.00	*124*	25.00	8.60	48.00	0.04	170.00	*46*	110.00	44.00	380.00	2.10	1500.00
Bicarbonates*****	*132*	108.58	32.33	183.00	7.32	427.00	*19*	207.40	26.84	380.64	6.10	695.40	*124*	170.80	112.85	219.60	21.52	553.88	*46*	158.60	117.12	244.00	6.10	683.20
Chloride***	*129*	3.40	0.90	10.00	0.16	170.00	*19*	310.00	55.00	690.00	9.50	3000.00	*124*	11.00	4.00	35.00	0.07	1100.00	*46*	815.00	260.00	1600.00	64.00	4200.00
Sulfates***	*131*	5.20	3.30	10.00	0.20	41.00	*18*	44.50	8.60	120.00	2.40	420.00	*124*	14.00	7.60	18.00	0.10	250.00	*46*	42.50	15.00	130.00	0.50	530.00
Barium**	*126*	0.0250	0.0100	0.0500	0.0030	0.3000	*19*	0.0540	0.0370	0.0800	0.0130	0.6500	*112*	0.0635	0.0235	0.1250	0.0060	1.2000	*46*	0.0820	0.0400	0.2200	0.0120	2.8000
Boron**	*75*	0.0120	0.0073	0.0210	0.0050	0.3500	*15*	0.2900	0.0160	0.3800	0.0130	0.6600	*115*	0.0500	0.0240	0.1200	0.0040	3.4000	*46*	0.2650	0.1400	0.4500	0.0060	1.9000
Strontium**	*132*	0.0910	0.0390	0.2100	0.0140	2.4000	*19*	0.3700	0.1500	1.4000	0.0160	7.8000	*121*	0.2800	0.1100	0.7400	0.0030	4.3000	*46*	3.750	0.89	13	0.1900	37.0000
Silicium**	*132*	5.9500	4.7500	7.6500	2.5000	14.0000	*19*	7.1000	6.0000	9.1000	1.3000	13.0000	*124*	5.6000	4.9000	6.7000	2.4000	16.0000	*46*	5.4500	4.6000	7.7000	0.2200	15.0000
Manganese**	*107*	0.0071	0.0014	0.0530	0.0004	2.4000	*18*	0.0380	0.0110	0.0710	0.0070	0.2800	*117*	0.0140	0.0040	0.0420	0.0004	1.0000	*44*	0.0620	0.0245	0.1020	0.0010	1.1000
Fluoride****	*68*	0.2000	0.1000	0.6000	0.1000	2.3000	*11*	1.3000	0.9000	1.7000	0.1000	2.9000	*112*	0.8500	0.4000	1.6000	0.1000	4.9000	*44*	1.3000	0.7100	1.6500	0.0600	3.0000
Aluminium**	*119*	0.0075	0.0041	0.0180	0.0020	0.1600	*17*	0.0120	0.0063	0.0290	0.0020	0.1700	*114*	0.0070	0.0039	0.0097	0.0010	0.2300	*43*	0.0070	0.0057	0.0120	0.0020	0.0260
Bromide***	*3*	0.4000	0.4000	0.5220	0.4000	0.5220	*9*	4.1050	1.6000	8.0000	1.1000	11.0000	*24*	0.5000	0.2000	2.0345	0.1000	15.8340	*41*	7.1000	2.3780	18.0000	0.2000	45.0000
Iron**	*55*	0.1100	0.0490	0.7800	0.0250	13.0000	*14*	0.1900	0.1300	1.3000	0.0410	5.4000	*65*	0.0980	0.0460	0.2400	0.0020	13.0000	*40*	0.1200	0.0465	0.4100	0.0050	35.0000
Lithium**	*5*	0.0120	0.0110	0.0130	0.0030	0.0180	*7*	0.0180	0.0120	0.0300	0.0090	0.0310	*26*	0.0110	0.0030	0.0150	0.0010	0.6000	*35*	0.0300	0.0130	0.0700	0.0030	0.5700
Zinc**	*113*	0.0180	0.0097	0.0540	0.0020	0.7100	*16*	0.0190	0.0125	0.0500	0.0070	0.1900	*98*	0.0130	0.0072	0.0250	0.0020	0.3500	*34*	0.0100	0.0067	0.0120	0.0020	0.1000
Lead**	*96*	0.0003	0.0002	0.0007	0.0001	0.0073	*12*	0.0003	0.0002	0.0010	0.0001	0.0021	*74*	0.0003	0.0002	0.0006	0.0001	0.0020	*21*	0.0006	0.0003	0.0080	0.0001	0.0100
Amonium****	*94*	0.0600	0.0400	0.1000	0.0200	0.8500	*14*	0.4650	0.0600	1.1000	0.0400	2.4000	*98*	0.0950	0.0500	0.2100	0.0200	0.7900	*21*	0.5100	0.1200	1.6000	0.0300	5.7000
Copper**	*104*	0.0056	0.0020	0.0130	0.0010	0.3500	*10*	0.0060	0.0020	0.0390	0.0010	0.0800	*79*	0.0038	0.0013	0.0120	0.0010	0.2600	*20*	0.0030	0.0014	0.0100	0.0010	0.0540
Molybdene**	*52*	0.0015	0.0007	0.0024	0.0010	0.0086	*9*	0.0020	0.0015	0.0030	0.0010	0.0060	*90*	0.0019	0.0011	0.0032	0.0010	0.0240	*20*	0.0020	0.0013	0.0050	0.0010	0.0150
Nickel**	*33*	0.0018	0.0014	0.0039	0.0010	0.0110	*4*	0.0020	0.0013	0.0020	0.0010	0.0020	*29*	0.0019	0.0011	0.0030	0.0010	0.0200	*16*	0.0020	0.0010	0.0020	0.0010	0.0150
Silver**	*34*	0.0002	0.0001	0.0003	0.0001	0.0007	*4*	0.0003	0.0001	0.0003	0.0001	0.0003	*38*	0.0002	0.0002	0.0003	0.0001	0.0020	*9*	0.0002	0.0001	0.0010	0.0001	0.0090
Uranium**	*12*	0.0016	0.0011	0.0022	0.0010	0.0034	*4*	0.0020	0.0012	0.0020	0.0010	0.0020	*35*	0.0029	0.0014	0.0055	0.0010	0.0200	*8*	0.0020	0.0018	0.0030	0.0020	0.0100
Chromium**	*20*	0.0010	0.0006	0.0014	0.0010	0.0021	*3*	0.0010	0.0005	0.0010	0.0010	0.0010	*19*	0.0012	0.0006	0.0016	0.0010	0.0110	*4*	0.0010	0.0009	0.0020	0.0010	0.0020
Nitrate***	*84*	0.3150	0.1000	0.9700	0.0200	8.6000	*8*	0.8300	0.2500	1.7000	0.0900	3.7000	*41*	0.2000	0.1000	0.7000	0.0200	4.4000	*3*	0.11	0.1000	1.2000	0.1000	1.2000
Sulfide***	*5*	0.3200	0.3000	0.5900	0.0600	0.7800	*0*	-	-	-	-	-	*8*	0.1350	0.0550	0.7050	0.0300	16.0000	*3*	0.1000	0.0400	1.4000	0.0400	1.4000
Cobalt**	*10*	0.0023	0.0010	0.0026	0.0010	0.0066	*2*	0.0010	-	-	-	-	*1*	0.0013	-	-	-	-	*2*	0.0010	-	-	-	-
Inorganic phosphorus****	*4*	0.1050	0.0550	0.3200	0.0400	0.5000	*6*	0.0650	0.0500	0.0900	0.0400	0.1100	*4*	0.3250	0.1750	0.4250	0.0500	0.5000	*2*	0.0500	-	-	-	-
Vanadium**	*11*	0.0027	0.0022	0.0042	0.0020	0.0069	*0*	-	-	-	-	-	*6*	0.0026	0.0026	0.0031	0.0020	0.0030	*1*	0.0020	-	-	-	-
Antimony**	*4*	0.0023	0.0013	0.0042	0.0010	0.0052	*0*	-	-	-	-	-	*5*	0.0016	0.0012	0.0020	0.0010	0.0020	*0*	-	-	-	-	-
Cadmium**	*4*	0.0003	0.0003	0.0005	0.0002	0.0007	*0*	-	-	-	-	-	*5*	0.0006	0.0003	0.0007	0.0003	0.0010	*0*	-	-	-	-	-
Selenium**	*0*	-	-	-	-	-	*0*	-	-	-	-	-	*1*	0.0420	-	-	-	-	*0*	-	-	-	-	-
Tin**	*1*	0.0021	-	-	-	-	*1*	0.0030	-	-	-	-	*1*	0.0011	-	-	-	-	*0*	-	-	-	-	-
Titanium**	*1*	0.0044	-	-	-	-	*0*	-	-	-	-	-	*2*	0.0012	-	-	-	-	*0*	-	-	-	-	-
Beryllium**	*1*	0.0044	-	-	-	-	*0*	-	-	-	-	-	*1*	0.0008	-	-	-	-	*0*	-	-	-	-	-
Bismuth**	*0*	-	-	-	-	-	*0*	-	-	-	-	-	*1*	0.0007	-	-	-	-	*0*	-	-	-	-	-

ANALYTICAL METHODS
* multiparameter probe (in situ)
**Inductively Coupled Plasma Mass Spectrometry (ICP-MS) (mg/L)
*** Ionic chromatography (mg/L)
**** Specific probe (mg/L)
***** Titration (mg/L)
25 and 75 header correspond to the first and the third quantiles
TDS is calculated using the software Aquachem v.5.0

For major, minor and trace elements, data are given in mg/L
If N = 1 or 2: data are underlined
If N = 1: unique measured value is presented
If N = 2: mean value is presented

ANNEXE 5 (Annexe 4; Chapitre 4): Résultats exprimés en pourcentage de la différence des concentrations médianes des paramètres de la base de données régionale avec les concentrations médianes des paramètres chimiques du jeu de données réduit (Δ m.c).

Chemical Parameters	Database Median (ppm)	Subset Median (ppm)	Δ m.c (%)
Chloride	10	37	370%
Amonium	0.08	0.23	288%
Sodium	14	40	286%
Boron	0.046	0.12	261%
Calcium	26	55	212%
Cadmium	0.00033	0.00067	203%
Magnesium	4.3	8.7	202%
Strontium	0.21	0.4	190%
Manganese	0.017	0.0305	179%
Potassium	2.1	3.5	167%
Sulfates	11	18	164%
Tin	0.0021	0.0034	162%
Cobalt	0.0014	0.0023	161%
Bicarbonates	146.4	207.4	142%
Bromide	2.5	3.5	140%
Chromium	0.00099	0.00134	135%
Barium	0.041	0.055	134%
Iron	0.12	0.15	125%
Lead	0.00033	0.00041	124%
Lithium	0.015	0.018	120%
Fluoride	0.7	0.8	114%
Silicium	5.7	6.5	114%
Antimony	0.0016	0.0017	106%
Molybdene	0.0017	0.0018	106%
Aluminium	0.007	0.00735	105%
Zinc	0.014	0.0145	104%
Nitrate	0.3	0.3	100%
Nickel	0.0019	0.0019	100%
Silver	0.00018	0.00018	100%
Vanadium	0.0026	0.0023	88%
Uranium	0.0021	0.0018	86%
Inorganic phosphorus	0.07	0.05	71%
Copper	0.0043	0.0027	63%
Selenium	0.042	-	-
Beryllium	0.0026	-	-
Titanium	0.0013	-	-
Bismuth	0.00072	-	

ANNEXE 6 (Annexe 5; Chapitre 4): Matrices de corrélation de la base de données régionale (321 échantillons) et du jeu de donnée réduit (51 échantillons).

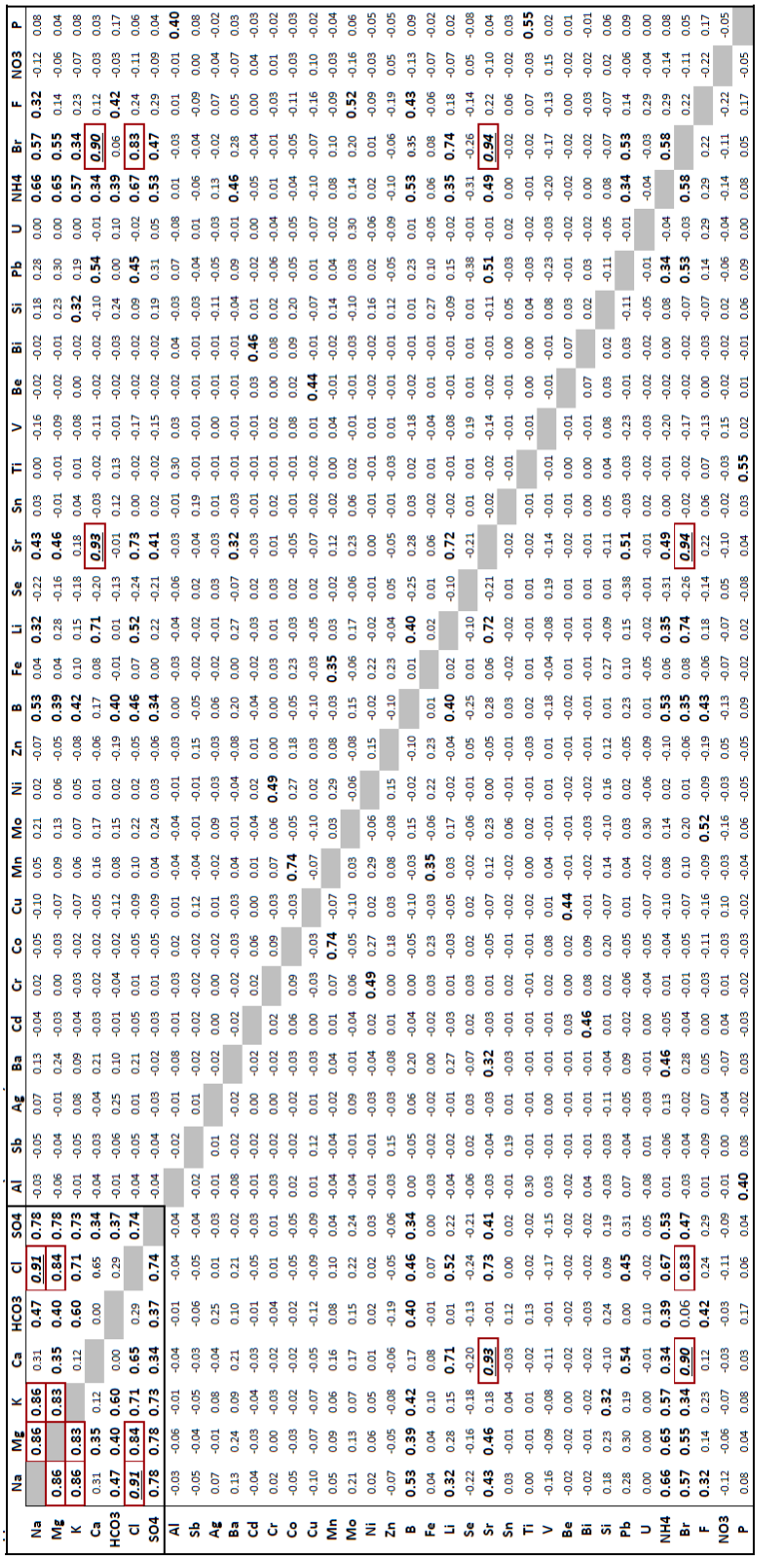

	Na	Mg	K	Ca	HCO3	Cl	SO4	Al	Sb	Ag	Ba	Cd	Cr	Co	Cu	Mn	Mo	Ni	Zn	B	Fe	Li	Se	Sr	Sn	Ti	V	Be	Bi	Si	Pb	U	NH4	Br	F	NO3	P
Na		0.86	0.86	0.31	0.47	0.91	0.78	-0.03	-0.05	0.07	0.13	-0.04	0.02	-0.05	-0.10	0.05	0.21	0.02	-0.07	0.53	0.04	0.32	-0.22	0.43	0.03	0.00	-0.16	-0.02	-0.02	0.18	0.28	0.00	0.66	0.57	0.32	-0.12	0.08
Mg	0.86		0.83	0.35	0.40	0.84	0.78	-0.06	-0.04	-0.01	0.24	-0.03	0.00	-0.03	-0.07	0.09	0.13	0.06	-0.05	0.39	0.04	0.28	-0.16	0.46	-0.01	-0.01	-0.09	-0.02	-0.01	0.23	0.30	0.00	0.65	0.55	0.14	-0.06	0.04
K	0.86	0.83		0.12	0.60	0.71	0.73	-0.01	-0.05	0.08	0.09	-0.04	-0.03	-0.02	-0.07	0.06	0.07	0.05	-0.08	0.42	0.10	0.15	-0.18	0.18	0.04	0.01	-0.08	0.00	-0.02	0.32	0.19	0.00	0.57	0.34	0.23	-0.07	0.08
Ca	0.31	0.35	0.12		0.00	0.65	0.34	-0.04	-0.03	-0.04	0.21	-0.03	-0.02	-0.02	-0.05	0.16	0.17	0.01	-0.06	0.17	0.08	0.71	-0.20	0.93	-0.03	0.12	-0.02	-0.02	-0.02	-0.10	0.54	-0.01	0.34	0.90	0.12	-0.03	0.03
HCO3	0.47	0.40	0.60	0.00		0.29	0.37	-0.01	-0.06	0.25	0.10	-0.01	-0.04	-0.02	-0.12	0.08	0.15	0.02	-0.19	0.40	-0.01	0.01	-0.13	-0.01	0.12	0.13	-0.01	-0.02	-0.03	0.24	0.00	0.10	0.39	0.06	0.42	-0.03	0.17
Cl	0.91	0.84	0.71	0.65	0.29		0.74	-0.04	-0.05	0.01	0.21	-0.05	0.01	-0.05	-0.09	0.10	0.22	0.02	-0.05	0.46	0.07	0.52	-0.24	0.73	0.00	-0.02	-0.17	-0.02	-0.02	0.09	0.45	-0.02	0.67	0.83	0.24	-0.11	0.06
SO4	0.78	0.78	0.73	0.34	0.37	0.74		-0.04	-0.04	-0.03	-0.02	-0.03	0.01	-0.05	-0.09	0.04	0.24	0.03	-0.06	0.34	0.00	0.22	-0.21	0.41	0.02	0.02	-0.15	-0.02	-0.02	0.19	0.31	0.05	0.53	0.47	0.29	-0.09	0.04
Al	-0.03	-0.06	-0.01	-0.04	-0.01	-0.04	-0.04		-0.02	-0.01	-0.08	-0.01	-0.03	0.02	0.01	-0.04	-0.04	-0.01	-0.03	0.00	-0.03	-0.04	-0.06	-0.03	-0.01	0.30	0.03	-0.02	0.04	-0.03	0.07	-0.08	0.01	-0.03	0.01	-0.01	0.40
Sb	-0.05	-0.04	-0.05	-0.03	-0.06	-0.05	-0.04	-0.02		0.01	-0.02	-0.02	-0.02	-0.02	0.12	-0.04	-0.01	-0.01	0.15	-0.05	-0.02	-0.02	0.02	-0.04	0.19	-0.01	-0.01	-0.01	-0.01	-0.03	-0.04	0.01	-0.06	-0.04	-0.09	0.00	0.08
Ag	0.07	-0.01	0.08	-0.04	0.25	0.01	-0.03	-0.01	0.01		-0.02	0.00	0.00	-0.02	0.01	-0.02	0.09	-0.03	-0.03	0.06	-0.02	-0.01	0.03	-0.03	0.01	-0.01	0.00	-0.01	-0.01	-0.11	-0.05	-0.03	0.13	-0.02	0.07	-0.04	-0.02
Ba	0.13	0.24	0.09	0.21	0.10	0.21	-0.02	-0.08	-0.02	-0.02		-0.02	-0.02	-0.03	-0.03	0.04	-0.01	-0.04	-0.08	0.20	0.00	0.27	-0.07	0.32	-0.03	-0.01	-0.01	-0.01	-0.04	0.09	-0.01	-0.01	0.46	0.28	0.05	-0.07	0.03
Cd	-0.04	-0.03	-0.04	-0.03	-0.01	-0.05	-0.03	-0.01	-0.02	0.00	-0.02		0.02	0.06	0.00	0.01	-0.04	0.02	0.01	-0.04	-0.02	-0.03	0.02	-0.03	-0.01	-0.01	-0.01	0.03	0.46	0.01	-0.02	0.00	-0.05	-0.04	0.00	0.04	-0.03
Cr	0.02	0.00	-0.03	-0.02	-0.04	0.01	0.01	-0.03	-0.02	0.00	-0.02	0.02		0.09	-0.03	0.07	0.06	0.49	0.00	0.00	0.03	0.01	0.03	0.01	0.02	-0.01	0.02	0.00	0.08	0.02	-0.06	-0.04	0.01	-0.01	-0.03	0.01	-0.02
Co	-0.05	-0.03	-0.02	-0.02	-0.02	-0.05	-0.05	0.02	-0.02	-0.02	-0.03	0.06	0.09		-0.03	0.74	-0.05	0.27	0.18	-0.05	0.23	-0.03	0.02	-0.05	-0.01	-0.01	0.08	0.02	0.09	0.20	-0.05	-0.05	-0.04	-0.05	-0.11	-0.03	-0.03
Cu	-0.10	-0.07	-0.07	-0.05	-0.12	-0.09	-0.09	0.01	0.12	0.01	-0.03	0.00	-0.03	-0.03		-0.07	-0.10	0.02	0.03	-0.10	-0.03	-0.05	0.02	-0.07	-0.02	-0.02	0.01	0.44	-0.01	-0.07	0.01	-0.07	-0.10	-0.07	-0.16	0.10	-0.02
Mn	0.05	0.09	0.06	0.16	0.08	0.10	0.04	-0.04	-0.04	-0.02	0.04	0.01	0.07	0.74	-0.07		0.03	0.29	0.08	-0.03	0.35	0.03	-0.02	0.12	-0.02	0.00	0.04	-0.01	-0.02	0.14	0.04	-0.02	0.08	0.10	-0.09	-0.03	-0.04
Mo	0.21	0.13	0.07	0.17	0.15	0.22	0.24	-0.04	-0.01	0.09	-0.01	-0.04	0.06	-0.05	-0.10	0.03		-0.06	-0.08	0.15	-0.06	0.17	-0.06	0.23	0.06	0.02	-0.01	-0.01	-0.03	-0.10	0.03	0.30	0.14	0.20	0.52	-0.16	0.06
Ni	0.02	0.06	0.05	0.01	0.02	0.02	0.03	-0.01	-0.01	-0.03	-0.04	0.02	0.49	0.27	0.02	0.29	-0.06		0.15	-0.02	0.22	-0.02	-0.01	0.00	-0.01	-0.01	0.01	-0.02	-0.02	0.16	-0.02	-0.06	0.02	0.01	-0.09	-0.03	-0.05
Zn	-0.07	-0.05	-0.08	-0.06	-0.19	-0.05	-0.06	-0.03	0.15	-0.03	-0.08	0.01	0.00	0.18	0.03	0.08	-0.08	0.15		-0.10	0.23	-0.04	0.05	-0.05	-0.01	-0.03	0.01	-0.01	-0.01	0.12	-0.05	-0.09	-0.10	-0.06	-0.19	0.05	-0.05
B	0.53	0.39	0.42	0.17	0.40	0.46	0.34	0.00	-0.05	0.06	0.20	0.04	0.00	-0.05	-0.10	-0.03	0.15	-0.02	-0.10		0.01	0.40	-0.25	0.28	0.03	0.02	-0.18	-0.02	-0.01	0.23	0.01	0.05	0.53	0.35	0.43	-0.13	0.09
Fe	0.04	0.04	0.10	0.08	-0.01	0.07	0.00	-0.03	-0.02	-0.02	0.00	-0.02	0.03	0.23	-0.03	0.35	-0.06	0.22	0.23	0.01		0.02	0.01	0.06	-0.02	0.01	-0.04	0.01	-0.01	0.27	0.10	-0.05	0.06	0.08	-0.06	-0.07	-0.02
Li	0.32	0.28	0.15	0.71	0.01	0.52	0.22	-0.04	-0.02	-0.01	0.27	-0.03	0.01	-0.03	-0.05	0.03	0.17	-0.02	-0.04	0.40	0.02		-0.10	0.72	-0.02	-0.01	-0.08	-0.01	-0.01	0.05	0.15	-0.02	0.35	0.74	0.18	-0.07	0.02
Se	-0.22	-0.16	-0.18	-0.20	-0.13	-0.24	-0.21	-0.06	0.02	0.03	-0.07	0.02	0.03	0.02	0.02	-0.02	-0.06	-0.01	0.05	-0.25	0.01	-0.10		-0.21	0.01	0.01	0.19	0.01	0.01	0.01	-0.38	-0.01	-0.31	-0.26	-0.14	0.07	-0.02
Sr	0.43	0.46	0.18	0.93	-0.01	0.73	0.41	-0.03	-0.04	-0.03	0.32	-0.03	0.01	-0.01	-0.02	-0.02	0.23	0.00	-0.05	0.28	0.06	0.72	-0.21		-0.02	-0.02	-0.14	-0.02	-0.01	0.11	0.51	-0.01	0.49	0.94	0.22	-0.10	0.04
Sn	0.03	-0.01	0.04	-0.03	0.12	0.00	0.02	-0.01	0.19	0.01	-0.03	-0.01	0.02	-0.01	-0.02	-0.02	0.06	-0.01	-0.01	0.03	-0.02	0.01	-0.02	-0.02		-0.01	-0.01	-0.01	0.00	0.05	-0.03	0.02	0.00	-0.02	0.06	-0.02	0.03
Ti	0.00	-0.01	0.01	-0.02	0.13	-0.02	-0.02	0.30	-0.01	0.00	-0.01	-0.01	-0.01	-0.02	0.00	0.02	0.30	-0.06	-0.09	0.01	-0.05	-0.02	-0.01	-0.01	-0.03		-0.01	-0.03	-0.02	-0.05	-0.01	-0.04	-0.03	0.29	-0.04	0.00	
V	-0.16	-0.09	-0.01	-0.11	-0.01	-0.17	-0.15	0.03	-0.01	0.00	-0.01	-0.01	0.02	-0.01	-0.02	0.04	-0.01	0.01	-0.05	0.28	0.06	-0.08	0.19	-0.14	-0.01	-0.01		-0.01	0.07	0.03	-0.01	-0.01	0.08	0.34	0.58	0.29	-0.14	0.08
Be	-0.02	-0.09	-0.08	-0.11	-0.01	-0.17	-0.15	0.03	-0.01	0.00	-0.01	-0.01	0.02	-0.01	-0.02	0.00	0.01	0.01	-0.09	0.01	-0.04	-0.08	0.19	-0.14	-0.01	-0.01	-0.01		0.07	0.03	-0.01	-0.01	0.08	-0.04	0.22	0.29	-0.11	0.05
Bi	-0.02	-0.02	0.00	-0.02	-0.02	-0.02	-0.02	-0.01	-0.01	-0.01	-0.01	0.03	0.08	0.20	-0.07	0.14	-0.10	0.02	-0.07	0.23	0.10	0.15	-0.02	-0.01	-0.03	-0.03	-0.20	-0.01		0.02	-0.01	-0.02	-0.03	-0.04	0.29	0.22	-0.05	0.08
Si	0.18	0.23	0.32	-0.10	0.24	0.09	0.19	-0.03	-0.03	-0.11	-0.04	0.01	0.02	0.20	-0.07	0.14	-0.10	0.16	0.12	0.01	0.10	0.15	-0.38	0.51	-0.03	-0.03	-0.23	-0.01	-0.01		-0.11	-0.02	0.34	0.53	-0.06	0.09
Pb	0.28	0.30	0.19	0.54	0.00	0.45	0.31	0.07	-0.04	-0.05	0.09	-0.02	-0.06	-0.05	0.01	0.04	0.03	0.02	-0.05	0.23	0.10	0.15	-0.38	0.51	-0.03	-0.02	-0.03	-0.02	-0.02	-0.11		-0.01	0.34	0.53	0.14	-0.06	0.09
U	0.00	0.00	0.00	-0.01	0.10	-0.02	0.05	-0.08	0.01	-0.03	-0.01	0.00	-0.04	-0.05	-0.07	-0.02	0.30	-0.06	-0.09	0.01	-0.05	-0.02	-0.01	-0.01	0.02	-0.02	-0.03	-0.20	-0.02	-0.05	-0.01		-0.04	-0.03	0.29	-0.04	0.00
NH4	0.66	0.65	0.57	0.34	0.39	0.67	0.53	0.01	-0.06	0.13	0.46	-0.05	0.01	-0.04	-0.10	0.08	0.14	0.02	-0.10	0.53	0.06	0.35	0.35	0.49	0.00	-0.01	-0.20	-0.02	0.00	0.08	0.34	-0.04		0.58	0.29	-0.14	0.08
Br	0.57	0.55	0.34	0.90	0.06	0.83	0.47	-0.03	-0.04	-0.02	0.28	-0.04	-0.01	-0.05	-0.07	0.10	0.20	0.01	-0.06	0.35	0.08	0.74	-0.26	0.94	-0.02	-0.02	-0.17	-0.02	-0.02	-0.07	0.53	-0.03	0.58		0.22	-0.11	0.05
F	0.32	0.14	0.23	0.12	0.42	0.24	0.29	0.01	-0.09	0.07	0.05	0.00	-0.03	-0.11	-0.16	-0.09	0.52	-0.09	-0.19	0.43	-0.06	0.18	-0.14	0.22	0.06	0.07	-0.13	0.00	-0.03	-0.07	0.14	0.29	0.29	0.22		-0.22	0.17
NO3	-0.12	-0.06	-0.07	-0.03	-0.03	-0.11	-0.09	-0.01	0.00	-0.04	-0.07	0.04	0.01	-0.03	0.10	-0.03	-0.16	-0.03	0.05	-0.13	-0.07	-0.07	0.05	-0.10	-0.02	-0.03	0.15	-0.02	-0.02	0.02	-0.06	-0.04	-0.14	-0.11	-0.22		-0.05
P	0.08	0.04	0.08	0.03	0.17	0.06	0.04	0.40	0.08	-0.02	0.03	-0.03	-0.02	-0.03	-0.02	-0.04	0.06	-0.05	-0.05	0.09	-0.02	0.02	-0.08	0.04	0.03	0.55	0.02	0.01	-0.01	0.06	0.09	0.00	0.08	0.05	0.17	-0.05	

> 0.3 Correlated
> 0.8 Highly correlated
> 0.9 Extremly high correlation

	Na	Mg	K	Ca	HCO3	Cl	SO4	Al	Sb	Ag	Ba	Cd	Cr	Co	Cu	Mn	Mo	Ni	Zn	B	Fe	Li	Se	Sr	Sn	Ti	V	Be	Bi	Si	Pb	U	NH4	Br	F	NO3	P
Na		**0.86**	**0.86**	**0.31**	**0.47**	***0.91***	**0.78**	-0.03	-0.05	0.07	0.13	-0.04	0.02	-0.05	-0.10	0.05	0.21	0.02	-0.07	**0.53**	0.04	**0.32**	-0.22	**0.43**	0.03	0.00	-0.16	-0.02	-0.02	0.18	0.28	0.00	**0.66**	**0.57**	**0.32**	-0.12	0.08
Mg	**0.86**		**0.83**	**0.35**	**0.40**	**0.84**	**0.78**	-0.06	-0.04	-0.01	0.24	-0.03	0.00	-0.03	-0.07	0.09	0.13	0.06	-0.05	**0.39**	0.04	0.28	-0.16	**0.46**	-0.01	-0.01	-0.09	-0.02	-0.01	0.23	0.30	0.00	**0.65**	**0.55**	0.14	-0.06	0.04
K	**0.86**	**0.83**		0.12	**0.60**	**0.71**	**0.73**	-0.01	-0.05	0.08	0.09	-0.04	-0.03	-0.02	-0.07	0.06	0.07	0.05	-0.08	**0.42**	0.10	0.15	-0.18	0.18	0.04	0.01	-0.08	0.00	-0.02	**0.32**	0.19	0.00	**0.57**	**0.34**	0.23	-0.07	0.08
Ca	**0.31**	**0.35**	0.12		0.00	**0.65**	**0.34**	-0.04	-0.03	-0.04	0.21	-0.03	-0.02	-0.02	-0.05	0.16	0.17	0.01	-0.06	0.17	0.08	**0.71**	-0.20	***0.93***	-0.03	-0.02	-0.11	-0.02	-0.02	-0.10	**0.54**	-0.01	**0.34**	***0.90***	0.12	-0.03	0.03
HCO3	**0.47**	**0.40**	**0.60**	0.00		0.29	**0.37**	-0.01	-0.06	0.25	0.10	-0.01	-0.04	-0.02	-0.12	0.08	0.15	0.02	-0.19	**0.40**	-0.01	0.01	-0.13	-0.01	0.12	0.13	-0.01	-0.02	-0.03	0.24	0.00	0.10	**0.39**	0.06	**0.42**	-0.03	0.17
Cl	***0.91***	**0.84**	**0.71**	**0.65**	0.29		**0.74**	-0.04	-0.05	0.01	0.21	-0.05	0.01	-0.05	-0.09	0.10	0.22	0.02	-0.05	**0.46**	0.07	**0.52**	-0.24	**0.73**	0.00	-0.02	-0.17	-0.02	-0.02	0.09	**0.45**	-0.02	**0.67**	**0.83**	0.24	-0.11	0.06
SO4	**0.78**	**0.78**	**0.73**	**0.34**	**0.37**	**0.74**		-0.04	-0.04	-0.03	-0.02	-0.03	0.01	-0.05	-0.09	0.04	0.24	0.03	-0.06	**0.34**	0.00	0.22	-0.21	**0.41**	0.02	-0.02	-0.15	-0.02	-0.02	0.19	**0.31**	0.05	**0.53**	**0.47**	0.29	-0.09	0.04
Al	-0.03	-0.06	-0.01	-0.04	-0.01	-0.04	-0.04		-0.02	-0.01	-0.08	-0.01	-0.03	0.02	0.01	-0.04	-0.04	-0.01	-0.03	0.00	-0.03	-0.04	-0.06	-0.03	-0.01	**0.30**	0.03	-0.02	0.04	-0.03	0.07	-0.08	0.01	-0.03	0.01	-0.01	**0.40**
Sb	-0.05	-0.04	-0.05	-0.03	-0.06	-0.05	-0.04	-0.02		0.01	-0.02	-0.02	-0.02	-0.02	0.12	-0.04	-0.01	-0.01	0.15	-0.05	-0.02	-0.02	0.02	-0.04	0.19	-0.01	-0.01	-0.01	-0.01	-0.03	-0.04	0.01	-0.06	-0.04	-0.09	0.00	0.08
Ag	0.07	-0.01	0.08	-0.04	0.25	0.01	-0.03	-0.01	0.01		-0.02	0.00	0.00	-0.02	0.01	-0.02	0.09	-0.03	-0.03	0.06	-0.02	-0.01	0.03	-0.03	0.01	-0.01	0.00	-0.01	-0.01	-0.11	-0.05	-0.03	0.13	-0.02	0.07	-0.04	-0.02
Ba	0.13	0.24	0.09	0.21	0.10	0.21	-0.02	-0.08	-0.02	-0.02		-0.02	-0.02	-0.03	-0.03	0.04	-0.01	-0.04	-0.08	0.20	0.00	0.27	-0.07	**0.32**	-0.03	-0.01	-0.01	-0.01	-0.01	-0.04	0.09	-0.01	**0.46**	0.28	0.05	-0.07	0.03
Cd	-0.04	-0.03	-0.04	-0.03	-0.01	-0.05	-0.03	-0.01	-0.02	0.00	-0.02		0.02	0.06	0.00	0.01	-0.04	0.02	0.01	-0.04	-0.02	-0.03	0.02	-0.03	-0.01	-0.01	-0.01	0.03	**0.46**	0.01	-0.02	0.00	-0.05	-0.04	0.00	0.04	-0.03
Cr	0.02	0.00	-0.03	-0.02	-0.04	0.01	0.01	-0.03	-0.02	0.00	-0.02	0.02		0.09	-0.03	0.07	0.06	**0.49**	0.00	0.00	0.03	0.01	0.03	0.01	0.02	-0.01	0.02	0.00	0.08	0.02	-0.06	-0.04	0.01	-0.01	-0.03	0.01	-0.02
Co	-0.05	-0.03	-0.02	-0.02	-0.02	-0.05	-0.05	0.02	-0.02	-0.02	-0.03	0.06	0.09		-0.03	**0.74**	-0.05	0.27	0.18	-0.05	0.23	-0.03	0.02	-0.05	-0.01	-0.01	0.08	0.02	0.09	0.20	-0.05	-0.05	-0.04	-0.05	-0.11	-0.03	-0.03
Cu	-0.10	-0.07	-0.07	-0.05	-0.12	-0.09	-0.09	0.01	0.12	0.01	-0.03	0.00	-0.03	-0.03		-0.07	-0.10	0.02	0.03	-0.10	-0.03	-0.05	0.02	-0.07	-0.02	-0.02	0.01	**0.44**	-0.01	-0.07	0.01	-0.07	-0.10	-0.07	-0.16	0.10	-0.02
Mn	0.05	0.09	0.06	0.16	0.08	0.10	0.04	-0.04	-0.04	-0.02	0.04	0.01	0.07	**0.74**	-0.07		0.03	0.29	0.08	-0.03	**0.35**	0.03	-0.02	0.12	-0.02	0.00	0.04	-0.01	-0.02	0.14	0.04	-0.02	0.08	0.10	-0.09	-0.03	-0.04
Mo	0.21	0.13	0.07	0.17	0.15	0.22	0.24	-0.04	-0.01	0.09	-0.01	-0.04	0.06	-0.05	-0.10	0.03		-0.06	-0.08	0.15	-0.06	0.17	-0.06	0.23	0.06	0.02	-0.01	-0.01	-0.03	-0.10	0.03	0.30	0.14	0.20	**0.52**	-0.16	0.06
Ni	0.02	0.06	0.05	0.01	0.02	0.02	0.03	-0.01	-0.01	-0.03	-0.04	0.02	**0.49**	0.27	0.02	0.29	-0.06		0.15	-0.02	0.22	-0.02	-0.01	0.00	-0.01	-0.01	0.01	-0.02	-0.02	0.16	0.02	-0.06	0.02	0.01	-0.09	-0.03	-0.05
Zn	-0.07	-0.05	-0.08	-0.06	-0.19	-0.05	-0.06	-0.03	0.15	-0.03	-0.08	0.01	0.00	0.18	0.03	0.08	-0.08	0.15		-0.10	0.23	-0.04	0.05	-0.05	-0.01	-0.03	0.01	-0.01	-0.01	0.12	-0.05	-0.09	-0.10	-0.06	-0.19	0.05	-0.05
B	**0.53**	**0.39**	**0.42**	0.17	**0.40**	**0.46**	**0.34**	0.00	-0.05	0.06	0.20	-0.04	0.00	-0.05	-0.10	-0.03	0.15	-0.02	-0.10		0.01	**0.40**	-0.25	0.28	0.03	0.02	-0.18	-0.02	-0.01	0.01	0.23	0.01	**0.53**	**0.35**	**0.43**	-0.13	0.09
Fe	0.04	0.04	0.10	0.08	-0.01	0.07	0.00	-0.03	-0.02	-0.02	0.00	-0.02	0.03	0.23	-0.03	**0.35**	-0.06	0.22	0.23	0.01		0.02	0.01	0.06	-0.02	0.01	-0.04	0.01	-0.01	0.27	0.10	-0.05	0.06	0.08	-0.06	-0.07	-0.02
Li	**0.32**	0.28	0.15	**0.71**	0.01	**0.52**	0.22	-0.04	-0.02	-0.01	0.27	-0.03	0.01	-0.03	-0.05	0.03	0.17	-0.02	-0.04	**0.40**	0.02		-0.10	**0.72**	-0.02	-0.01	-0.08	-0.01	-0.01	-0.09	0.15	-0.02	**0.35**	**0.74**	0.18	-0.07	0.02
Se	-0.22	-0.16	-0.18	-0.20	-0.13	-0.24	-0.21	-0.06	0.02	0.03	-0.07	0.02	0.03	0.02	0.02	-0.02	-0.06	-0.01	0.05	-0.25	0.01	-0.10		-0.21	0.01	0.01	0.19	0.01	0.01	0.01	-0.38	-0.01	-0.31	-0.26	-0.14	0.05	-0.08
Sr	**0.43**	**0.46**	0.18	***0.93***	-0.01	**0.73**	**0.41**	-0.03	-0.04	-0.03	**0.32**	-0.03	0.01	-0.05	-0.07	0.12	0.23	0.00	-0.05	0.28	0.06	**0.72**	-0.21		-0.02	-0.02	-0.14	-0.02	-0.01	-0.11	**0.51**	-0.01	**0.49**	***0.94***	0.22	-0.10	0.04
Sn	0.03	-0.01	0.04	-0.03	0.12	0.00	0.02	-0.01	0.19	0.01	-0.03	-0.01	0.02	-0.01	-0.02	-0.02	0.06	-0.01	-0.01	0.03	-0.02	-0.02	0.01	-0.02		-0.01	-0.01	-0.01	0.00	0.05	-0.03	0.02	0.00	-0.02	0.06	-0.02	0.03
Ti	0.00	-0.01	0.01	-0.02	0.13	-0.02	-0.02	**0.30**	-0.01	-0.01	-0.01	-0.01	-0.01	-0.01	-0.02	0.00	0.02	-0.01	-0.03	0.02	0.01	-0.01	0.01	-0.02	-0.01		-0.01	0.00	0.00	0.04	-0.03	-0.02	-0.01	-0.02	0.07	-0.03	**0.55**
V	-0.16	-0.09	-0.08	-0.11	-0.01	-0.17	-0.15	0.03	-0.01	0.00	-0.01	-0.01	0.02	0.08	0.01	0.04	-0.01	0.01	0.01	-0.18	-0.04	-0.08	0.19	-0.14	-0.01	-0.01		-0.01	-0.01	0.08	-0.23	-0.03	-0.20	-0.17	-0.13	0.15	0.02
Be	-0.02	-0.02	0.00	-0.02	-0.02	-0.02	-0.02	-0.02	-0.01	-0.01	-0.01	0.03	0.00	0.02	**0.44**	-0.01	-0.01	-0.02	-0.01	-0.02	0.01	-0.01	0.01	-0.02	-0.01	0.00	-0.01		0.07	0.03	-0.01	-0.02	-0.02	-0.02	0.00	-0.02	0.01
Bi	-0.02	-0.01	-0.02	-0.02	-0.03	-0.02	-0.02	0.04	-0.01	-0.01	-0.01	**0.46**	0.08	0.09	-0.01	-0.02	-0.03	-0.02	-0.01	-0.01	-0.01	-0.01	0.01	-0.01	0.00	0.00	-0.01	0.07		0.02	0.03	-0.02	0.00	-0.02	-0.03	-0.02	-0.01
Si	0.18	0.23	**0.32**	-0.10	0.24	0.09	0.19	-0.03	-0.03	-0.11	-0.04	0.01	0.02	0.20	-0.07	0.14	-0.10	0.16	0.12	0.01	0.27	-0.09	0.01	-0.11	0.05	0.04	0.08	0.03	0.02		-0.11	-0.05	0.08	-0.07	-0.07	0.02	0.06
Pb	0.28	0.30	0.19	**0.54**	0.00	**0.45**	**0.31**	0.07	-0.04	-0.05	0.09	-0.02	-0.06	-0.05	0.01	0.04	0.03	0.02	-0.05	0.23	0.10	0.15	-0.38	**0.51**	-0.03	-0.03	-0.23	-0.01	0.03	-0.11		-0.01	**0.34**	**0.53**	0.14	-0.06	0.09
U	0.00	0.00	0.00	-0.01	0.10	-0.02	0.05	-0.08	0.01	-0.03	-0.01	0.00	-0.04	-0.05	-0.07	-0.02	0.30	-0.06	-0.09	0.01	-0.05	-0.02	-0.01	-0.01	0.02	-0.02	-0.03	-0.02	-0.02	-0.05	-0.01		-0.04	-0.03	0.29	-0.04	0.00
NH4	**0.66**	**0.65**	**0.57**	**0.34**	**0.39**	**0.67**	**0.53**	0.01	-0.06	0.13	**0.46**	-0.05	0.01	-0.04	-0.10	0.08	0.14	0.02	-0.10	**0.53**	0.06	**0.35**	-0.31	**0.49**	0.00	-0.01	-0.20	-0.02	0.00	0.08	**0.34**	-0.04		**0.58**	0.29	-0.14	0.08
Br	**0.57**	**0.55**	**0.34**	***0.90***	0.06	**0.83**	**0.47**	-0.03	-0.04	-0.02	0.28	-0.04	-0.01	-0.05	-0.07	0.10	0.20	0.01	-0.06	**0.35**	0.08	**0.74**	-0.26	**0.94**	-0.02	-0.02	-0.17	-0.02	-0.02	-0.07	**0.53**	-0.03	**0.58**		0.22	-0.11	0.05
F	**0.32**	0.14	0.23	0.12	**0.42**	0.24	0.29	0.01	-0.09	0.07	0.05	0.00	-0.03	-0.11	-0.16	-0.09	**0.52**	-0.09	-0.19	**0.43**	-0.06	0.18	-0.14	0.22	0.06	0.07	-0.13	0.00	-0.03	-0.07	0.14	0.29	0.29	0.22		-0.22	0.17
NO3	-0.12	-0.06	-0.07	-0.03	-0.03	-0.11	-0.09	-0.01	0.00	-0.04	-0.07	0.04	0.01	-0.03	0.10	-0.03	-0.16	-0.03	0.05	-0.13	-0.07	-0.07	0.05	-0.10	-0.02	-0.03	0.15	-0.02	-0.02	0.02	-0.06	-0.04	-0.14	-0.11	-0.22		-0.05
P	0.08	0.04	0.08	0.03	0.17	0.06	0.04	**0.40**	0.08	-0.02	0.03	-0.03	-0.02	-0.03	-0.02	-0.04	0.06	-0.05	-0.05	0.09	-0.02	0.02	-0.08	0.04	0.03	**0.55**	0.02	0.01	-0.01	0.06	0.09	0.00	0.08	0.05	0.17	-0.05	

> 0.3 Correlated

> 0.8 Highly correlated

> 0.9 Extremly high correlatation

ANNEXE 7 (Annexe 6; Chapitre 4): Diagramme Eh-pH combiné du fer et du manganèse. Les échantillons sont représentés par un symbole qui permet d'identifier la grappe à laquelle ils appartiennent obtenue à partir de l'analyse statistique multivariée du jeu de données réduit. Il existe des gammes de pH et de Eh pour lesquelles le fer et le manganèse ne coexistent pas sous forme dissoute. C'est le cas de la plupart des échantillons du jeu de donnée réduit.